**UNIVERSITÀ
DEGLI STUDI
DI BRESCIA**

DOTTORATO DI RICERCA IN INGEGNERIA CIVILE, AMBIENTALE, DELLA COOPERAZIONE INTERNAZIONALE E DI MATEMATICA

Settore Scientifico Disciplinare ICAR/08

Metodi e Modelli Matematici per l'Ingegneria

XXXV CICLO

VARIATIONAL PRINCIPLES FOR EVOLUTION PROBLEMS

DOTTORANDA
Francesca Levi

SUPERVISORE
Prof. Angelo Carini

CO-SUPERVISORE
Prof. Andrea Panteghini

CO-SUPERVISORE
Dott.ssa Francesca Fantoni

Variational principles for evolution problems

Francesca Levi

University of Brescia

PhD in Civil and Environmental Engineering, International cooperation and Mathematics

Curriculum: Mathematical Methods and Models for Engineering (XXXV Cycle)

Supervisor:
Prof. Angelo Carini

Co-Supervisor:
Prof. Andrea Panteghini

Co-Supervisor:
Dott.ssa Francesca Fantoni

To mum and dad

Acknowledgments

Abstract

The study of phenomena that evolve over time is often conducted through their modelling as dynamic systems, whose mathematical formulation generally requires the resolution of systems of differential equations with initial conditions.

Solving the governing equations of a physical phenomenon means determining its evolution over time starting from a set of initial conditions; for example, considering mechanical systems, through a mathematical law that determines its position and speed as functions of time.

However, the equations governing motion cannot be often solved analytically and therefore, numerical integration techniques are used in order to obtain an accurate approximation of the solution.

Treating the problem of studying a physical system from a variational point of view may be a different approach, motivated by the Lagrangian formulation of classical mechanics. The idea of replacing a given problem with an equivalent one in variational form is certainly not new: the interest in this formulation is in fact justified by the validity of the so-called *direct methods* of the calculation of variations. These methods are valid both for a qualitative study of the problem (verification of existence and uniqueness of the solution, its regularity, etc.), and for a quantitative study, namely from a numerical point of view (evaluation of convergence, estimation of the error of the approximate solution).

In this thesis, evolution problems of engineering interest are analysed, formulated in a variational way. Firstly, the linear viscoelastic problem is numerically solved using three different variational formulation, such as Gurtin's variational formulation, Split Gurtin formulation and the Huet formulation.

The Finite Element Method is used for the space discretization and the Ritz method is used for the time discretization.

Then, the heat conduction problem is taken into account. Two formulations are considered: the first one based on a convolutive bilinear form, the second one based on a biconvolutive bilinear form. Several numerical examples highlight the goodness of the two different approaches.

Next, the problem of the determination of upper and lower bounds for the mechanical properties of composite materials, consisting of phases having viscoelastic constitutive laws, is addressed. Subsequently, the problem of the evolution of a fracture is analyzed both in an elastic medium and in a viscoelastic medium. In the first case, an extremal formulation, similar to that of Capurso and Maier, is proposed, valid in the elastoplastic field.

Finally, the dynamical stability of plane systems with just one lumped mass, subjected to follower forces, is considered.

Sommario

Lo studio di fenomeni che evolvono nel tempo è spesso condotto attraverso la loro modellazione come sistemi dinamici, la cui formulazione matematica, in genere, richiede la risoluzione di sistemi di equazioni differenziali a condizioni iniziali. Risolvere le equazioni che governano un fenomeno fisico evolutivo significa determinarne l'evoluzione nel tempo a partire da un insieme di condizioni iniziali; ad esempio, considerando i sistemi meccanici, attraverso una legge matematica che ne determina la posizione e la velocità in funzione del tempo.

Tuttavia, le equazioni che governano il moto spesso non possono essere risolte analiticamente e quindi vengono utilizzate tecniche di integrazione numerica per ottenere un'approssimazione accurata della soluzione.

Trattare il problema dello studio di un sistema fisico da un punto di vista variazionale può essere un approccio diverso, motivato dalla formulazione Lagrangiana della meccanica classica. L'idea di sostituire un dato problema con uno equivalente in forma variazionale non è certo nuova: l'interesse per questa formulazione è infatti giustificato dalla validità dei cosiddetti *metodi diretti* del calcolo delle variazioni. Questi metodi sono validi sia per uno studio qualitativo del problema (verifica dell'esistenza e unicità della soluzione, la sua regolarità, ecc.), sia per uno studio quantitativo, cioè da un punto di vista numerico (valutazione della convergenza, stima dell'errore della soluzione approssimata).

In questa tesi vengono analizzati problemi evolutivi di interesse ingegneristico, formulati per via variazionale. In primo luogo, il problema viscoelastico lineare viene risolto numericamente utilizzando tre diverse formulazioni variazionali: la formulazione di Gurtin, la formulazione di Gurtin "splittata"e la formulazione di Huet.

Il metodo degli elementi finiti viene utilizzato per la discretizzazione spaziale e il metodo Ritz viene utilizzato per la discretizzazione temporale.

Successivamente, si prende in considerazione il problema della conduzione del calore. Vengono considerate due formulazioni: la prima basata su una forma bilineare convolutiva, la seconda su una forma bilineare biconvolutiva. Numerosi esperimenti numerici mettono in luce la bontà dei due diversi approcci.

Viene poi affrontato il tema della determinazione di upper e lower bounds per le proprietà meccaniche di materiali compositi costituiti da fasi aventi legami costitutivi viscoelastici.

Successivamente viene analizzato il problema dell'evoluzione di una frattura sia in un mezzo elastico sia in un mezzo viscoelastico. Nel primo caso viene proposta una formulazione estremale analoga a quella di Capurso e Maier, valida in ambito elastoplastico.

Infine, viene considerata la stabilità dinamica di sistemi piani con una sola massa concentrata e soggetti a forze follower.

Contents

List of Figures

List of Tables

Chapter 1

Introduction

The study of phenomena that evolve over time, like the swing of a pendulum, the motion of celestial bodies, molecular dynamics, etc., is often conducted through their modelling as dynamic systems, whose mathematical formulation generally requires the resolution of systems of differential equations with initial conditions. Solving the governing equations of a physical phenomenon means determining its evolution over time starting from a set of initial conditions; for example, considering mechanical systems, through a mathematical law that determines its position and speed as a function of time.

However, the equations governing motion cannot be often solved analytically and therefore, numerical integration techniques are used in order to obtain an accurate approximation of the solution.

Treating the problem of studying a physical system from a variational point of view may be a different approach, motivated by the Lagrangian formulation of classical mechanics. The idea of replacing a given problem with an equivalent one in variational form is certainly not new: the interest in this formulation is in fact justified by the validity of the so-called *direct methods* of the calculus of variations. These methods are valid both for a qualitative study of the problem (study of existence and uniqueness of the solution, its regularity, etc.), and for a quantitative study, namely from a numerical point of view (evaluation of convergence, estimation of the error of the approximate solution). The first results of the calculus of variations concerned analytical mechanics and were subsequently extended to elastodynamics and field theory, as reported in several texts (Levi-Civita and Amaldi, (1927); Whittaker, (1917); Lanczos, (1970)). In particular, due to their importance, it is appropriate to recall Gauss's principle of least constraint and Hertz's principle of least curvature (which is a geometric interpretation of Gauss's principle in the case of zero active forces and time-independent constraints).

Another classic variational principle of mechanics is Hamilton's principle, whose importance was recognized after World War II by the use Feynman (1948) and Dirac (1930), in the field of quantum mechanics, made of it. However, all applications and extensions of Hamilton's law are not strictly variational formulations, since the equations of motion do not derive from the stationarity or from the minimum of a functional, but can only be considered quasi-variational (or weak) formulations.

In fact, Hamilton's principle is a true variational principle but, generally, it cannot be used to find solutions to the dynamic problem. The reason for this lies in the fact that, in order to find the stationary value of the Hamilton functional, it is necessary to consider functions that vanish both at the initial instant and at the final instant of a given time interval. Since, for a time-dependent field, the field at the final time is usually unknown, it is not possible to use the direct methods of variational calculus. In fact, the functions used in these methods must

satisfy the final condition which is known a priori. Furthermore, Hamilton's principle is not, in general, a minimum principle and it transforms the real problem (with initial conditions) in another with boundary conditions that does not always have a solution and the solution may not be unique. Despite all these criticisms, Hamilton's principle had considerable success in theoretical physics, also because attention was often addressed to differential equations, while the initial conditions were neglected.

In this thesis, evolution problems of engineering interest are presented, formulated in a variational way. In each Chapter a problem is introduced and analysed.

1.1   Thesis outline

Chapter 2 takes into account classical variational formulations for the linear viscoelastic problem (Section 2.1), such as Gurtin's variational formulation (1963), Split Gurtin formulation (Carini and Mattei, 2015) and the Huet (1992) formulation.
Firstly, the linear viscoelastic problem and its governing equations are introduced (Section 2.2). Properties regarding the relaxation kernel and the creep kernel are described. Then, a brief reminder to the convolutive bilinear form, which the formulations are based on, is made.
Gurtin's formulation is derived from the method of the adjoint equation, but it proves to be only a stationary principle.
Performing a decomposition of the integration time interval into two subintervals of the same amplitude leads to the definition of the Split Gurtin formulation. From the positiveness of the operator defined over the first subinterval, a minimum-stationary principle is obtained.
Finally, Huet formulation is described. He introduced a pseudo-convolutive bilinear form, which is not commutative in general, thus it is not symmetric even for relaxation kernels, which have the universal symmetries of linear elasticity. This is the main reason why Huet's formulations are subjected to limitations. To overcome this issue, a so-called "t-symmetrization" is performed and a minimum principle is derived. Nevertheless, the usage of Huet's functional is acceptable only with step-by-step marching procedures.
Tonti's extended formulations (1973) are introduced as a comparison (Section 2.3).
Three numerical simulations are performed (Section 2.4):

1. Bernulli-Navier viscoelastic beam, subject to a uniform load, with two rigid end supports and an elastic support in the middle;

2. cable stayed bridge, subject to a uniform load, with viscoelastic girder and piers and elastic stays;

3. reinforced cylinder under internal pressure.

The Finite Element Method is used for the space discretization and the Ritz method is used for the time discretization.
The different formulations are applied and the results are compared in order to define the best approach (Section 2.5).

Chapter 3 starts with the description of classical variational formulations for the heat conduction problem (Section 3.1).

Firstly, the linear transient heat conduction problem and its governing equations are introduced (Section 3.2). The problem can be written in three different forms: a three-fields operatorial form, a two-fields operatorial form and in a one-field form. Then the convolutive bilinear form (already introduced in the previous Chapter) and the biconvolutive bilinear form are defined. The latter depends on using a particular function of time, which recalls the relaxation function governing the linear viscoelastic problem. Stationary principles are obtained.

Gurtin's functionals (1963), using both the convolutive and the biconvolutive bilinear forms, are thus written (Section 3.3).

Performing a decomposition of the integration time interval into two subintervals of the same amplitude leads to the definition of different stationary principles (Section 3.4):

- a min-max principle of Tonti's type using the convolutive bilinear form;

- a minimum-stationary principle using the biconvolutive bilinear form.

Numerical simulations are performed (Section 3.5). Two examples are introduced: a finite rod with null initial temperature and a prescribed temperature at its ends and a finite square element with null initial temperature and a prescribed temperature at its boundary with no heat generation within the solid.

The Finite Element Method is used for the space discretization and the Ritz method is used for the time discretization.

The different formulations are applied and the results are compared in order to define the best approach (Section 3.6).

In *Chapter 4* the upper and lower bounds defined by Voigt and Reuss for elasticity are extended to the viscoelastic case, only to the deviatoric part of the relaxation and creep kernels (Section 4.1).

Firstly, an analysis of a system with elastic and viscoelastic materials arranged in series is performed, using the TPE-type functional introduced by Carini and Mattei (2015).

Macroscopically isotropic composite materials are considered. The lower bounds are satisfied and the upper bounds are proved only for the deviatoric part and they are also tested for the volumetric part of the relaxation and creep kernels.

Starting from the deviatoric strains, several square RVEs have been constructed, each possessing inclusions with different shapes. A plane strain simple shear problem was considered, applying, in the case of relaxation, boundary displacements corresponding to a constant unit value for the average in-plane shear strain, and, for creep, boundary tractions corresponding to a unit value for the average in-plane shear stress.

The analysis is conducted using the software ABAQUS and all the results confirm the prescribed bound (Section 4.3).

As for the the volumetric strains, two examples are taken into account, each structure possessing inclusions with different shapes (Section 4.4):

- sphere consisting of two phases, an elastic and a viscoelastic one. The internal phase is also redistributed equally into smaller symmetrical portions and the phases are also inverted (Section 4.4.1);

- RVE consisting of two phases, an elastic and a viscoelastic one. The internal phase consists of several spherical inclusions of different volume and the phases are also inverted (Section 4.4.2).

For the relaxation kernel, boundary displacements corresponding to a constant unit value for volumetric strain are applied.

All these analysis prove that the upper bound is not valid for systems with volumetric strains.

Chapter 5 starts from Capurso-Maier functional (Corradi dell'Acqua, 1992) used in plasticity in an incremental form and extend it to the case of fracture mechanics. A straight crack in an infinite domain Ω_∞ is considered first. From the definition of the energy-release rate a new component is added to the functional, which symbolizes (in the case of plasticity) a negative hardening (Sections 5.2.2-5.2.3). The Kuhn-Tucker complementary conditions are extended for the process zone (Section 5.2.4), which is the plastic zone according to the analogy with plasticity. A minimum principle is thus obtained for the Total Potential Energy type functional. The functional is then reformulated, from a two-field form to a one-field form and an analogy with the functional introduced by Salvadori and Carini (2011) is presented (Section 5.2.6). Subsequently, the functional is generalized to the case of a finite body in a two/three-dimensional space and a minimum formulation is performed (resorting to a Bramble and Pasciak method, in Section 5.2.7). A hint on a possible Free-Energy functional is given for the viscoelastic fracture mechanics, deriving from Francfort-Marigo formulation (2008) of the fracture mechanics problem (Section 5.3).

In *Chapter 6* firstly a brief reminder to the variational approach for the evaluation of dynamic instability performed by Leipholz (1970) is made (Section 6.1). In the first part of the Chapter, the dynamical stability of plane systems with just one lumped mass is discussed. The lumped-mass idealization, together with the assumption of negligible axial strain and the adoption of the second-order theory, reduces the considered systems to a single Lagrangian coordinate. In this way, static methods could be applied to derive the analytical expression of the stiffness coefficient and to study the dynamic stability. In particular, if instability is due to divergence at infinity, one can consider an auxiliary structure, differing from the original one in that the lumped mass is replaced by a constraint blocking the corresponding Lagrangian coordinate. Thus, the critical load of such new structure is due to divergence and it coincides with the critical load by divergence at infinity of the original structure. Firstly a new lumped mass system is studied: a straight-axis beam with constant cross-sectional area and stiffness, mass-free, hinged at one end, simply supported at an intermediate point (with a sliding plane parallel to the beam axis) and with the other end free, where a lumped mass is present and a follower force (concentrated or distributed) is applied. For this particular problem there should exist a position of the intermediate support, which divides divergence at infinity and Eulerian instability (Section 6.2.2).

Numerical analysis are performed, the transition values are obtained (Section 6.2.3) and a new rule for the determination of the critical load of dynamical systems, using only analytical methods, is established (Section 6.2.4).

In the second part of the Chapter, structures showing instability in tension are addressed. A recall to the work of Zaccaria et al. (2011) is made, regarding the example of two inextensible elastic rods clamped at one end and joint through a slider (see Fig. 6.7). Then, two conservative systems showing instability due to a tensile load are presented (Feriani and Carini, 2017), obtained by symmetrizing a follower load. This analysis corresponds to summing Beck's and Reut's non conservative loading conditions, where in each case the vertical load is equal to $P/2$. The resulting applied load is conservative (Section 6.3.2). In Section 6.3.3 a new system is studied: a straight-axis beam of length l with constant cross-sectional area and stiffness, hinged at one end, simply supported at an intermediate point is presented and two different

follower forces causing traction are applied. Results regarding the analysis with a concentrated and distributed loads are presented.

References

Carini, A., Mattei, O., 2015. Variational formulations for the linear viscoelastic problem in the time domain. European Journal of Mechanics A/Solids, 54, 146-159.

Corradi dell'Acqua, L., 1992. Meccanica delle strutture, il comportamento dei mezzi continui. Ed. McGraw-Hill, Milano.

Dirac, P. A., 1930. The principles of quantum mechanics. Oxford at the Clarendon Press.

Feriani, A., Carini, A., 2017. Some considerations on dynamic stability. in A. Zingoni (Ed.), Insights and Innovations in Structural Engineering, Mechanics and Computation, Proceedings of Sixth International Conference on Structural Engineering, Mechanics and Computation, Cape Town (South Africa), 2016-09-05 / 2016-09-07.

Feynman, R.P., 1948. Space-Time Approach to Non-Relativistic Quantum Mechanics. Reviews of Modern Physics 20, 367.

Francfort, G., Marigo, J., 2008. The Variational Approach to Fracture. Journal of Elasticity, 91.

Gurtin, M.E., 1963. Variational principles in the linear theory of viscoelasticity. Archive for Rational Mechanics and Analysis, 16 (1), 34-50.

Huet, C., 1992. Minimum theorems for elasticity. European Journal of Mechanics A/Solids 11 (5), 653-684.

Leipholz, H., 1970. Stability Theory. Academic Press, London.

Lanczos, C., 1970. The variational principles of mechanics. Dover, Toronto, Fourth Ed.

Levi-Civita, T., Amaldi, U., 1927. Lezioni di meccanica razionale. Ed. Zanichelli, Bologna.

Salvadori, A., Carini, A., 2011. Minimum theorems in incremental linear elastic fracture mechanics. International Journal of Solids and Structures, 48, 1362-1369.

Tonti, E., 1973. On the variational formulation for linear initial value problems. Annali di Matematica Pura ed Applicata, Serie Quarta XCV, 331-359.

Whittaker, E. T., 1917. A Treatise on the analytical dynamics of particles and rigid bodies; with an introduction to the problem of three bodies. Cambridge University Press, Cambridge, Second ed.

Zaccaria, D., Bigoni, D., Misseroni, D., Noselli, G., 2011. Structures buckling under tensile dead load. Proceedings of the Royal Society of London A 467, 16861700.

Chapter 2

On the effectiveness of convolutive type variational principles in the numerical solution of viscoelastic problems

Notation

Greek and latin letters

- Ω: Region occupied by a solid body;

- x_r, $r = 1, 2, 3$: Cartesian coordinates;

- V: Volume of the solid body;

- Γ: External surface of the solid body;

- $n_i(x_r)$: Unit outward normal vector components;

- $u_i(x_r, t)$: Displacement vector components;

- $\epsilon_{ij}(x_r, t)$: Small strain tensor components;

- $\sigma_{ij}(x_r, t)$: Stress tensor components;

- $[0, 2T]$: Time interval;

- $b_i(x_r, t)$: Body force vector components;

- $p_i(x_r, t)$: Surface traction vector components;

- Γ_p: Loaded region of the boundary;

- $\bar{u}_i(x_r, t)$: Prescribed displacement vector components;

- Γ_u: Constrained region of the boundary;

- R_{ijhk}: Relaxation tensor or kernel;

- C_{ijhk}: Creep tensor or kernel;

- $\boldsymbol{u}$: Displacement vector with components u_i;

- $\boldsymbol{b}$: Vector of the known terms;

- $\boldsymbol{v}$: Unknown vector of the adjoint problem;

- $\boldsymbol{a}$: Arbitrary known term;

- $\Phi(T)$: Free energy density;

- $D(T)$: Dissipation power density;

- $N(x,t)$: Axial force;

- $M(x,t)$: Bending moment;

- $\chi(x,t)$: Curvature;

- $A(x)$: Cross-section area;

- $J(x)$: Moment of inertia;

- $q(x,t)$: Transversal component of the distributed load;

- l^e: Length of the finite element;

- r_i: Interpolation functions;

- $\boldsymbol{\delta}$: Vector of the degrees of freedom;

- $\boldsymbol{\beta}_i$: Vector of the time degrees of freedom;

- $\boldsymbol{m}_i$: Vector of time shape functions;

- E_0, E_1 Elastic moduli;

- η: Relaxation time;

- k_m: Elastic stiffness of the spring;

- α: Tikhonov regularization parameter.

Symbols

- $=::$ Is defined as;

- $\circ$: Convolution product;

- $\tilde{}$: Adjoint operator;

- $'$: Admissible term;

- $_1$: Variable defined over the first subinterval;

- $_2$: Variable defined over the second subinterval;

- $\square$: Pseudo-convolution;

- $\hat{}$: Fictitious solution;

- $\subseteq$: Is included in;

- $\supseteq$: Includes.

Operators and functions

- $_{/i}$: Partial derivative operation;

- $\dot{\ }$: Derivation with respect to the time variable;

- $\mathcal{L}$: Navier operator;

- F^{MF}: Morse and Feshbach functional;

- $\langle\,,\,\rangle$: Standard bilinear form with time integral in the sense of Stieltjes;

- $\langle\,,\,\rangle_c$: Bilinear form with time integral in the sense of Stieltjes but standard with respect to space;

- F^G: Gurtin's functional;

- F^{SG}: Split Gurtin functional;

- $\mathcal{K}$: Tonti's linear positive-definite operator;

- $\mathcal{S}$: Linear elastic part of $\mathcal{L}$;

- $H(t)$: Heaviside function;

- F^H: Huet's functional.

2.1   Introduction

The first theme of this thesis is the numerical use of variational principles for linear viscoelasticity. As observed by Tonti (1973), variational formulations for initial value problems are not possible in the classical context of the Calculus of Variations. This is because the linear operators relevant to linear initial value problems are not self-adjoint with respect to the standard bilinear form, meaning the scalar product given by:

$$\int_0^T f(t)g(t)dt \tag{2.1.1}$$

or one of its variants. Historically, this problem was overcome by introducing artificial conditions, thus converting the original initial value problem into a boundary value problem, which is governed by a symmetric, self-adjoint operator (method of the formally self-adjoint operators). Therefore, the new problem admits a variational formulation and this method was profusely used in mechanics and theoretical physics (Hamilton principle, the stationary action principles of electromagmetism, quantum mechanics, general relativity, etc.).

A variational formulation, valid simultaneously for the given problem and the adjoint problem, was provided by Morse and Feshbach (1953). By using this method it is always possible to rephrase any linear problem in a variational way, considering that the method of the formally self-adjoint operators cannot be applied when the operator is not at least self adjoint. This method considers, alongside with the original initial value problem, another artificial one governed by the adjoint operator, then with final conditions. The use of the adjoint operator, whether explicitly or implicitly, inspired a significant number of papers, especially for diffusion problems. Nevertheless, justifying the attachment of the adjoint problem from a physical point of view constitutes a great issue.

The earliest variational formulations for the viscoelastic problem, although under very restrictive assumptions, date back to Biot (1956), Olszak and Perzyna (1959), Breuer and Onat (1964), Hlaváček (1966), who proposed extremum formulations for isotropic viscoelastic materials with Poisson's ratio invariant in time, and Christensen (1968, 1971), who proposed an extremum variational formulation, valid under restrictive assumptions, since the isotropy of the material and separation of space and time in the expressions of the solution to the viscoelasticity problem are required, using state functions such as the free energy.

The first true variational formulation for initial value problems dates back to Gurtin's work (1963, 1964a, 1964b). It is based on the use of convolution integrals, generalizing the classical elasticity principles to the linear viscoelastic case, and it is valid for a large class of linear time-dependent problems, including viscoelasticity, elastodynamics, and the heat conduction problem. This approach is perfectly described by Tonti (1973): *The choice of different bilinear forms becomes the key to try to give variational formulation to new class of equations.* Gurtin's approach consisted in converting the original initial-boundary value problem into an equivalent boundary value problem, governed by integro-differential equations, through the application of Laplace transorms.

Gurtin's method was applied to the linear theory of viscoelasticity by many authors (Schapery (1964), Leitman (1966), Taylor et al. (1970), Brilla (1972), Reddy (1976), just to name a few) and is has also been extended to the method of boundary integral equations (Carini et al. (1991)).

It should be emphasized that Gurtin's variational principles and relevant generalizations are not extremum principles. Nevertheless, Benthien and Gurtin (1970) showed that the Laplace transform of the Gurtin-type stationarity formulations are in fact minimum formulations in the transformed domain.

Rafalski (1969) has the merit of having obtained extremal formulations for linear problems with initial values. The limit of his results is that it is necessary to study the whole history, from the time of the initial assignment of data to infinity. The work of Rafalski was later perfected by Reiss (1978), who introduced a method, whereby the functional of Benthien and Gurtin could be transformed back to the original space-time domain, while preserving the extremizing characteristic of the functional, and by Reiss and Haug (1978), who formulated extremal principles for problems with initial values, including the problem of hereditary viscoelasticity and who explored the possibility of finding those functionals which return an extremum principle for linear initial value problems.

Huet (1992), through the use of pseudo-convolutive and pseudo-biconvolutive bilinear forms introduced in 1952 by Staverman and Schwarzl and extended in 1966-1969 by Mandel and Brun (SSMB theory), although under restrictive assumptions, obtained two principles, extensions of the minimum principles of the Total Potential Energy and the Complementary Energy related to linear elasticity.

Tonti (1984) generalized the method to any non-linear problem through the application of an "integrating operator" that transforms the differential original problem into an integro-differential one which admits a variational formulation. Tonti proved that not only does an integrating operator always exists but that there is an infinite numbers of such operators. Moreover, integrating operators can be found such that the functional is an extremum at the solution. The latter approach was applied also to the linear viscoelasticity case by Carini et al. (1995) and Carini and De Donato (2004).

In Carini and Mattei (2015) five principles are formulated: four of the variational type and one of the minimum type. Minimum-stationary type formulations are obtained for the linear viscoelastic problem. In the following these formulations are called "split Gurtin's formulations", whose name derives from the division of the time domain into two equal subintervals, thus doubling the original unknowns of the viscoelastic problem. Citing the article: *The use of a convolutive bilinear form and the decomposition of the time domain into two equal subintervals are the necessary ingredients to reformulate the viscoelastic problem in terms of a minimum variational problem, with evident advantages, both theoretical and computational.*

To the authors' knowledge, there does not appear to be any significant work in the literature concerning the use of variational formulations for the numerical solution of the linear viscoelasticity problem. In particular, variational principles based on convolutive bilinear forms with respect to time do not seem to have had any place so far in computational procedures for the numerical determination of the viscoelastic response of solids or structures subjected to external actions. In this Chapter we try to start filling this gap with reference to Gurtin's formulation and those related to it which have been mentioned above.

The Chapter is organized as follows. In Subsection 2, the linear viscoelastic problem and the relative equations are introduced. In Subsection 3, Gurtin's variational formulation and those derived from it are presented, i.e., the split Gurtin formulation and the Huet formulation. In Subsection 4, by using the Finite Element technique in space and the Ritz method in time, a discretized formulation is applied and three numerical examples, of increasing complexity, are shown with the aim of testing the effectiveness of the presented Gurtin type variational formulations in the numerical solution of the linear viscoelastic problem. The first example is a viscoelastic beam on elastic support subjected to a constant distributed load. The second example is a cable-stayed bridge with girder and piers made of concrete and stays made of steel, subjected to a constant distributed load. The third and last example is e a plane strain cylinder of viscoelastic material, surrounded by an elastic steel casing and subjected to an internal pressure history (first constant, and then variable over three time intervals). In Subsection 5,

conclusions and open issues are discussed, therefore a list of references is presented.

2.2 The linear viscoelastic problem

Consider a solid body $\Omega \subset \mathbb{R}^3$ made of a linear viscoelastic material, possibly anisotropic. An orthogonal Cartesian reference system is used, with coordinates x_r, $r = 1, 2, 3$. The components of vectors, second order, and fourth order tensors are indicated with the usual indicial notation. Einstein's convention over repeated indices is adopted, for which when an index variable appears twice in a single term and is not otherwise defined, it implies summation of that term over all the values of the index.

Denote by V the volume of the region Ω and by Γ its external surface, with unit outward normal $n_i(x_r)$. Let $u_i(x_r, t)$, $\epsilon_{ij}(x_r, t)$ and $\sigma_{ij}(x_r, t)$ be, respectively, the displacement, strain, and stress fields at the point $x_r \in \Omega$, at the time $t \in [0, 2T]$. The solid may be subjected to a history of body forces $b_i(x_r, t)$, to a history of surface tractions $p_i(x_r, t)$ acting on the loaded region Γ_p of the boundary, and to a history of prescribed displacements $\bar{u}_i(x_r, t)$ acting on the constrained boundary Γ_u, with $\Gamma_u \cup \Gamma_p = \Gamma$.

The body is undisturbed for $t < 0$ and the whole loading history is supposed to be defined in the given time range $t \in [0, 2T]$, $2T$ being the end time of the loading process.

The stress field $\sigma_{ij}(x_r, t)$, with $\sigma_{ij}(x_r, t) = 0$ for $t < 0$, satisfies the equilibrium equations:

$$\begin{aligned}
\sigma_{ij/j}(x_r, t) + b_i(x_r, t) &= 0 \quad \text{in } \Omega \times [0, 2T] \\
\sigma_{ij}(x_r, t) n_j(x_r) &= p_i(x_r, t) \quad \text{on } \Gamma_p \times [0, 2T]
\end{aligned} \tag{2.2.1}$$

where the symbol / indicates the partial derivative operation.
The displacement field $u_i(x_r, t)$ and the strain field $\epsilon_{ij}(x_r, t)$ with $u_i(x_r, t) = 0$ and $\epsilon_{ij}(x_r, t) = 0$ for $t < 0$, fulfill the strain-displacement relations:

$$\begin{aligned}
\epsilon_{ij}(x_r, t) &= \frac{1}{2}(u_{i/j}(x_r, t) + u_{j/i}(x_r, t)) \quad \text{in } \Omega \times [0, 2T] \\
u_i(x_r, t) &= \bar{u}_i(x_r, t) \quad \text{on } \Gamma_u \times [0, 2T]
\end{aligned} \tag{2.2.2}$$

Here, we deal only with non-aging materials (i.e., we consider only the hereditary viscoelasticity case), for which the direct constitutive law, that relates a known strain field $\epsilon_{ij}(x_r, t)$ to the corresponding stress field $\sigma_{ij}(x_r, t)$, can be written as follows (this form derives from the Boltzmann superposition principle, and it describes the stress field at the time t, in the fixed point $x_r \in \Omega$, due to the strain increments $\mathrm{d}\epsilon_{hk}(x_r, \tau)$, for $\tau \in [0, t]$):

$$\sigma_{ij}(x_r, t) = \int_{0^-}^{t} R_{ijhk}(x_r, t - \tau) \, \mathrm{d}\epsilon_{hk}(x_r, \tau) \tag{2.2.3}$$

where $R_{ijhk}(x_r, t)$, with $t > 0$ (we assume that $R_{ijhk}(x_r, t) = 0$ for $t < 0$), is the relaxation tensor, or kernel and the integral has to be meant in the Stieltjes sense.
We recall that, considering two functions f and g, the convolution product can be written in two different forms, i.e. the Stieltjes-type convolution:

$$\langle f(t), g(t) \rangle_{Sc} = \int_{0^-}^{t} f(t - \tau) \, dg(\tau) \tag{2.2.4}$$

and the Lebesgue-type convolution:

$$\langle f(t), g(t) \rangle_{Lc} = \int_{0}^{t} f(t - \tau) g(\tau) \, d\tau \tag{2.2.5}$$

Using the latter, the direct constitutive law (2.2.3) can be written in the Volterra form:

$$\sigma_{ij}(x_r, t) = R_{ijhk}(x_r, 0)\epsilon_{hk}(x_r, t) + \int_0^t \dot{R}_{ijhk}(x_r, t - \tau)\epsilon_{hk}(x_r\tau)\, \mathrm{d}\tau \tag{2.2.6}$$

where the dot indicates derivation with respect to the time variable.

We assume that the relaxation tensor satisfies the same symmetry properties enjoyed also by the linear elasticity constitutive tensors:

$$R_{ijhk}(x_r, t) = R_{jihk}(x_r, t) = R_{ijkh}(x_r, t) = R_{hkij}(x_r, t) \quad \forall x_r \in \Omega, \forall t \in [0, 2T] \tag{2.2.7}$$

and that the following inequalities hold:

$$R^0_{ijhk}(x_r)\, \lambda_{ij}\, \lambda_{hk} > 0 \quad, \qquad R^\infty_{ijhk}(x_r)\, \lambda_{ij}\, \lambda_{hk} > 0 \tag{2.2.8}$$

for every $x_r \in \Omega$ and for every non-vanishing symmetric second order tensor λ_{ij}, $R^0_{ijhk}(x_r)$ and $R^\infty_{ijhk}(x_r)$ being defined, respectively, as

$$R^0_{ijhk}(x_r) := \lim_{t \to 0} R_{ijhk}(x_r, t) \quad, \qquad R^\infty_{ijhk}(x_r) := \lim_{t \to +\infty} R_{ijhk}(x_r, t). \tag{2.2.9}$$

We further assume that the constitutive laws (2.2.3) and (2.2.6) are invertible, with the inverse forms written as:

$$\epsilon_{ij}(x_r, t) = \int_{0^-}^t C_{ijhk}(x_r, t - \tau)\, \mathrm{d}\sigma_{hk}(x_r, \tau) \tag{2.2.10}$$

$$\epsilon_{ij}(x_r, t) = C_{ijhk}(x_r, 0)\sigma_{hk}(x_r, t) + \int_0^t \dot{C}_{ijhk}(x_r, t - \tau)\sigma_{hk}(x_r\tau)\, \mathrm{d}\tau \tag{2.2.11}$$

in which the symbol $C_{ijhk}(x_r, t)$ denotes the creep tensor, or kernel, which enjoys the same properties as $R_{ijhk}(x_r, t)$.

For the conditions of invertibility of equations (2.2.3) and (2.2.6), see for instance Fabrizio (1992), and Bozza and Gentili (1995).

The equilibrium equations in terms of displacements (Navier's equations) are:

$$-\frac{\partial}{\partial x_i}\int_{0^-}^t R_{ijhk}(x_r, t - \tau)\frac{1}{2}\,\mathrm{d}\left(u_{h/k} + u_{k/h}\right)(\tau) = b_j \quad \text{in } \Omega \times [0, 2T]$$

$$n_i \int_{0^-}^t R_{ijhk}(x_r, t - \tau)\frac{1}{2}\,\mathrm{d}\left(u_{h/k} + u_{k/h}\right)(\tau) = p_j \quad \text{on } \Gamma_p \times [0, 2T] \tag{2.2.12}$$

with u_i satisfying the kinematic boundary conditions $u_i = \bar{u}_i$ on Γ_u. Equation (2.2.12a) can be written in the following operatorial form:

$$\mathcal{L}\mathbf{u} = \mathbf{b} \tag{2.2.13}$$

with $\mathbf{u}$ the displacement vector with components u_i, $\mathbf{b}$ the vector of the known terms with components b_i and $\mathcal{L}$ the Navier operator.

2.3 Variational formulations in viscoelasticity

In viscoelasticity, the lack of symmetry of the constitutive operators of eqs. (2.2.3) and (2.2.10), with respect to standard bilinear forms (see for example Tonti, 1973, 1984), has severely hindered the development of variational formulations. Some results have been obtained in the

past making reference to *convolutive* bilinear forms (Gurtin, 1963; Tonti, 1973). Given any two functions $f(x_r, t)$ and $g(x_r, t)$, we introduce the following notation for the basic convolution integral, such as the one adopted in eqs. (2.2.3) and (2.2.10):

$$f(x_r, t) \circ g(x_r, t) := \int_{0^-}^{t} f(x_r, t - \tau) \mathrm{d}g(x_r, \tau) = \int_{0^-}^{t} g(x_r, t - \tau) \mathrm{d}f(x_r, \tau) = g(x_r, t) \circ f(x_r, t). \tag{2.3.1}$$

The symbol $\circ$ introduced in the above formula and used by several Authors (see, for instance, Huet (1992), Charpin and Sanahuja (2017)), is a simplification of the symbol $\otimes$ adopted, for instance, by Mandel (1966) and Leitman and Fisher (1973). The symbol $\circ$ is not to be confused with the standard convolution symbol $*$, see, e.g. Gurtin and Sternberg (1962).
The properties of the convolution are listed below:

$$\begin{aligned}
&f \circ g = g \circ f; \\
&f \circ g = 0 \text{ implies either } f = 0 \text{ } or \text{ } g = 0; \\
&f \circ (g \circ h) = (f \circ g) \circ h = f \circ g \circ h; \\
&f \circ (g + h) = f \circ g + f \circ h.
\end{aligned} \tag{2.3.2}$$

In this Subsection we present and discuss the variational formulations adopted in the next Subsection for the numerical determination of the viscoelastic response of solids and structures subjected to external actions. In particular, Gurtin's formulation and the formulations derived from it, i.e. the split Gurtin formulation and the Huet formulation, will be taken into consideration. Tonti's "extended" formulation will be used as a comparison. The formulation based on adding the adjoint equation (see Morse and Feshbach (1953)) is somehow related to Gurtin's formulation.

1) The method of the adjoint equation and Gurtin's formulation

Gurtin's formulation can be derived directly from the method of adding the adjoint equation (see Morse and Feshbach (1953)). In fact, consider the Navier equation (2.2.12a) (here we suppose, for simplicity, homogeneous boundary conditions) and write the adjoint equation with respect to the standard bilinear form (see the definition (2.3.9)) as follows:

$$-\frac{\partial}{\partial x_i} \int_{2T}^{t} R_{ijhk}(x_r, \tau - t) \frac{1}{2} \mathrm{d} \left(v_{h/k} + v_{k/h} \right) (\tau) = a_j \quad \text{in } \Omega \times [0, 2T] \tag{2.3.3}$$

or, in operatorial form

$$\tilde{\mathcal{L}} \mathbf{v} = \mathbf{a} \tag{2.3.4}$$

with $\mathbf{v}$ the unknown vector of the adjoint problem with components v_i and $\mathbf{a}$ is an arbitrary known term with components a_i. The two equations, the original one and the adjoint one, can be represented in symmetrical matrix form as follows:

$$\mathbf{S}\mathbf{z} = \mathbf{h} \tag{2.3.5}$$

with

$$\mathbf{S} := \begin{bmatrix} 0 & \tilde{\mathcal{L}} \\ \mathcal{L} & 0 \end{bmatrix}, \quad \mathbf{z} := \begin{bmatrix} \mathbf{u} \\ \mathbf{v} \end{bmatrix}, \quad \mathbf{h} := \begin{bmatrix} \mathbf{a} \\ \mathbf{b} \end{bmatrix}. \tag{2.3.6}$$

By the symmetry of the operator $\mathbf{S}$, with respect to the standard bilinear form, a variational formulation becomes possible and the solution $\mathbf{z}$ of the equation (2.3.5) can be obtained by the solution of the following stationarity problem:

$$F^{MF}(\mathbf{z}) = \operatorname*{stat}_{\mathbf{z}'} F^{MF}(\mathbf{z}') \tag{2.3.7}$$

where $\mathbf{z}'$ is any vector belonging to the domain of $\mathbf{S}$ and

$$F^{MF}(\mathbf{z}') = F^{MF}(\mathbf{u}', \mathbf{v}') = \frac{1}{2}\langle \mathbf{S}\mathbf{z}', \mathbf{z}'\rangle - \langle \mathbf{h}, \mathbf{z}'\rangle = \langle \mathcal{L}\mathbf{u}', \mathbf{v}'\rangle - \langle \mathbf{b}, \mathbf{v}'\rangle - \langle \mathbf{a}, \mathbf{u}'\rangle \qquad (2.3.8)$$

where $\langle \mathbf{b}, \mathbf{v}'\rangle$ is the standard bilinear form with time integral in the sense of Stieltjes

$$\langle \mathbf{b}, \mathbf{v}'\rangle := \int_\Omega \int_{0-}^{2T} b_i(x,t)\, \mathrm{d}v_i'(x,t)\, \mathrm{d}\Omega. \qquad (2.3.9)$$

If we take

$$\mathbf{a}(t) = \mathbf{b}(2T - t) \qquad (2.3.10)$$

and by making the change of variables $2T - \tau = \bar{\tau}$ e $2T - t = \bar{t}$, the adjoint equation (2.3.3) becomes

$$-\frac{\partial}{\partial x_i}\int_0^{\bar{t}} R_{ijhk}(x_r, \bar{t} - \bar{\tau})\frac{1}{2}\,\mathrm{d}\left(v_{h/k} + v_{k/h}\right)(2T - \bar{\tau}) = b_j(\bar{t}) \quad \text{in } \Omega \times [0, 2T] \qquad (2.3.11)$$

which, compared with the starting equation (2.2.12a) allows us to easily deduce that

$$\mathbf{v}(t) = \mathbf{u}(2T - t) \qquad (2.3.12)$$

and, therefore, F^{MF} is a function only of $\mathbf{u}'$:

$$F^{MF}(\mathbf{u}') = \langle \mathcal{L}\mathbf{u}', \mathbf{u}'(2T - t)\rangle - \langle \mathbf{b}, \mathbf{u}'(2T - t)\rangle - \langle \mathbf{b}(2T - t), \mathbf{u}'\rangle = \langle \mathcal{L}\mathbf{u}', \mathbf{u}'\rangle_c - 2\langle \mathbf{b}, \mathbf{u}'\rangle_c. \quad (2.3.13)$$

where

$$\langle \mathbf{b}, \mathbf{u}'\rangle_c := \int_\Omega \int_{0-}^{2T} b_i(x, 2T - t)\, \mathrm{d}u_i'(x,t)\, \mathrm{d}\Omega \qquad (2.3.14)$$

is a bilinear form convolutive (in the sense of Stieltjes) with respect to time but standard with respect to space.

In the case of homogeneous boundary conditions, the functional of the Total Potential Energy type obtained by Gurtin (1963) coincides with (2.3.13), the one obtained by the method of the adjoint equation. Gurtin derived his functional starting from the bilinear form (2.3.14). In the case of inhomogeneous boundary conditions, Gurtin's functional takes the more general form:

$$\begin{aligned} F^G(u_i') = &\frac{1}{2}\int_\Omega \int_{0-}^{2T}\int_{0-}^{2T-t} R_{ijhk}(x, 2T - t - \tau)\, \mathrm{d}\epsilon_{ij}'(x,t)\ \mathrm{d}\epsilon_{hk}'(x,\tau)\, d\Omega \\ &- \int_\Omega \int_{0-}^{2T} b_j(x, 2T - t)\, \mathrm{d}u_j'(x,t)\, \mathrm{d}\Omega - \int_{\Gamma_p}\int_{0-}^{2T} p_j(x, 2T - t)\mathrm{d}u_j'(x,t)\, \mathrm{d}\Gamma_p \end{aligned} \qquad (2.3.15)$$

under the kinematically admissiblility constraints $\epsilon_{ij}' = \frac{1}{2}(u_{i/j}' + u_{j/i}')$ (definition equation) and $u_i' = \bar{u}_i$ on Γ_u

2) Split Gurtin's formulation

In Carini and Mattei (2015) five new variational formulations for the viscoelastic problem are derived, one of which is of the minimum type. Here, these new formulations are conveniently interpreted as obtained from the decomposition of the time interval $[0, 2T]$ into two sub-intervals ($[0, T]$ and $[T, 2T]$) of equal length (see, also, Huet (1999, 2001a, 2001b)). The unknowns are

thus formally doubled: the variables defined in the first sub-interval and those defined in the second one. Accordingly, the strain and stress fields can be written, respectively, as:

$$\epsilon_{ij}(t) = \begin{cases} \epsilon_{1_{ij}}(t) & \text{for } t \in [0, T] \\ \epsilon_{2_{ij}}(t) & \text{for } t \in [T, 2T] \end{cases} \tag{2.3.16}$$

$$\sigma_{ij}(t) = \begin{cases} \sigma_{1_{ij}}(t) & \text{for } t \in [0, T] \\ \sigma_{2_{ij}}(t) & \text{for } t \in [T, 2T] \end{cases} \tag{2.3.17}$$

(from here on, unless strictly necessary, we will omit indicating the dependence on the space coordinate x_r) where subscript 1 refers to the quantities defined over the time interval $[0, T]$, and subscript 2 indicates quantities defined over $[T, 2T]$. As a consequence, the constitutive law operator is split into sub-operators, that can be arranged into a two-by-two matrix symmetric with respect to Gurtin's convolutive bilinear form (see Carini and Mattei, 2015).

The direct constitutive law (2.2.3), by virtue of (2.3.16) and (2.3.17) and thanks to Boltzmann's superposition principle, can be split as follows:

$$\sigma_{1_{ij}}(t) = \int_{0^-}^t R_{ijhk}(t - \tau)\,\mathrm{d}\epsilon_{1_{hk}}(\tau) \quad \text{for } t \in [0, T] \tag{2.3.18}$$

$$\sigma_{2_{ij}}(t) = \int_{0^-}^T R_{ijhk}(t - \tau)\,\mathrm{d}\epsilon_{1_{hk}}(\tau) + \int_T^t R_{ijhk}(t - \tau)\,\mathrm{d}\epsilon_{2_{hk}}(\tau) \quad \text{for } t \in [T, 2T]. \tag{2.3.19}$$

Eqs. (2.3.18) and (2.3.19) can be rewritten in the following compact, and symmetric, matricial form:

$$\boldsymbol{\sigma} = \mathbf{L}\,\boldsymbol{\epsilon} \tag{2.3.20}$$

with

$$\mathbf{L} := \begin{bmatrix} A & B \\ C & 0 \end{bmatrix} := \begin{bmatrix} \int_{0^-}^T R_{ijhk}(t - \tau)\,\mathrm{d}(.) & \int_T^t R_{ijhk}(t - \tau)\,\mathrm{d}(.) & \text{for } t \in [T, 2T] \\ \int_{0^-}^t R_{ijhk}(t - \tau)\,\mathrm{d}(.) & 0 & \text{for } t \in [0, T] \end{bmatrix} \tag{2.3.21}$$

$$\boldsymbol{\epsilon} := \begin{bmatrix} \epsilon_{1_{ij}}(t) \\ \epsilon_{2_{ij}}(t) \end{bmatrix}; \qquad \boldsymbol{\sigma} := \begin{bmatrix} \sigma_{2_{ij}}(t) \\ \sigma_{1_{ij}}(t) \end{bmatrix} \tag{2.3.22}$$

The convolutive bilinear form was introduced by Gurtin (1963) (see also Tonti, 1973) and, for our purposes, fixed a material point x_r of the viscoelastic solid, and a time $2T > 0$, from here on is defined (in the Stieltjes sense) as follows:

$$\left(\sigma'_{ij}, \epsilon''_{ij}\right)_c := \sigma'_{ij}(2T) \circ \epsilon''_{ij}(2T) := \int_{0^-}^{2T} \sigma'_{ij}(2T - t)\,\mathrm{d}\epsilon''_{ij}(t) \tag{2.3.23}$$

where quantities with one or two apexes denote generic symmetric stress and strain tensors, and $2T$ denotes the end time of the considered loading history.

Operator A is self-adjoint with respect to (2.3.23), i.e.:

$$\left(A\epsilon'_{1ij}, \epsilon''_{1ij}\right)_c = \int_{0^-}^T \int_{0^-}^T R_{ijhk}(2T - t - \tau)\mathrm{d}\epsilon'_{1ij}(\tau)\,\mathrm{d}\epsilon''_{1ij}(t) = \left(A\epsilon''_{1ij}, \epsilon'_{1ij}\right)_c \tag{2.3.24}$$

while B is the adjoint operator of C, that is:

$$
\begin{aligned}
\left(B\epsilon'_{2ij}, \epsilon''_{1ij}\right)_c &= \int_{0^-}^{T} \int_{T}^{2T-t} R_{ijhk}(2T - t - \tau) \mathrm{d}\epsilon'_{2ij}(\tau) \, \mathrm{d}\epsilon''_{1ij}(t) \\
&= \int_{T}^{2T} \int_{0^-}^{2T-t} R_{ijhk}(2T - t - \tau) \mathrm{d}\epsilon'_{1ij}(\tau) \, \mathrm{d}\epsilon''_{2ij}(t) = \left(C\epsilon''_{1ij}, \epsilon'_{2ij}\right)_c = \left(\tilde{B}\epsilon''_{1ij}, \epsilon'_{2ij}\right)_c
\end{aligned}
\tag{2.3.25}
$$

in which the superscript ˜ denotes the adjoint operator with respect to the adopted convolutive bilinear form. The operatorial formulation (2.3.20) is therefore symmetric, and it is equivalent to the constitutive law (2.3.18)-(2.3.19). Operator A is also, in general, positive semi-definite. In fact, the following quadratic form

$$
\phi(T) = \left(A\,\epsilon'_{1ij}, \epsilon'_{1ij}\right)_c = \int_{0^-}^{T} \int_{0^-}^{T} R_{ijhk}(2T - t - \tau) \, \mathrm{d}\epsilon'_{1hk}(\tau) \, \mathrm{d}\epsilon'_{1ij}(t)
\tag{2.3.26}
$$

has the physical meaning of the free energy per unit volume of the material (see Mandel 1966), a non-negative quantity, which explains the positive semi-definition of operator A of eq. (2.3.21). Note that this operator has not the form of eq. (2.2.3), owing to its upper integration limit. Therefore, even though we have assumed the constitutive operator (2.2.3) to be invertible, nothing can be said, in general, about the invertibility of operator A.

A completely analogous path allows one to introduce a symmetric split formulation for the inverse constitutive law, expressed in terms of the creep kernel, which we skip here for the sake of brevity (see Carini and Mattei, 2015).

From this new split approach, exploiting symmetry only, Carini and Mattei (2015) were able to derive several saddle-point formulations, of which the first one (of the Total Potential Energy type) is especially interesting for the purposes of the present work and reads as follows:

$$
F^{SG}(u_{1i}, u_{2i}) = \min_{u'_{1i}} \operatorname{stat}_{u'_{2i}} F^{SG}(u'_{1i}, u'_{2i})
\tag{2.3.27}
$$

where

$$
\begin{aligned}
F^{SG}[u'_{1i}, u'_{2i}] = \frac{1}{2} \int_{\Omega} &\left(A\epsilon'_{1ij}(2T) \circ \epsilon'_{1ij}(2T) + 2\tilde{B}\epsilon'_{1ij}(2T) \circ \epsilon'_{2ij}(2T) \right) \mathrm{d}\Omega \\
&- \int_{\Omega} b_{2i}(2T) \circ u'_{1i}(2T) \, \mathrm{d}\Omega - \int_{\Omega} b_{1i}(2T) \circ u'_{2i}(2T) \, \mathrm{d}\Omega \\
&- \int_{\Gamma_p} p_{2i}(2T) \circ u'_{1i}(2T) \, \mathrm{d}\Gamma - \int_{\Gamma_p} p_{1i}(2T) \circ u'_{2i}(2T) \, \mathrm{d}\Gamma.
\end{aligned}
\tag{2.3.28}
$$

Here $u_{1i}(t)$ and $u_{2i}(t)$ are the exact solution of the problem, and $u'_{1i}(t)$, $u'_{2i}(t)$, $\epsilon'_{1ij}(t)$, and $\epsilon'_{2ij}(t)$ are arbitrary but compatible displacement and strain fields.

A mixed minimum formulation was also derived in Carini and Mattei (2015), by transforming the problem operator $\mathbf{L}$ of eq. (2.3.21) into a positive definite one. Despite looking very promising, precisely because it is a true minimum principle, this formulation is quite hard to be adopted as a basis for further calculations, since it involves operator A^{-1}, which, even assuming it to exist, is extremely difficult to be suitably characterized. Note that the inversion of operator A on the main diagonal of $\mathbf{L}$ in eq. (2.3.21) requires, as a necessary condition, that it be positive definite, not just positive semi-definite as it was shown to be in general. This happens, for example, when the relaxation tensor $R_{ijhk}(x_r, t)$ is completely monotonic (see Del

Piero and Deseri, 1996).

The use of a convolutive bilinear form and the decomposition of the time domain into two equal subintervals are the necessary ingredients to reformulate the viscoelastic problem in terms of a minimum variational problem, with evident advantages, both theoretical and computational. In the following numerical applications, if the external actions remain constant from a certain time T_0 onwards and if T is long enough one attains a purely minimum principle, as the solution on the second subinterval $[T, 2T]$ is substantially constant.

3) Huet's formulation

The extremum theorems derived by Huet (1992) are valid only under severe restrictions and were proposed for linear quasi-static viscoelasticity without aging, with material, isotropic or not, for which a free energy density per unit volume $\phi(T)$ and a dissipation power density $D(T)$ can be expressed from the relaxation function or the creep function. As demonstrated by Mandel (1966) and Brun (1965, 1969), by their extensions of the results obtained by Staverman and Schwarzl (1952 a, b), this occurs at least for the behaviours which can be dealt with through an internal variable approach. An essential ingredient for Huet's approach are Brun's (1965, 1969) formal identities giving viscoelastic analogues to the Clapeyron equation of elasticity. Huet (1992) introduced a pseudo-convolutive formalism based on results obtained by Brun (1965, 1969). In particular Brun gave a generalization of the Clapeyron equation for the non-aging viscoelastic case, which expresses $D(T)$ and ϕ (Helmholtz free energy) in terms of ϵ_{ij} and σ_{ij} only:

$$D(T) = -\left(\int_{0^-}^{T} - \int_{T}^{2T}\right) \dot{\sigma}_{ij}(2T - t)\,\mathrm{d}\epsilon_{ij}(t); \tag{2.3.29}$$

$$\phi(T) = \frac{1}{2}\left(\int_{0^-}^{T} - \int_{T}^{2T}\right) \sigma_{ij}(2T - t)\,\mathrm{d}\epsilon_{ij}(t). \tag{2.3.30}$$

This is a bilinear form in σ_{ij} and ϵ_{ij}, which restitutes the Staverman and Schwarzl formulas when replacing σ_{ij} by its value given by the constitutive equation:

$$D(T) = -\left(\int_{0^-}^{T} - \int_{T}^{2T}\right) \dot{\sigma}_{ij}(2T - t)\,\mathrm{d}\epsilon_{ij}(t) =$$

$$= -\left(\int_{0^-}^{T} - \int_{T}^{2T}\right) \int_{0^-}^{2T-t} \dot{R}_{ijhk}(2T - t - \tau)\,\mathrm{d}\epsilon_{ij}(\tau)\,\mathrm{d}\epsilon_{hk}(t) =$$

$$= -\int_{0^-}^{T} \int_{0^-}^{T} \dot{R}_{ijhk}(2T - t - \tau)\,\mathrm{d}\epsilon_{ij}(\tau)\,\mathrm{d}\epsilon_{hk}(t).$$

$$\phi(T) = \frac{1}{2}\left(\int_{0^-}^{T} - \int_{T}^{2T}\right) \sigma_{ij}(2T - t)\,\mathrm{d}\epsilon_{ij}(t) =$$

$$= \frac{1}{2}\left(\int_{0^-}^{T} - \int_{T}^{2T}\right) \int_{0^-}^{2T-t} R_{ijhk}(2T - t - \tau)\,\mathrm{d}\epsilon_{ij}(\tau)\,\mathrm{d}\epsilon_{hk}(t) =$$

$$= \frac{1}{2}\int_{0^-}^{T} \int_{0^-}^{T} R_{ijhk}(2T - t - \tau)\,\mathrm{d}\epsilon_{ij}(\tau)\,\mathrm{d}\epsilon_{hk}(t).$$

Huet introduced from the form exhibited by the free energy density a pseudo-convolution $a\Box b$ of two functions $a(t)$ and $b(t)$ from the forms exhibited by the free energy:

$$a\Box b = \left(\int_{0^-}^{T} - \int_{T}^{2T}\right) a(2T - t)\,\mathrm{d}b(t). \tag{2.3.31}$$

It is important to note that the pseudo-convolution $a\square b$ is not commutative in general:

$$a\square b \neq b\square a. \tag{2.3.32}$$

This means that, in contrast with the bilinear form associated to the Staverman and Schwarzl quadratic one, the pseudo-convolution is not symmetric even for kernels R_{ijhk} having the universal symmetries of linear elasticity. This is the basic reason for which the minimum theorems derived by Huet (1992) are subjected to restrictions.

To overcome the problem, Huet introduced the so-called "t-symmetrizing" virtual field. A t-symmetrizing virtual field $\tilde{\epsilon}_{ij}$ verifies:

$$\int_\Omega R_{ijhk} \circ \tilde{\epsilon}_{ij}\square\epsilon_{hk}\,\mathrm{d}V = \int_\Omega R_{ijhk} \circ \epsilon_{ij}\square\tilde{\epsilon}_{hk}\,\mathrm{d}V. \tag{2.3.33}$$

$\tilde{\epsilon}_{ij}$ has to be kinematically admissible, but it is not required for it to satisfy the constitutive equations. The Total Potential Energy type formulation introduced by Huet, a minimum theorem for the displacements, can be expressed as follows:
among all the kinematically admissible (that is $\tilde{\epsilon}_{ij} = \frac{1}{2}(\tilde{u}_{i/j} + \tilde{u}_{j/i})$ and $\tilde{u}_i = \bar{u}_i$ on Γ_u) and "t-symmetrizing" virtual displacement and strain field histories, the actual solution field histories is the solution of the following minimum problem:

$$F^H(\hat{u}) = \min_{\tilde{u}_i} F^H(\tilde{u}_i) \tag{2.3.34}$$

where

$$F^H(\tilde{u}_i) = \frac{1}{2}\int_\Omega R_{ijhk} \circ \tilde{\epsilon}_{ij}\square\tilde{\epsilon}_{hk}\,\mathrm{d}V - \int_\Omega F_i\square\tilde{u}_i\,\mathrm{d}V - \int_{\Gamma_p} p_i\square\tilde{u}_i\,\mathrm{d}\Gamma =$$

$$= \frac{1}{2}\int_\Omega \int_{0^-}^{T} \int_{0^-}^{T} R_{ijhk}(2T - t - \tau)\,\mathrm{d}\tilde{\epsilon}_{ij}(\tau)\,\mathrm{d}\tilde{\epsilon}_{hk}(t)\,\mathrm{d}V \tag{2.3.35}$$

$$-\int_\Omega \left(\int_{0^-}^{T} - \int_{T}^{2T}\right) F_i(2T - t)\,\mathrm{d}\tilde{u}_i(t)\,\mathrm{d}V - \int_{\Gamma_p} \left(\int_{0^-}^{T} - \int_{T}^{2T}\right) p_i(2T - t)\,\mathrm{d}\tilde{u}_i(t)\,\mathrm{d}\Gamma.$$

In general, the solution $\hat{u}_i$ of the problem (2.3.34) sought without the constraint (2.3.33) on $\tilde{u}_i$ and $\tilde{\epsilon}_{ij}$ differs from the true solution. In the following we will call $\hat{u}_i$ a "fictitious" solution. In the case $u(t)$ remains constant from T onwards, it is possible to show, however, that the "fictitious" solution "contains" in itself the real one if one sets, in it, $t = T$.

In fact, in this case, imposing the stationarity of Huet's functional (2.3.35) one gets the following equilibrium conditions (using the notation previously introduced, i.e. subscript 1 and 2 refer to the quantities defined over $[0, T]$ and $[T, 2T]$, respectively):

$$-\frac{\partial}{\partial x_i}\left[\int_{0^-}^{T} R_{ijhk}(2T - t - \tau)\,\mathrm{d}\epsilon_{1hk}(\tau)\right] = b_{2j}(2T - t) \quad \text{in } \Omega \tag{2.3.36}$$

$$n_i\left[\int_{0^-}^{T} R_{ijhk}(2T - t - \tau)\,\mathrm{d}\epsilon_{1hk}(\tau)\right] = p_{2j}(2T - t) \quad \text{on } \Gamma_p \tag{2.3.37}$$

with $0 \leq t \leq T$. Observe that, as said, in this equilibrium condition one has explicit functions of both t and T.

It can now be seen that the solution $\hat{\epsilon}_{1ij}(t, T)$ to problem (2.3.36)-(2.3.37) coincides, at time $t = T$, with the solution of the starting problem. In fact, setting $t = T$ in eqs. (2.3.36)-(2.3.37), one obtains

$$-\frac{\partial}{\partial x_i}\left[\int_{0^-}^{T} R_{ijhk}(T - \tau)\,\mathrm{d}\epsilon_{1hk}(\tau)\right] = b_{2j}(T) \quad \text{in } \Omega \tag{2.3.38}$$

$$n_i \left[\int_{0^-}^{T} R_{ijhk}(T - \tau)\, \mathrm{d}\epsilon_{1hk}(\tau) \right] = p_{2j}(T) \quad \text{on } \Gamma_p \tag{2.3.39}$$

which coincide with the true equilibrium equations for $\epsilon_{1ij}(t)$ at time $t = T$ if the loading terms fulfill the following continuity condition at time $t = T$:

$$b_{2i}(T) = b_{1i}(T); \quad p_{2i}(T) = p_{1i}(T). \tag{2.3.40}$$

In a step-by-step time marching procedure, for each step, a displacement field constant over time and satisfying the kinematic boundary conditions can be considered a "t-symmetrizing" virtual field.

4) Tonti's extended formulation

Consider the problem (2.2.13). Since $\mathcal{L}$ is not a symmetric operator with respect to the standard bilinear form, it is not possible to reformulate the problem as a classical variational statement. Nevertheless, Tonti (1984) proved that it is possible to transform the equation (2.2.13) into an "extended" linear symmetric one as follows:

$$\tilde{\mathcal{L}}\mathcal{K}\mathcal{L}\mathbf{u} = \tilde{\mathcal{L}}\mathcal{K}\mathbf{b} \tag{2.3.41}$$

where $\tilde{\mathcal{L}}$ is the adjoint of $\mathcal{L}$ and $\mathcal{K}$ is a linear positive definite, invertible operator, symmetric with respect to the standard bilinear form, the so-called "integrating" or "kernel" operator, with $D(\mathcal{K}) \supseteq R(\mathcal{L})$ (where $D(\mathcal{K})$ is the domain of the operator $\mathcal{K}$ and $R(\mathcal{L})$ is the range of operator $\mathcal{L}$) and $R(\mathcal{K}) \subseteq D(\tilde{\mathcal{L}})$. The transformation of equation (2.2.13) into the equivalent symmetric one (2.3.41) leads to what is called an "extended variational formulation". In fact, it is easy to prove that the solution of problem (2.3.41) minimizes the following "extended" functional (Tonti, 1984):

$$F^{ext}(\mathbf{u}') = \frac{1}{2}\langle \mathcal{L}\mathbf{u}' - 2\mathbf{b}, \mathcal{K}\mathcal{L}\mathbf{u}' \rangle \tag{2.3.42}$$

where $\langle .,. \rangle$ is the standard bilinear form. Tonti's statement is invertible: a function $\mathbf{u}'$ which minimizes the functional (2.3.42) is also the solution $\mathbf{u}$ of the problem (2.3.41), if this problem admits a solution. The choice of the kernel operator $\mathcal{K}$ is crucial in determining the conditioning of the problem which arises from imposing the stationarity of the functional (2.3.42). For instance, if the kernel is chosen as simply the identity operator, than the extremal property of the extended functional (2.3.42) reduces to a least square formulation, well known for its bad conditioning. Here, we consider, for the linear viscoelastic problem, the formulation proposed by Carini, Gelfi, Marchina (1995) in which $\mathcal{K} = \mathcal{S}^{-1}$ where $\mathcal{S}$ is the linear elastic part of $\mathcal{L}$. In the next Section the formulation proposed by Carini, Gelfi and Marchina (1995) will be used as a comparison.

5) Particularization of the previous functionals to plane frame structures

In the case of plane frame structures, the classical hypothesis of Bernoulli-Navier and a first-order beam theory are assumed. Let the kinematic of a straight beam be defined by the vector $\mathbf{u} = \begin{bmatrix} u \\ v \end{bmatrix}$ where u and v are the x and y displacements of the centroid of the cross section at x (x is the longitudinal axis of the beam and y the transversal one). Denoting with $N(x,t)$ and $M(x,t)$ the axial force and the bending moment, the constitutive viscoelastic law

may be written as

$$N(x,t) = \int_{t_0^-}^t R(x, t-\tau) A(x) \, d\epsilon(x, \tau) \tag{2.3.43}$$

$$M(x,t) = \int_{t_0^-}^t R(x, t-\tau) J(x) \, d\chi(x, \tau) \tag{2.3.44}$$

where $\epsilon = \partial u/\partial x$ and $\chi = -\partial^2 v/\partial x^2$ are the axial strain and curvature, respectively, while $A(x)$, $J(x)$ and $R(x,t)$ are the cross-section area, its moment of inertia and the relaxation function, respectively. Then, denoting with $p(x,t)$ and $q(x,t)$ the longitudinal and transversal components of the distributed load, the general beam equilibrium equations become:

$$-\frac{\partial}{\partial x} \int_{t_0^-}^t R(x, t-\tau) A(x) \frac{\partial \, du(x,\tau)}{\partial x} = p(x,t) \tag{2.3.45}$$

$$\frac{\partial^2}{\partial x^2} \int_{t_0^-}^t R(x, t-\tau) J(x) \frac{\partial^2 \, dv(x,\tau)}{\partial x^2} = q(x,t). \tag{2.3.46}$$

Using the previous notation, in the case of structures composed by a number m of straight beams (the index e is added to any quantity relevant to the generic beam e, $e = 1, ..., m$), Gurtin's functional, split Gurtin's functional and Huet's functional are shown in Table 2.1.

Gurtin	$F^G(u,v) = \sum_{e=1}^m \left\{ \frac{1}{2} \int_0^{l^e} \int_{0^-}^{2T} \int_{0^-}^{2T-t} [R^e(x, 2T-t-\tau) A^e \, d\epsilon^e(x,t) \, d\epsilon^e(x,\tau) \right.$ $+ R^e(x, 2T-t-\tau) J^e \, d\chi^e(x,t) \, d\chi^e(x,\tau)] \, dx$ $\left. - \int_0^{l^e} \int_{0^-}^{2T} p^e(x, 2T-t) \, du^e(x,t) \, dx - \int_0^{l^e} \int_{0^-}^{2T} q^e(x, 2T-t) \, dv^e(x,t) \, dx \right\}$
Split Gurtin	$F^{SG}(u_1, u_2, v_1, v_2) = \sum_{e=1}^m \left\{ \frac{1}{2} \int_0^{l^e} \int_{0^-}^T \int_{0^-}^T [R^e(x, 2T-t-\tau) A^e \, d\epsilon_1^e(x,t) \, d\epsilon_1^e(x,\tau) \right.$ $+ R^e(x, 2T-t-\tau) J^e \, d\chi_1^e(x,t) \, d\chi_1^e(x,\tau)] \, dx$ $+ \int_0^{l^e} \int_T^{2T} \int_{0^-}^{2T-t} [R^e(x, 2T-t-\tau) A^e \, d\epsilon_1^e(x,\tau) \, d\epsilon_2^e(x,t)$ $+ R^e(x, 2T-t-\tau) J^e \, d\chi_1^e(x,\tau) \, d\chi_2^e(x,t)] \, dx$ $- \int_0^{l^e} \left[\int_{0^-}^T p_2^e(x, 2T-t) \, du_1^e(x,t) \, dx + \int_T^{2T} p_1^e(x, 2T-t) \, du_2^e(x,t) \, dx \right]$ $\left. - \int_0^{l^e} \left[\int_{0^-}^T q_2^e(x, 2T-t) \, dv_1^e(x,t) \, dx + \int_T^{2T} q_1^e(x, 2T-t) \, dv_2^e(x,t) \, dx \right] \right\}$
Huet	$F^H(u,v) = \sum_{e=1}^m \left\{ \frac{1}{2} \int_0^{l^e} \int_{0^-}^T \int_{0^-}^T [R^e(x, 2T-t-\tau) A^e \, d\epsilon^e(x,t) \, d\epsilon^e(x,\tau) \right.$ $+ R^e(x, 2T-t-\tau) J^e \, d\chi^e(x,t) \, d\chi^e(x,\tau)] \, dx$ $\left. - \int_0^{l^e} \left(\int_{0^-}^T - \int_T^{2T} \right) p^e(x, 2T-t) \, du^e(x,t) \, dx - \int_0^{l^e} \left(\int_{0^-}^T - \int_T^{2T} \right) q^e(x, 2T-t) \, dv^e(x,t) \, dx \right\}$

Table 2.1: Functionals for plane frame structures.

2.4   Numerical simulations

In the case of *planar frame structures*, standard finite elements of length l^e with two nodes will be considered, with three degrees of freedom in each node, with linear interpolation functions for the "extensional" degrees of freedom r_1 and r_2 and with cubic interpolation functions for the "bending" degrees of freedom r_3, r_4, r_5, r_6 (see Fig. 2.12c). Each beam can be subdivided into several straight finite elements.

The six shape functions n_i $(i = 1, ..., 6)$ relevant to the degrees of freedom $1, ..., 6$ are:

$$
\begin{aligned}
n_1(x) &= 1 - \frac{x}{l^e}; \\
n_2(x) &= \frac{x}{l^e}; \\
n_3(x) &= 1 - \frac{3x^2}{l^{e2}} + \frac{2x^3}{l^{e3}}; \\
n_4(x) &= l^e \cdot \left(\frac{x}{l^e} - \frac{2x^2}{l^{e2}} - \frac{x^3}{l^{e3}} \right); \\
n_5(x) &= \frac{3x^2}{l^{e2}} - \frac{2x^3}{l^{e3}}; \\
n_6(x) &= l^e \cdot \left(-\frac{x^2}{l^{e2}} + \frac{x^3}{l^{e3}} \right).
\end{aligned}
\tag{2.4.1}
$$

In the following we will suppose, for simplicity, that each element has constant cross-section (i.e. A^e and J^e are independent of x) and homogeneous material.

In the case of a *three-dimensional body* analysed in 2D, let's subdivide the solid into N finite elements. In the following we will suppose, for the sake of simplicity, that each element is constituted by a homogeneous material (i.e., $R^e_{ijhk} = R^e_{ijhk}(t)$) and we will assume zero given displacements on Γ_u. Let $\mathbf{u}^e(\mathbf{x}, t)$ be the displacement vector of an internal point $\mathbf{x}$ of the finite element e $(e = 1, ..., N)$, u^e, v^e, w^e being the displacement components along x, y, z, respectively.

In the following we will denote with $\boldsymbol{\delta}(t)$ (with components $\delta_1, ..., \delta_{n_s}$) the vector of the n_s degrees of freedom of the assembled solid, with respect to the global reference system both in the case of three-dimensional bodies and in the case of plane frame structures.

Time discretization. Each component $\delta_i(t)$ of the spatial degrees of freedom vector of the assembled solid is now written as a function of n_t time degrees of freedom $\boldsymbol{\beta}_i$ (with components $\beta_{i1}, \beta_{i2}, ...\beta_{in_t}$) through time interpolation functions collected into the matrix $\mathbf{M}(t)$, with $t \in 2T$:

$$
\boldsymbol{\delta}(t) = \begin{bmatrix} \delta_1(t) \\ . \\ . \\ . \\ \delta_{n_s}(t) \end{bmatrix} = \begin{bmatrix} \mathbf{m}_1(t) & & \\ & ... & \\ & & \mathbf{m}_{n_s}(t) \end{bmatrix} \cdot \begin{bmatrix} \boldsymbol{\beta}_1 \\ ... \\ \boldsymbol{\beta}_{n_s} \end{bmatrix} = \mathbf{M}(t)\boldsymbol{B}. \tag{2.4.2}
$$

In every example shown hereafter, all the spatial degrees of freedom $\delta_i(t)$ are discretized with respect to time using the same interpolation functions, i.e.

$$
\mathbf{m}_1 = ... = \mathbf{m}_{n_s} = \mathbf{m} = [m_1 ... m_{n_t}]. \tag{2.4.3}
$$

In this way, $n_s \times n_t$ is the total number of degrees of freedom.

In the examples discussed in the next Section two different procedures will be adopted, specified case by case. In a first one the solution is sought in a single step over the entire

time interval $2T$. In this case the numerical response is not obtained by means of a step-by-step method, but is given immediately on the whole temporal range without the need of a time integration procedure. In a second procedure the variational technique is applied on subintervals of the original integration time range $2T$, therefore becoming a step-by-step procedure.

Here we introduce three examples of calculation of the structural effects of creep. For the first two examples we use the hereditary Kelvin-Voigt model (see Fig. 2.12d). For the Kelvin-Voigt model the relaxation function R and the creep function C for the uniaxial case are:

$$R(t - \tau) = E_0 - \frac{E_0^2}{E_0 + E_1}\left(1 - e^{-(E_0 + E_1)(t-\tau)/\eta}\right) = E_\infty + (E_0 - E_\infty)\,e^{-(t-\tau)/T^*} \tag{2.4.4}$$

$$C(t - \tau) = \frac{1}{E_0} + \frac{1}{E_1}\left(1 - e^{-E_1(t-\tau)/\eta}\right) = \frac{1}{E_\infty} + \left(\frac{1}{E_0} + \frac{1}{E_1}\right)e^{-(t-\tau)/\tau^*} \tag{2.4.5}$$

where

$$E_\infty = \frac{E_0 E_1}{E_0 + E_1}; \quad \tau^* = \frac{\eta}{E_1}; \quad T^* = \frac{\eta}{E_0 + E_1}. \tag{2.4.6}$$

The extension to the multiaxial case is straightforward.

Whereas, for the third and last example, only the deviatoric part of the constitutive law is viscoelastic and we use a classical Maxwell model, for which the relaxation function R and the creep function C for the uniaxial case are:

$$R(t - \tau) = E_0 e^{-E_0(t-\tau)/\eta} \tag{2.4.7}$$

$$C(t - \tau) = \frac{1}{E_0} + \frac{t}{\eta} \tag{2.4.8}$$

In all the examples, negative exponential time interpolation functions are used:

$$\mathbf{m} = \left[1, e^{-t/t^*}, e^{-t/10t^*}, e^{-t/100t^*}, ...\right]. \tag{2.4.9}$$

where t^* is a parameter to be defined and has the meaning of a relaxation time. For the examples considered herein, these interpolation functions were empirically found to be better than polynomial or damped polynomial functions.

The asymptotic character of the viscoelastic responses over large time intervals justifies the above choice of the negative exponential interpolation functions which appear more suitable for a good approximation of the structural behaviour even in the presence of a small number of temporal degrees of freedom, especially when solving the problem over the entire time interval. Polynomial time interpolation functions could also be chosen, but only for short enough time intervals.

The sequence of relaxation times t^*, $10t^*$, $100t^*$, ..., adopted for the time interpolation functions in (2.4.9), has provided good numerical results. Both this type of sequence and the numerical values of t^*, in the absence of theoretical indications, have been found by trial and error.

For each example, significant displacements and/or stresses are plotted versus time, for different time intervals and, in the case of a single step solution (first procedure, see above) for 1, 2, 3, 4, and 5 time degrees of freedom. In each diagram both the exact solution and the percentage error are also plotted.

Example a: viscoelastic beam on elastic support.

The structure is a Bernoulli-Navier built in beam of length $2l$, with an elastic support (a spring of stiffness k_m) in the middle; the beam is homogeneous and has a constant cross-section. A uniformly distributed transversal load q is applied at time $t_0 = 0$ and remains constant. The beam is subdivided into two finite elements of the type described previously.

First, we consider *Gurtin's formulation*. After the spatial discretization, Gurtin's functional takes the following form:

$$
\begin{aligned}
F^G = {} & \frac{1}{2} k_m \int_{0^-}^{2T} v'(l, 2T - t) \, \mathrm{d}v'(l, t) \\
& + \frac{1}{2} \left[\frac{24J}{l^3} \right] \int_{0^-}^{2T} \mathrm{d}v'(l, t) \int_{0^-}^{2T-t} R(2T - t - \tau) \, \mathrm{d}v'(l, \tau) \\
& - l \int_{0^-}^{2T} q(2T - t) \, \mathrm{d}v'(l, t)
\end{aligned}
\tag{2.4.10}
$$

where $v(l, t)$, the only non-zero δ degree of freedom, is the vertical displacement of the middle section of the beam.

We start by discussing the results obtained finding the entire solution in a single step. In Fig. 2.1, the ratio between the displacement $v(l, t)$ of the middle section at time t and the initial elastic displacement $v(l, 0)$ is plotted. The exact solution of this problem was determined analytically through the correspondence principle. The time shape functions are of the negative exponential type (2.4.9) with $t^* = 70$, 130 and 180 days, the time $2T$ ranges from 0 to 1500 days and the number of time degrees of freedom from 2 to 5. After 750 days, $v(l)$ remains practically constant over time. The diagrams show that the presented method allows a good interpretation of the viscoelastic behaviour of the structure. With three time degrees of freedom the solution is satisfactory within the entire time range.

The accuracy of the numerical results depends on the choices of t^*. In this example, for $t^* = 130$ days very precise results are obtained with just two temporal degrees of freedom. The optimal determination of t^* remains an open problem.
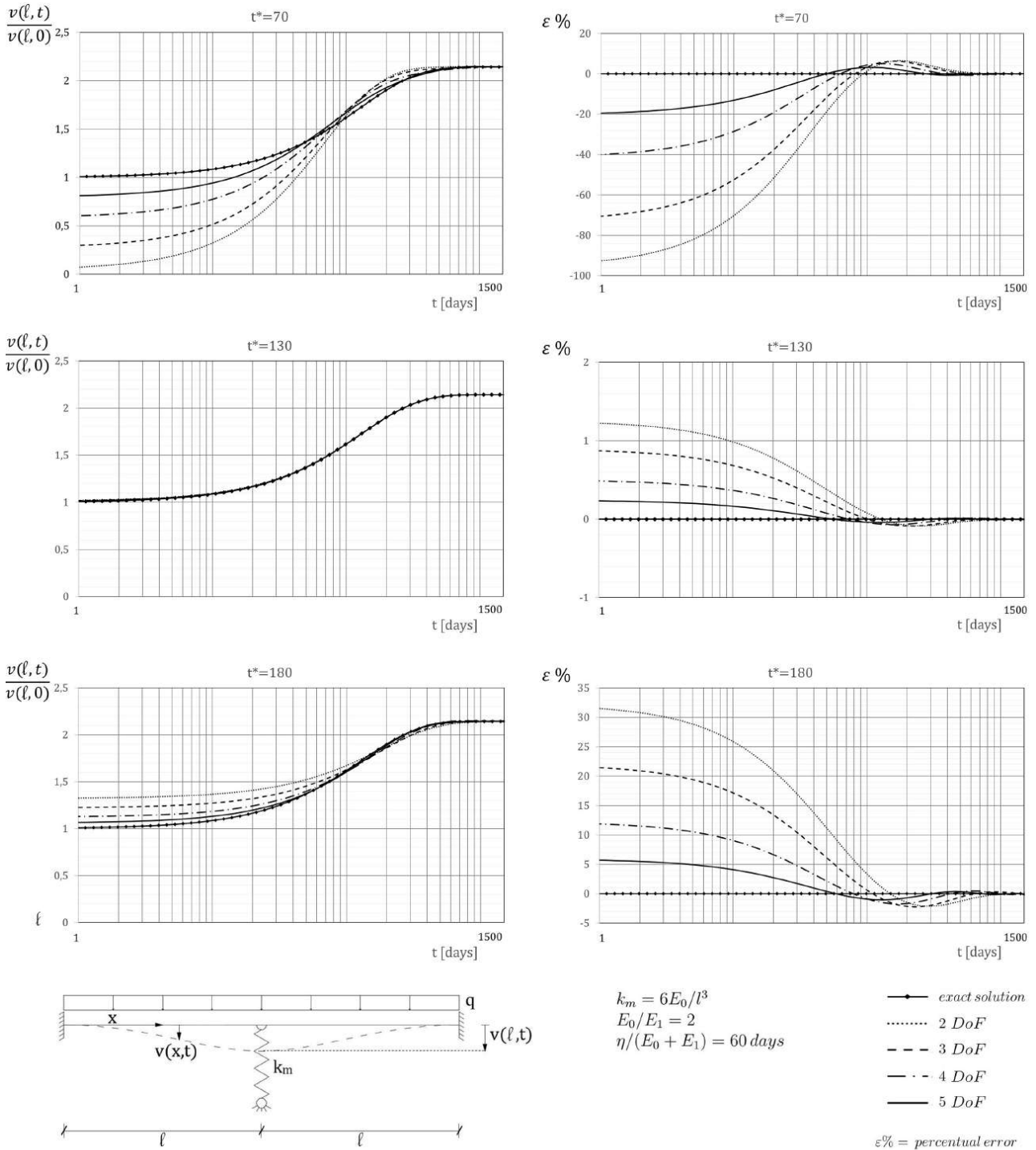
Figure 2.1: Example a: Beam on elastic support. Numerical results using Gurtin's formulation.

Fig. 2.2 shows the numerical results obtained by splitting the loading time interval $2T = 1500$ days into two equal parts and using the *split Gurtin's formulation* (2.3.27). After the spatial discretization, functional (2.3.28) takes the following form:

$$
\begin{aligned}
F^{SG} = {} & \frac{1}{2} \, k_m \int_{0-}^{T} v_2'(l, 2T - t) \, \mathrm{d}v_1'(l, t) \\
& + \frac{1}{2} \, k_m \int_{T}^{2T} v_1'(l, 2T - t) \, \mathrm{d}v_2'(l, t) \\
& + \frac{1}{2} \left[\frac{24J}{l^3} \right] \int_{0-}^{T} \mathrm{d}v_1'(l, t) \int_{0-}^{T} R(2T - t - \tau) \, \mathrm{d}v_1'(l, \tau) \\
& + \frac{1}{2} \left[\frac{24J}{l^3} \right] \int_{0-}^{T} \mathrm{d}v_1'(l, t) \int_{T}^{2T-t} R(2T - t - \tau) \, \mathrm{d}v_2'(l, \tau) \\
& + \frac{1}{2} \left[\frac{24J}{l^3} \right] \int_{T}^{2T} \mathrm{d}v_2'(l, t) \int_{0-}^{2T-t} R(2T - t - \tau) \, \mathrm{d}v_1'(l, \tau) \\
& - l \int_{0-}^{T} q_2(2T - t) \, \mathrm{d}v_1'(l, t) \\
& - l \int_{T}^{2T} q_1(2T - t) \, \mathrm{d}v_2'(l, t)
\end{aligned}
\tag{2.4.11}
$$

Here we have considered from 2 to 5 time degrees of freedom both in the first and in the second sub-interval. Of course, the accuracy increases significantly in the case of splitting, due to a doubling of the degrees of freedom. As it is possible to see in Fig. 2.2, a constant time function is sufficient to approximate well the solution in the second sub-interval, given the asymptotical nature of the viscoelastic problem. For this reason, an attempt has been made in reducing the degrees of freedom in the second subinterval, in order to reduce the computational cost and to obtain a purely minimum principle. Fig. 2.3 shows the numerical results for the same example, obtained using n_t degrees of freedom on the first sub-interval and $(n_t - 1)$ time degrees of freedom on the second one. It is noted that the solution in the first sub-interval significantly worsens compared to the case of an equal number of degrees of freedom in both sub-intervals.

Fig. 2.4 shows the case of $(n_t - 2)$ degrees of freedom in the second sub-interval: the solution in the first sub-interval further deteriorates respect to the case of $(n_t - 1)$ number of degrees of freedom in the second sub-interval. To understand the reason for this strange behaviour, considering that just one degree of freedom is enough to obtain a good approximation in the second sub-interval, the exact solution in the second sub-interval was replaced in the functional, thus reducing the variational problem to a minimum problem only in the first sub-interval. The obtained numerical result implies $v_1(l)$ becoming unbounded.

This strong instability can be explained by analysing the equation obtained by imposing the stationarity of the functional, that is:

$$
\int_{0-}^{T} R(2T - t - \tau) \, \mathrm{d}v(l, \tau) = f(t)
\tag{2.4.12}
$$

or, in operatorial form:

$$
Av = f
\tag{2.4.13}
$$

with $f(t)$ the known term obtained by the sum of the original known term and the one resulting from the integral on the second sub-interval.
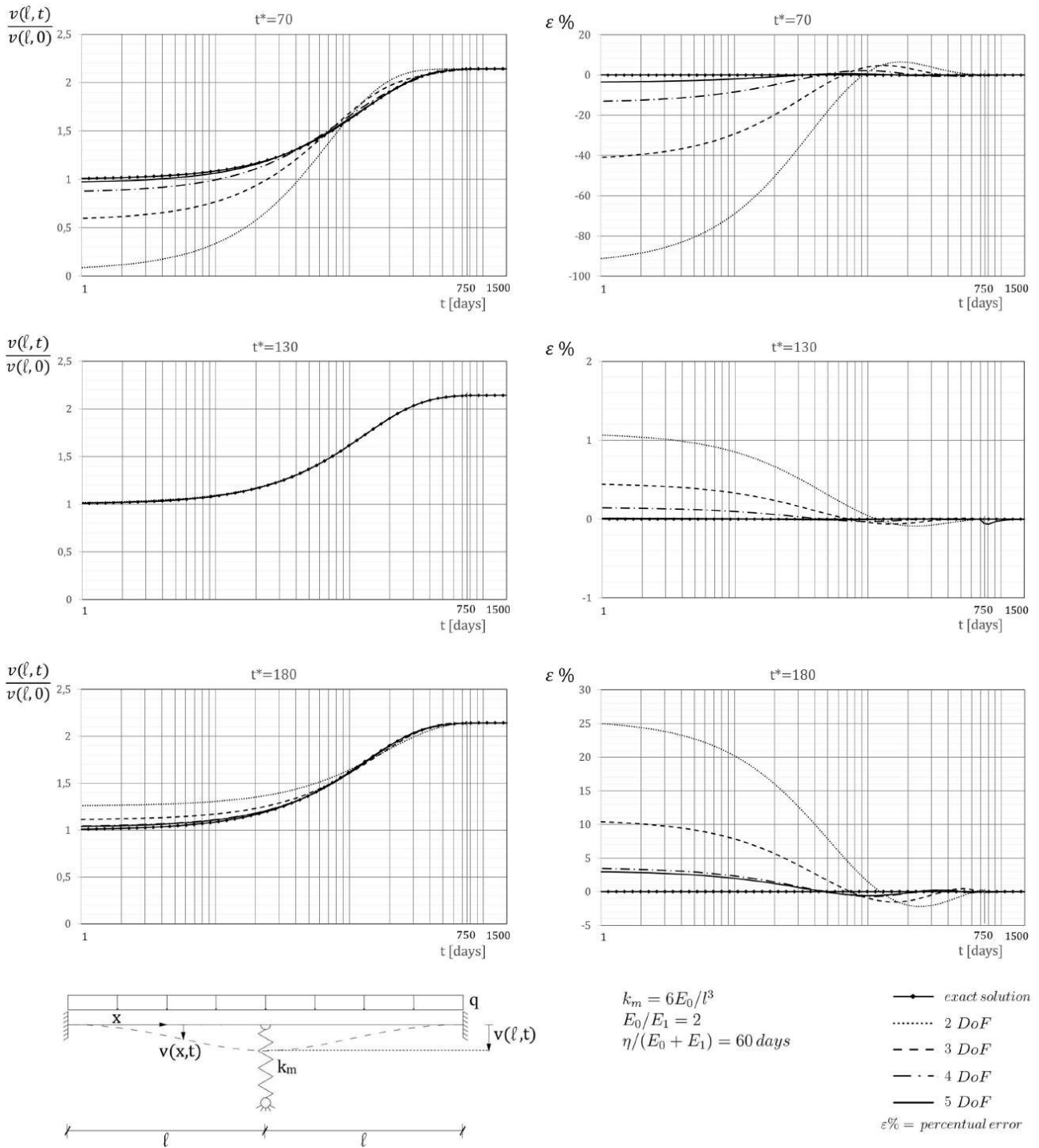
Figure 2.2: Example a: Beam on elastic support. Numerical results using split Gurtin's formulation with same number of time degrees of freedom in the first and in the second time sub-interval.
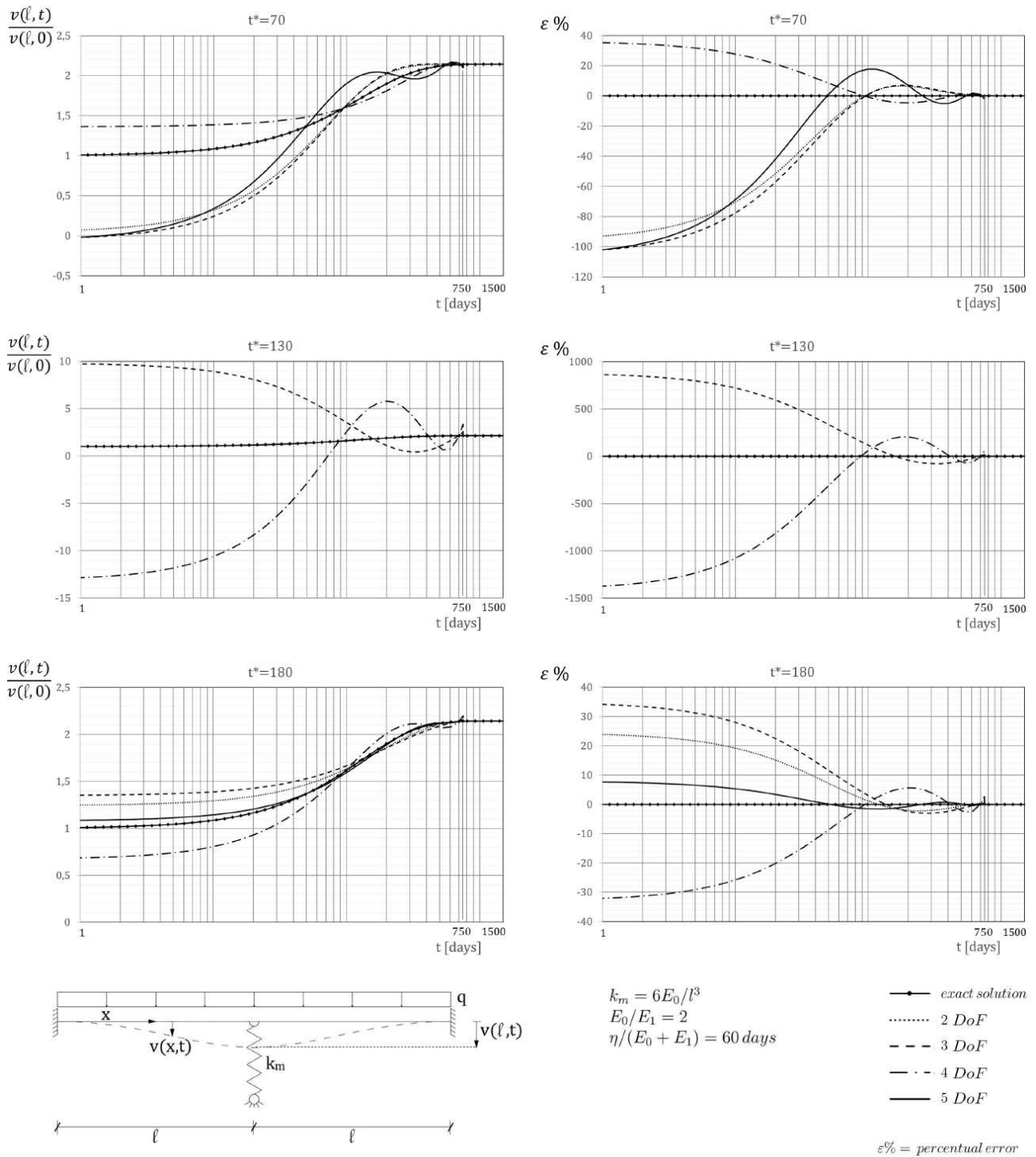
Figure 2.3: Example a: Beam on elastic support. Numerical results using split Gurtin's formulation with n degrees of freedom in the first sub-interval and $(n-1)$ DoF in the second sub-interval.
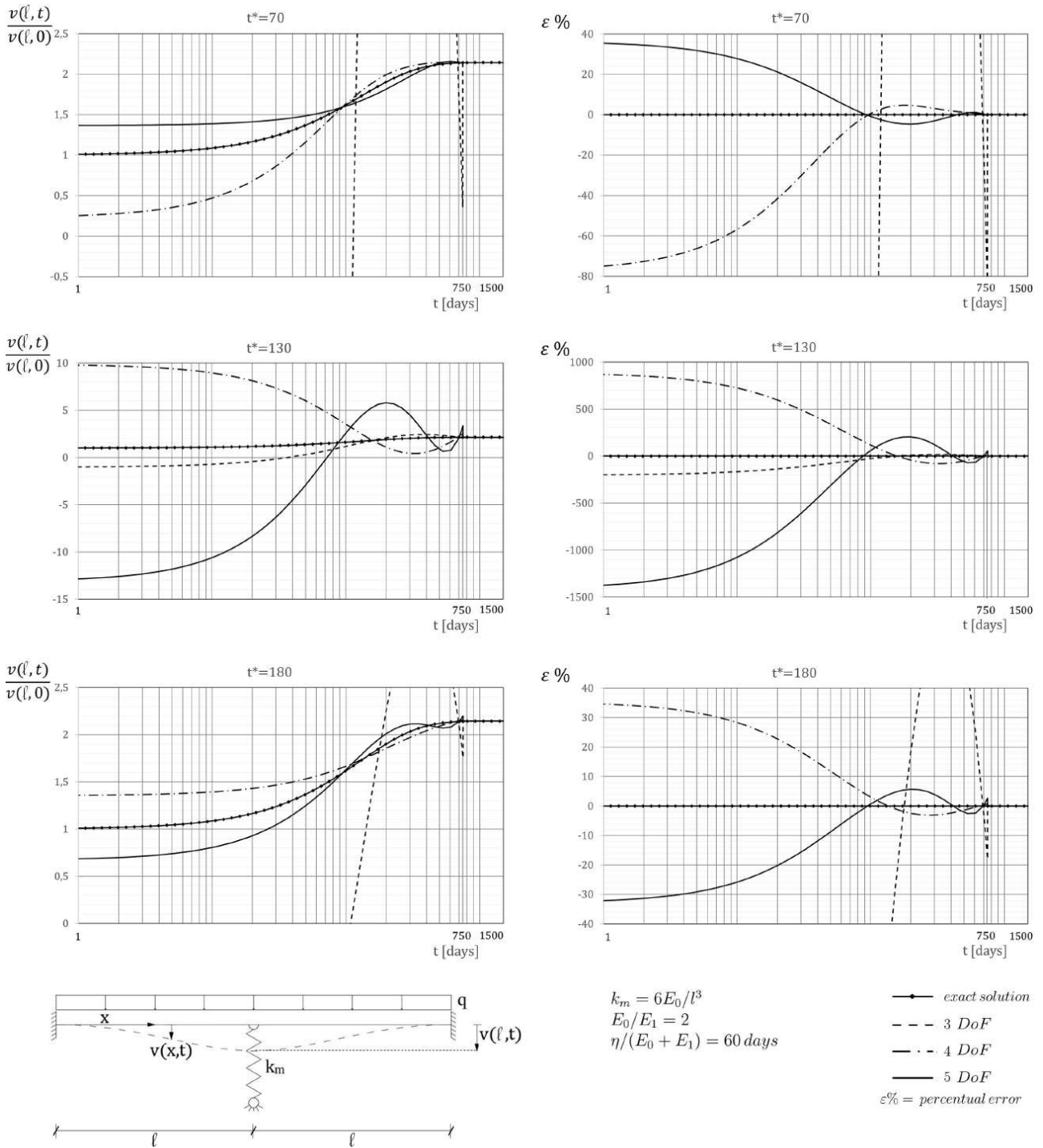
Figure 2.4: Example a: Beam on elastic support. Numerical results using split Gurtin's formulation with n degrees of freedom in the first sub-interval and $(n-2)$ DoF in the second sub-interval.

The equation $Av = f$ is called well-posed or properly posed if A is bijective and the inverse operator A^{-1} is continuous. In fact, Hadamard postulated three requirements for a problem to satisfy in order to be well posed:

1. existence of a solution;

2. uniqueness of a solution;

3. continuous dependence of the solution on the data.

Otherwise the equation is called ill-posed or improperly posed. Our operator A is not surjective, then equation $Av = f$ is not solvable for all f (nonexistence), and A is also not injective, so that the equation may have more than one solution (nonuniqueness).

In general, linear integral equations of the first kind with continuous (as in our case) or weakly singular kernels provide typical examples of ill-posed problems.

One of the fundamental facts in the theory of operatorial equations of the first kind is that the inverse of a completely continuous operator is not bounded. So, even if f_a and f_b are two mutually close elements in a Hilbert space and both equations $Av = f_a$ and $Av = f_b$ are solvable, the respective solutions $v_a = A^{-1}f_a$ and $v_b = A^{-1}f_b$ can differ strongly from each other. Therefore, a small difference in the known term of the starting equation can lead to a large error in the solution (see, for instance, Kress, 1989).

The ill-posed nature of an equation, of course, has consequences on its numerical treatment. The fact that an operator A does not have a bounded inverse means that the condition numbers of its finite dimensional approximations grow with the quality of the approximation. This means that increasing the accuracy of the approximation for the operator A will cause the approximate solution to the equation to become less and less reliable.

To at least partially mitigate these instabilities, a Tikhonov "regularization" was considered (see, for example, Kress, 1989). A regularizing "penalty" term $\frac{1}{2}\alpha \int_{0-}^{T} v^{'2}(l,t)\,dt$, dependent on a parameter α, has therefore been added to the functional (2.4.11). This means replacing the given equation of the first kind with the following equation of the second kind:

$$\alpha v(l,t) + \int_{0-}^{T} R(2T - t - \tau)\,dv(l,\tau) = f(t). \tag{2.4.14}$$

The choice of α is very important but linked in general to great difficulties, and we made it by trial and error. The results of this regularization, shown in Fig. 2.5, is not very satisfactory. Fig. 2.6 shows the regularized result obtained by adding the modified quadratic term $\frac{1}{2}\alpha \int_{0-}^{T} v^{'2}(l, 2T - t)\,dt$ to the functional (2.4.11). In this case a good result is obtained by using two temporal degrees of freedom and $\alpha = 0.007925$.
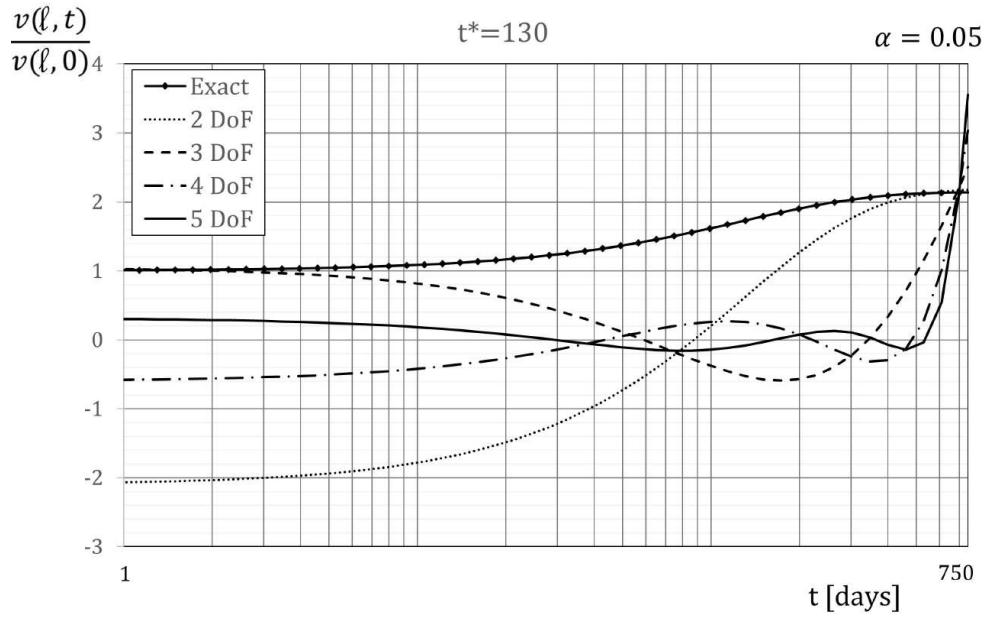
Figure 2.5: Example a: Beam on elastic support. Numerical results using a Tikhonov regularization with the addition of $\frac{1}{2}\alpha \int_{0-}^{T} v'^2(l,t)\,\mathrm{d}t$ to functional (2.4.11) ($t^* = 130$ days, $\alpha = 0.05$).
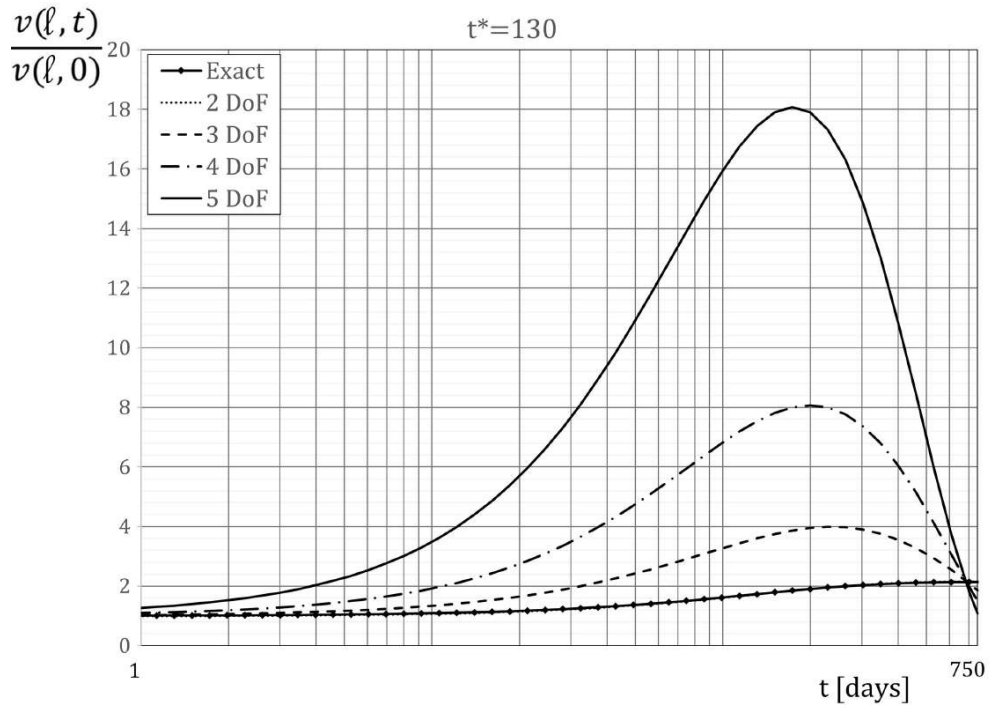
Figure 2.6: Example a: Beam on elastic support. Numerical results using a Tikhonov regularization with the addition of $\frac{1}{2}\alpha \int_{0-}^{T} v'^2(l, 2T - t)\,\mathrm{d}t$ to functional (2.4.11). ($t^* = 130$ days, $\alpha = 0.007925$ for 2 DoF; $\alpha = 0.06594$ for 3 DoF; $\alpha = 0.29431$ for 4 DoF; $\alpha = 1.40348$ for 5 DoF).

Let us now analyse the behaviour of *Huet's formulation*.

Because of the theoretical restrictions summarized in Section 3, Huet's formulation does not work numerically if applied in a single loading step, unless during the step the solution tends to becomes constant. For this reason, in the next examples we have considered step-by-step procedures only, with a reasonably large number of time steps.

Once again because of the same theoretical restrictions, standard step-by-step techniques, in the case of Huet's formulation, become rapidly unstable with an increasing number of time degrees of freedom in a single time step: actually, they seem to work only by adopting a single time degree of freedom in each step. By standard we mean a procedure in which (i) the time integrals are computed only on the current time step and (ii) the initial conditions at each time step are the end conditions at the previous time step.

Nevertheless, considering the convolutive nature of the involved functionals, one is lead to adopt non standard step-by-step procedure in which (i) all the time integrals are computed starting from the global loading initial time $t = 0$, and (ii) the time interpolation functions are defined as the sum of Heaviside step functions, each starting at the beginning of a new time step. In this way, the degrees of freedom can be obtained in a simple recursive form and the solution seems to be more accurate with respect to a standard one with the same numbers of unknowns. This happens because in this way the past history is "remembered". In the sequel, we will apply this idea also to Gurtin's approach.

Since the integrals in Huet's functional are defined between 0 and T, in this case the solution must be found in this interval only. The time interval $[0, T]$ is subdivided into n temporal subintervals defined by the sequence of instants $T_0, T_1, ..., T_i, ..., T_n = T$. The analysis is carried out in sequence in the intervals $T_0 \leq t \leq T_1$, $T_0 \leq t \leq T_2$, etc., always assuming, as initial conditions, the conditions at the initial time $t = 0$.

Following this idea, all the time interpolation functions used in the previous steps are prolonged to the current temporal step by means of the Heaviside function. This means that the approximating function at the step $T_{i-1} - T_i$ is represented using a sum of step time interpolation functions (see Fig. 2.7)

$$v^{'}(l, t) = \sum_{n=1}^{i} a_n H(t - T_{n-1}), \quad T_{i-1} \leq t \leq T_i \tag{2.4.15}$$

with $a_1, ..., a_{i-1}$ already known from the previous steps. The time marching procedure starts from the initial time, adding a new interpolation function to each step. By imposing the stationarity of the Huet functional, rewritten for the example here studied and for time interval $T_0 \leq t \leq T_i$

$$F^H(v^{'}(l, t, T_i)) = \frac{1}{2} k_m v^{'2}(l, T_i) + \frac{1}{2} \left[\frac{24J}{l^3} \right] \int_{0^-}^{T_i} \int_{0^-}^{T_i} R(2T_i - t - \tau) \, \mathrm{d}v^{'}(l, \tau) \, \mathrm{d}v^{'}(l, t)$$
$$- l \int_{0^-}^{T_i} q(2T_i - t) \, \mathrm{d}v^{'}(l, t) \tag{2.4.16}$$

and making $t \to T_i$, we go back to the starting equation (see Section 3.3). Using (2.4.15) as an admissible function, we obtain:

$$a_n = \frac{q\left(2T_n - T_{n-1}\right)l - \sum_{i=1}^{n-1} a_i \left[(24J/l^3) R\left(2T_n - T_{i-1} - T_{n-1}\right) + k_m\right]}{(24J/l^3) R\left(2T_n - 2T_{n-1}\right) + k_m}, \quad n \geq 2. \tag{2.4.17}$$

Fig. 2.8 shows the results from 0 to 750 days for $t \to T_i$, and, as a test, $t \to T_{i-1} + \Delta T_i/2$, $t \to T_{i-1} + \Delta T_i/4$, $t \to T_{i-1} + \Delta T_i/8$, $t \to T_{i-1}$ (with $\Delta T_i = T_i - T_{i-1}$).

Surprisingly, the best results are obtained for $t \to T_{i-1} + \Delta T_i/4$ and not for $t \to T_i$, as instead explained by the theory summarized in Section 3.3. In Figures 2.9, 2.10, and 2.11 the results obtained using both the Huet formulation and the Gurtin formulation (now used with the same non standard step-by-step procedure) are reported for a constant load, for a load that varies linearly over time and for a load that varies sinusoidally over time, respectively. It should be noted that with Gurtin's formulation one has not the problem of finding an optimal t. Gurtin's results can be derived from the following formula:

$$a_n = \frac{l \cdot \int_{T_{n-1}}^{T_n} q(t)\,dt - (24J/l^3) \cdot \sum_{i=1}^{n-1} a_i \cdot \int_{T_{i-1}}^{T_i} \int_0^{T_1} \frac{\partial R(T_n - t - \tau)}{\partial(T_n - t - \tau)}\,d\tau\,dt}{(24J/l^3 + k_m) \cdot (T_n - T_{n-1}) + \gamma \cdot \int_{T_{n-1}}^{T_n} \int_0^{T_n-t} \frac{\partial R(T_n - t - \tau)}{\partial(T_n - t - \tau)}\,d\tau\,dt}$$

(2.4.18)

and they are slightly better than Huet's results for the first two cases while they are slightly worse for the last case.
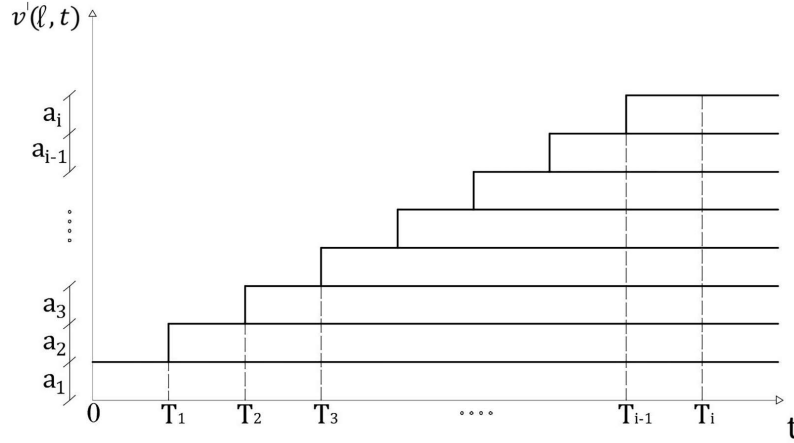
Figure 2.7: Example a: Beam on elastic support, non standard step-by-step procedure. Step time interpolation functions.
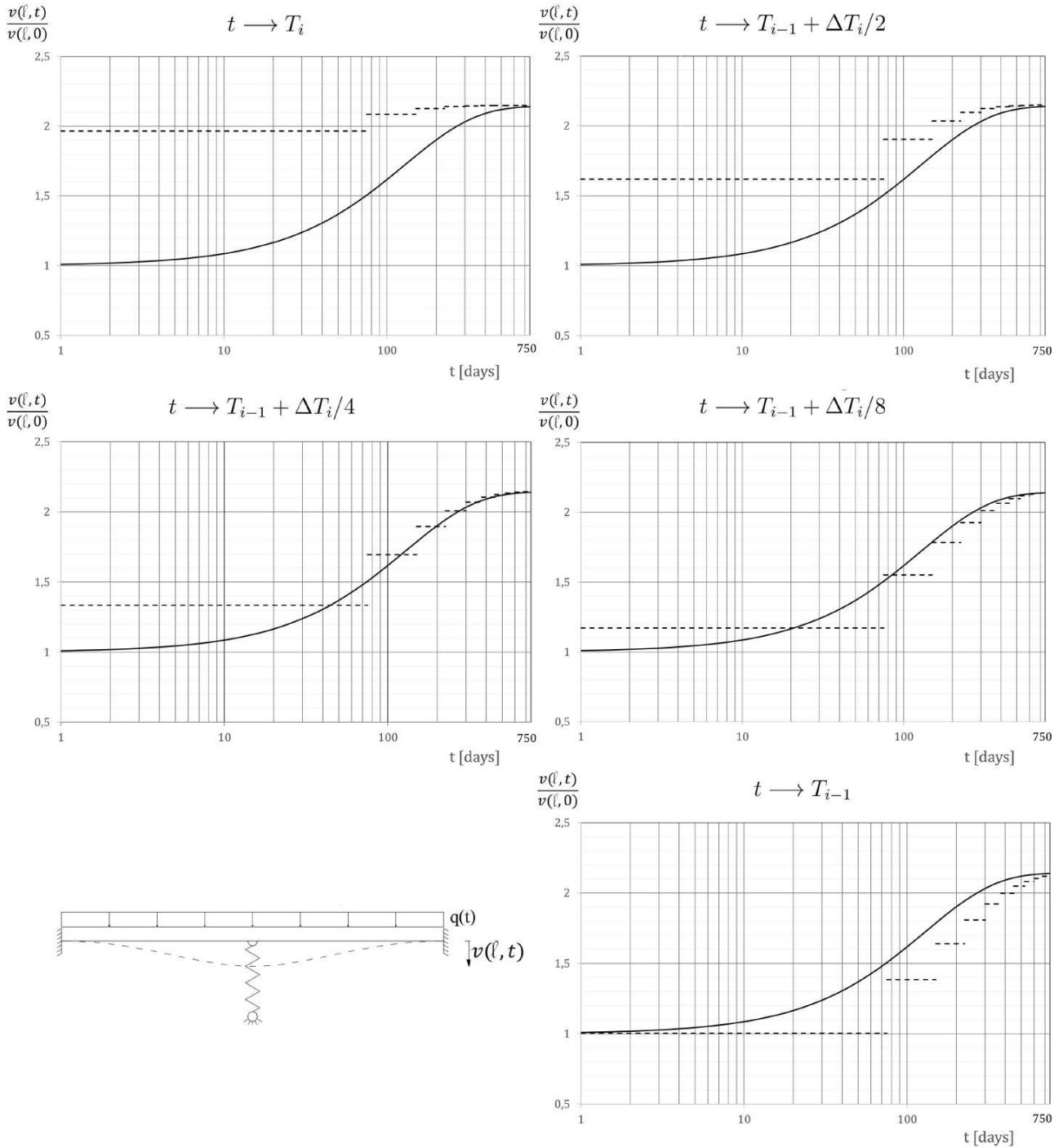
Figure 2.8: Example a: Beam on elastic support. Numerical results using step time interpolation functions in the case of constant load.
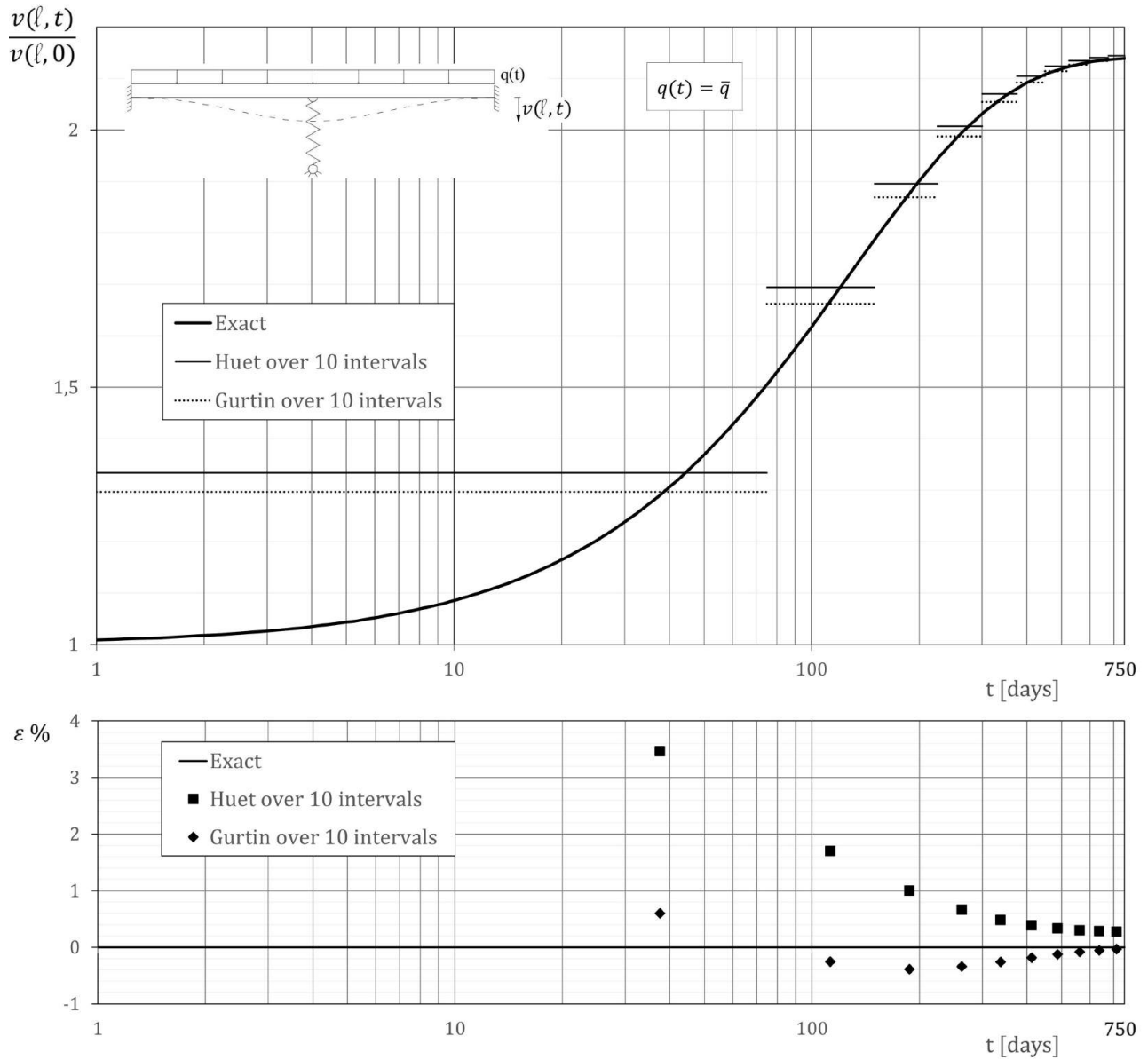
Figure 2.9: Example a: Beam on elastic support. Numerical results using step time interpolation functions in the case of constant load, using Huet's formulation and Gurtin's formulation.
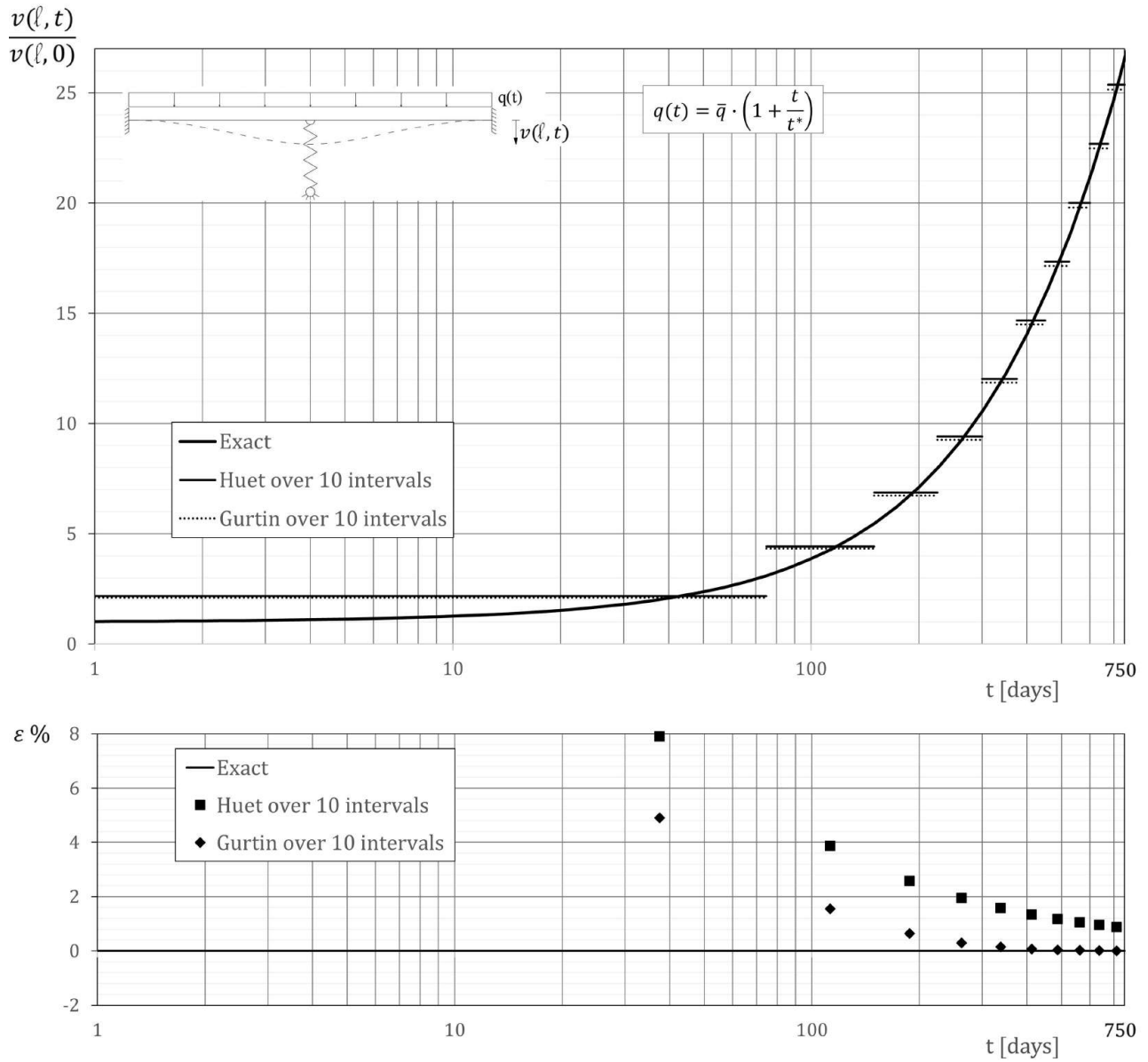
Figure 2.10: Example a: Beam on elastic support. Numerical results using step time interpolation functions in the case of load q linearly varying over time, using Huet's formulation and Gurtin's formulation.
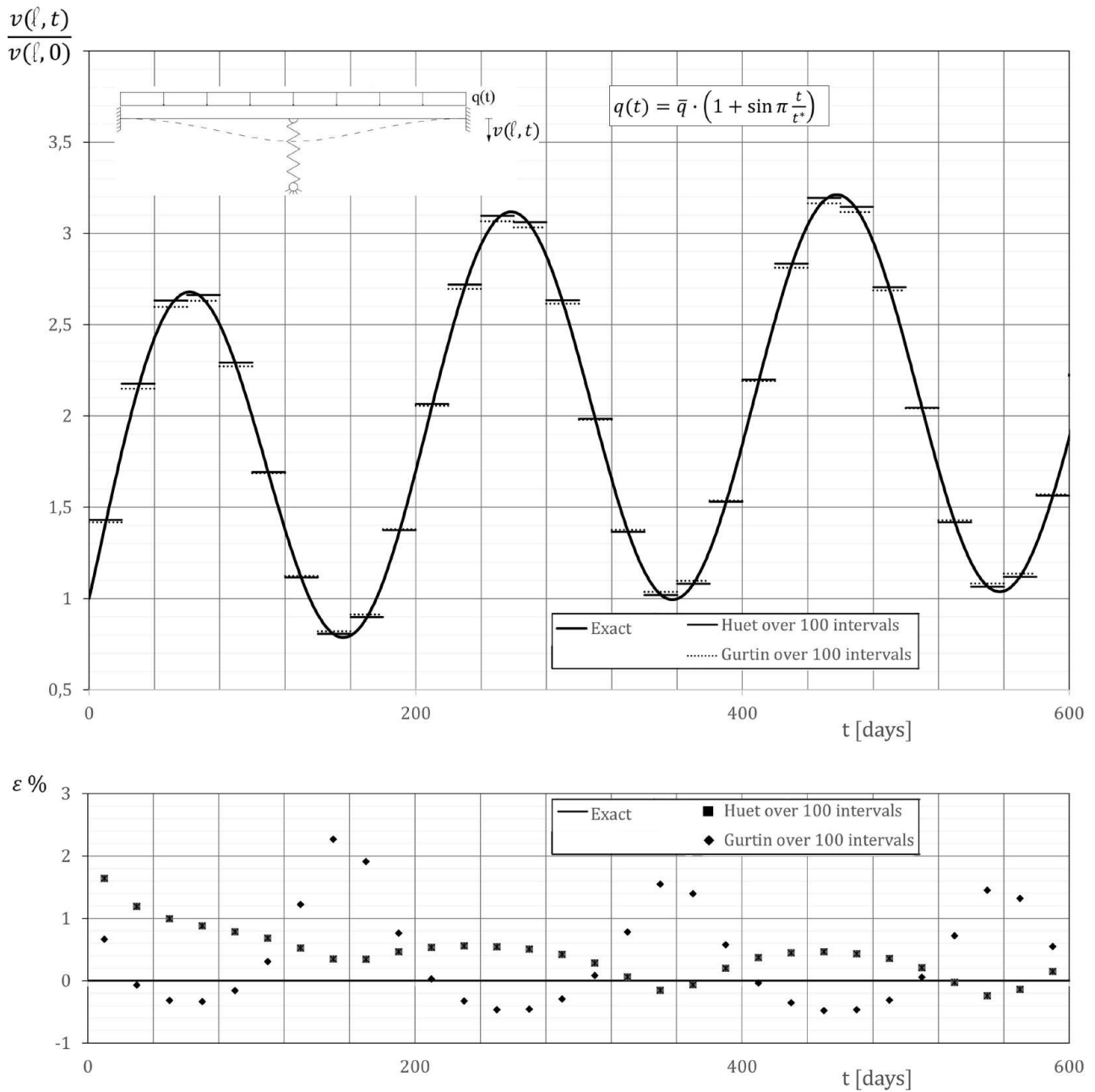
Figure 2.11: Example a: Beam on elastic support. Numerical results using step time interpolation functions in the case of load q sinusoidally varying over time, using Huet's formulation and Gurtin's formulation.

Example b: cable-stayed bridge.

The structure (Fig. 2.12) represents a simple cable stayed bridge. The girder and the piers are of concrete with geometrical and rheological properties constant along the axis; the stays are made of steel. The uniform load q is applied on the girder at time $t_0 = 28$ days and remains constant in time. The structure is discretized with seven beam elements having the characteristics shown in Fig. 2.12. The reference solution is obtained with the program ABAQUS (ABAQUS Manuals, 2018).

Once again, the solution is here found in a single time step. Negative exponential time interpolation functions are used, as in the first solutions of the previous example. The results obtained in Carini, Gelfi, Marchina (1995), using the same interpolation functions, are compared with the present ones and, therefore, as in that work, $t^* = 120$ days is taken. Physical phenomena start at 28 days because the structure is designed in reinforced concrete. Two and three temporal degrees of freedom are considered. The numerical results, using Gurtin's approach, are reported in Fig. 2.13 for three distinct time intervals: 28-100, 28-1000 and 28-10000 days. Fig. 2.13 also shows the reference solution obtained with the ABAQUS program with a considerable degree of precision and, therefore, to be considered "exact" from an engineering point of view. As can be seen, the approximate solution is already good with only two temporal degrees of freedom over the entire time interval analysed, showing errors lower than 5% almost everywhere.

Fig. 2.14 shows the results obtained with the split Gurtin's formulation and the same interpolation functions. The results are not very different from those obtained with the unsplit Gurtin's formulation, in spite of a doubling of the unknowns. Table 2.2 compares the conditioning indexes of the matrices of the coefficients of the resolving systems in the case of use 1) of the least squares method, 2) of the method based on Tonti's extended functionals, 3) of Gurtin's method. The results related to the least square method and to the Tonti method are taken from Carini, Gelfi, Marchina (1995). The results with 1 or 2 temporal degrees of freedom, obtained by the different methods, are comparable to each other. It is noted that the conditioning index of Gurtin's method is of the same order of magnitude as that associated to Tonti's extended functional, orders of magnitude lower than the method of least squares. Furthermore, the Gurtin method is much less expensive because it does not require the inversion of the elastic operator, as necessary in the case of Tonti's extended functional where the inverse of the elastic operator acts as a preconditioning operator.

The conditioning indexes related to the split Gurtin method are similar to those of the unsplit Gurtin method, except for the case related to the interval 28-10000 days and for 2 and 3 degrees of freedom where the conditioning index jumps to very high levels. Using time interpolation functions that are still negative exponential but with different relaxation times ($10\,t^*$ and $100\,t^*$ for the second and third degrees of freedom, respectively) yielded conditioning indices comparable to those for the Gurtin approach (see the last column of Table 2.2).
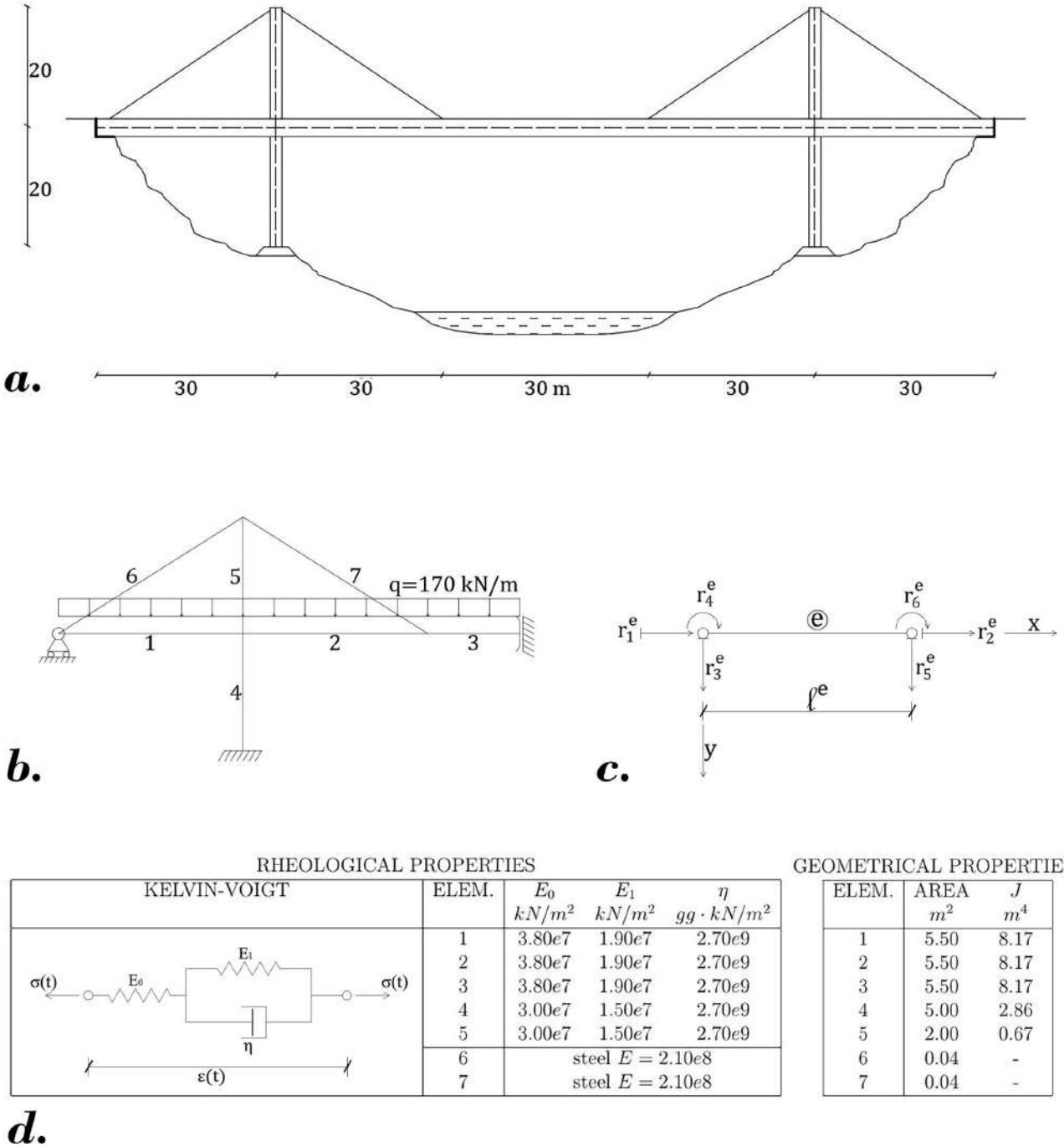
Figure 2.12: Example b: Cable-stayed bridge (a) - Finite Element mesh (b), beam finite element (c), geometrical properties and rheological properties (d).
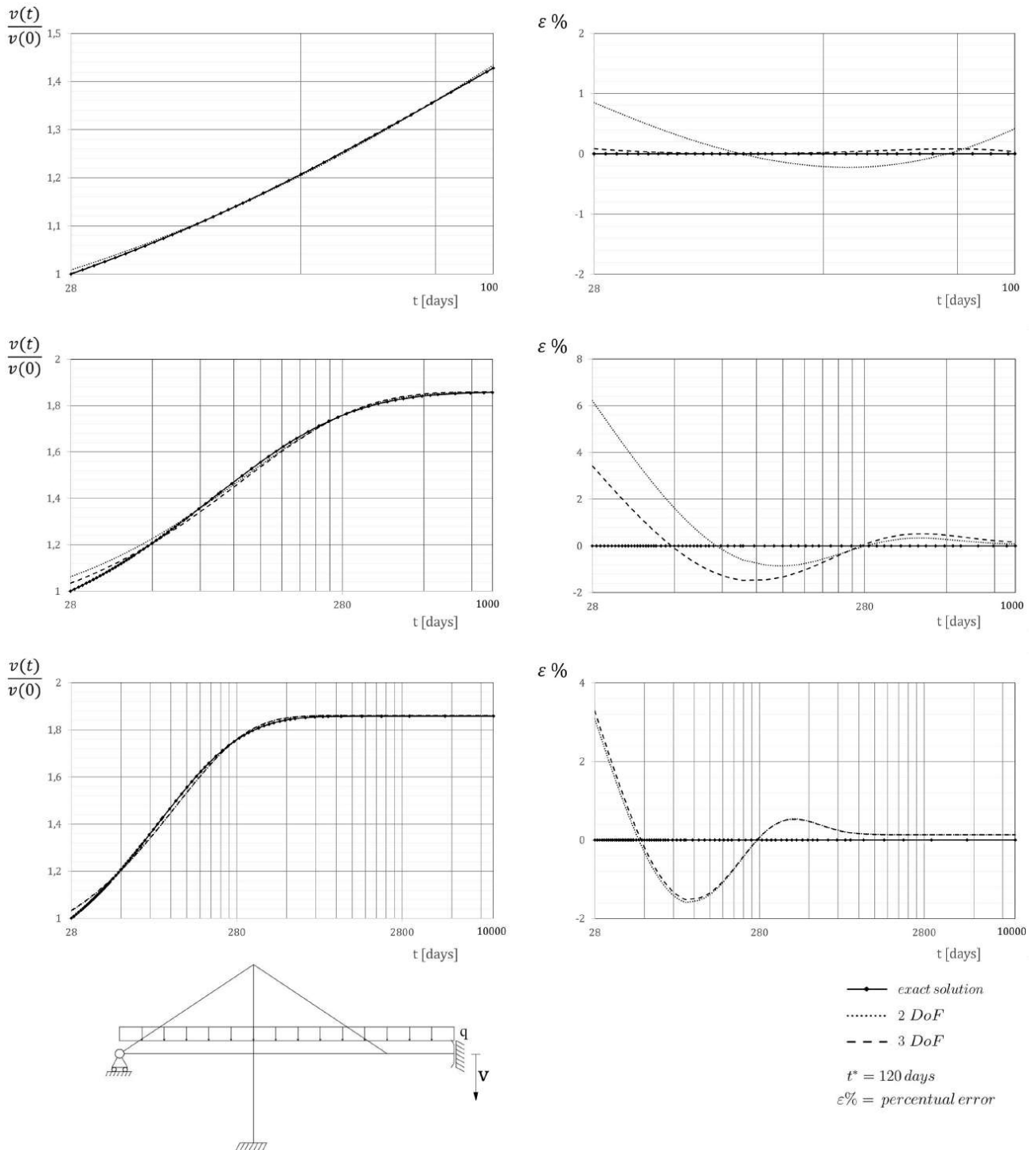
Figure 2.13: Example b: Cable-stayed bridge. Numerical results using Gurtin's approach.
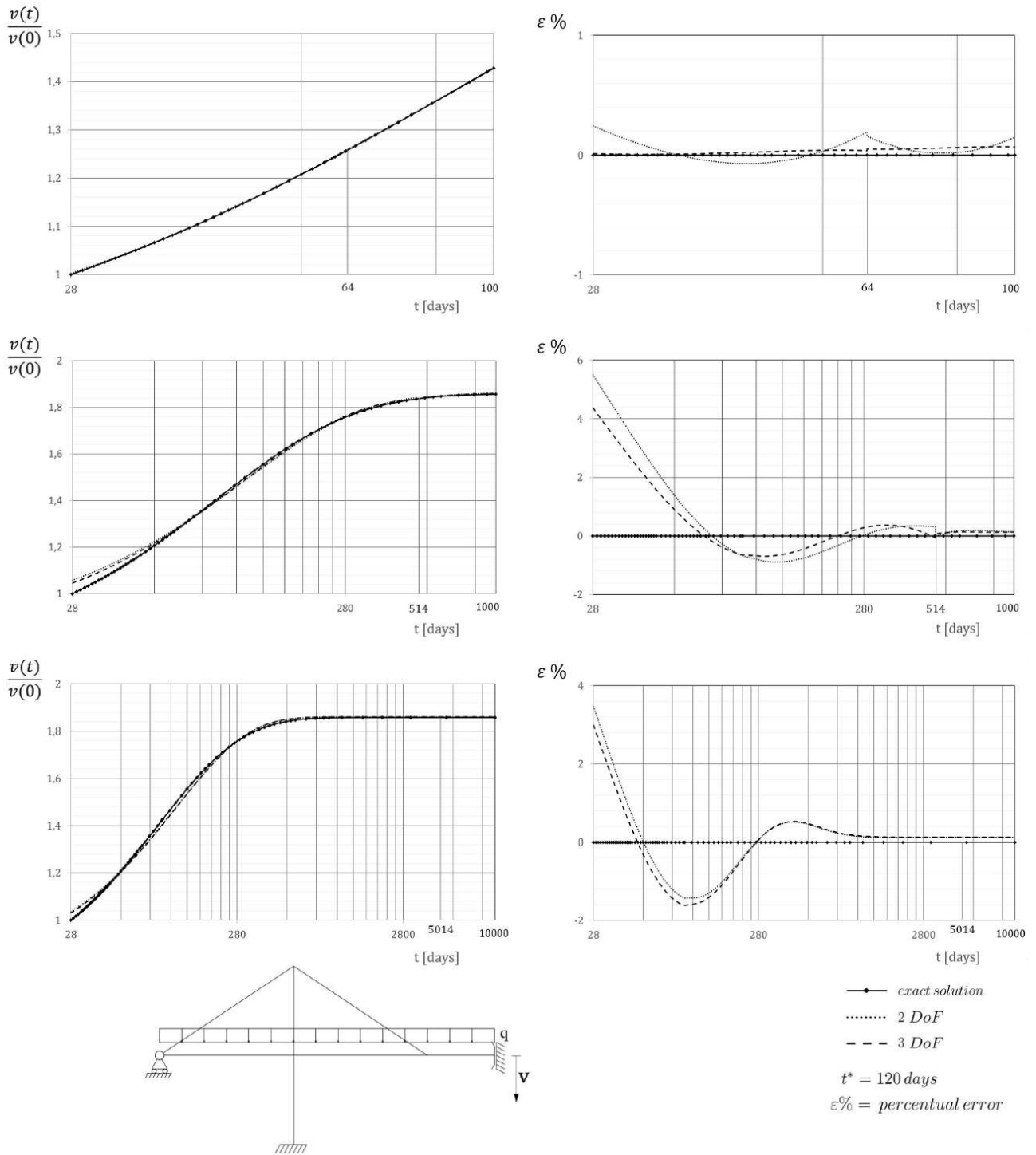
Figure 2.14: Example b: Cable-stayed bridge. Numerical results using the split Gurtin's approach.

$2T$ (days)	Time d.o.f.	Conditioning index				
		Least square	Extended functional	Gurtin	Split Gurtin	Split Gurtin*
28-100	1	1.555×10^7	3.635×10^3	4.032×10^3	5.638×10^3	
	2	7.389×10^8	2.118×10^5	4.655×10^5	2.735×10^6	2.459×10^7
	3	2.705×10^9	2.328×10^7	1.049×10^{10}	2.367×10^{11}	2.542×10^{13}
28-1000	1	5.944×10^6	2.248×10^3	3.117×10^3	3.681×10^3	
	2	2.195×10^8	1.051×10^5	2.350×10^5	5.640×10^6	3.361×10^5
	3	1.715×10^{10}	4.932×10^6	1.112×10^6	1.158×10^8	9.123×10^8
28-10000	1	8.891×10^6	2.064×10^3	3.001×10^3	3.058×10^3	
	2	2.695×10^9	1.001×10^6	2.095×10^7	5.969×10^{24}	3.878×10^7
	3	5.796×10^{12}	8.667×10^7	1.754×10^9	6.036×10^{36}	1.537×10^8
		$\tilde{\mathcal{L}}\mathcal{L}\mathbf{u}$ $= \tilde{\mathcal{L}}\mathbf{b}$ $\langle \cdot , \cdot \rangle$ standard	$\tilde{\mathcal{L}}\mathcal{K}\mathcal{L}\mathbf{u}$ $= \tilde{\mathcal{L}}\mathcal{K}\mathbf{b}$ $\langle \cdot , \cdot \rangle$ standard	$\mathcal{L}\mathbf{u} = \mathbf{b}$ $\langle \cdot , \cdot \rangle_c$		

Shape functions	$\begin{cases} \textit{Least square/Extended functional } [1\,,\, e^{-t/t^*}\,,\, e^{-2t/t^*}] \\ \textit{Gurtin's/Split Gurtin's functional } [1\,,\, e^{-t/t^*}\,,\, e^{-0.1t/t^*}] \\ {}^*\textit{Split Gurtin's functional} \begin{cases} 1^{st} \textit{ subinterval } [1\,,\, e^{-t/t^*}\,,\, e^{-0.1t/t^*}] \\ 2^{nd} \textit{ subinterval } [1\,,\, e^{-0.1t/t^*}\,,\, e^{-0.01t/t^*}] \end{cases} \end{cases}$

Table 2.2: Cable-stayed bridge. Conditioning indexes of the coefficient matrixes.

Example c: reinforced cylinder under internal pressure.

With this example we want to test the effectiveness of Gurtin's approach in the case of more complex geometry and load history. In this example a plane strain cylinder of viscoelastic material is surrounded by a steel casing and subjected to an internal pressure history. Shown in Fig. 2.15 are the geometric dimensions of the solid (2.15a), the mechanical properties of the materials (2.15b) (the material properties are assumed as in Zienkiewicz et al. (1968)), the used finite element mesh (2.15c). In particular, a quarter of cylinder is subdivided in 48 four nodes isoparametric finite elements, with 63 total nodes for the assembled structure, and two load histories; the first one (2.15d) is a pressure suddenly applied at time t=28 days and then held constant over time, the second (2.15e) is a pressure suddenly applied at time t=28 days, held constant for 100 days, suddenly doubled for the next 100 days and then suddenly removed. The reference solution has been obtained analytically through the correspondence principle.

Using Gurtin's approach, and with reference to the pressure history (2.15d), in Fig. 2.16 the radial displacements (calculated in correspondence of two representative nodes) with the relevant percentage errors are plotted while the variation of radial stress and variation of the tangential stress (calculated in correspondence of two points inside two representative finite elements) are plotted in Fig. 2.17. Table 2.3 reports the conditioning indexes of the coefficient matrices. Figure 2.18 shows the results obtained with Gurtin's formulation in the case of the more complex loading history (2.15e). The results were obtained by solving the problem in three time steps, adopting a variation of the non standard step-by-step procedure described earlier. In the case of the three loading steps, in the first step the solution for the first 100 days was calculated. Then the solution for 100 more days was calculated using the functional for the first 200 days and using the solution already found in the first interval.

Finally, the solution was found in the third interval, between 228 and 328 days by considering the functional over the entire time interval, starting at 28 days and using the solution already found in the first two intervals. Basically, a step-by-step procedure was used with large time steps and using two temporal degrees of freedom for each step, only. As shown in Fig. 2.18, Gurtin's approach leads to very good results with low computational cost.

PROPERTIES

Geometrical		$r_0 = 4\,in$	$r_i = 2\,in$	$s = 4/33\,in$
Rheological	Steel casing	$E = 3 \times 10^7\,lb/in^2$		$\nu = 0.3015$
	Viscoelastic material	Volumetric part (elastic)		$K = 1 \times 10^5\,lb/in^2$
		Deviatoric part		$G = 3.75 \times 10^4\,lb/in^2$, Relaxation time= $10\,days$
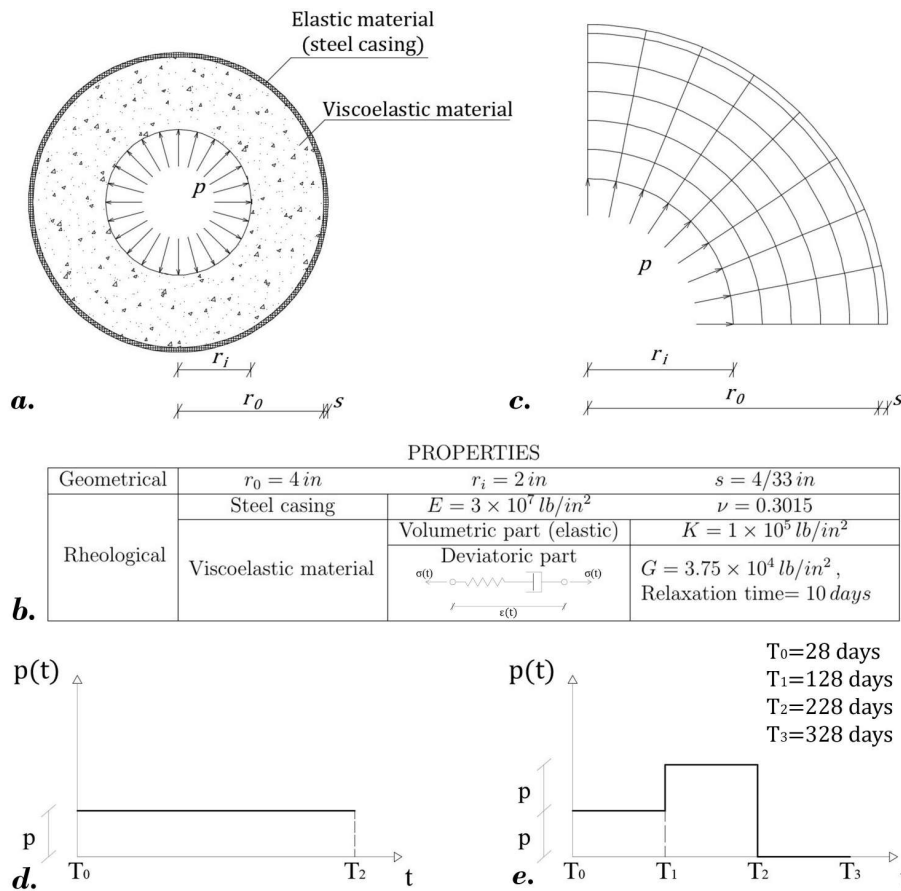
Figure 2.15: Example c: Reinforced cylinder under internal pressure (a), Geometrical properties and rheological properties (b), Finite Element mesh (c), First load history (d), Second load history (e).
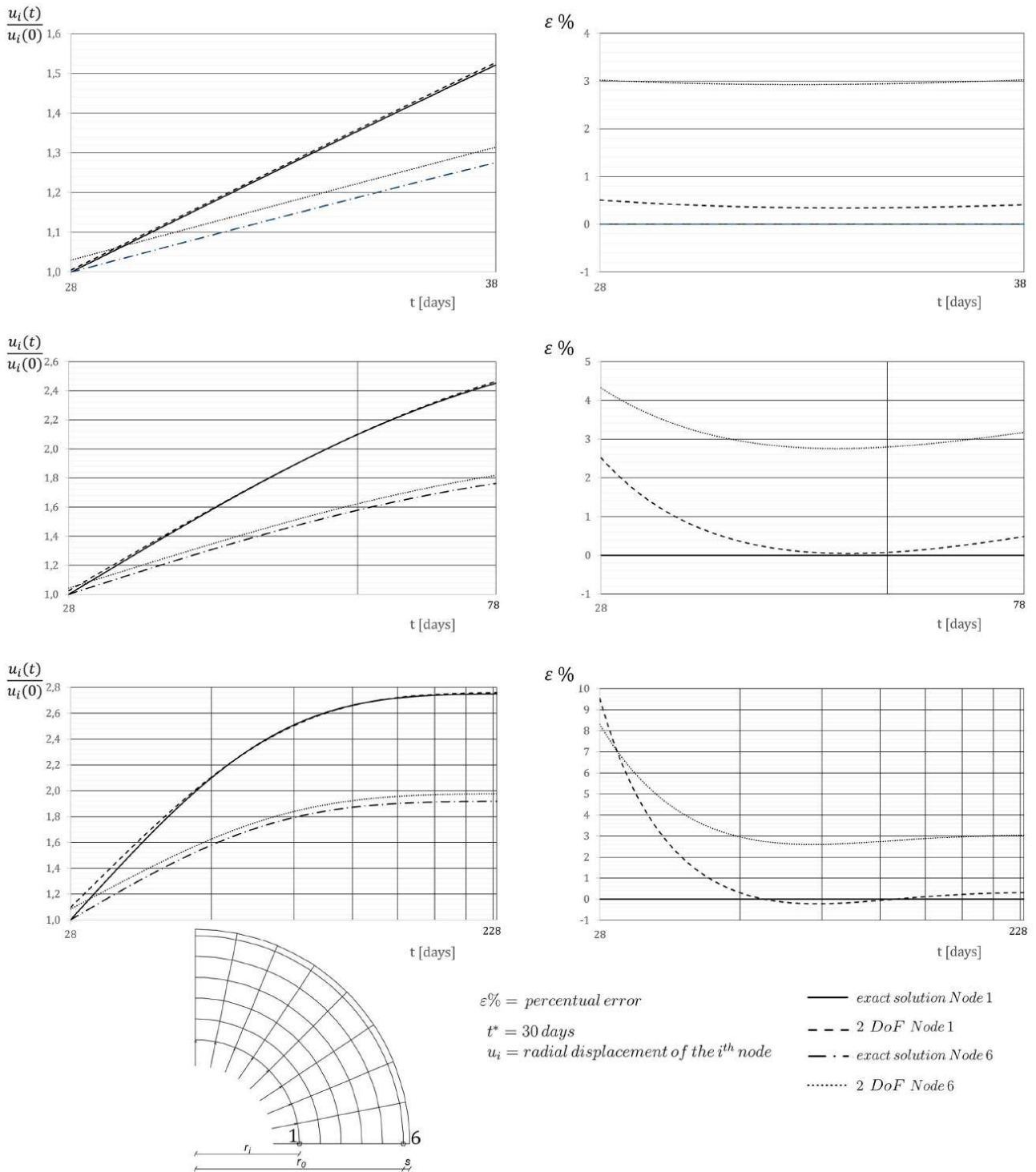
Figure 2.16: Example c: Reinforced cylinder under suddenly applied constant internal pressure. Radial displacements plots.
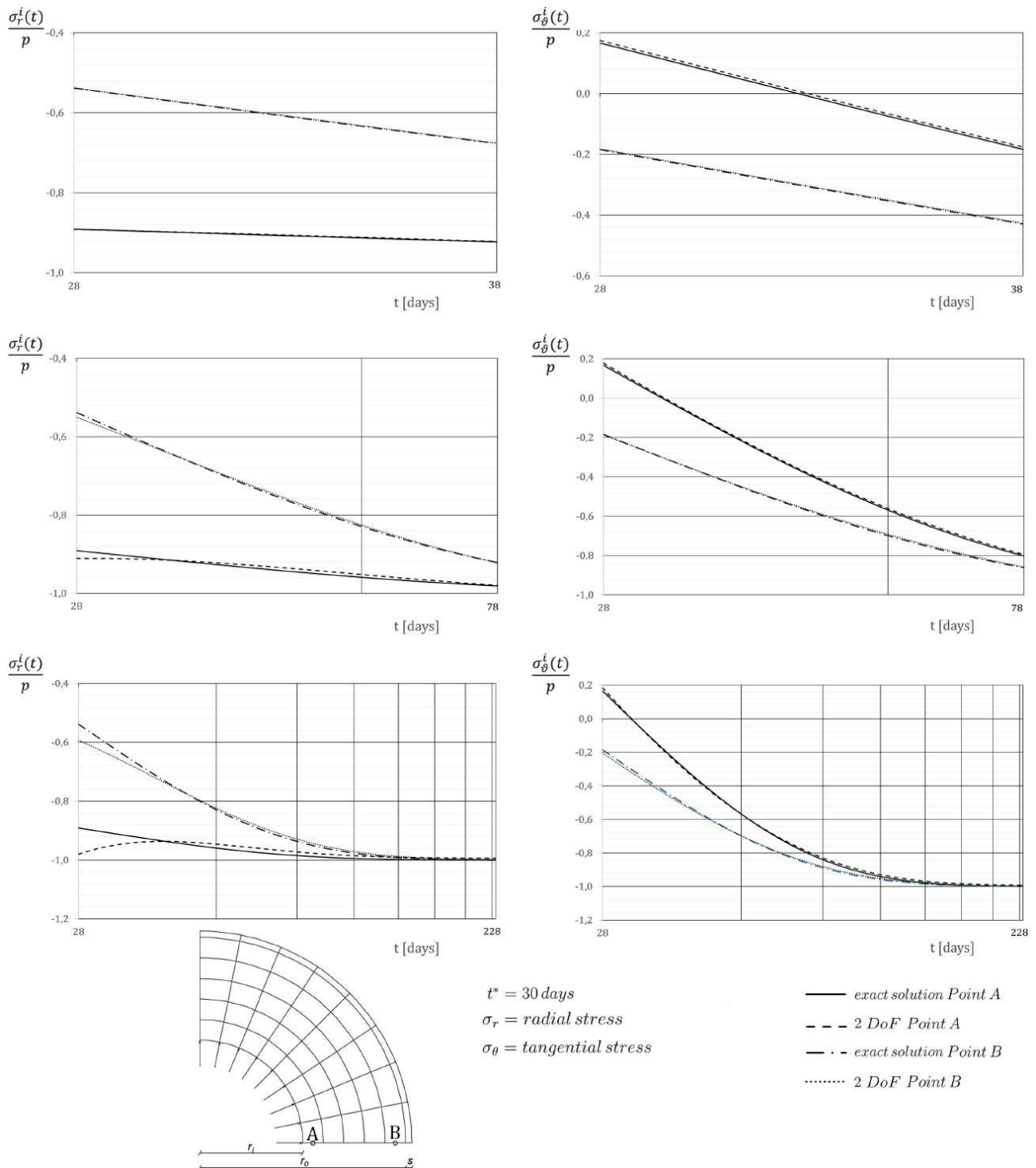
Figure 2.17: Example c: Reinforced cylinder under suddenly applied constant internal pressure. Radial and tangential stress plots.
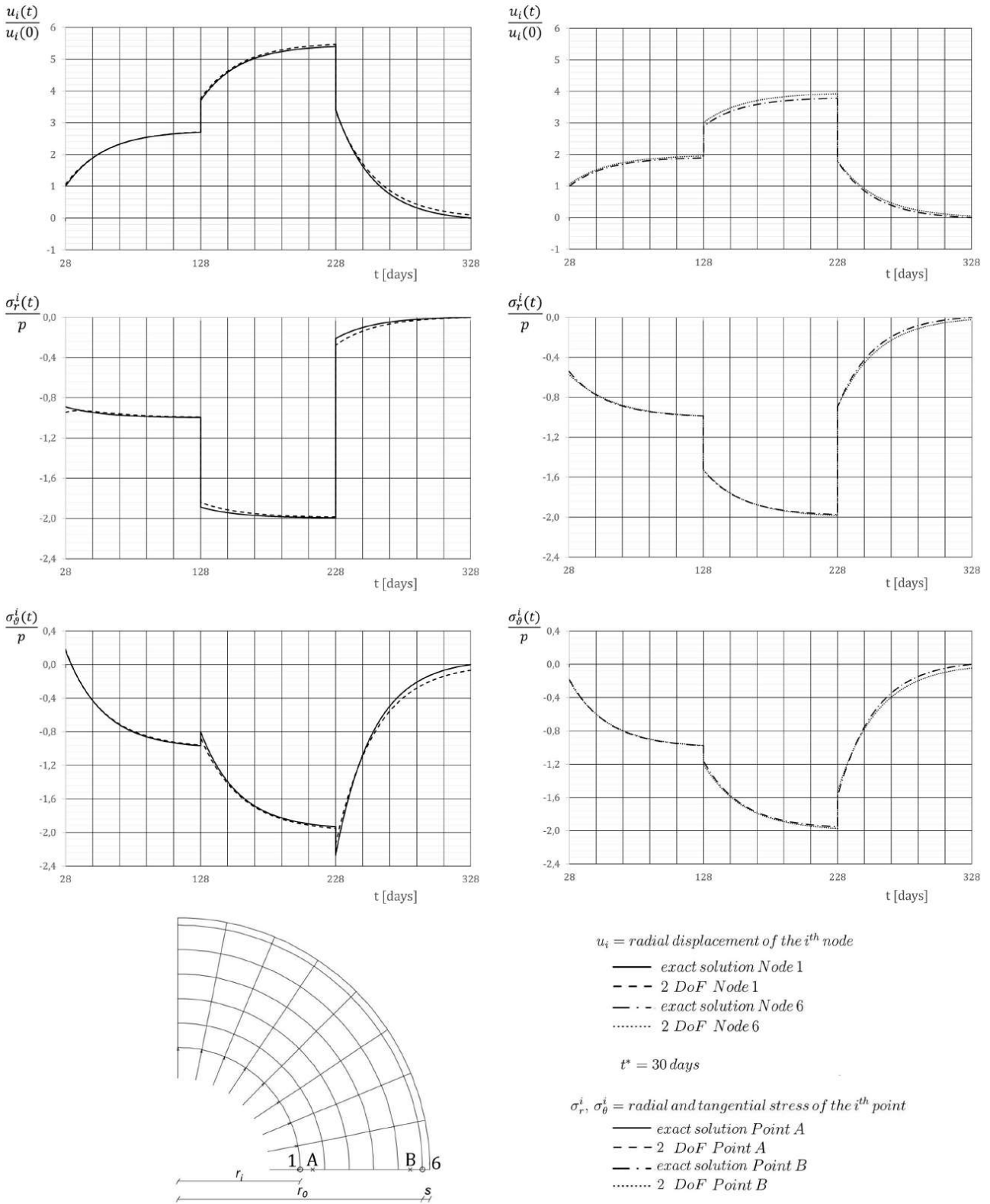
Figure 2.18: Example c: Reinforced cylinder under internal pressure depicted in fig. 2.15e.

$2T$ (days)	No. of time degrees of freedom	Conditioning index Gurtin's functional
	1	9.4777×10^5
28-38	2	3.2489×10^8
	3	2.6005×10^{13}
	1	1.6799×10^6
28-78	2	3.3209×10^7
	3	3.8077×10^{10}
	1	2.4283×10^6
28-228	2	1.5416×10^8
	3	8.1938×10^8
		$\mathcal{L}\mathbf{u} = \mathbf{b}$ $\langle \cdot, \cdot \rangle_c$

Table 2.3: Reinforced cylinder under suddenly applied constant internal pressure: conditioning indexes of the coefficient matrices.

2.5 Conclusions

To the authors' knowledge, no significant work seems to exist in the literature concerning the use of variational formulations for the numerical solution of the linear viscoelasticity problem. In particular, variational principles based on convolutional bilinear forms with respect to time do not seem to have had any place so far in computational procedures for the numerical determination of the viscoelastic response of solids or structures subject to external actions. This Chapter aims at investigating the effectiveness of numerical procedures based on these variational formulations.

Three variational formulations for the linear viscoelastic problem are critically reviewed and numerically tested with the purpose of investigating their effectiveness in the numerical solution of viscoelastic problem. Numerical examples with reference to hereditary Kelvin-Voigt and Maxwell material model are presented.

In the case of finding the viscoelastic solution over a finite time interval in a single step, Gurtin's formulation works well in the sense that the numerical solutions are obtained with errors lower than 5%, using only two or three temporal degrees of freedom; by carefully choosing the temporal interpolation functions, Gurtin's formulation leads to numerical results comparable to those obtained with Tonti's "extended" variational formulation in terms of accuracy, but with lower computational costs.

With Gurtin's formulation, the results are more sensitive to the choice made of interpolation functions over time. Polynomial interpolation functions are appropriate only for short time intervals. The interpolation functions that have given the best results are the negative exponential functions because they capture well the typically damped trend of the viscoelastic solution. The conditioning indexes are comparable to those obtained with the "extended" Tonti's formulation. In the case of using the Gurtin formulation in a step-by-step procedure, the results are comparable to those obtained with a traditional time integration technique.

The split Gurtin formulation gives good results only for an equal number of degrees of freedom in the first and second time sub-interval. For a lower number in the former there is no solution while for a lower number in the latter there arise numerical instabilities that, in the worst cases, are difficult to overcome even with the help of a Tikhonov regularization. From

the numerical point of view it does not seem to provide any improvement over the unsplit formulation. In any case, the doubling of unknowns makes the method less competitive than the unsplit Gurtin's method. The split Gurtin functional, however, could have advantages from the theoretical point of view, as shown in Carini and Mattei (2015). In fact, the formulation is of the min-max type and, by the adopted time splitting, one is able to isolate a part of the functional that represents the free energy of the system and is, therefore, in general, semidefinite positive.

In the case of the Gurtin and split Gurtin functionals, the problem of the optimal choice of the relaxation time to be used in the negative exponential interpolation functions remains unsolved.

Huet's formulation, in general, can provide a wrong solution. It provides the true solution only under very restrictive assumptions, as in the case of integration times long enough for the solution to have become constant, but even in these cases the formulation has numerical instabilities similar to those presented by the split Gurtin formulation. Huet's formulation works well only for short time intervals embedded in a standard step-by-step procedure. From a theoretical point of view it is interesting because the quadratic part of the functional has the physical meaning of a free energy.

In conclusion, of the three formulations presented here and numerically tested, Gurtin's original formulation seems to be the most effective in numerically solving the linear hereditary viscoelastic problem.

References

ABAQUS Manuals, rel. 2018. Dassault Systèmes/SIMULIA, Jonston, Rhode Island, US. Hibbit, H.D., Karlsson, B., Sorensen, P.

Benthien, G., Gurtin, M.E., 1970. A principle of minimum transformed energy in linear elastodynamics. Journal of Applied Mechanics, 37 (4), 1147-1149.

Biot, M.A., 1956. Variational and Lagrangian methods in viscoelasticity, Deformation and Flow of Solids. Ed. R. Grammel, IUTAM, Kolloquium Madrid, sept. 26-30 1955, Springer-Verlag, 252-263.

Bozza, A., Gentili, G., 1995. Inversion and Quasi-Static Problems in Linear Viscoelasticity. Meccanica 30, 321-335.

Breuer, S., Onat, E.T., 1964. On the determination of free energy in linear viscoelastic solids. Journal of Applied Mathematics and Physics, 15, 184-191.

Brilla, J., 1972. Convolution variational principles and methods in linear viscoelasticity, Variational Methods in Engineering. Ed. Department of Civil Engineering University of Southampton, Proceedings of an Int. Conf. Southampton, 25 sept.

Brun, L., 1965. Sur deux espressions, analogues à la formule de Clapeyron, donnant l'énergie libre et la puissance dissipée pour un corp viscoélastique, Comptes Rendus de l'Acadmie des Sciences. Paris 261, 41-44.

Brun, L., 1969. Méthodes énergétiques dans les systèmes évolutif linéaires. Première partie: Séparation des énergies. Journal de Mécanique 8 (1), 125-166.

Carini, A., De Donato, O., 2004. Inelastic analysis by symmetrization of the constitutive law. Meccanica 39 (4), 297-312.

Carini, A.,Diligenti, M., Maier, G., 1991. Boundary integral equation analysis in linear viscoelasticity: variational and saddle point formulations. Computational Mechanics, 39. 8, 87-89.

Carini, A., Gelfi, P., Marchina, E., 1995. An energetic formulation for the linear viscoelastic problem. Part I: Theoretical results and first calculations. International Journal for Numerical Methods in Engineering, 38, 37-62.

Carini, A., Mattei, O., 2015. Variational formulations for the linear viscoelastic problem in the time domain. European Journal of Mechanics A/Solids, 54, 146-159.

Charpin, L., Sanahuja, J., 2017. Creep and relaxation Poisson's ratio: Back to the foundations of linear viscoelasticity. Application to concrete. International Journal of Solids and Structures, 110-111, 2-14

Christensen, R.M., 1968. Variational and minimum theorems for the linear theory of viscoelasticity. Journal of Applied Mathematics and Physics, 19, 233-243.

Christensen, R.M., 1971. Theory of viscoelasticity. Academic Press, New York, London.

Del Piero, G., Deseri, L., 1996. On the analytic expression of the free energy in linear viscoelasticity. Journal of Elasticity 43, 247278.

Fabrizio, M., 1992. Sull'invertibilità dell'equazione costitutiva della viscoelasticità lineare. Rendiconti Lincei Matematica e Applicazioni s.9, 3, 141-148.

Gurtin, M.E., 1963. Variational principles in the linear theory of viscoelasticity. Archive for Rational Mechanics and Analysis, 16 (1), 34-50.

Gurtin, M.E., 1964. Variational principles for linear elastodynamics. Archive for Rational Mechanics and Analysis, 13 (3), 179-191.

Gurtin, M.E., 1964. Variational principles for linear initial-value problems. Quarterly of Applied Mathematics, 22, 252-256.

Gurtin, M.E., Sternberg, E., 1962. On the linear theory of viscoelasticity. Archive for Rational Mechanics and Analysis, 11, 291-356.

Hlaváček, I., 1966. Sur quelques théorèmes variationnels dans la théorie du fluage linéaire. Aplikace Matematiky, Swazek 11, Č 4, 283-294.

Huet, C., 1992. Minimum theorems for elasticity. European Journal of Mechanics - A/Solids, 11 (5), 653-684.

Huet, C., 1999. Coupled size and boundary-condition effects in viscoelastic heterogeneous and composite bodies. Mechanics of Materials, 31, 787-829.

Huet, C., 2001. Extended Clapeyron formulae for viscoelasticity problems in the time domain and application to the boundary-condition effect in random composite bodies. Journal of the Mechanics and Physics of Solids, 49, 675-706.

Huet, C., 2001. Comparison and minimum theorems in the time domain for viscoelasticity and other convolutive initial-boundary value problems with applications to random inhomogeneous materials. Journal of the Mechanics and Physics of Solids, 49, 1569-1602.

Kress, R., 1989. Linear Integral Equations. Springer-Verlag.

Leitman, M.J., 1966. Variational principles in the linear dynamic theory of viscoelasticity. Quart. Appl. Math. XXIV, 1, 37-46.

Leitman, M.J., Fisher, G.M.C. The linear theory of viscoelasticity. In Encyclopedia of Physics, Chief Editor: S. Flugge, Vol. VIa/3, Mechanics of Solids III, Editor: C. Truesdell, Springer-Verlag, 1973.

Mandel, J., 1966. Cours de mécanique des milieux continus, Tome II. Gauthier-Villars, Paris.

Morse, P.M., Feshbach, H., 1953. Methods of Theoretical Physics, Vol. I. McGraw-Hill.

Olszak, W., Perzyna, P., 1959. Variational theorems in general viscoelasticity. Ingenieur-Archiv XXVIII, 246-250.

Rafalski. P., 1969. The orthogonal projection method III. Linear viscoelastic problem. Bulletin of the Polish Academy of Sciences: Technical Sciences, 17, 167.

Reiss, R., 1978. Minimum principles for linear elastodynamics. Journal of Elasticity, 8(1), 35-45.

Reiss, R., Haug, E.J., 1978. Extremal principles for linear initial value problems of mathematical physics. The International Journal of Engineering Science, 16, 231-251.

Reddy, J.N., 1976. Variational principles for linear coupled dynamic theory of thermoviscoelasticity. The International Journal of Engineering Science, 14, 605-616.

Schapery, R.A., 1964. On the time dependence of viscoelastic variational solutions. Quarterly of Applied Mathematics, 22, 207-216.

Staverman, A.J., Schwarzl, F., 1952a. Thermodynamics of Viscoelastic Behavior. Proceedings of the National Academy of Sciences, The Netherlands 55, 474-485.

Staverman, A.J., Schwarzl, F., 1952b. Non-equilibrium Thermodynamics of Viscoelastic Behavior. Proc. Kowink. Nederl., Akad Van Wettenschappen B-55, 486-492.

Taylor, R.L., Pister, K.S., Goudreau G.L., 1970. Thermo-mechanical Analysis of Viscoelastic Solids. International Journal for Numerical Methods in Engineering, 2, 45-59.

Tonti, E., 1973. On the variational formulation for linear initial value problems. Annali di Matematica Pura ed Applicata, Serie Quarta XCV, 331-359.

Tonti, E., 1984. Variational formulations for every nonlinear problem. International Journal of Engineering Science, 22 (11-12), 1343-1371.

Zienkiewicz, O.C., Watson, M., King, I.P., 1968. A numerical method of visco-elastic stress analysis. International Journal of Mechanical Sciences, 10, 807-827.

Chapter 3

Variational principles and numerical integration methods for the heat conduction problem

Notation

Greek and latin letters

- Ω: Region occupied by a solid body;

- V: Volume of the solid body;

- Γ: External surface of the solid body;

- $n_i(x_r)$: Unit outward normal vector components;

- $x_r,\ r = 1, 2, 3$: Cartesian coordinates;

- $\theta(x_r, t)$: Temperature field;

- $q_i(x_r, t)$: Heat flux vector components;

- $[0, 2T]$: Time interval;

- Γ_q: Loaded region of the boundary;

- $\bar{\theta}(x_r, t)$: Prescribed temperatures;

- $\bar{q}_i(x_r, t)$: Prescribed heat flux vector components;

- $k(x_r)$: Thermal conductivity;

- $\gamma(x_r)$: Specific heat;

- $\rho(x_r)$: Mass density;

- $a(x_r, t)$: Rate of heat production per unit volume;

- Γ_θ: Constrained region of the boundary;

- $r(t)$: Function for the biconvolutive bilinear form;

- l^e: Length of the finite element;

- $\boldsymbol{\alpha}$: Vector of the degrees of freedom;

- $\boldsymbol{\beta}_i$: Vector of the time degrees of freedom;

- $\boldsymbol{m}_i$: Vector of time shape functions;

- L: Length of the rod;

- A: Cross-sectional area.

Symbols

- $=::$ Is defined as;

- $*$: Convolution product;

- $\circ$: Convolution product over half time range;

- $'$: Admissible term;

- $_1$: Variable defined over the first subinterval;

- $_2$: Variable defined over the second subinterval;

- $\subseteq$: Is included in;

- $\supseteq$: Includes.

Operators and functions

- $_{/i}$: Partial derivative operation;

- $\dot{\ }$: Derivation with respect to the time variable;

- I: Identity Operator;

- $\langle\, ,\, \rangle_c$: Convolutive bilinear form;

- $\langle\, ,\, \rangle_{cc}$: Biconvolutive bilinear form;

- $\mathcal{F}^G$: Gurtin's functional;

- $\mathcal{F}^{SG}$: Split Gurtin functional;

- $H(t)$: Heaviside function.

3.1 Introduction

This Chapter starts from the theories and results obtained in the previous Chapter and it aims at the numerical use of variational principles applied on the heat conduction problem.

In the past, many attempts were carried out to provide variational formulations, especially of extremum type, also for the heat conduction problem. The research of variational formulations led to a variety of quasi-variational principles (or weak forms) and restricted variational principles, where the adjective "restricted" refers to the fact that certain variables are kept constant during the variation process. For example, Rosen (1953) formulated a variational principle for diffusional processes, modifying Osanger's principle of minimum dissipation, holding the temperature field fixed.

Glansdorff and Prigogine (1964,1965) extended the theorem of minimum entropy production to obtain a universal evolution criterion, valid in the whole range of macroscopic physics, deriving local potentials which open the way to the use of variational techniques.

Gyarmati (1969) derived a universal form of the integral principle of thermodynamics, whose validity could be extended to certain types of non-linear problems, and discussed its relation to Vojta's functional variational principle.

Finlayson (1983) obtained a series of variational principles (based on a functional, or not) for heat conduction problems.

According to Biot (1970), by introducing a new vector field called by Biot himself the "heat displacement vector", one can rewrite the heat equation in a canonical form, which corresponds to a variational principle involving the potential and the thermal dissipation of the system. According to Biot's analysis, such a principle may be considered similar to d'Alembert's thermodynamic principle of analytical mechanics. In fact, many of the variational principles proposed in the past for the heat conduction problem were inspired by similar principles put forward for problems of analytical mechanics, such as Hamilton's principle, the principle of least action, and Gauss' principle of least constraint (see Levi-Civita and Amaldi, 1927).

For example, in Vujanovic's work (1971,1974), with the aim to formulate a variational principle of Hamilton's type, the conduction problem (parabolic) is transformed into a hyperbolic one, depending on one parameter. This is achieved by adding, to the original equation, a term including the second time derivative and depending on a parameter. The original equation is re-obtained when the parameter goes to zero in the first variation, set equal to zero. It should be noted that the parameter has a clear physical interpretation: it is related to the relative speed of the heat wave (see Cattaneo, 1948). Changes to such a variational principle have been proposed: the parameter may be replaced by a "vanishing" function (Djukic and Vujanovic, 1971, who defined the so-called "DV method", Vujanovic, 1976a, Schlup, 1975).

The principle analogue to that of the least action is based on the abandonment of the well-known rule: *the variation of the derivative is equal to the derivative of the variation* and on the consideration of non-commutative derivation rules to include non-conservative dynamical systems. Atanackovic, in a series of papers (1977, 1978, 1980, 1983), gave an interpretation to the variational principle with non-commutative laws in terms of directional Gateaux derivatives. Namely, the Gateaux derivative of the conservative part of the action integral vanishes for a certain set of directions. He also examinates the conditions which ensure the existence of a local minimum of the functional used in a variational principle with non-commutative rules (the second Gateaux derivative must be positive).

Also the method of least squares, inspired by Gauss' principle of least constraint, has been widely used for the initial value problems and, in particular, for the elastodynamic problem and for the heat conduction problem. The problem is reduced to the algebraic minimization of a

quadratic form with respect to some physical parameters. See, for example, Vujanovic (1976b), Vujanovic and Baclic (1976), Vujanovic and Atanackovic (1978) and Djukic and Atanackovic (1981).

An extension of the method of least squares was proposed by Tonti (1984) with the so-called extended variational principles, based on the choice of a bilinear form with respect to which a suitable "integral operator" is symmetric and positive definite. Regardless, Ortiz (1985) used a similar method to provide a variational formulation to the convection-diffusion problem, minimizing the weighted residuals of the solution uniformly. Furthermore, a generalization of Tonti's approach to the case of non-differentiable operators has been established by Auchmuty (1988, 1993).

A variational formulation valid simultaneously for the given problem and the adjoint problem was provided by Morse and Feshback (1953). By using this method it is always possible to rephrase any linear problem in a variational way, considering that the method of the formally self-adjoint operators cannot be applied when the operator is not at least self adjoint. This method considers, alongside with the original initial value problem, another artificial one governed by the adjoint operator, therefore with final conditions. The use of the adjoint operator, whether explicitly or implicitly, inspired a significant number of papers, especially for diffusion problems. Nevertheless, justifying the attachment of the adjoint problem from a physical point of view constitutes a great issue. Herrera (1974) found two extreme principles for the heat equation which were then extended (Herrera and Bielak, 1976) to diffusion problems. In these works, Herrera also uses the solution of the adjoint problem on a given time interval and introduces functions either even or odd in time with respect to the midpoint of the time interval used. He derives a functional which is minimum over a set of constraints and maximum with respect to a second set thereby obtaining dual extremum principles.

Subsequently, Collins (1977), using Herrera's ideas, has derived dual complementary variational principles in which explicit use of the adjoint equation and the extremum principles are used to obtain bounds of quantity of interest for the heat equation. Bivariational bounds, based on the use of the adjoint equation, were obtained by Barnsley and Robinson (1974, 1975), and Cole (1980).

The first true variational formulation dates back to Gurtin's work (1964). It is based on the use of convolution integrals and it is valid for a large class of linear time-dependent problems, including the heat conduction problem. Gurtin's idea consists of a preliminary transformation of differential equations into integro-differential equations with convolutive integrals. Filippov and Skorokhodov (1977), for a one-dimensional problem, provided a functional involving spatial integrals rather than time integrals.

Gurtin's method has then been simplified by Tonti (1973) who, with the introduction of a convolutive bilinear form, prevents the transformation of the differential problem into an integro-differential one. Magri (1974) generalizes the results of Gurtin and Tonti, providing an infinite number of bilinear forms, dependent on a symmetric kernel function, with respect to which the problem of heat conduction is symmetric, thus admits a variational formulation. The convolutive bilinear form was also used to obtain variational formulations in space and time for the heat conduction problem written in terms of boundary integral equations (Carini, Diligenti, Maier, 1991; Carini, Diligenti, Salvadori, 1999).

Rafalski (1969) has the merit of having obtained extremal formulation for linear problems with initial values. The limit of his results is that it is necessary to study the whole story, from the time of the initial assignment of data to infinity. The work of Rafalski was later perfected by Reiss and Haug (1978), who formulated extremal principles for problems with initial values and who explored the possibility of finding those functionals which return an extremum principle

for linear initial value problems.

The Chapter is organized as follows. In Subsection 2, the linear transient heat conduction problem is introduced. In Subsection 3 two bilinear forms will be defined (the convolutive bilinear form and the biconvolutive bilinear form) and two stationarity principles are derived. In Subsection 4 a splitting of the time integration interval is performed and several extremal principles are obtained. In Subsection 5, by using the finite element method in space and the Ritz method in time, a discretized formulation is applied and the behaviour of a finite rod with superimposed temperature at its ends and of finite square element with null initial temperature, a prescribed temperature at its boundary and with no heat generation within the solid is analysed. In Subsection 6, conclusions and open issues are discussed, therefore a list of references is presented.

3.2 The linear transient heat conduction problem

Consider a solid body $\Omega \subset \mathbb{R}^3$, with volume V and external surface Γ with unit outward normal $n_i(x_r)$.

An orthogonal Cartesian reference system is used, with coordinates x_r, $r = 1, 2, 3$. The components of vectors, second order and fourth order tensors are indicated with the usual indicial notation. Einstein's convention over repeated indices is adopted, for which when an index variable appears twice in a single term and is not otherwise defined, it implies summation of that term over all the values of the index.

The constituent material is supposed to be thermally isotropic, i.e., when a point x_r is heated, the heat spreads out equally well in all directions. Furthermore, the material might be thermally inhomogeneous, i.e., the conditions of conduction may be different from point to point.

The purpose of the present work is to describe the temperature field $\theta(x_r, t)$ and the heat flux $q_i(x_r, t)$, at the point $x_r \in \Omega$, at the time $t \in [0, 2T]$ with $T > 0$.

The body is undisturbed for $t < 0$; in particular, suppose that the body is in a steady state of conduction for $t < 0$, i.e. the temperature difference driving the conduction is constant and the spatial distribution of the temperature in the region Ω does not change any further in time, with $\theta(\mathbf{x}, t) = \theta_0(\mathbf{x})$ for every $\mathbf{x} \in \Omega$ and for $t < 0$.

The constitutive law, that relates the heat flux $q_i(x_r, t)$ to the temperature $\theta(x_r, t)$ may be written as follows:

$$k(x_r) \cdot p_i(x_r, t) - q_i(x_r, t) = 0 \tag{3.2.1}$$

where $k(x_r)$ is the thermal conductivity in $Jm^{-1}s^{-1}K^{-1}$ and $p_i(x_r, t)$ is derived from the definition equation:

$$-\frac{\partial \theta(x_r, t)}{\partial x_i} - p_i(x_r, t) = 0 \tag{3.2.2}$$

The latter equation (3.2.2) asserts that the vector $p_i(x_r, t)$ is the opposite in sign to the temperature gradient. By combining equations (3.2.1) and (3.2.2), one obtains the following well-known equation:

$$q_i(x_r, t) = -k(x_r) \cdot \frac{\partial \theta(x_r, t)}{\partial x_i} \tag{3.2.3}$$

derived by Fourier in 1822 by observing that heat transfer is in the direction of decreasing temperature.

The equilibrium equations in terms of temperature is:

$$\gamma(x_r)\rho(x_r) \cdot \frac{\partial\theta(x_r,t)}{\partial t} - \frac{\partial}{\partial x_i}\left(k(x_r) \cdot \frac{\partial\theta(x_r,t)}{\partial x_i}\right) = a(x_r,t) \quad \text{in } \Omega \times [0,2T]$$

$$k(x_r) \cdot \frac{\partial\theta(x_r,t)}{\partial x_i} \cdot n_i(x_r) = \bar{q}(x_r,t) \quad \text{on } \Gamma_q \times [0,2T]$$

(3.2.4)

where $\gamma(x_r)$ is the specific heat in $JK^{-1}kg^{-1}$ depending upon the position within the body, $\rho(x_r)$ is the mass density in $kg\,m^{-3}$ of the material and the given function $a(x_r,t)$ represents the rate of heat production per unit volume in $Jm^{-3}s^{-1}$.

When the range of temperature is limited, as supposed in the present Chapter, the dependence upon $\theta(x_r,t)$ can be neglected and $k(\mathbf{x})$ can be considered constant. The balance equation (3.2.4a) is prototypical example of a parabolic partial differential equation and it represents the principle of energy conservation applied to a differential control volume through which energy transfer is exclusively by conduction.

The balance, definition and constitutive equations are equipped with the boundary conditions reported below. On the portion Γ_θ of the boundary Γ ($\Gamma = \Gamma_\theta \cup \Gamma_q$, Γ_q and Γ_θ being complementary parts of Γ ($\Gamma_\theta \cap \Gamma_q = \emptyset$)), the surface temperature $\bar{\theta}(\mathbf{x},t)$, that may be constant or a function of time, or position, or both, is assigned, that is

$$\theta(\mathbf{x},t) = \bar{\theta}(\mathbf{x},t) \quad \text{on } \Gamma_\theta \times [0,2T] \qquad \text{(Dirichlet boundary condition)} \qquad (3.2.5)$$

whereas on Γ_q the flux of heat $q(\mathbf{x},t)$ across the surface is prescribed:

$$q(\mathbf{x},t) = q_i(\mathbf{x},t)n_i(\mathbf{x}) = \bar{q}(\mathbf{x},t) \quad \text{on } \Gamma_q \times [0,2T] \qquad \text{(Neumann boundary condition)} \quad (3.2.6)$$

where $n_i(\mathbf{x})$ is the outward-drawn unit normal and $\bar{q}(\mathbf{x},t)$ is the given flux.

For simplicity, we do not consider the "linear radiation boundary condition" for which the flux across the surface is proportional to the temperature difference between the surface and the surrounding medium. We do not consider non-linear boundary conditions either, such as the "black-body radiation", for which the fourth power of the temperature field is prescribed on the boundary, or the "natural convection", regarding powers of the temperature field close to 5.4 (see Carslaw and Jaeger (1959)).

Finally, the initial condition reads

$$\theta(\mathbf{x},t) = \theta_0(\mathbf{x}) \quad \text{in } \Omega, \, t = 0 \tag{3.2.7}$$

For the sake of simplicity, throughout the following the dependence upon the variable $\mathbf{x} = (x_i)_{i=1,2,3}$ will be omitted, unless strictly required.

The heat conduction problem can be written in a three-fields operatorial form, as follows

$$\begin{bmatrix} \gamma\rho\frac{\partial(.)}{\partial t} & 0 & \frac{\partial(.)}{\partial x_i} \\ 0 & k & -I \\ -\frac{\partial(.)}{\partial x_i} & -I & 0 \end{bmatrix} \begin{bmatrix} \theta \\ p_i \\ q_i \end{bmatrix} = \begin{bmatrix} a \\ 0 \\ 0 \end{bmatrix} \quad \text{in } \Omega \times [0,2T] \tag{3.2.8}$$

$$\begin{bmatrix} 0 & 0 & -n_i \\ 0 & 0 & 0 \\ n_i & 0 & 0 \end{bmatrix} \begin{bmatrix} \theta \\ p_i \\ q_i \end{bmatrix} = \begin{bmatrix} -\bar{q} \\ 0 \\ n_i\bar{\theta} \end{bmatrix} \quad \begin{array}{l} \text{on } \Gamma_q \times [0,2T] \\ \\ \text{on } \Gamma_\theta \times [0,2T] \end{array} \tag{3.2.9}$$

$$\begin{bmatrix} \gamma\rho & 0 & 0 \\ 0 & 0 & 0 \\ 0 & 0 & 0 \end{bmatrix} \begin{bmatrix} \theta \\ p_i \\ q_i \end{bmatrix} = \begin{bmatrix} \gamma\rho\theta_0 \\ 0 \\ 0 \end{bmatrix} \quad \text{in } \Omega, \, t = 0 \tag{3.2.10}$$

with I the identity operator, or, in a compact form, with obvious meaning of the symbols:

$$\mathbf{M}_I \mathbf{z}_I = \mathbf{a}_I \quad \text{in } \Omega \times [0, 2T] \tag{3.2.11}$$

$$\mathbf{B}_I \mathbf{z}_I = \mathbf{g}_I \quad \text{on } \Gamma \times [0, 2T] \tag{3.2.12}$$

$$\mathbf{T}_I \mathbf{z}_I = \mathbf{h}_I \quad \text{in } \Omega, \, t = 0 \tag{3.2.13}$$

or, finally, in the following condensed form:

$$\mathbf{N}_I \mathbf{z}_I = \mathbf{f}_I \tag{3.2.14}$$

By eliminating the variable $p_i(t)$, one gets the following two-fields operatorial form:

$$\begin{bmatrix} -\gamma\rho\frac{\partial(.)}{\partial t} & -\frac{\partial(.)}{\partial x_i} \\ \frac{\partial(.)}{\partial x_i} & \frac{1}{k} \end{bmatrix} \begin{bmatrix} \theta \\ q_i \end{bmatrix} = \begin{bmatrix} -a \\ 0 \end{bmatrix} \quad \text{in } \Omega \times [0, 2T] \tag{3.2.15}$$

$$\begin{bmatrix} 0 & n_i \\ -n_i & 0 \end{bmatrix} \begin{bmatrix} \theta \\ q_i \end{bmatrix} = \begin{bmatrix} \bar{q} \\ -n_i\bar{\theta} \end{bmatrix} \quad \begin{array}{l} \text{on } \Gamma_q \times [0, 2T] \\ \text{on } \Gamma_\theta \times [0, 2T] \end{array} \tag{3.2.16}$$

$$\begin{bmatrix} -\gamma\rho & 0 \\ 0 & 0 \end{bmatrix} \begin{bmatrix} \theta \\ q_i \end{bmatrix} = \begin{bmatrix} -\gamma\rho\,\theta_0 \\ 0 \end{bmatrix} \quad \text{in } \Omega, \, t = 0 \tag{3.2.17}$$

or, in a compact form:

$$\mathbf{M}_{II} \mathbf{z}_{II} = \mathbf{a}_{II} \quad \text{in } \Omega \times [0, 2T] \tag{3.2.18}$$

$$\mathbf{B}_{II} \mathbf{z}_{II} = \mathbf{g}_{II} \quad \text{on } \Gamma \times [0, 2T] \tag{3.2.19}$$

$$\mathbf{T}_{II} \mathbf{z}_{II} = \mathbf{h}_{II} \quad \text{in } \Omega, \, t = 0 \tag{3.2.20}$$

or, finally, in the condensed form:

$$\mathbf{N}_{II} \mathbf{z}_{II} = \mathbf{f}_{II} \tag{3.2.21}$$

At last, consider the following one-field operatorial formulation:

$$\gamma\rho\frac{\partial\theta}{\partial t} - \frac{\partial}{\partial x_i}\left(k\frac{\partial\theta}{\partial x_i}\right) = a \quad \text{in } \Omega \times [0, 2T] \tag{3.2.22}$$

$$-k\frac{\partial\theta}{\partial x_i}n_i = \bar{q} \quad \text{on } \Gamma_q \times [0, 2T] \tag{3.2.23}$$

$$\theta = \theta_0 \quad \text{in } \Omega, \, t = 0 \tag{3.2.24}$$

where the temperature field must satisfy a priori the boundary condition on Γ_θ, i.e.

$$\theta = \bar{\theta} \quad \text{on } \Gamma_\theta \times [0, 2T] \tag{3.2.25}$$

In a compact form, the one-field problem reads:

$$\mathbf{M}_{III} \mathbf{z}_{III} = \mathbf{a}_{III} \quad \text{in } \Omega \times [0, 2T] \tag{3.2.26}$$

$$\mathbf{B}_{III} \mathbf{z}_{III} = \mathbf{g}_{III} \quad \text{on } \Gamma \times [0, 2T] \tag{3.2.27}$$

$$\mathbf{T}_{III} \mathbf{z}_{III} = \mathbf{h}_{III} \quad \text{in } \Omega, \, t = 0 \tag{3.2.28}$$

or, in a condensed form:

$$\mathbf{N}_{III} \mathbf{z}_{III} = \mathbf{f}_{III} \tag{3.2.29}$$

3.3 Variational formulations for the heat conduction problem

The operator $\mathbf{N}_i$, $i = I, II, III$, proves to be symmetric with respect to the following non-degenerate *convolutive bilinear form*:

$$\langle \mathbf{z}'_i, \mathbf{N}_i \, \mathbf{z}''_i \rangle_c = \int_\Omega \mathbf{z}'_i * \mathbf{M}_i \, \mathbf{z}''_i \, \mathrm{d}\Omega + \int_\Gamma \mathbf{z}'_i * \mathbf{B}_i \, \mathbf{z}''_i \, \mathrm{d}\Gamma + \int_\Omega \mathbf{z}'_i(0) \mathbf{T}_i \, \mathbf{z}''_i(2T) \, \mathrm{d}\Omega \qquad (3.3.1)$$

where $\mathbf{z}'_i$ and $\mathbf{z}''_i$ are arbitrary vectors, belonging to the domain of $\mathbf{N}_i$, $i = I, II, III$, and the symbol $*$ represents the following convolution product with respect to the time variable: given any two functions $f(x_r, t)$ and $g(x_r, t)$, the basic convolutive integral (in the sense of Lebesgue) is defined as:

$$f(x_r, t) * g(x_r, t) = \int_0^t f(x_r, t - \tau) \, g(x_r, \tau) \, d\tau = \int_0^t g(x_r, t - \tau) \, f(x_r, \tau) \, d\tau = g(x_r, t) * f(x_r, t) \qquad (3.3.2)$$

Therefore, the compact problem

$$\mathbf{N}_i \, \mathbf{z}_i = \mathbf{f}_i \qquad (3.3.3)$$

with $i = I, II, III$, proves to be equivalent[1] to the following variational formulation:

$$\mathcal{F}^c_i(\mathbf{z}_i) = \operatorname*{stat}_{\mathbf{z}'_i} \mathcal{F}^c_i(\mathbf{z}'_i) \qquad (3.3.4)$$

where

$$\begin{aligned} \mathcal{F}^c_i(\mathbf{z}'_i) = \ & \frac{1}{2} \langle \mathbf{z}'_i, \mathbf{N}_i \, \mathbf{z}'_i \rangle_c - \langle \mathbf{z}'_i, \mathbf{f}_i \rangle_c \\ = \ & \frac{1}{2} \int_\Omega \mathbf{z}'_i * \mathbf{M}_i \, \mathbf{z}'_i \, \mathrm{d}\Omega + \frac{1}{2} \int_\Gamma \mathbf{z}'_i * \mathbf{B}_i \, \mathbf{z}'_i \, \mathrm{d}\Gamma + \frac{1}{2} \int_\Omega \mathbf{z}'_i(0) \mathbf{T}_i \, \mathbf{z}'_i(2T) \, \mathrm{d}\Omega \\ & - \int_\Omega \mathbf{a}_i * \mathbf{z}'_i \, \mathrm{d}\Omega - \int_\Gamma \mathbf{g}_i * \mathbf{z}'_i \, \mathrm{d}\Gamma - \int_\Omega \mathbf{h}_i \, \mathbf{z}'_i(2T) \, \mathrm{d}\Omega \end{aligned} \qquad (3.3.5)$$

$\mathbf{z}'_i$ being any admissible vector, that is, any vector belonging to the domain of $\mathbf{N}_i$, and $\mathbf{z}_i$ the solution of the problem, with $i = I, II, III$.

Also, the operator $\mathbf{N}_i$, $i = I, II, III$, proves to be symmetric with respect to the following non-degenerate *biconvolutive bilinear form*:

$$\langle \mathbf{z}'_i, \mathbf{N}_i \, \mathbf{z}''_i \rangle_{cc} = \int_\Omega \mathbf{z}'_i * r * \mathbf{M}_i \, \mathbf{z}''_i \, \mathrm{d}\Omega + \int_\Gamma \mathbf{z}'_i * r * \mathbf{B}_i \, \mathbf{z}''_i \, \mathrm{d}\Gamma + \int_\Omega \mathbf{z}'_i(0) \mathbf{T}_i \, \mathbf{z}''_i(2T) \, \mathrm{d}\Omega \qquad (3.3.6)$$

where $\mathbf{z}'_i$ and $\mathbf{z}''_i$ are arbitrary vectors, belonging to the domain of $\mathbf{N}_i$, $i = I, II, III$. The biconvolutive integral is defined as:

$$f(x_r, t) * r * g(x_r, t) = \int_0^t \int_0^{t-\tau} r(t - \tau - \eta) \, r(x_r, \eta) \, f(x_r, \tau) \, d\tau dt \qquad (3.3.7)$$

where $r(t)$ recalls the relaxation function governing the linear viscoelastic problem. In the following numerical examples, $r(t)$ will assume different forms.

---

[1]The equivalence is guaranteed by the non-degeneracy of the chosen bilinear form on the domain and on the range of the operator $\mathbf{N}_i$ (see Magri (1974), for instance).

Therefore, the compact problem (3.3.3) proves to be equivalent to the following variational formulation:

$$\mathcal{F}_i^{cc}(\mathbf{z}_i) = \underset{\mathbf{z}_i'}{\text{stat}} \, \mathcal{F}_i^{cc}(\mathbf{z}_i') \tag{3.3.8}$$

where

$$
\begin{aligned}
\mathcal{F}_i^{cc}(\mathbf{z}_i') =& \frac{1}{2}\langle \mathbf{z}_i', \mathbf{N}_i \, \mathbf{z}_i'\rangle_{cc} - \langle \mathbf{z}_i', \mathbf{f}_i\rangle_{cc} \\
=& \frac{1}{2}\int_\Omega \mathbf{z}_i' * r * \mathbf{M}_i \, \mathbf{z}_i' \, \mathrm{d}\Omega + \frac{1}{2}\int_\Gamma \mathbf{z}_i' * r * \mathbf{B}_i \, \mathbf{z}_i' \, \mathrm{d}\Gamma + \frac{1}{2}\int_\Omega \mathbf{z}_i'(0)\mathbf{T}_i \, \mathbf{z}_i'(2T) \, \mathrm{d}\Omega \\
& - \int_\Omega \mathbf{a}_i * r * \mathbf{z}_i' \, \mathrm{d}\Omega - \int_\Gamma \mathbf{g}_i * r * \mathbf{z}_i' \, \mathrm{d}\Gamma - \int_\Omega \mathbf{h}_i \, \mathbf{z}_i'(2T) \, \mathrm{d}\Omega
\end{aligned} \tag{3.3.9}
$$

$\mathbf{z}_i'$ being any admissible vector, that is, any vector belonging to the domain of $\mathbf{N}_i$, and $\mathbf{z}_i$ the solution of the problem, with $i = I, II, III$.

Gurtin's formulation

Gurtin's functional and Split Gurtin functional are now introduced for the resolution of the linear transient heat conduction problem.

Gurtin's formulation leads to a Total Potential Energy type functional (dependant only on the temperature field). Using the convolutive bilinear form, it assumes the general form:

$$
\begin{aligned}
\mathcal{F}_c^G(\theta') =& \frac{1}{2}\int_\Omega \theta' * \gamma\rho\frac{\partial\theta'}{\partial t}\, d\Omega + \frac{1}{2}\int_\Omega k\frac{\partial\theta'}{\partial x_i} * \frac{\partial\theta'}{\partial x_i}\, d\Omega + \frac{1}{2}\int_\Omega \gamma\rho\theta' \cdot \theta'(0)\, d\Omega \\
& - \int_\Omega \theta' * a\, d\Omega + \int_{\Gamma_q} \theta' * \bar{q}\, d\Gamma - \int_\Omega \theta' \cdot \gamma\rho\theta_0\, d\Omega
\end{aligned} \tag{3.3.10}
$$

while, using the biconvolutive bilinear form over the time interval $[0, 2T]$, it assumes the form:

$$
\begin{aligned}
\mathcal{F}_{cc}^G(\theta') =& \frac{1}{2}\int_\Omega \theta' * r * \gamma\rho\frac{\partial\theta'}{\partial t}\, d\Omega + \frac{1}{2}\int_\Omega k\frac{\partial\theta'}{\partial x_i} * r * \frac{\partial\theta'}{\partial x_i}\, d\Omega + \frac{1}{2}\int_\Omega (\gamma\rho\theta' * r) \cdot \theta'(0)\, d\Omega \\
& - \int_\Omega \theta' * r * a\, d\Omega + \int_{\Gamma_q} \theta' * r * \bar{q}\, d\Gamma - \int_\Omega (\theta' * r) \cdot \gamma\rho\theta_0\, d\Omega \\
=& \frac{1}{2}\int_\Omega \gamma\rho\theta' * (r(0)\theta' + \dot{r} * \theta')\, d\Omega + \frac{1}{2}\int_\Omega k\frac{\partial\theta'}{\partial x_i} * r * \frac{\partial\theta'}{\partial x_i}\, d\Omega \\
& - \int_\Omega \theta' * r * a\, d\Omega + \int_{\Gamma_q} \theta' * r * \bar{q}\, d\Gamma - \int_\Omega (\theta' * r) \cdot \gamma\rho\theta_0\, d\Omega
\end{aligned} \tag{3.3.11}
$$

under the constraints $\theta(x_r, t) = \bar{\theta}(x_r, t)$ on Γ_θ.

3.4   Reformulation of the problem

By decomposing the time domain into two equal subintervals (Section 3.4.1), it is possible to derive a min-max variational formulation, as shown in Subsection 3.4.2, using the convolutive bilinear form. And in Subsection 3.4.3, through the use of the biconvolutive bilinear form, a minimum-stationarity principle is presented, which is later applied to the numerical examples.

3.4.1 Decomposition of the time domain

In Carini and Mattei (2015) five new variational formulations for the viscoelastic problem are derived, one of which is of the minimum type. Here, these new formulations are conveniently interpreted as obtained from the decomposition of the time interval $[0, 2T]$ into two sub-intervals ($[0, T]$ and $[T, 2T]$) of equal length. Accordingly, the variables of the problem, $\theta(t)$, $p_i(t)$ and $q_i(t)$, formally double as follows:

$$\theta(t) = \begin{cases} \theta_1(t) & \text{for } t \in [0, T] \\ \theta_2(t) & \text{for } t \in [T, 2T] \end{cases} \tag{3.4.1}$$

$$p_i(t) = \begin{cases} p_{1_i}(t) & \text{for } t \in [0, T] \\ p_{2_i}(t) & \text{for } t \in [T, 2T] \end{cases} \tag{3.4.2}$$

$$q_i(t) = \begin{cases} q_{1_i}(t) & \text{for } t \in [0, T] \\ q_{2_i}(t) & \text{for } t \in [T, 2T] \end{cases} \tag{3.4.3}$$

Hereafter, the subscript 1 will refer to quantities defined over the time subinterval $[0, T]$, whereas the subscript 2 will be used in reference to quantities defined over $[T, 2T]$.

3.4.2 Min-max variational formulation of Tonti's type with the convolutive bilinear form

With the purpose to provide the expression of the functional $\mathcal{F}_i$, with $i = I, II, III$, given by (3.3.5), in terms of the six new variables, let us start considering the case $i = I$. In particular, let us begin from the decomposition, over the two time subintervals, of the term $\int_\Omega \mathbf{z}'_I * \mathbf{M}_I \, \mathbf{z}'_I \, \mathrm{d}\Omega$, the explicit expression of which is

$$\int_\Omega \mathbf{z}'_I * \mathbf{M}_I \, \mathbf{z}'_I \, \mathrm{d}\Omega = \gamma\rho \int_\Omega \frac{\partial \theta'}{\partial t} * \theta' \, \mathrm{d}\Omega + \int_\Omega \frac{\partial q'_i}{\partial x_i} * \theta' \, \mathrm{d}\Omega + \int_\Omega p'_i * k \, p'_i \, \mathrm{d}\Omega$$
$$- 2 \int_\Omega p'_i * q'_i \, \mathrm{d}\Omega - \int_\Omega \frac{\partial \theta'}{\partial x_i} * q'_i \, \mathrm{d}\Omega \tag{3.4.4}$$

The first integral, involving a partial differentiation with respect to the time variable, may be split in several ways. Two possible decompositions are:

$$\text{(a)} \quad \gamma\rho \int_\Omega \frac{\partial \theta'}{\partial t} * \theta' \, \mathrm{d}\Omega = 2\gamma\rho \int_\Omega \int_0^T \frac{\partial \theta'(t)}{\partial t} \theta'(2T - t) \, \mathrm{d}t \, \mathrm{d}\Omega - C \tag{3.4.5}$$

$$\text{(b)} \quad \gamma\rho \int_\Omega \frac{\partial \theta'}{\partial t} * \theta' \, \mathrm{d}\Omega = 2\gamma\rho \int_\Omega \int_T^{2T} \frac{\partial \theta'(t)}{\partial t} \theta'(2T - t) \, \mathrm{d}t \, \mathrm{d}\Omega + C \tag{3.4.6}$$

where C has the following expression:

$$C = \gamma\rho \int_\Omega \int_0^T \frac{\partial \theta'(t)}{\partial t} \theta'(2T - t) \, \mathrm{d}t \, \mathrm{d}\Omega - \gamma\rho \int_\Omega \int_T^{2T} \frac{\partial \theta'(t)}{\partial t} \theta'(2T - t) \, \mathrm{d}t \, \mathrm{d}\Omega \tag{3.4.7}$$

By means of an integration by parts, the latter turns into

$$C = \gamma\rho \int_\Omega \theta'^2(T) \, \mathrm{d}\Omega - \gamma\rho \int_\Omega \theta'(2T) \, \theta'(0) \, \mathrm{d}\Omega \tag{3.4.8}$$

Hence, equations (3.4.5) and (3.4.6) become, respectively

(a) $\quad \gamma \rho \int_\Omega \frac{\partial \theta'}{\partial t} * \theta' \, d\Omega = 2\gamma\rho \int_\Omega \int_0^T \frac{\partial \theta_1'(t)}{\partial t} \theta_2'(2T - t) \, dt \, d\Omega - \gamma\rho \int_\Omega \theta_1'^2(T) \, d\Omega$

$$+ \gamma\rho \int_\Omega \theta_2'(2T) \, \theta_1'(0) \, d\Omega \quad (3.4.9)$$

(b) $\quad \gamma \rho \int_\Omega \frac{\partial \theta'}{\partial t} * \theta' \, d\Omega = 2\gamma\rho \int_\Omega \int_T^{2T} \frac{\partial \theta_2'(t)}{\partial t} \theta_1'(2T - t) \, dt \, d\Omega + \gamma\rho \int_\Omega \theta_2'^2(T) \, d\Omega$

$$- \gamma\rho \int_\Omega \theta_2'(2T) \, \theta_1'(0) \, d\Omega \quad (3.4.10)$$

where the aforementioned notation regarding the subscripts 1 and 2 has been applied. It is worth noting that other decompositions, different from (3.4.9) and (3.4.10), may be used, but the ones illustrated above have the advantage of leading to a negative quadratic term in θ_1 (see (3.4.9)) and a positive quadratic term in θ_2 (see (3.4.10)), fundamental to enunciate maximum and minimum variational principles, respectively.

The remaining terms in (3.4.4), not involving differentiation in time, can be decomposed by simply splitting the time integrals. For instance, the second term in (3.4.4) turns into

$$\int_\Omega \frac{\partial q_i'}{\partial x_i} * \theta' \, d\Omega = \int_\Omega \int_0^T \frac{\partial q_{1_i}'(t)}{\partial x_i} \theta_2'(2T - t) \, d\Omega + \int_\Omega \int_T^{2T} \frac{\partial q_{2_i}'(t)}{\partial x_i} \theta_1'(2T - t) \, d\Omega \qquad (3.4.11)$$

Therefore, the following variational principles hold:

$$\mathcal{F}_I^a(\theta_1, \theta_2, p_{1_i}, p_{2_i}, q_{1_i}, q_{2_i}) = \max_{\theta_1'} \underset{\theta_2', p_{1_i}', p_{2_i}', q_{1_i}', q_{2_i}'}{\text{stat}} \mathcal{F}_I^a(\theta_1', \theta_2', p_{1_i}', p_{2_i}', q_{1_i}', q_{2_i}') \qquad (3.4.12)$$

$$\mathcal{F}_I^b(\theta_1, \theta_2, p_{1_i}, p_{2_i}, q_{1_i}, q_{2_i}) = \min_{\theta_2'} \underset{\theta_1', p_{1_i}', p_{2_i}', q_{1_i}', q_{2_i}'}{\text{stat}} \mathcal{F}_I^b(\theta_1', \theta_2', p_{1_i}', p_{2_i}', q_{1_i}', q_{2_i}') \qquad (3.4.13)$$

where here and henceforth the superscripts a and b refer, respectively, to decompositions (3.4.9) and (3.4.10). The expression of functionals $\mathcal{F}_I^a$ and $\mathcal{F}_I^b$ is not given explicitly for the sake of brevity.

The same procedure applied to the functional $\mathcal{F}_{II}$ leads to the following variational principles:

$$\mathcal{F}_{II}^a(\theta_1, \theta_2, q_{1_i}, q_{2_i}) = \min_{\theta_1'} \underset{\theta_2', q_{1_i}', q_{2_i}'}{\text{stat}} \mathcal{F}_{II}^a(\theta_1', \theta_2', q_{1_i}', q_{2_i}') \qquad (3.4.14)$$

$$\mathcal{F}_{II}^b(\theta_1, \theta_2, q_{1_i}, q_{2_i}) = \max_{\theta_2'} \underset{\theta_1', q_{1_i}', q_{2_i}'}{\text{stat}} \mathcal{F}_{II}^b(\theta_1', \theta_2', q_{1_i}', q_{2_i}') \qquad (3.4.15)$$

Finally, for $\mathcal{F}_{III}$ the following results hold:

$$\mathcal{F}_{III}^a(\theta_1, \theta_2) = \max_{\theta_1'} \underset{\theta_2'}{\text{stat}} \mathcal{F}_{III}(\theta_1', \theta_2') \qquad (3.4.16)$$

$$\mathcal{F}_{III}^b(\theta_1, \theta_2) = \min_{\theta_2'} \underset{\theta_1'}{\text{stat}} \mathcal{F}_{III}(\theta_1', \theta_2') \qquad (3.4.17)$$

with

$$\mathcal{F}^a_{III}(\theta'_1, \theta'_2) = \gamma\rho \int_\Omega \frac{\partial\theta'_1}{\partial t} \circ \theta'_2 \, d\Omega + \frac{1}{2}\int_\Omega \frac{\partial\theta'_1}{\partial x_i} \circ k\frac{\partial\theta'_2}{\partial x_i} \, d\Omega + \frac{1}{2}\int_\Omega \frac{\partial\theta'_2}{\partial x_i} \circ k\frac{\partial\theta'_1}{\partial x_i} \, d\Omega$$
$$- \int_\Omega \theta'_1 \circ a_2 \, d\Omega - \int_\Omega a_1 \circ \theta'_2 \, d\Omega + \int_{\Gamma_q} \theta'_1 \circ \overline{q}_2 \, d\Gamma$$
$$+ \int_{\Gamma_q} \overline{q}_1 \circ \theta'_2 \, d\Gamma - \gamma\rho \int_\Omega \theta_0 \, \theta'_2(2T) \, d\Omega + \gamma\rho \int_\Omega \theta'_1(0)\theta'_2(2T) \, d\Omega$$
$$- \frac{1}{2}\gamma\rho \int_\Omega (\theta'_1(T))^2 \, d\Omega \tag{3.4.18}$$

$$\mathcal{F}^b_{III}(\theta'_1, \theta'_2) = \gamma\rho \int_\Omega \theta'_1 \circ \frac{\partial\theta'_2}{\partial t} \, d\Omega + \frac{1}{2}\int_\Omega \frac{\partial\theta'_1}{\partial x_i} \circ k\frac{\partial\theta'_2}{\partial x_i} \, d\Omega + \frac{1}{2}\int_\Omega \frac{\partial\theta'_1}{\partial x_i} \circ k\frac{\partial\theta'_2}{\partial x_i} \, d\Omega$$
$$- \int_\Omega \theta'_1 \circ b_2 \, d\Omega - \int_\Omega b_1 \circ \theta'_2 \, d\Omega + \int_{\Gamma_q} \theta'_1 \circ \overline{q}_2 \, d\Gamma$$
$$+ \int_{\Gamma_q} \overline{q}_1 \circ \theta'_2 \, d\Gamma - \gamma\rho \int_\Omega \theta_0 \, \theta'_2(2T) \, d\Omega + \frac{1}{2}\gamma\rho \int_\Omega (\theta'_2(T))^2 \, d\Omega \tag{3.4.19}$$

where θ'_1 and θ'_2 are admissible fields, satisfying boundary condition (3.2.5), and the symbol $\circ$ represents the convolution product restricted to the subinterval $[0, T]$ or $[T, 2T]$, e.g.

$$\theta'_1 \circ a_2 = \int_0^T \theta'_1(t) \, a_2(2T - t) \, dt = \int_T^{2T} \theta'_1(2T - t) \, a_2(t) \, dt \tag{3.4.20}$$

It is interesting to observe that imposing the stationarity of the functionals $\mathcal{F}^a_i$, $i = I, II, III$, with respect to θ'_1 yields also the following continuity condition:

$$\theta_1(T) = \theta_2(T) \tag{3.4.21}$$

whereas, for the functionals $\mathcal{F}^b_i$, $i = I, II, III$, the same condition is obtained by imposing the stationarity with respect to the variable θ'_2.

A min-max variational principle can be achieved by considering the sum of the functionals $\mathcal{F}^a_{III}$ and $\mathcal{F}^b_{III}$. In effect,

$$\mathcal{F}^c_{III} = \mathcal{F}^a_{III} + \mathcal{F}^b_{III} = \gamma\rho \int_\Omega \frac{\partial\theta'_1}{\partial t} \circ \theta'_2 \, d\Omega + \gamma\rho \int_\Omega \theta'_1 \circ \frac{\partial\theta'_2}{\partial t} \, d\Omega + 2\int_\Omega \frac{\partial\theta'_1}{\partial x_i} \circ k\frac{\partial\theta'_2}{\partial x_i} \, d\Omega$$
$$- 2\int_\Omega \theta'_1 \circ a_2 \, d\Omega - 2\int_\Omega a_1 \circ \theta'_2 \, d\Omega + 2\int_{\Gamma_q} \theta'_1 \circ \overline{q}_{2_i} n_i \, d\Gamma$$
$$+ 2\int_{\Gamma_q} \overline{q}_{1_i} n_i \circ \theta'_2 \, d\Gamma - 2\gamma\rho \int_\Omega \theta_0 \, \theta'_2(2T) \, d\Omega + \gamma\rho \int_\Omega \theta'_1(0)\theta'_2(2T) \, d\Omega$$
$$- \frac{1}{2}\gamma\rho \int_\Omega (\theta'_1(T))^2 \, d\Omega + \frac{1}{2}\gamma\rho \int_\Omega (\theta'_2(T))^2 \, d\Omega \tag{3.4.22}$$

is such that the following variational principle holds:

$$\mathcal{F}^c_{III}(\theta_1, \theta_2) = \min_{\theta'_2} \max_{\theta'_1} \mathcal{F}^c_{III}(\theta'_1, \theta'_2) \tag{3.4.23}$$

In particular, the stationarity of the above functional with respect to θ_1' and θ_2' leads, respectively, to

$$\delta_{\theta_1'} \mathcal{F}_{III}^c = 0 \Rightarrow \begin{cases} \gamma\rho\frac{\partial\theta_2'}{\partial t} - \frac{\partial}{\partial x_i}\left(k\frac{\partial\theta_2'}{\partial x_i}\right) = a_2 & \text{in } \Omega \times [T, 2T] \\ -k\frac{\partial\theta_2'}{\partial x_i}n_i = \bar{q}_2 & \text{on } \Gamma_q \times [T, 2T] \end{cases} \tag{3.4.24}$$

$$\delta_{\theta_2'} \mathcal{F}_{III}^c = 0 \Rightarrow \begin{cases} \gamma\rho\frac{\partial\theta_1'}{\partial t} - \frac{\partial}{\partial x_i}\left(k\frac{\partial\theta_1'}{\partial x_i}\right) = a_1 & \text{in } \Omega \times [0, T] \\ -k\frac{\partial\theta_1'}{\partial x_i}n_i = \bar{q}_1 & \text{on } \Gamma_q \times [0, T] \\ \theta_1'(0) = \theta_0 & \text{in } \Omega \\ \theta_1'(T) = \theta_2'(T) & \text{in } \Omega \end{cases} \tag{3.4.25}$$

3.4.3 Split Gurtin's formulation with biconvolutive bilinear form and min-stat principle

The splitting of the integration time interval $[0, 2T]$ will be analysed using only the biconvolutive bilinear form, for which the typical splitting assumes the form:

$$\langle\theta', \theta'\rangle_{cc} = \theta' \circ r \circ \theta' = \int_0^T \int_0^T r(2T-\tau-\eta)\,\theta_1'(\tau)\,\theta_1'(t)\,d\tau dt + 2\cdot\int_0^T \int_T^{2T-t} r(2T-\tau-\eta)\,\theta_2'(\tau)\,\theta_1'(t)\,d\tau dt \tag{3.4.26}$$

Function $r(t)$ is defined as follows:

$$r(t) := \int_0^\infty \phi(\alpha)e^{-\alpha(2d-t)}\,d\alpha \tag{3.4.27}$$

With ϕ positive and bounded function and $d > T$.

Function $r(t)$ recalls the relaxation function governing the linear viscoelastic problem, in case the relaxation tensor is completely monotonic.

This biconvolutive bilinear form owns the following properties:

$$\theta_1' \circ \dot{r} \circ \theta_1' = \int_0^T \int_0^T \dot{r}(2T-t-\tau)\theta_1'(\tau)\theta_1'(t)\,d\tau\,dt > 0 \tag{3.4.28}$$

$$p_{1_i}' \circ r \circ p_{1_i}' = \int_0^T \int_0^T r(2T-t-\tau)p_{1_i}'(\tau)p_{1_i}'(t)\,d\tau\,dt > 0 \tag{3.4.29}$$

From this new split approach, exploiting symmetry only, Carini and Mattei (2015) were able to derive several saddle-point formulations, the first of which (of the Total Potential Energy type) is used in the following Section for the numerical resolution of the problem:

$$\begin{aligned}
\mathcal{F}_{cc}^{SG}(\theta_1', \theta_2') =&\frac{1}{2}\int_\Omega (\gamma\rho\theta_1' \circ r(0)\theta_2' + \gamma\rho\theta_2' \circ r(0)\theta_1')\,d\Omega \\
&+ \frac{1}{2}\int_\Omega (\theta_1' \circ \dot{r} \circ \gamma\rho\theta_1' + \theta_1' \circ \dot{r} \circ \gamma\rho\theta_2' + \theta_2' \circ \dot{r} \circ \gamma\rho\theta_1')\,d\Omega \\
&+ \frac{1}{2}\int_\Omega \left(k\frac{\partial\theta_1'}{\partial x_i} \circ r \circ \frac{\partial\theta_1'}{\partial x_i} + k\frac{\partial\theta_1'}{\partial x_i} \circ r \circ \frac{\partial\theta_2'}{\partial x_i} + k\frac{\partial\theta_2'}{\partial x_i} \circ r \circ \frac{\partial\theta_1'}{\partial x_i}\right)\,d\Omega \\
&- \int_\Omega (\theta_1' \circ r \circ a_1 + \theta_1' \circ r \circ a_2 + \theta_2' \circ r \circ a_1)\,d\Omega \\
&+ \int_{\Gamma_q} (\theta_1' \circ r \circ \bar{q}_1 + \theta_1' \circ r \circ \bar{q}_2 + \theta_2' \circ r \circ \bar{q}_1)\,d\Gamma \\
&- \int_\Omega (\theta_1' \circ r + \theta_2' \circ r) \cdot \gamma\rho\bar{\theta}_0\,d\Omega
\end{aligned} \tag{3.4.30}$$

By explicitly expressing the convolutive integrals the former functional becomes:

$$
\begin{aligned}
\mathcal{F}_{cc}^{SG}(\theta_1', \theta_2') = & \int_\Omega \int_0^T \gamma\rho\theta_1'(t)r(0)\theta_2'(2T-t)\,dtd\Omega \\
& + \frac{1}{2}\int_\Omega \int_0^T \gamma\rho\theta_1'(t)\int_0^T \dot{r}(2T-t-\tau)\theta_1'(\tau)\,d\tau dtd\Omega \\
& + \int_\Omega \int_0^T \gamma\rho\theta_1'(t)\int_T^{2T-t} \dot{r}(2T-t-\tau)\theta_2'(\tau)\,d\tau dtd\Omega \\
& + \frac{1}{2}\int_\Omega k\int_0^T \frac{\partial\theta_1'(t)}{\partial x_i}\int_0^T r(2T-t-\tau)\frac{\partial\theta_1'(\tau)}{\partial x_i}\,d\tau dtd\Omega \\
& + \int_\Omega k\int_0^T \frac{\partial\theta_1'(t)}{\partial x_i}\int_T^{2T-t} r(2T-t-\tau)\frac{\partial\theta_2'(\tau)}{\partial x_i}\,d\tau dtd\Omega \\
& - \int_\Omega \int_0^T \theta_1'(t)\int_0^T r(2T-t-\tau)a_1(\tau)\,d\tau dtd\Omega \\
& - \int_\Omega \int_0^T \theta_1'(t)\int_T^{2T-t} r(2T-t-\tau)a_2(\tau)\,d\tau dtd\Omega \\
& - \int_\Omega \int_T^{2T} \theta_2'(t)\int_0^{2T-t} r(2T-t-\tau)a_1(\tau)\,d\tau dtd\Omega \\
& + \int_{\Gamma_q} \int_0^T \theta_1'(t)\int_0^T r(2T-t-\tau)\bar{q}_1(\tau)\,d\tau dtd\Gamma \\
& + \int_{\Gamma_q} \int_0^T \theta_1'(t)\int_T^{2T-t} r(2T-t-\tau)\bar{q}_2(\tau)\,d\tau dtd\Gamma \\
& + \int_{\Gamma_q} \int_T^{2T} \theta_2'(t)\int_0^{2T-t} r(2T-t-\tau)\bar{q}_1(\tau)\,d\tau dtd\Gamma \\
& - \int_\Omega \gamma\rho\bar{\theta}_0\int_0^T r(2T-t)\theta_1'(t)\,dtd\Omega - \int_\Omega \gamma\rho\bar{\theta}_0\int_T^{2T} r(2T-t)\theta_2'(t)\,dtd\Omega
\end{aligned}
\tag{3.4.31}
$$

It is possible to notice that, using the biconvolutive bilinear form, one obtains the following principle:

$$
\mathcal{F}_{cc}^{SG}(\theta_1, \theta_2) = \min_{\theta_1'}\operatorname{stat}_{\theta_2'} \mathcal{F}_{cc}^{SG}(\theta_1', \theta_2')
\tag{3.4.32}
$$

Here θ_1, θ_2 are the exact solution of the problem, while θ_1', θ_2' are arbitrary but compatible temperature fields.

3.5   Numerical simulations

Example a: a finite rod of length L and constant cross-sectional area A (Fig. 3.1(a)) with null temperature for $t < 0$ and a prescribed temperature at its ends for $t \geq 0$ will be considered. The spatial discretization is performed with standard finite elements of length l^e with two nodes, with one degree of freedom in each node.

For simplicity, the rod is made of the same homogeneous material.

The rod is subdivided into N finite elements (Fig. 3.1(b)), and $\boldsymbol{\alpha}(t) = [\alpha_1, ..., \alpha_{n_s}]^T$ is the vector on the n_s degrees of freedom of the assembled structure.
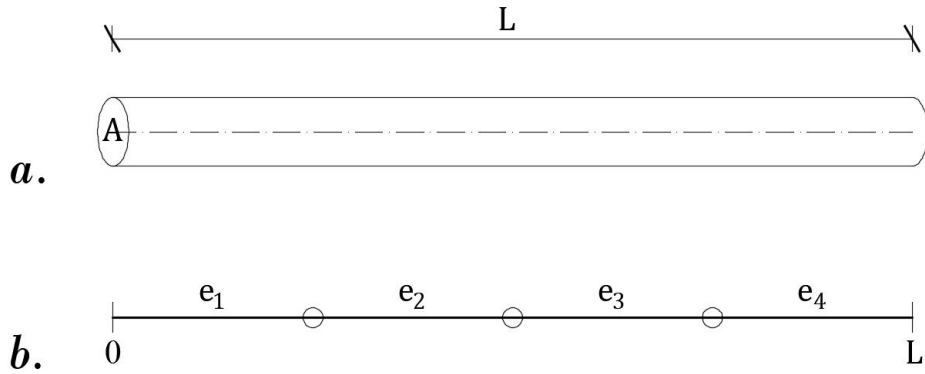
Figure 3.1: Geometrical properties (a) and Finite Element Discretization (b) of the finite rod.

Time discretization. The vector $\boldsymbol{\alpha}(t)$ of the degrees of freedom of the assembled structure is now written as a function of time degrees of freedom $\boldsymbol{\beta}(t) = [\beta_1, ..., \beta_{n_t}]^T$ through shape functions collected into the matrix $\boldsymbol{M}(t)$, with $t \in T$:

$$\boldsymbol{\alpha}(t) = \begin{bmatrix} \alpha_1(t) \\ \cdot \\ \cdot \\ \cdot \\ \alpha_{n_s}(y) \end{bmatrix} = \begin{bmatrix} m_1^T(t) & & \\ & \cdots & \\ & & m_{n_s}^T(y) \end{bmatrix} \cdot \begin{bmatrix} \beta_1(t) \\ \cdots \\ \beta_{n_s}(y) \end{bmatrix} = \boldsymbol{M}(t)\boldsymbol{\beta} \tag{3.5.1}$$

In every example shown here, all the spatial degrees of freedom $\alpha_i(t)$ are discretized with respect to time using the same interpolation functions, i.e

$$\boldsymbol{m}_1 = ... = \boldsymbol{m}_{n_s} = \boldsymbol{m} = [m_1, ..., m_{n_t}]^T \tag{3.5.2}$$

In this way $n_s \times n_t$ is the total number of degrees of freedom.

The initial temperature of the rod and the rate of heat production per unit volume are null, but at its ends the temperature is assigned and constant.
The exact solution of the problem can be found in literature (Carslaw, Jaeger, 1986):

$$\theta(x,t) = \frac{2}{L} \sum_{n=1}^{\infty} e^{-\frac{n^2\pi^2 t}{L^2}} \sin\frac{n\pi x}{L} \left[\int_0^L \bar{\theta} \sin\frac{n\pi x}{L} dx + \frac{n\pi}{L} \int_0^t e^{\frac{n^2\pi^2 \lambda}{L^2}} (\theta_0 - (-1)^n\theta_L)d\lambda \right] \tag{3.5.3}$$

where L is the total length of the rod, $\bar{\theta}$ is the initial temperature and $\theta_0 = \theta_L$ is the assigned temperature at its ends.
For our specific case, we have:

$$\theta(x,t) = \frac{2}{\pi} \sum_{n=1}^{\infty} \frac{1}{n}(\theta_0 - (-1)^n\theta_L) \sin\frac{n\pi x}{L} \left(1 - e^{-\frac{n^2\pi^2 t}{L^2}} \right) \tag{3.5.4}$$

This problem is analysed using different forms for the $r(t)$ function:

1. $r(t) = \int_0^{\infty} e^{-\alpha(2d-t)} d\alpha$ with $d > T$, $d = 1.5T$;

2. $r(t) = t^2 \ln t$;

3. $r(t) = \ln t$;

4. $r(t) = t$;

5. $r(t) = t^2$.

In all examples, negative exponential time shape functions are used:

$$\boldsymbol{m}_e^T = [1,\ e^{-t/t^*},\ e^{-0.1t/t^*},\ ...] \tag{3.5.5}$$

where t^* is a parameter to be defined through the trial error method and has the meaning of a relaxation time.

For each analysis, the internal temperatures (calculated in correspondence of the internal nodes) are plotted versus time for different time intervals and for 2 and 3 degrees of freedom.

First, *Gurtin's formulation* is considered. After spatial discretization (the rod is subdivided into four linear finite elements), Gurtin's functional is reduced to the following form (first using the convolutive bilinear form, than using the biconvolutive bilinear form):

$$
\begin{aligned}
\mathcal{F}_c^G = {} & \frac{l}{3} \int_0^{2T} \theta_2(2T - t)\dot{\theta}_2(t)\, dt + \frac{l}{12} \int_0^{2T} \theta_2(2T - t)\dot{\theta}_3(t)\, dt + \frac{1}{l} \int_0^{2T} \theta_2(2T - t)\theta_2(t)\, dt \\
& - \frac{1}{l} \int_0^{2T} \theta_2(2T - t)\theta_3(t)\, dt + \frac{l}{3} \int_0^{2T} \theta_3(2T - t)\dot{\theta}_3(t)\, dt + \frac{l}{12} \int_0^{2T} \theta_3(2T - t)\dot{\theta}_2(t)\, dt \\
& + \frac{l}{12} \int_0^{2T} \theta_3(2T - t)\dot{\theta}_4(t)\, dt + \frac{1}{l} \int_0^{2T} \theta_3(2T - t)\theta_3(t)\, dt - \frac{1}{l} \int_0^{2T} \theta_3(2T - t)\theta_4(t)\, dt \\
& + \frac{l}{3} \int_0^{2T} \theta_4(2T - t)\dot{\theta}_4(t)\, dt + \frac{l}{12} \int_0^{2T} \theta_4(2T - t)\dot{\theta}_3(t)\, dt + \frac{1}{l} \int_0^{2T} \theta_4(2T - t)\theta_4(t)\, dt \\
& - \frac{1}{l} \int_0^{2T} \theta_2(2T - t)\theta_0(t)\, dt - \frac{1}{l} \int_0^{2T} \theta_4(2T - t)\theta_L(t)\, dt \\
& + \frac{l}{3}\theta_2(2T)\theta_2(0)\, dt + \frac{l}{3}\theta_3(2T)\theta_3(0)\, dt + \frac{l}{3}\theta_4(2T)\theta_4(0) \\
& + \frac{l}{12}\theta_2(2T)\theta_3(0) + \frac{l}{12}\theta_3(2T)\theta_2(0) \\
& + \frac{l}{12}\theta_3(2T)\theta_4(0) + \frac{l}{12}\theta_4(2T)\theta_3(0)
\end{aligned}
\tag{3.5.6}
$$

$$\mathcal{F}_{cc}^{G} = \frac{l}{3} \int_0^{2T} \theta_2(t) \int_0^{2T-t} r(2T-t-\tau)\dot{\theta}_2(\tau)\,d\tau\,dt + \frac{l}{12} \int_0^{2T} \theta_2(t) \int_0^{2T-t} r(2T-t-\tau)\dot{\theta}_3(\tau)\,d\tau\,dt$$

$$+ \frac{1}{l} \int_0^{2T} \theta_2(t) \int_0^{2T-t} r(2T-t-\tau)\theta_2(\tau)\,d\tau\,dt - \frac{1}{2l} \int_0^{2T} \theta_2(t) \int_0^{2T-t} r(2T-t-\tau)\theta_3(\tau)\,d\tau\,dt$$

$$+ \frac{l}{3} \int_0^{2T} \theta_3(t) \int_0^{2T-t} r(2T-t-\tau)\dot{\theta}_3(\tau)\,d\tau\,dt + \frac{l}{12} \int_0^{2T} \theta_3(t) \int_0^{2T-t} r(2T-t-\tau)\dot{\theta}_2(\tau)\,d\tau\,dt$$

$$+ \frac{l}{12} \int_0^{2T} \theta_3(t) \int_0^{2T-t} r(2T-t-\tau)\dot{\theta}_4(\tau)\,d\tau\,dt + \frac{1}{l} \int_0^{2T} \theta_3(t) \int_0^{2T-t} r(2T-t-\tau)\theta_3(\tau)\,d\tau\,dt$$

$$- \frac{1}{2l} \int_0^{2T} \theta_3(t) \int_0^{2T-t} r(2T-t-\tau)\theta_2(\tau)\,d\tau\,dt - \frac{1}{2l} \int_0^{2T} \theta_3(t) \int_0^{2T-t} r(2T-t-\tau)\theta_4(\tau)\,d\tau\,dt$$

$$+ \frac{l}{3} \int_0^{2T} \theta_4(t) \int_0^{2T-t} r(2T-t-\tau)\dot{\theta}_4(\tau)\,d\tau\,dt + \frac{l}{12} \int_0^{2T} \theta_4(t) \int_0^{2T-t} r(2T-t-\tau)\dot{\theta}_3(\tau)\,d\tau\,dt$$

$$+ \frac{1}{l} \int_0^{2T} \theta_4(t) \int_0^{2T-t} r(2T-t-\tau)\theta_4(\tau)\,d\tau\,dt - \frac{1}{2l} \int_0^{2T} \theta_4(t) \int_0^{2T-t} r(2T-t-\tau)\theta_3(\tau)\,d\tau\,dt$$

$$- \frac{1}{l} \int_0^{2T} \theta_2(t) \int_0^{2T-t} r(2T-t-\tau)\theta_0(\tau)\,d\tau dt - \frac{1}{l} \int_0^{2T} \theta_4(t) \int_0^{2T-t} r(2T-t-\tau)\theta_L(\tau)\,d\tau dt$$

$$+ \frac{l}{3} \int_0^{2T} \theta_2(t) r(2T-t)\theta_2(0)\,dt + \frac{l}{3} \int_0^{2T} \theta_3(t) r(2T-t)\theta_3(0)\,dt + \frac{l}{3} \int_0^{2T} \theta_4(t) r(2T-t)\theta_4(0)\,dt$$

$$+ \frac{l}{12} \int_0^{2T} \theta_2(t) r(2T-t)\theta_3(0)\,d\tau\,dt + \frac{l}{12} \int_0^{2T} \theta_3(t) r(2T-t)\theta_2(0)\,dt$$

$$+ \frac{l}{12} \int_0^{2T} \theta_3(t) r(2T-t)\theta_4(0)\,dt + \frac{l}{12} \int_0^{2T} \theta_4(t) r(2T-t)\theta_3(0)\,dt$$

$$(3.5.7)$$

By performing an integration by parts on the integrals containing a time derivation on the temperature variable and adding the corresponding integrals, the former functional becomes:

$$
\begin{aligned}
\mathcal{F}_{cc}^{G} = &\frac{l}{3} \int_0^{2T} \theta_2(t) \int_0^{2T-t} \dot{r}(2T-t-\tau)\theta_2(\tau)\,d\tau\,dt + \frac{r(0) \cdot l}{3} \int_0^{2T} \theta_2(t)\theta_2(2T-t)\,dt \\
&+ \frac{l}{6} \int_0^{2T} \theta_2(t) \int_0^{2T-t} \dot{r}(2T-t-\tau)\theta_3(\tau)\,d\tau\,dt + \frac{r(0) \cdot l}{6} \int_0^{2T} \theta_2(t)\theta_3(2T-t)\,dt \\
&+ \frac{1}{l} \int_0^{2T} \theta_2(t) \int_0^{2T-t} r(2T-t-\tau)\theta_2(\tau)\,d\tau\,dt - \frac{1}{l} \int_0^{2T} \theta_2(t) \int_0^{2T-t} r(2T-t-\tau)\theta_3(\tau)\,d\tau\,dt \\
&+ \frac{l}{3} \int_0^{2T} \theta_3(t) \int_0^{2T-t} \dot{r}(2T-t-\tau)\theta_3(\tau)\,d\tau\,dt + \frac{r(0) \cdot l}{3} \int_0^{2T} \theta_3(t)\theta_3(2T-t)\,dt \\
&+ \frac{l}{6} \int_0^{2T} \theta_3(t) \int_0^{2T-t} \dot{r}(2T-t-\tau)\theta_4(\tau)\,d\tau\,dt + \frac{r(0) \cdot l}{6} \int_0^{2T} \theta_3(t)\theta_4(2T-t)\,dt \\
&+ \frac{1}{l} \int_0^{2T} \theta_3(t) \int_0^{2T-t} r(2T-t-\tau)\theta_3(\tau)\,d\tau\,dt - \frac{1}{l} \int_0^{2T} \theta_3(t) \int_0^{2T-t} r(2T-t-\tau)\theta_4(\tau)\,d\tau\,dt \\
&+ \frac{l}{3} \int_0^{2T} \theta_4(t) \int_0^{2T-t} \dot{r}(2T-t-\tau)\theta_4(\tau)\,d\tau\,dt + \frac{r(0) \cdot l}{3} \int_0^{2T} \theta_4(t)\theta_4(2T-t)\,dt \\
&+ \frac{1}{l} \int_0^{2T} \theta_4(t) \int_0^{2T-t} r(2T-t-\tau)\theta_4(\tau)\,d\tau\,dt \\
&- \frac{1}{l} \int_0^{2T} \theta_2(t) \int_0^{2T-t} r(2T-t-\tau)\theta_0(\tau)\,d\tau dt - \frac{1}{l} \int_0^{2T} \theta_4(t) \int_0^{2T-t} r(2T-t-\tau)\theta_L(\tau)\,d\tau dt
\end{aligned}
\tag{3.5.8}
$$

where θ_i, $i = 2, 3, 4$ refers to the temperature of the ith node and l is the length of the single finite element.

In Figure 3.2, the ratio between the temperature at the ith node of the rod at time t and the assigned temperature at its ends θ_L is plotted using the convolutive bilinear form. The time shape functions are of exponential type (3.5.5) with $t^* = 1.667$ days.

The time ranges from 0 to 1-10-20 days and the number of degrees of freedom goes from 2 to 3.

The diagrams show that the method using exponential time shape functions allows a good interpretation of the internal temperature of the rod. The solution is satisfactory, in particular, when longer time ranges are considered.

In figures 3.3-3.7 the results of the method using the biconvolutive bilinear form are presented with the five different forms of the $r(t)$ functions mentioned above. As before, exponential time shape functions allow a acceptable interpretation of thermal behaviour of the rod, expecially for longer time ranges.

Figure 3.2: Numerical results using Gurtin's formulation with the convolutive bilinear form and exponential time shape functions.

Figure 3.3: Numerical results using Gurtin's formulation with the biconvolutive bilinear form and exponential time shape functions. Here, $r(t) = \int_0^\infty e^{-\alpha(2d-t)}\, d\alpha$.

Figure 3.4: Numerical results using Gurtin's formulation with the biconvolutive bilinear form and exponential time shape functions. Here, $r(t) = t^2 \ln t$.
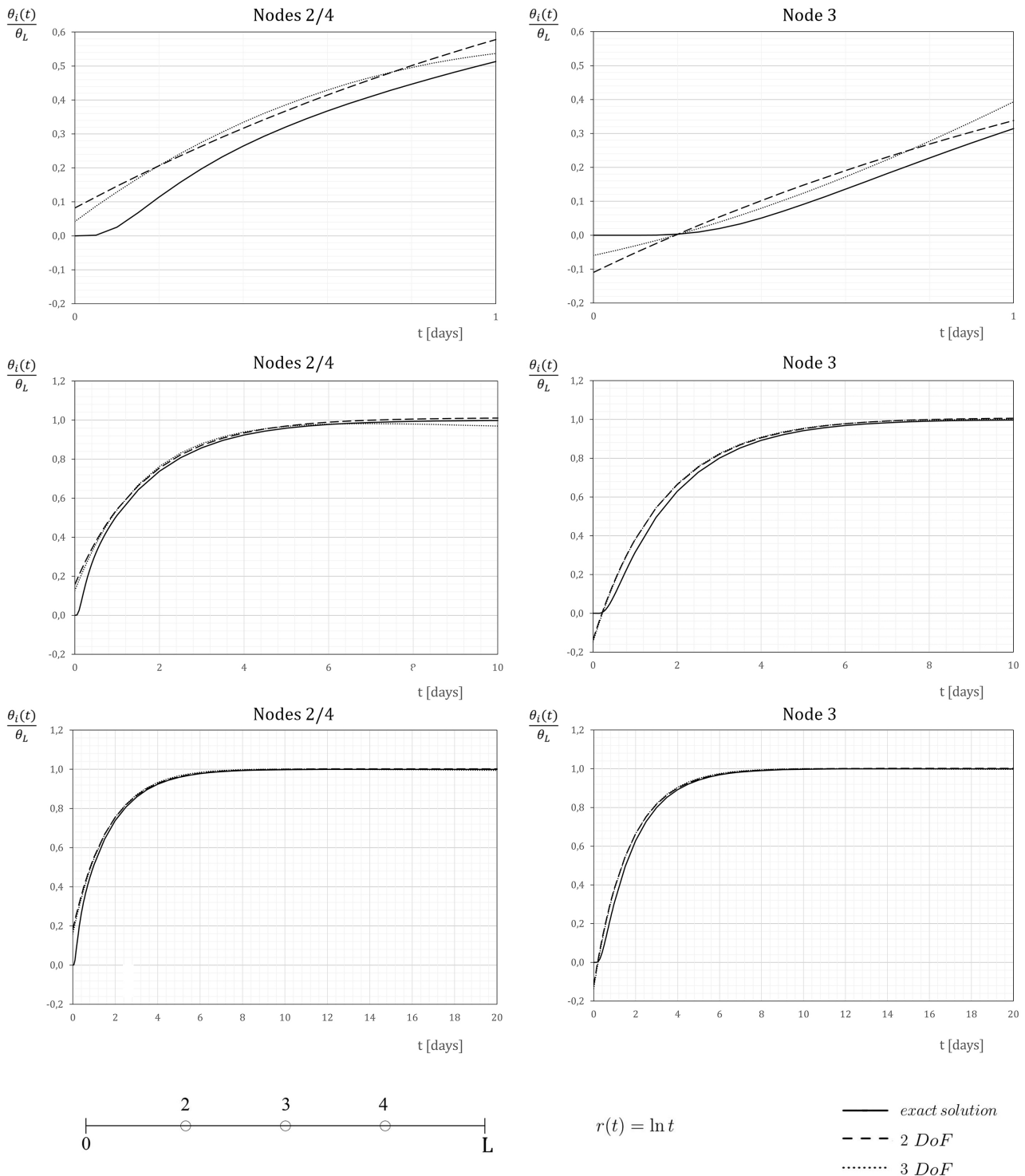
Figure 3.5: Numerical results using Gurtin's formulation with the biconvolutive bilinear form and exponential time shape functions. Here, $r(t) = \ln t$.
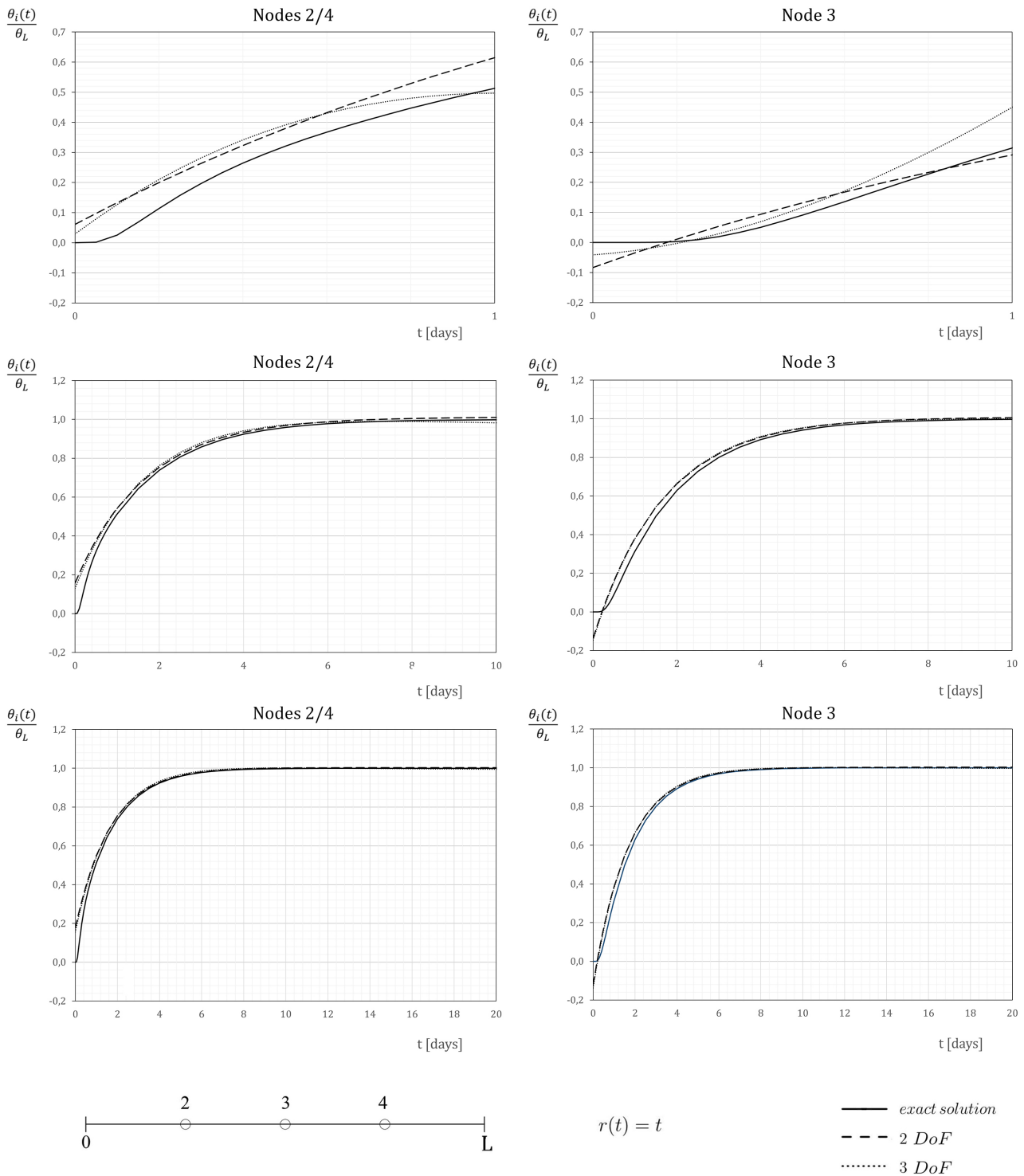
Figure 3.6: Numerical results using Gurtin's formulation with the biconvolutive bilinear form and exponential time shape functions. Here, $r(t) = t$.
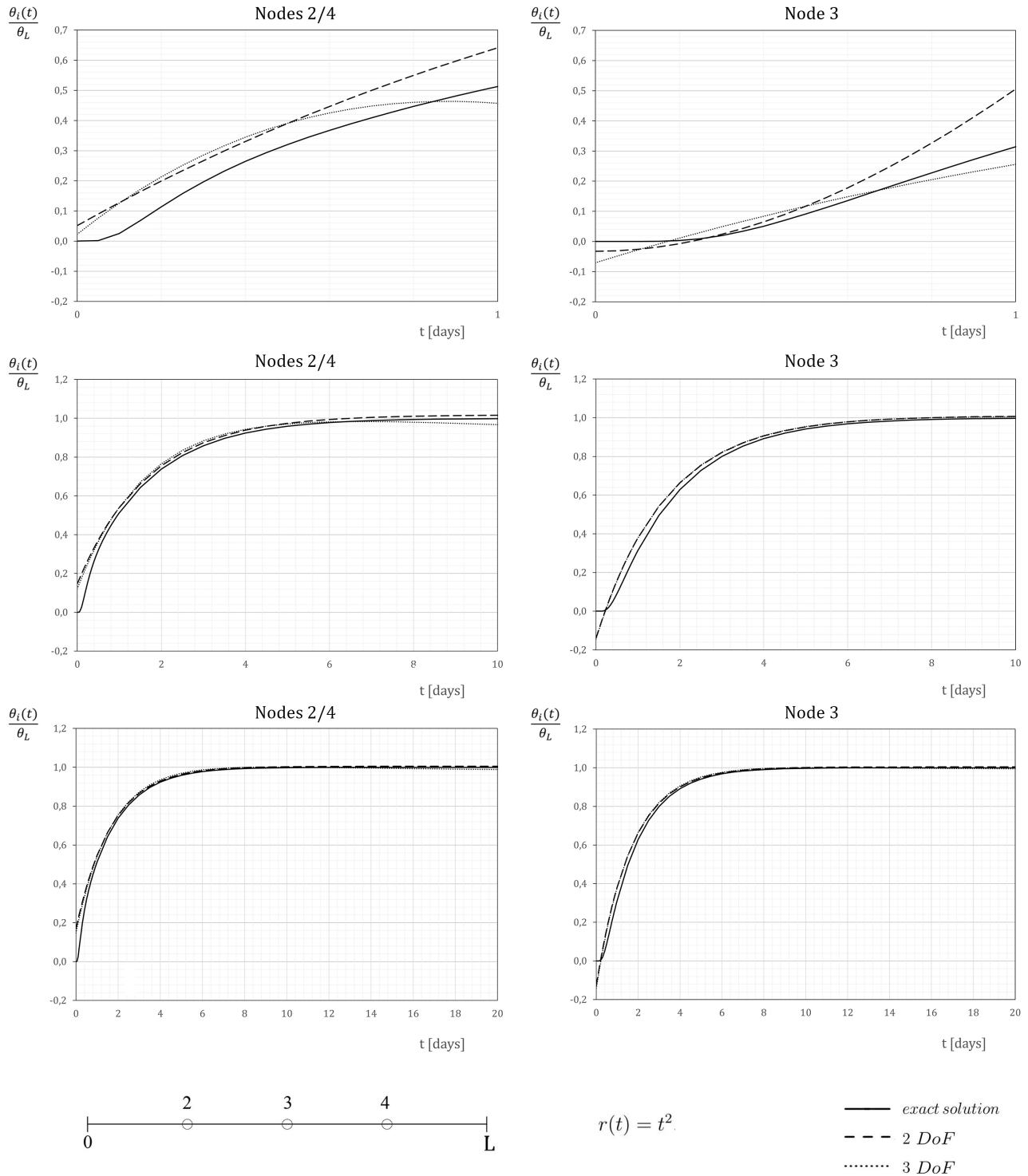
Figure 3.7: Numerical results using Gurtin's formulation with the biconvolutive bilinear form and exponential time shape functions. Here, $r(t) = t^2$.

Now, *split Gurtin's formulation* is considered, using the biconvolutive bilinear form and exponential time shape functions.

It is important to notice that the results obtained using $r(t) = \ln t$ are not reported, since the percentual error is significantly higher compared to the results obtained using the four other functions $r(t)$.

Figures 3.8-3.11 show the numerical results obtained by splitting the time interval 0-20 days into two equal parts. In each figure, in the first line of diagrams, we have considered from 2 to 3 degrees of freedom both in the first and in the second sub-interval and, surprisingly, in all cases, the results are worse than those obtained using Gurtin's functional.

As it is possible to see, a constant time function is sufficient to approximate well the solution in the second sub-interval. So, in the second and third lines of diagrams of each figure, in the first subinterval n_t time degrees of freedom are considered, whereas, in the second one, $n_t - 1$ (in the second line) and $n_t - 2$ (in the third line) time degrees of freedom are considered. It is noted that the solutions improve and the percentual error decreases in each case.

Furthermore it is also possible to analyse the split Gurtin's functional inserting the exact solution in the second subinterval, which is constant from a certain moment, reducing consequently the unknowns only in the first subinterval. If one tries this analysis, the numerical results obtained would slightly differ from the ones already presented in figures 3.8-3.11.
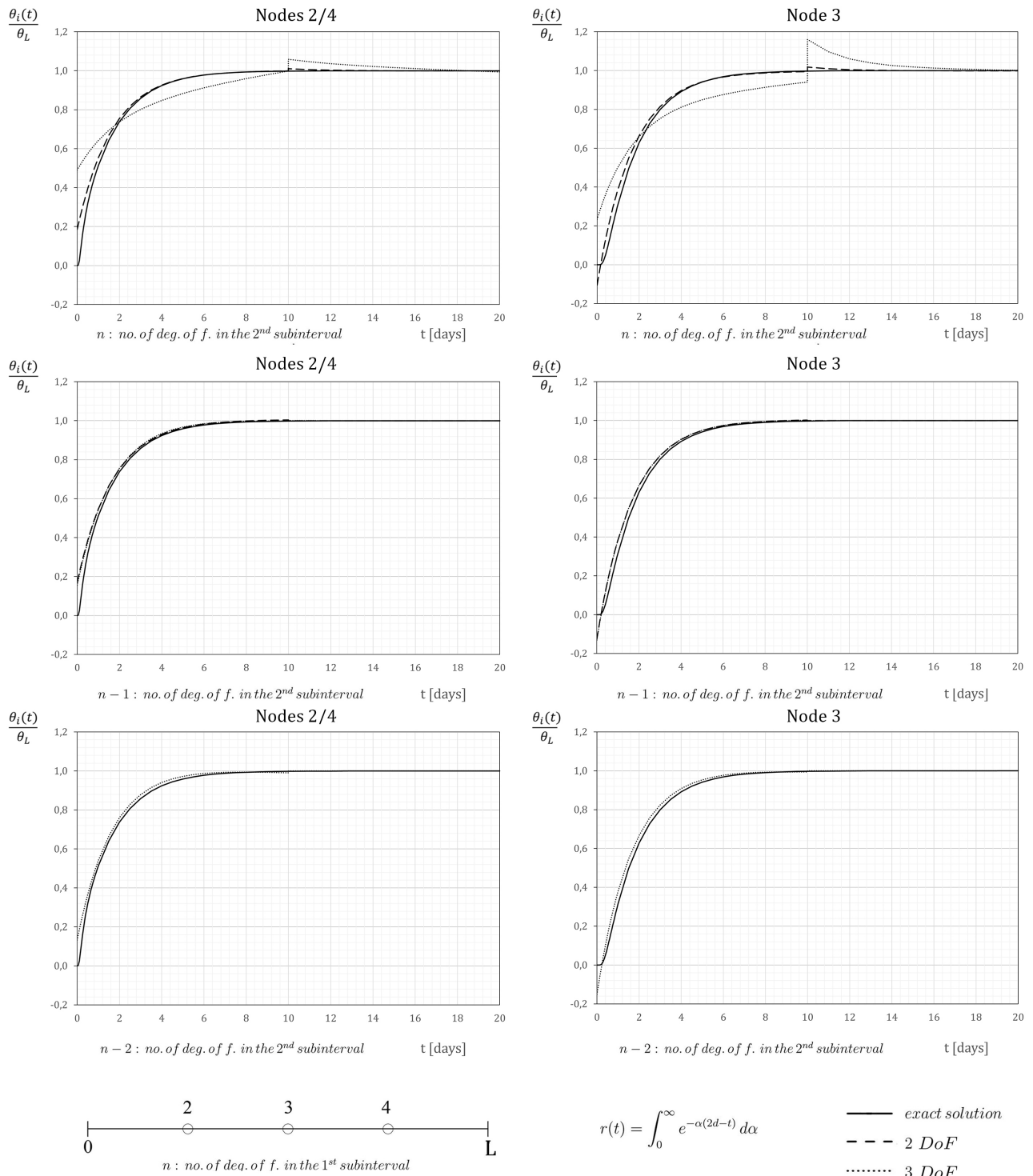
Figure 3.8: Numerical results using split Gurtin's formulation with the biconvolutive bilinear form and exponential time shape functions. Here, $r(t) = \int_0^\infty e^{-\alpha(2d-t)} \, d\alpha$.
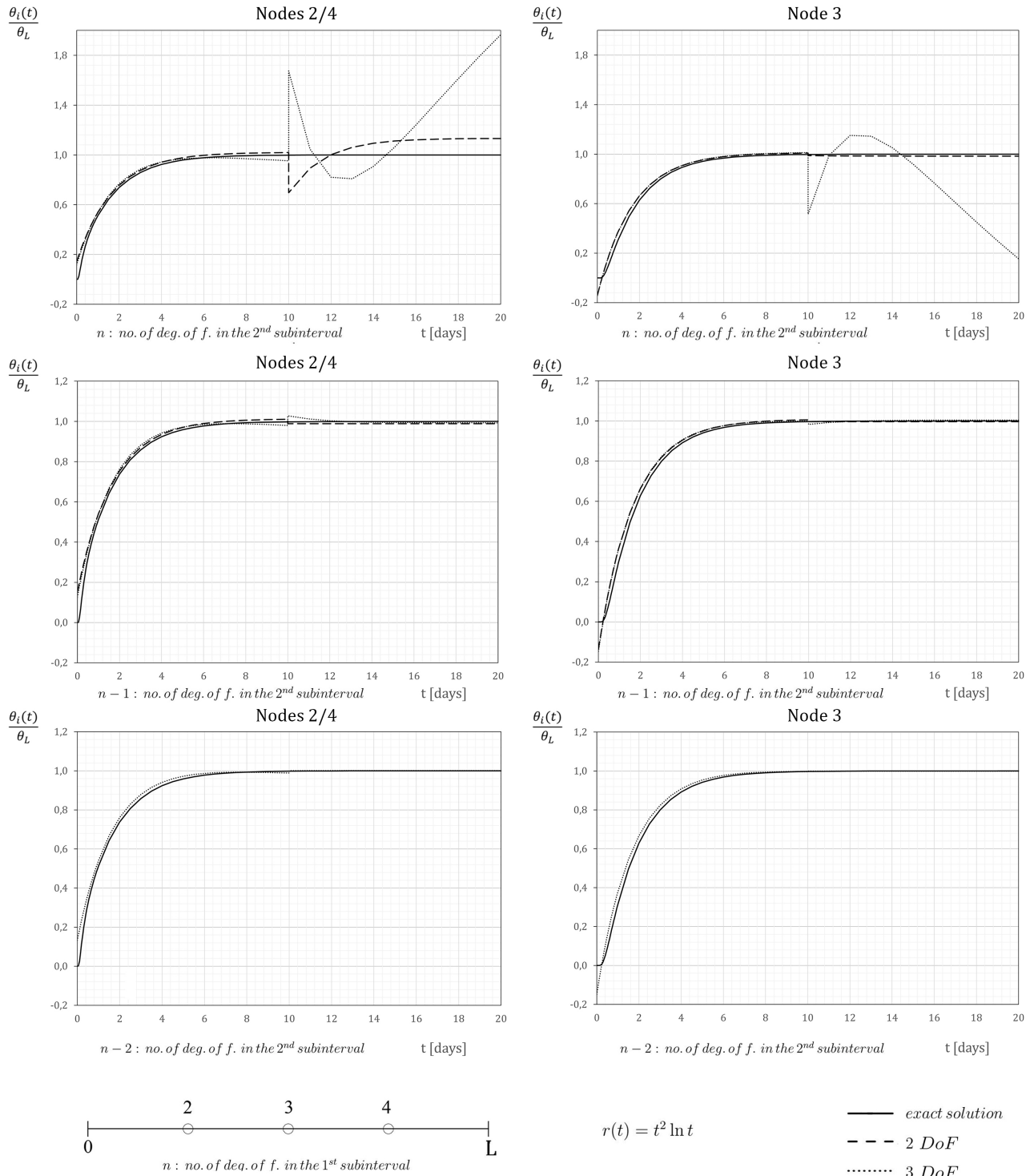
Figure 3.9: Numerical results using split Gurtin's formulation with the biconvolutive bilinear form and exponential time shape functions. Here, $r(t) = t^2 \ln t$.
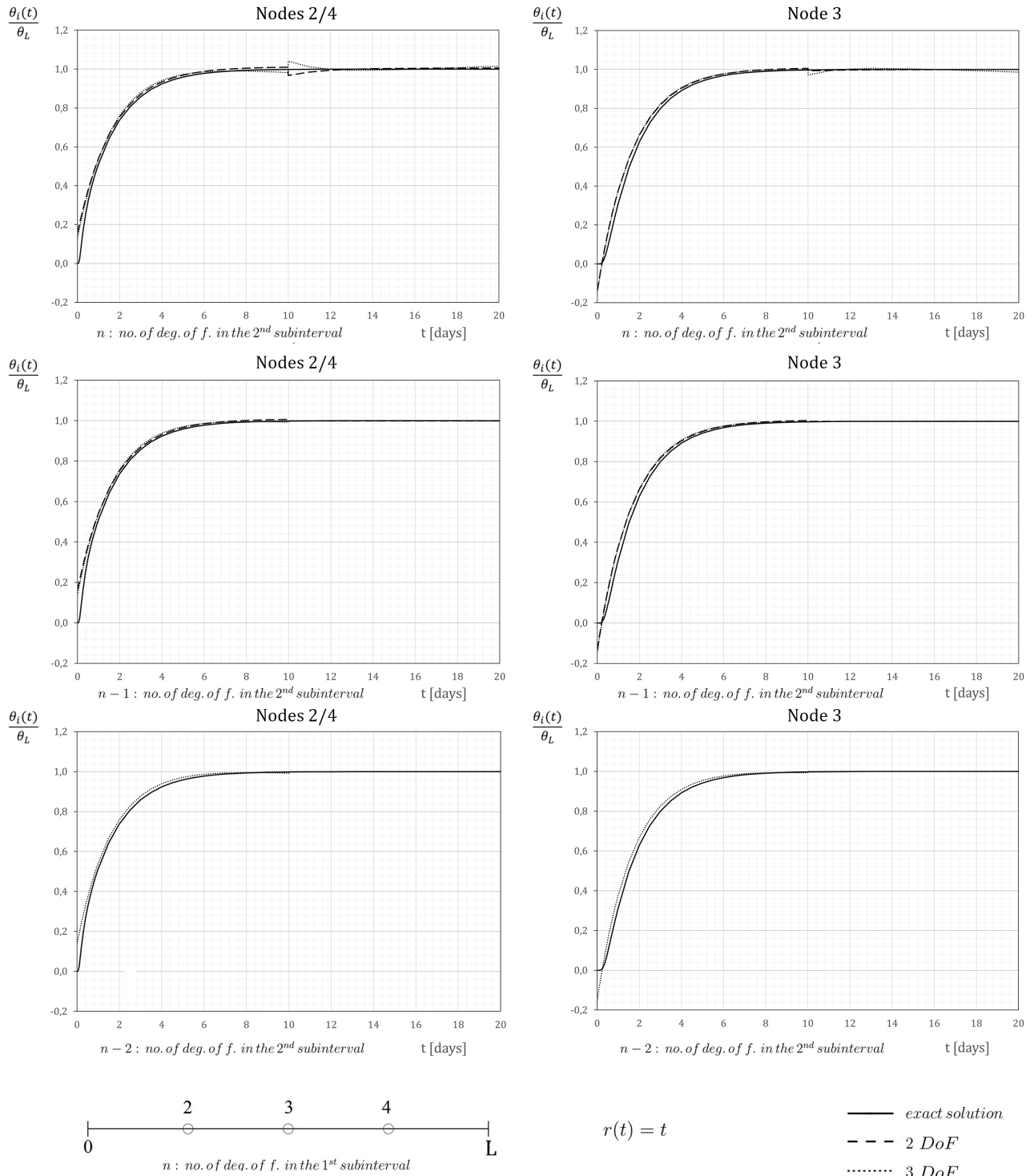
Figure 3.10: Numerical results using split Gurtin's formulation with the biconvolutive bilinear form and exponential time shape functions. Here, $r(t) = t$.
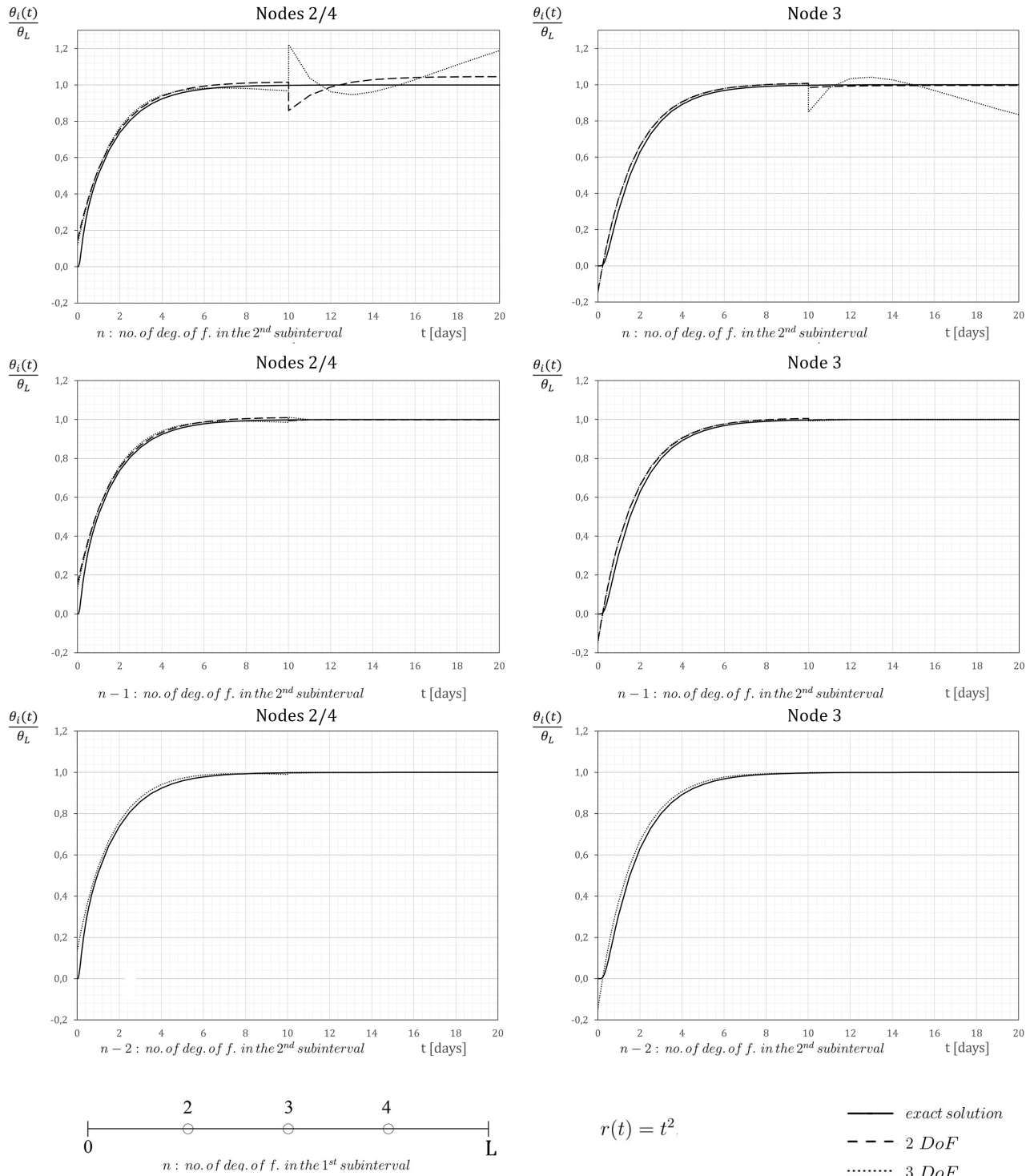
Figure 3.11: Numerical results using split Gurtin's formulation with the biconvolutive bilinear form and exponential time shape functions. Here, $r(t) = t^2$.

Example b: a finite square element with side $L = \pi/10$ with null temperature for $t < 0$ and a prescribed temperature at its boundary for $t \geq 0$ will be considered. The initial temperature is null and there is no heat generation within the solid. The boundary at $y = 0$ is kept at a temperature independent on time $\phi(x)$ and the remaining boundaries are kept at zero temperature (see Fig. 3.12)
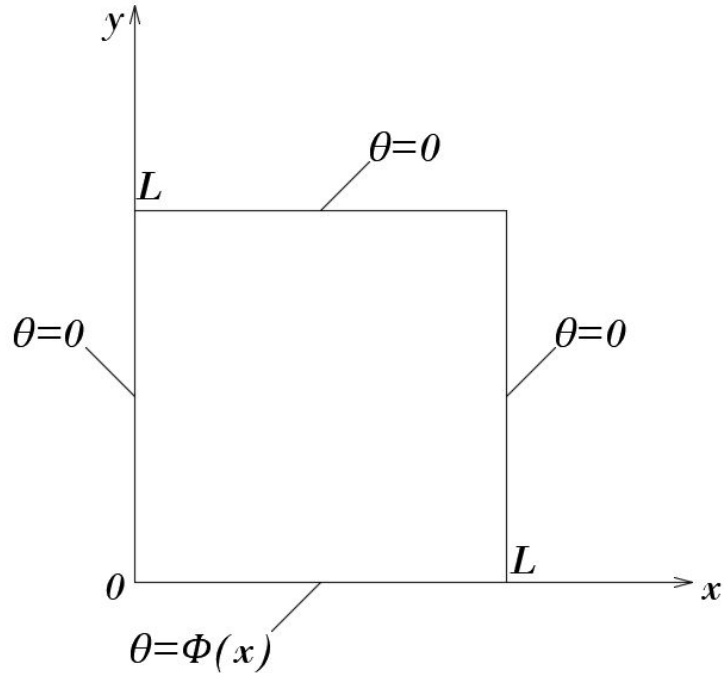
Figure 3.12: A finite square element with side L with null temperature for $t < 0$ and a prescribed temperature at its boundary for $t \geq 0$.

The equations governing the problem are:

$$
\begin{cases}
\dfrac{\partial \theta}{\partial t} - \dfrac{\partial^2 \theta}{\partial x^2} - \dfrac{\partial^2 \theta}{\partial y^2} = 0 & \Omega \times [0, 2T] \\[2ex]
\theta(0, x, y) = 0 & \Omega \times \ t = 0 \\[2ex]
\theta(t, 0, y) = 0 & x = 0 \times [0, 2T] \\[2ex]
\theta(t, L, y) = 0 & x = L \times [0, 2T] \\[2ex]
\theta(t, x, 0) = \phi(t, x) = \sin(20x) & y = 0 \times [0, 2T] \\[2ex]
\theta(t, x, L) = 0 & y = L \times [0, 2T]
\end{cases}
\tag{3.5.9}
$$

The spatial discretization is performed with standard 2-D finite elements of side l^e with four nodes, with one degree of freedom in each node.

For simplicity, the square is made of the same homogeneous material.

The square is subdivided into onehundred forty-four finite elements, and $\boldsymbol{\alpha}(t) = [\alpha_1, ..., \alpha_{n_s}]^T$

is the vector on the n_s degrees of freedom of the assembled structure.

The exact solution of the problem can be found in literature (Ozisik, 1968):

$$\theta(x, y, t) = \frac{4}{ab} \sum_{m=1}^{\infty} \sum_{n=1}^{\infty} \frac{\nu_n}{\beta_m^2 + \nu_n^2} \cdot \sin(\beta_m x) \cdot \sin(\nu_n y) \cdot \left(1 - e^{-(\beta_m^2 + \nu_n^2) \cdot t}\right) \cdot \int_{x'=0}^{a} \phi(x') \cdot \sin(\beta_m x') \, dx' \tag{3.5.10}$$

where a is the horizontal side and b is the vertical side (in this case both equal to L) and

$$\begin{aligned} \nu_n &= \frac{\pi \cdot n}{b} \\ \beta_m &= \frac{\pi \cdot m}{a} \\ \phi(x) &= \sin(20x) \end{aligned} \tag{3.5.11}$$

This problem is analysed using different forms for the $r(t) = t^2$ function.

Negative exponential time shape functions are used:

$$\boldsymbol{m}_e^T = [1, \; e^{-t/t^*}, \; e^{-0.1t/t^*}, \; ...] \tag{3.5.12}$$

where t^* is a parameter to be defined through the trial error method and has the meaning of a relaxation time.

For each analysis, the internal temperature calculated in correspondence of the internal node of coordinates $(L/4, L/4)$ is plotted versus time for different time intervals for 2 degrees of freedom.

First, *Gurtin's formulation* is considered.

Gurtin's functional can be written as follows:

$$\begin{aligned} \mathcal{F}_{cc}^G = &\frac{1}{2} \int_0^L \int_0^L \int_0^{2T} \theta(t) \int_0^{2T-t} r(2T - t - \tau) \dot{\theta}(\tau) \, d\tau \, dt \, dxdy \\ &+ \frac{1}{2} \int_0^L \int_0^L \int_0^{2T} \frac{\partial \theta}{\partial x}(t) \int_0^{2T-t} r(2T - t - \tau) \frac{\partial \theta}{\partial x}(\tau) \, d\tau \, dt \, dxdy \\ &+ \frac{1}{2} \int_0^L \int_0^L \int_0^{2T} \frac{\partial \theta}{\partial y}(t) \int_0^{2T-t} r(2T - t - \tau) \frac{\partial \theta}{\partial y}(\tau) \, d\tau \, dt \, dxdy \end{aligned} \tag{3.5.13}$$

In Figure 3.13, the ratio between the temperature calculated in correspondence of the internal node od coordinates $(L/4, L/4)$ at time t and the assigned temperature at $(L/4, 0)$ is plotted using the biconvolutive bilinear form with $r(t) = t^2$. The time shape functions are of exponential type (3.5.12).

The time ranges from 0-0.002-0.008-0.0012 to 0.030 days and the number of degrees of freedom is 2.

The diagrams show that the method using exponential time shape functions allows a good interpretation of the internal temperature of the rod. The solution is satisfactory using different values of t^*.
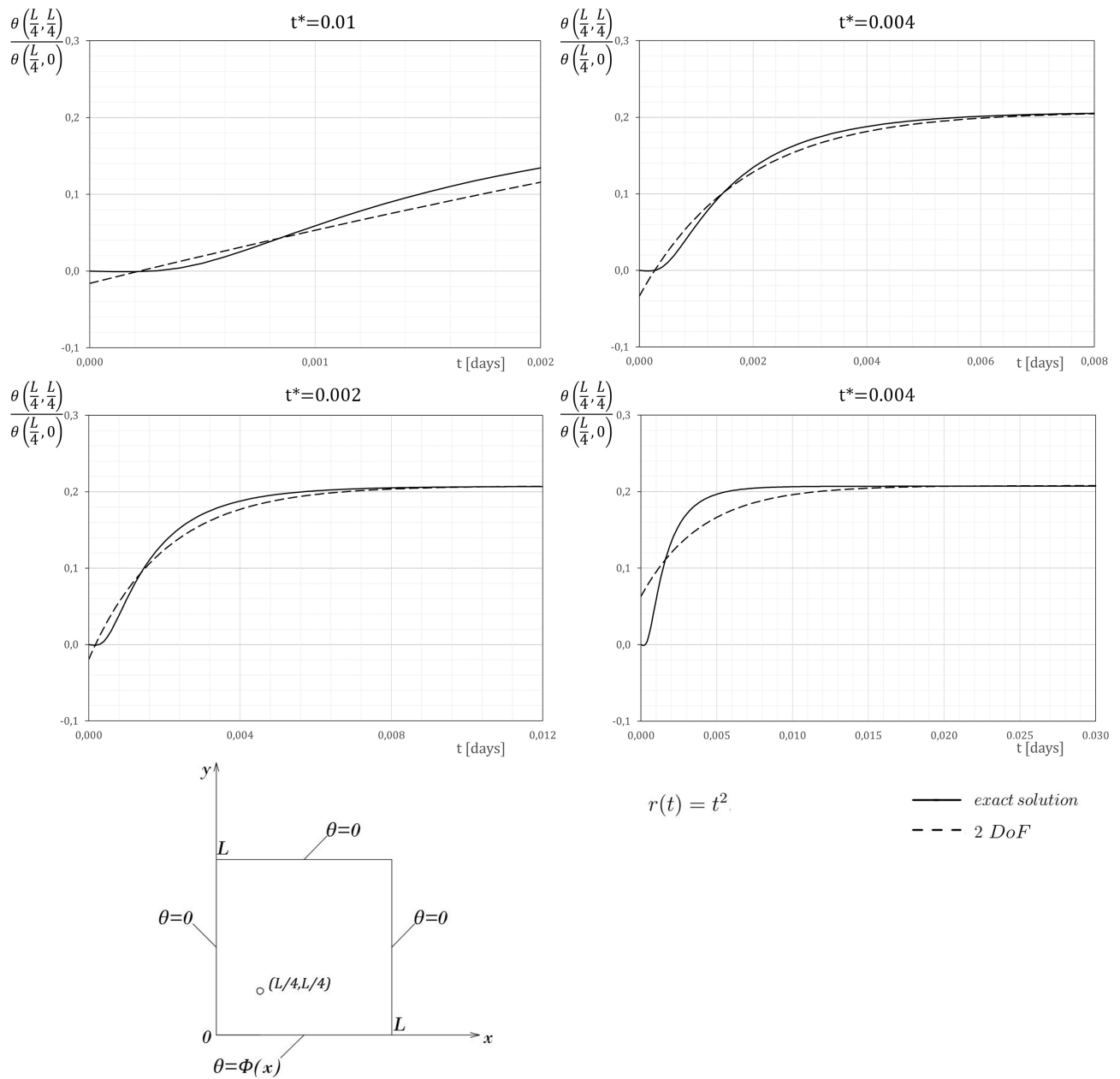
Figure 3.13: Numerical results using Gurtin's formulation with the biconvolutive bilinear form and exponential time shape functions. Here, $r(t) = t^2$.

Now, *split Gurtin's formulation* is considered, using the biconvolutive bilinear form and exponential time shape functions.

Figure 3.14 shows the numerical results obtained by splitting the time interval 0-0.03 days into two equal parts. In the first column, we have considered 2 degrees of freedom both in the first and in the second sub-interval and, surprisingly, the results are worse than those obtained using Gurtin's functional.

As it is possible to see, a constant time function is sufficient to approximate well the solution in the second sub-interval. So, in the second column, in the first subinterval n_t time degrees of freedom are considered, whereas, in the second one, $n_t - 1$ time degrees of freedom are considered. It is noted that the solutions improve.
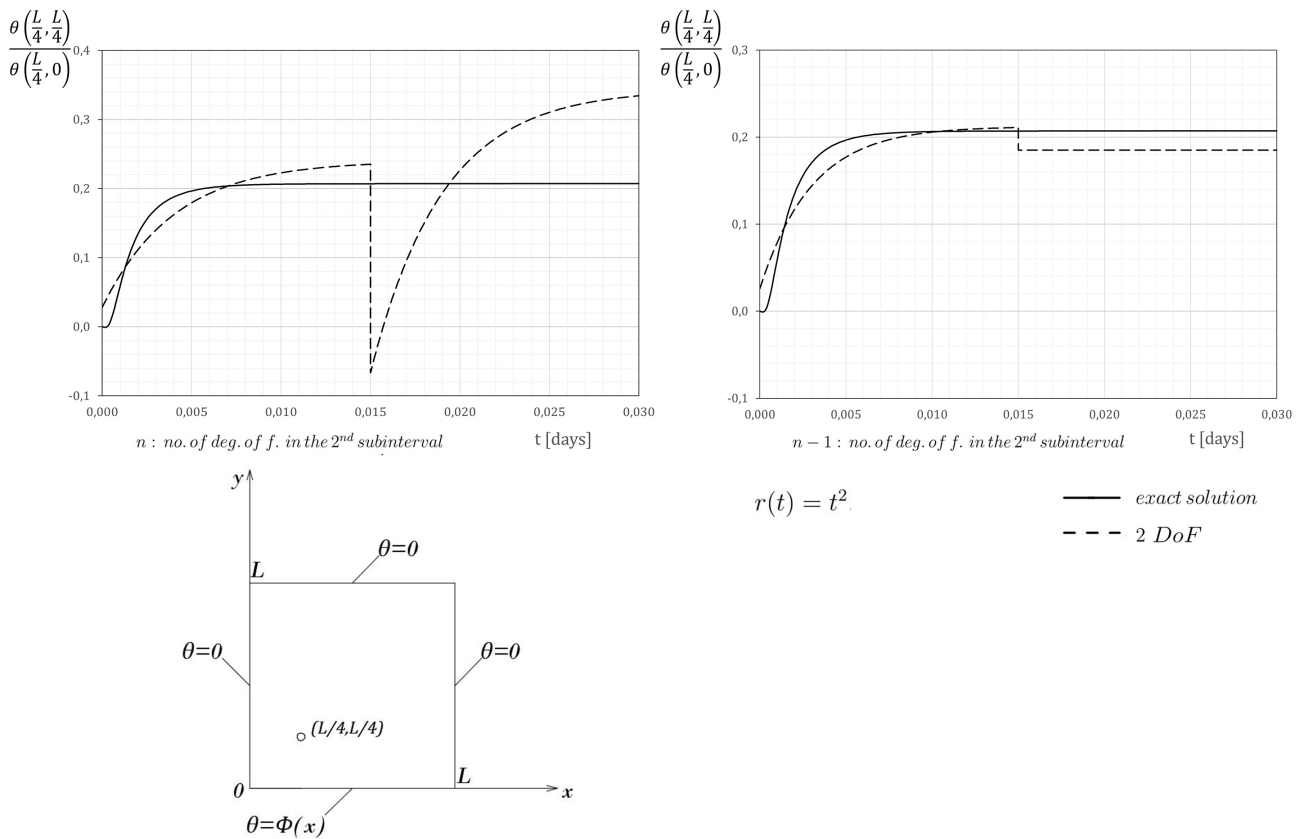
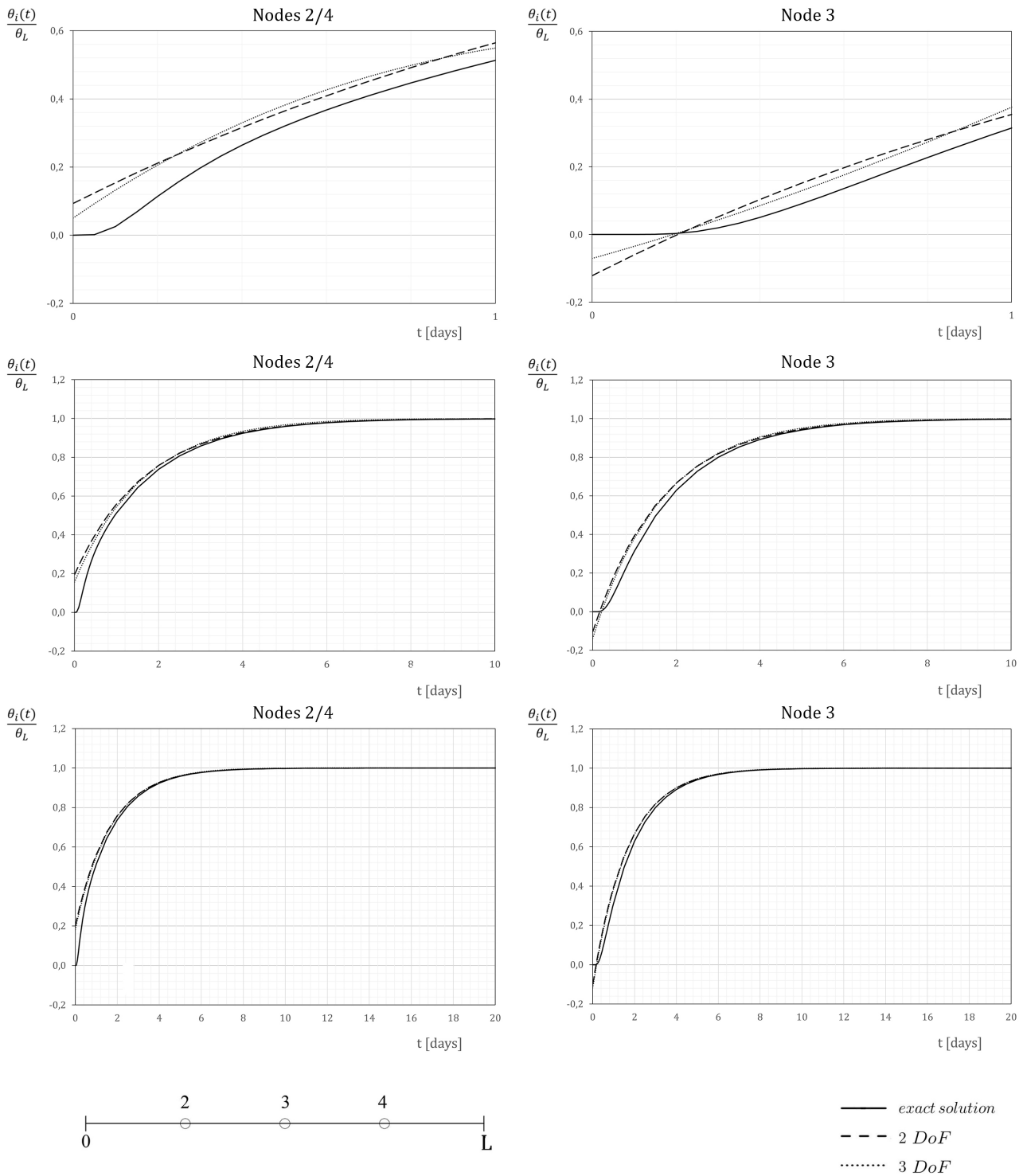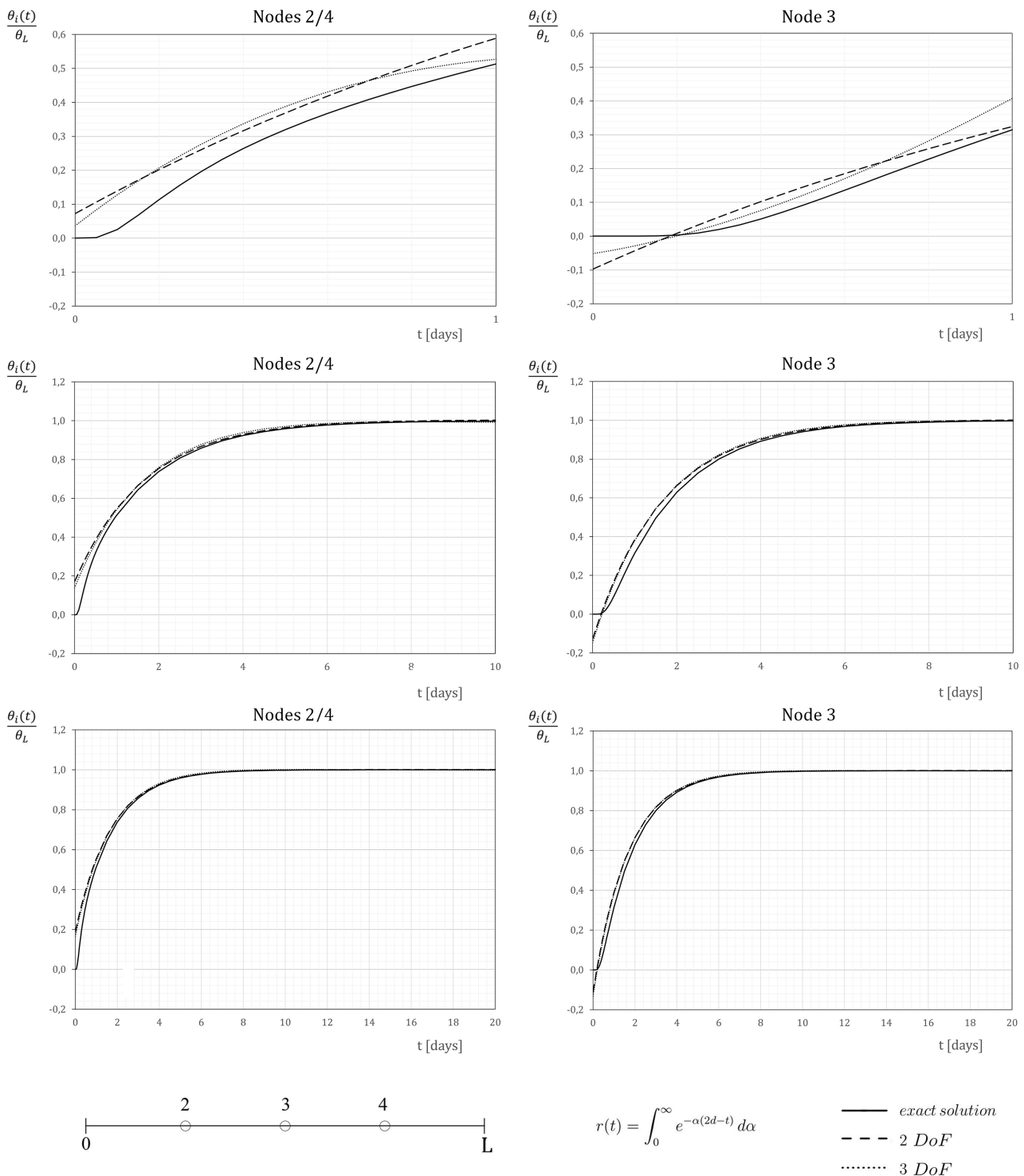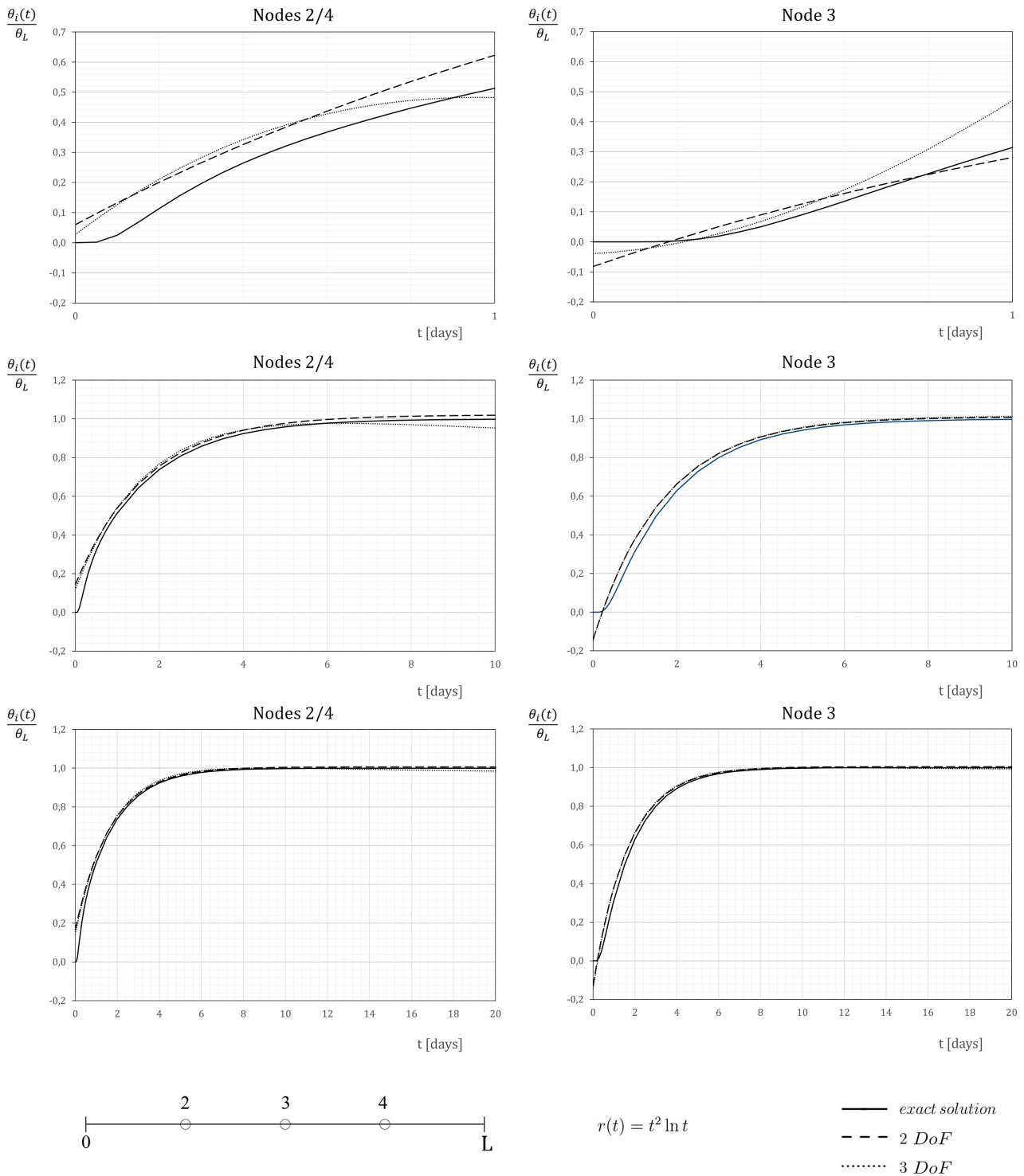Figure 3.14: Numerical results using split Gurtin's formulation with the biconvolutive bilinear form and exponential time shape functions. Here, $r(t) = t^2$.

3.6   Conclusions

To the authors' knowledge, no significant work seems to exist in the literature concerning the use of variational formulations for the numerical solution of the heat conduction problem. In particular, variational principles based on convolutional bilinear forms with respect to time do not seem to have had any place so far in computational procedures for the heat conduction problem. This Chapter aims at investigating the effectiveness of numerical procedures based on these variational formulations.

In particular, another interesting bilinear form is introduced: a so-called biconvolutive bilinear form. Through the exploitation of particular functions (that in this Chapter were called $r(t)$) the operator of the problem proves to be symmetric with respect to this new bilinear form. Also, new variational formulations and extremal principles are thus derived.

Two variational formulations for the linear viscoelastic problem are critically reviewed and numerically tested with the purpose of investigating their effectiveness in the numerical solution of the heat conduction problem.

In the case of finding the solution over a finite time interval in a single step, Gurtin's formulation works well, using only two or three temporal degrees of freedom; by carefully choosing the temporal interpolation functions, Gurtin's formulation leads to interesting numerical results, in particular, using negative exponential time shape functions.

With Gurtin's formulation, the results are more sensitive to the choice made of interpolation functions over time. Polynomial interpolation functions are appropriate only for short time intervals. The interpolation functions that have given the best results are the negative exponential functions because they capture well the typically damped trend of the solution.

The split Gurtin formulation gives good results, expecially for a lower number of temporal degrees of freedom in second subinterval. From the numerical point of view it does not seem to provide any improvement over the unsplit formulation. In any case, the doubling of unknowns makes the method less competitive than the unsplit Gurtin's method. The split Gurtin functional, however, could have advantages from the theoretical point of view, as shown in Carini and Mattei (2015). In fact, the formulation is of the min-max type and, by the adopted time splitting, one is able to isolate a part of the functional that represents the free energy of the system and is, therefore, in general, semidefinite positive.

In the case of the Gurtin and split Gurtin functionals, the problem of the optimal choice of the relaxation time to be used in the negative exponential interpolation functions remains unsolved.

In conclusion, of the three formulations presented here and numerically tested, Gurtin's original formulation seems to be the most effective in numerically solving the linear transient heat conduction problem.

References

Atanackovic, T.M., 1977. A Note on a Variational Principle for Simple Elastic Materials. Acta Mechanica, 26, 331-335.

Atanackovic, T.M., 1978. On a Stationary Principle for Non-Conservative Dynamica Systems. International Journal of Non-Linear Mechanics, 13, 139-143.

Atanackovic, T.M., 1980. A Stationary Principle for Simple Elastic Materials. ZAMM, 60, T 94-T 95.

Atanackovic, T.M., 1983. The Sufficient Condition for an Extremum in the Variational Principle with Non-Commutative Variational Rules. Proceedings of the IUTAM-ISIMM Symposium on Modern Developments in Analytical Mechanics. Atti dell'Accademia delle Scienze di Torino, Supplemento al n. 117, 463-467.

Auchmuty, G., 1988. Variational Principles for Operator Equations and Initial Value Problems. Nonlinear Analysis, Theory, Methods and Applications, 12(5), 531-564.

Auchmuty, G., 1993. Saddle-Points and Existence-Uniqueness for Evolution Equations. Differential and Integral Equations, 6(5), 1161-1171.

Barnsley, M.F., Robinson P.D., 1974. Bivariational Bounds. Proceedings of the Royal Society of London, Ser. A, 338, 527-533.

Barnsley, M.F., Robinson P.D., 1975. Bivariational Bounds Associated with Nonself-adjoint Linear Operators. Proceedings of the Royal Society od Edinburgh, 75A (9), 109-128.

Biot, M.A., 1970. Variational Principles in Heat Transfer (A Unified Lagrangian Analysis of Dissipative Phenomena). Clarendon Press, Oxford.

Carini, A., Feriani, A., 2020. Minimum formulations for linear initial-value problems. Technical reports, Università degli Studi di Brescia.

Cattaneo, C., 1948. On the Conduction of Heat. Atti del Seminario Matematico e Fisico, (Università di Modena), 3, 83-101.

Carini, A.,Diligenti, M., Maier, G., 1991. Boundary integral equation analysis in linear viscoelasticity: variational and saddle point formulations. Computational Mechanics, 39. 8, 87-89.

Carini, A.,Diligenti, M., Salvadori, A., 1999. Implementation of a symmetric boundary element method in transient heat conduction with semi-analytical integrations. International Journal for Numerical Methods in Engineering, 46, 1819-1843.

Carini, A., Mattei, O., 2015. Variational formulations for the linear viscoelastic problem in the time domain. European Journal of Mechanics A/Solids, 54, 146-159.

Carslaw, H.S., Jaeger, J.C., 1959. Conduction of heat in solids. Clarendon Press, Oxford.

Cole, R.J., 1980. Complementary Bivariational Principles for Linear Problems Involving Non-self-Adjoint Operators. Proceedings of the Royal Society of Edinburgh, 86A, 115,128.

Collins, W.D., 1977. Dual Extremum Principles for the Heat Equation. Proceedings of the Royal Society of Edinburgh, 77A, 273-292.

Djukic, Dj., Vujanovic, B., 1971. On a New Variational Principle of Hamiltonian Type for Classical Field Theory. ZAMM, 51, 611-616.

Djukic, Dj., Atanackovic, T.M., 1981. The Least Squares Method: Kantorovich Approach. International Journal of Heat and Mass Transfer, 24, 443-448.

Filippov, V.M., Skorokhodov, A.N., 1977. A Quadratic Functional for the Heat-Conduction Equation. Differential Equations, 13, 770-776.

Finlayson, B.A., 1983. Variational Principles for Heat Transfer in Numerical Properties and Methodologies in Heat Transfer. Proceedings of the Second National Symposium. T.M. shih Editor. Hemisphere Publishing Corporation, 17-31.

Glansdorff, P., Prigogine, I., 1964. On a Generalized Evolution Criterion in Macroscopic Physics. Physica, 30, 351-374.

Glansdorff, P., Prigogine, I., 1965. Variational Properties and Fluctuation Theory. Physica, 31, 1242-1254.

Gurtin, M.E., 1964. Variational principles for linear initial-value problems. Quarterly of Applied Mathematics, 22, 252-256.

Gyarmati, I., 1969. On the Governing Principle of Dissipative Processes and its Extension to Non-Linear Problems. Annals of Physics, 23, 353-378.

Herrera, I., 1974. A General Formulation of Variational Principles. Rep. Inst. Ing. Univ. Nac. Autonoma Mexico, E10.

Herrera, I., Bielak, J., 1976. Dual Variational Principles for Diffusion Equations. Quarterly of Applied Mathematics, 34, 85-102.

Levi-Civita, T., Amaldi, U., 1927. Lezioni di Meccanica Razionale, Parte Seconda. Zanichelli, Bologna.

Magri, F., 1974. Variational Formulations for Every Linear Equation. International Journal of Engineering Science, 12, 537-549.

Morse, P.M., Feshbach, H., 1953. Methods of Theoretical Physics, Vol. I. McGraw-Hill.

Ortiz, P., 1985. A variational Formulation for Convection-Diffusion Problems. International Journal of Engineering Science, 23(7), 717-731.

Ozisik, M.N., 1968. Boundary Value Problems of Heat Conduction. Dover Publications INC., Mineola, New York.

Rafalski. P., 1969. The orthogonal projection method III. Linear viscoelastic problem. Bulletin of the Polish Academy of Sciences: Technical Sciences, 17, 167.

Reiss, R., Haug, E.J., 1978. Extremal principles for linear initial value problems of mathematical physics. International Journal of Engineering Science, 16, 231-251.

Rosen, P., 1953. On Variational Principles for Irreversible Processes. The Journal of Chemical Physics, 21, 1220-1221.

Schlup, W.A., 1975. A Test of the DV Method with an Exactly Soluble Transport Problem. Journal of Physics A: Mathematical and Theoretical, 8, 1373-1378.

Tonti, E., 1973. On the variational formulation for linear initial value problems. Annali di Matematica Pura ed Applicata, Serie Quarta XCV, 331-359.

Tonti, E., 1984. Variational formulations for every nonlinear problem. International Journal of Engineering Science, 22 (11-12), 1343-1371.

Vujanovic, B., 1971. On Approach to Linear and Nonlinear Heat-Transfer Problem Using a Lagrangian. AIAA Journal, 9, 131-135.

Vujanovic, B., 1974. On One Variational Principle for Irreversible Phenomena. Acta Mechanica, 19, 259-275.

Vujanovic, B., 1976. Applications of Analytical Mechanics to Nonconservative Field Theory. Rendiconti del Seminario Matematico Università Politecnico di Torino, 35, 88-95.

Vujanovic, B., 1976. The Practical Use of Gauss' Principle of Least Constraint.Journal of Applied Mechanics, 98, 491-496.

Vujanovic, B., Baclic, B., 1976. Applications of Gauss' Principle of Least Constraint to Nonlinear Heat-Transfer Problem. International Journal of Heat and Mass Transfer, 19, 721-730.

Vujanovic, B., Atanackovic, T.M., 1978. On the Use of Jourdain's Variational Principle in Nonlinear Mechanics and Transport Phenomena. Acta Mechanica, 29, 229-238.

Chapter 4

Time domain analytical bounds to the overall properties of linear viscoelastic composites: explicit bounds to the homogenized relaxation and creep kernels

Notation

Greek and latin letters

- Ω: Region occupied by a solid body;

- Γ_p: Loaded region of the boundary;

- Γ_u: Constrained region of the boundary;

- Γ: External surface of the solid body;

- $n_i(x_r)$: Unit outward normal vector components;

- $u_i(x_r, t)$: Displacement vector components;

- $\epsilon_{ij}(x_r, t)$: Small strain tensor components;

- $\sigma_{ij}(x_r, t)$: Stress tensor components;

- $u_i^0(x_r, t)$: Prescribed displacement vector components;

- $b_j^B(x_r, t)$: Body force vector components;

- $p_j^B(x_r, t)$: Surface traction vector components;

- V: Volume of the body;

- N: Number of phases in the composite material;

- $R^{(i)}$: Relaxation kernel of the phase (i);

- c_i: Volumic fraction of phase (i);

- R^h: Homogenized relaxation function;

- $C^{(i)}$: Creep kernel of the phase (i);

- C^h: Homogenized creep function;

- $R_S^{(i)}$: Shear relaxation kernel of phase (i);

- G_E, G_V: Shear moduli of the viscoelastic material;

- G_{el}: Shear modulus of the elastic material;

- η_V: Viscosity coefficient;

- $C_S^{(i)}$: Shear creep kernel of phase (i);

- $\tau^{(i)}$: Shear stress of phase (i);

- γ: Shear strain;

- ν: Poisson's ratio;

- $R_V^{(i)}$: Volumetric relaxation kernel of phase (i);

- K_E, K_V: Bulk moduli of the viscoelastic material;

- K_{el}: Bulk modulus of the elastic material;

- $C_V^{(i)}$: Volumetric creep kernel of phase (i);

- p: Hydrostatic pressure;

- ϵ^{vol}: Volumetric strain;

- $\delta(t)$: Superimposed displacement.

Symbols

- $*$: Convolution product;

- $\forall$: For all;

- $\tilde{\ }$: Adjoint operator;

- $'$: Admissible term;

- $_1$: Variable defined over the first subinterval;

- $_2$: Variable defined over the second subinterval.

Operators and functions

- $\langle \, \rangle$: Volume average;

- TPE: Total Potential Energy functional;

- TCE: Total Complementary Energy functional.

- $\mathcal{H}(t)$: Heaviside function;

- $_{/i}$: Partial derivative operation;

- $\mathcal{L}$: Laplace transform.

4.1 Introduction

The viscoelastic problem was proved in Gurtin (1963) to be symmetric with respect to the convolutive bilinear form; nevertheless, even exploiting this symmetry, and despite a rather intense research activity (see for example Carini and Mattei, 2015, and references quoted therein), no usable extremum formulation has ever been obtained for linear viscoelasticity in the time domain[1], and only few standard, explicit, analytical bounds in the time domain to the homogenized viscous kernels for viscoelastic composites have been obtained so far. To the best of our knowledge, the main contribution, in this sense, has been given by Huet (1995), where a strict lower bound to the homogenized relaxation kernel has been proposed, together with other bounds, both lower and upper, on the *rates* of both the homogenized creep and relaxation kernels. From these last, Huet (1995) has obtained bounds also for total quantities which, however, appear of difficult practical application. Moreover, the same Huet (1995) points out, in his conclusions, that *"there are still classical results of the elasticity theory that cannot be transferred through to the viscoelastic case (...) For this, true viscoelasticity minimum theorems (...) are still needed"*.

In recent times, Carini and Mattei (2015) were able to exploit older ideas by Staverman and Schwarzl (1952), and by Mandel (1966), to obtain several new min-stat, or even minimum, formulations in viscoelasticity. None of these, unfortunately, could be adopted directly to obtain bounds to the homogenized viscous kernels (see also Mattei and Milton, 2016).

Extremum principles for linear viscoelasticity have been derived from the theory presented in Carini and Mattei (2015), only considering deviatoric strains. From these, upper and lower bounds to the homogenized viscous kernels of viscoelastic composites are derived in a general form. Subsequently, simple explicit expressions are obtained for the simplest case, i.e., first-order bounds for macroscopically isotropic composites with any number of isotropic phases.

The validity of the bounds presented herein is finally checked by comparison with reference numerical solutions, concerning RVEs, obtained by means of Finite Element analyses.

Carini-Mattei Functional

When the aim is to obtain bounds to the homogenized viscous kernels of viscoelastic composites, the loading is chosen in a very specific way.

In fact, when studying RVEs for deriving estimates or bounds to the homogenized viscous kernels of viscoelastic composites, it is customary, and specially convenient, to adopt either "affine" displacements prescribed on the constrained boundary $\Gamma_u = \Gamma$ of the RVE, or surface tractions on $\Gamma_p = \Gamma$ corresponding to uniform stresses in the homogenized solid; for both these cases, a unit-step time history is usually considered, as it will be done in the sequel of this work.

Let us examine, for example (all the other cases could be approached in the same way), the case in which one wants to obtain bounds to the homogenized relaxation kernel. It is convenient to choose as a specific loading for the considered heterogeneous RVE, "affine" prescribed

---

[1]Analytical minimum principles for linear viscoelasticity have been proposed in Rafalski (1969), Reiss and Haug (1978), and Carini et al. (1995). Nevertheless, none of these can be adopted to obtain bounds to the homogenized viscous kernels of viscoelastic composites in the time domain. The formulation proposed in Carini et al. (1995) can be adopted as a basis for time integration, but not for analytical developments leading to homogenization, whereas the other two can be adopted to obtain bounds only to the Laplace transforms of the homogenized viscous kernels.

Cherkaev and Gibiansky (1994), and Milton (1990), formulated extremum principles for linear initial value problems, including the hereditary viscoelastic one, in the frequency domain. The work by Milton (1990) can be extended to the time domain, even though it was not explicitly formulated with this purpose.

displacements on $\Gamma_u = \Gamma$, of the type

$$u_i^0(x_r, t) = \langle \epsilon_{ij}(x_r, t) \rangle x_j = \epsilon_{ij}^0(t) x_j, \quad 0 \le t \le 2T \tag{4.1.1}$$

and zero body forces b_j. This loading corresponds to a known strain $\epsilon_{ij}^0(t)$, independent of space, in the homogenized RVE.

The definition of the loading terms is made complete by assuming the following time history for the loading strain:

$$\langle \epsilon_{ij}(x_r, t) \rangle = \epsilon_{ij}^0(t) = \bar{\epsilon}_{ij} \mathcal{H}(t), \quad 0 \le t \le 2T \tag{4.1.2}$$

$\bar{\epsilon}_{ij}$ being a prescribed constant strain tensor, and $\mathcal{H}(t)$ the Heaviside function; this time history for the applied strains is the one usually adopted in practice to perform relaxation tests. Given any generic function $f(x_r, t)$, we adopt the notation $\langle f(t) \rangle$ to denote the volume average of $f(x_r, t)$ over the solid body Ω, i.e.,:

$$\langle f(t) \rangle = \frac{1}{V} \int_\Omega f(x_r, t) \, d\Omega \tag{4.1.3}$$

In Carini and Mattei (2015), the equations governing the viscoelastic problem are presented:

- Equilibrium equations

$$\begin{aligned} \sigma_{ij/j}(x_r, t) + b_i(x_r, t) = 0 \quad &\text{in } \Omega \times [0, 2T] \\ \sigma_{ij}(x_r, t) n_j(x_r) = p_i(x_r, t) \quad &\text{on } \Gamma_p \times [0, 2T]; \end{aligned} \tag{4.1.4}$$

- Kinematic compatibility

$$\begin{aligned} \epsilon_{ij}(x_r, t) = \frac{1}{2}(u_{i/j}(x_r, t) + u_{j/i}(x_r, t)) \quad &\text{in } \Omega \times [0, 2T] \\ u_i(x_r, t) = u_i^0(x_r, t) \quad &\text{on } \Gamma_u \times [0, 2T]; \end{aligned} \tag{4.1.5}$$

- Constitutive law:

$$\sigma_{ij}(x_r, t) = \int_{0^-}^t R_{ijhk}(x_r, t - \tau) \, d\epsilon_{hk}(x_r, \tau). \tag{4.1.6}$$

Therefore, a Total Potential Energy like functional is defined, based on the convolutive bilinear form (chosen due to the lack of symmetry of the classical bilinear forms).
The convolution integral is written as, considering any two functions $f(x_r, t)$ and $g(x_r, t)$:

$$f(x_r, t) * g(x_r, t) := \int_{0^-}^t f(x_r, t - \tau) dg(x_r, \tau) \tag{4.1.7}$$

Thus, the convolutive bilinear form is written as:

$$(\sigma'_{ij}, \epsilon'_{ij})_c = \sigma'_{ij}(2T) * \epsilon'_{ij}(2T) = \int_{0^-}^{2T} \sigma'_{ij}(2T - t) d\epsilon'_{ij}(t) \tag{4.1.8}$$

The functionals described in Carini and Mattei (2015) are obtained after a splitting procedure of the time interval $[0, 2T]$ into two subinterval of the same amplitude $[0, T]$ and $[T, 2T]$, thus formally doubling the unknowns of the problem:

$$\epsilon_{ij}(t) = \begin{cases} \epsilon_{1ij}(t) & \text{for } t \in [0, T] \\ \epsilon_{21ij}(t) & \text{for } t \in [T, 2T] \end{cases} \tag{4.1.9}$$

$$\sigma_{ij}(t) = \begin{cases} \sigma_{1ij}(t) \text{ for } t \in [0, T] \\ \sigma_{21ij}(t) \text{ for } t \in [T, 2T] \end{cases} \tag{4.1.10}$$

The subscript 1 refers to the quantities defined over the time interval $[0, T]$, and subscript 2 indicates quantities defined over $[T, 2T]$.

Accounting for the loading conditions (4.1.1) and (4.1.2), it writes as follows:

$$\text{TPE}[u'_{1i}, u'_{2i}] = \frac{1}{2} \int_{\Omega} \left(A\epsilon'_{1ij}(2T) * \epsilon'_{1ij}(2T) + 2\widetilde{B}\epsilon'_{1ij}(2T) * \epsilon'_{2ij}(2T) \right) d\Omega \tag{4.1.11}$$

which can also be rewritten in the following form:

$$\frac{1}{V}\text{TPE}[u'_{1i}, u'_{2i}] = \frac{1}{2}\left\langle A\epsilon'_{1ij}(2T) * \epsilon'_{1ij}(2T)\right\rangle + \left\langle \widetilde{B}\epsilon'_{1ij}(2T) * \epsilon'_{2ij}(2T)\right\rangle \tag{4.1.12}$$

where the operators are defined as:

$$A(\cdot) = \int_{0^-}^{T} R_{ijhk}(t - \tau) \, d(\cdot)$$

$$B(\cdot) = \int_{T}^{t} R_{ijhk}(t - \tau) \, d(\cdot) \tag{4.1.13}$$

$$\widetilde{B}(\cdot) = \int_{0^-}^{t} R_{ijhk}(t - \tau) \, d(\cdot)$$

and where $u'_{1i}, u'_{2i}, \epsilon'_{1ij}, \epsilon'_{2ij}$ are arbitrary but compatible displacement and strain fields. Operator A is symmetric with respect to the bilinear form (4.1.8).

In Carini and Mattei (2015) it is demonstrated that the Total Potential Energy like functional (4.1.11) is a min-stat functional, whose stationarity provide the (unique) solution of the real viscoelastic problem:

$$\text{TPE}[u_{1i}, u_{2i}] = \min_{u'_{1i}} \text{stat}_{u'_{2i}} \text{TPE}[u'_{1i}, u'_{2i}] \tag{4.1.14}$$

Unfortunately, in order to obtain bounds for the viscous kernels of viscoelastic composites, it is necessary to consider extremum theorems and, as already stated, functional (4.1.11) is only a min-stat one.

Nevertheless, it is possible to deduce a minimum principle from (4.1.11), considering particular loading conditions for the RVE.

It is possible to prove that, under the following conditions:

1. macroscopically isotropic viscoelastic composites,

2. for the RVE loading described as (4.1.1) and (4.1.2),

3. under deviatoric loading applied to the RVE and

4. for suitable choices of the admissible displacement u'_{1i},

the second term in eq. (4.1.12) is identically equal to zero. This means that, under these assumptions, the Total Potential Energy functional (4.1.12) reduces only to the first quadratic term in ϵ'_{1ij}, deriving a true minimum principle.

In fact, clearly if one inserts the true solution $\epsilon_{2ij}(2T)$, a minimum theorem is automatically obtained, but, unfortunately, the exact solution is not available. Nevertheless, if one assumes to have it available, and then selects an admissible displacement u'_{1j} that cancels the term $\langle \widetilde{B}\epsilon'_{1ij}(2T) * \epsilon_{2ij}(2T) \rangle$, a fully usable minimum theorem is thus obtained.

To pursue this idea, one can define as *strictly admissible* a displacement field u'_{1j} which (i) is admissible in the standard sense (compatible and satisfying the kinematic boundary conditions) and (ii) is such that the following holds: $\langle \widetilde{B}\epsilon'_{1ij}(2T) * \epsilon_{2ij}(2T) \rangle = 0$.

It is important to observe that the real solution $u_{1j}(t)$ is strictly admissible in the above sense. Therefore, it is obvious that among all the strictly admissible displacements the real one makes the first integral in functional (4.1.12) a minimum.

It is now possible to prove that also the choice $u'_{1j}(t) = \epsilon^0_{ij}(t)x_j = \bar{\epsilon}_{ij}x_j\mathcal{H}(t)$, extended to all the points of the RVE, is strictly admissible in the special case of a purely deviatoric type of kinematic loading on the RVE.

Proof. Lets' write Carini-Mattei functional for an admissible function:

$$\frac{1}{V}\text{TPE}[u'_{1i}] = \frac{1}{2}\langle A\epsilon'_{1ij}(2T) * \epsilon'_{1ij}(2T) \rangle + \langle \widetilde{B}\epsilon'_{1ij}(2T) * \epsilon_{2ij}(2T) \rangle \tag{4.1.15}$$

In the second member of the functional, $\langle \widetilde{B}\epsilon'_{1ij}(2T) * \epsilon_{2ij}(2T) \rangle$, the term $\epsilon_{2ij}(2T)$ is known, whereas $\epsilon'_{1ij}(2T)$ is an admissible function.

Considering that operator $\widetilde{B}$ is the adjoint of B, one can write:

$$\langle \widetilde{B}\epsilon'_{1ij}(2T) * \epsilon_{2ij}(2T) \rangle = \langle B\epsilon_{2ij}(2T) * \epsilon'_{1ij}(2T) \rangle \tag{4.1.16}$$

Defining:

$$B\epsilon_{2ij}(2T) = \sigma^B_{2ij}(2T) \tag{4.1.17}$$

Equation (4.1.16) becomes (recalling (4.1.3)):

$$\langle B\epsilon_{2ij} * \epsilon'_{1ij} \rangle = \langle \sigma^B_{2ij} * \epsilon'_{1ij} \rangle = \frac{1}{V}\int_\Omega \sigma^B_{2ij} * \epsilon'_{1ij}\, d\Omega = \frac{1}{V}\int_\Omega \sigma^B_{2ij} * u'_{1j/i}\, d\Omega$$
$$= \frac{1}{V}\int_\Omega \left(\sigma^B_{2ij} * u'_{1j}\right)_{/i} d\Omega - \frac{1}{V}\int_\Omega \sigma^B_{2ij/i} * u'_{1j}\, d\Omega \tag{4.1.18}$$

$\sigma^B_{2ij/i}$ is force per unit volume and it will be denoted as $-b^B_j$.
Thus, (4.1.18) becomes:

$$\langle B\epsilon_{2ij} * \epsilon'_{1ij} \rangle = \frac{1}{V}\int_\Gamma \sigma^B_{2ij}n_i * u'_{1j}\, d\Gamma + \frac{1}{V}\int_\Omega b^B_j * u'_{1j}\, d\Omega$$
$$= \frac{1}{V}\int_\Gamma p^B_j * u'_{1j}\, d\Gamma + \frac{1}{V}\int_\Omega b^B_j * u'_{1j}\, d\Omega \tag{4.1.19}$$

The first integral is constant, because u'_{1j} is assigned on the boundary and $\sigma^B_{2ij}n_i$ is a surface traction p^B_j, depending on ϵ_{2ij}.

As for the second integral, considering the "affine" displacement hypothesis:

$$u'_{1j} = \bar{\epsilon}_{1ij}x_i\mathcal{H}(t), \tag{4.1.20}$$

it becomes

$$\int_\Omega b^B_j * u'_{1j}\, d\Omega = \int_\Omega b^B_j \bar{\epsilon}_{1ij}x_i\, d\Omega = \int_\Omega b^B_j x_i\, d\Omega \cdot \bar{\epsilon}_{1ij} \tag{4.1.21}$$

94

Body forces b_j^B have a resultant force and a resultant moment, both null for symmetry reasons. In fact, let's suppose that the body forces have resultant $\boldsymbol{F}$ different from zero:
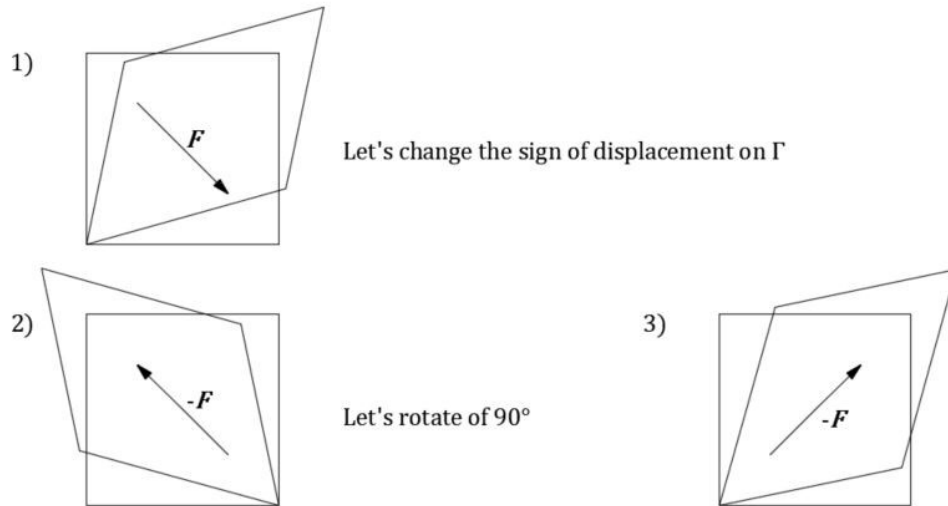
Figure 4.1: Proof that the resultant forces are null.

with these procedures, we obtain the same starting situation with $\boldsymbol{F}$ rotated by 90 degrees, therefore, $\boldsymbol{F} = 0$ must be valid.

Let's suppose that the body forces have resultant moment different from zero:
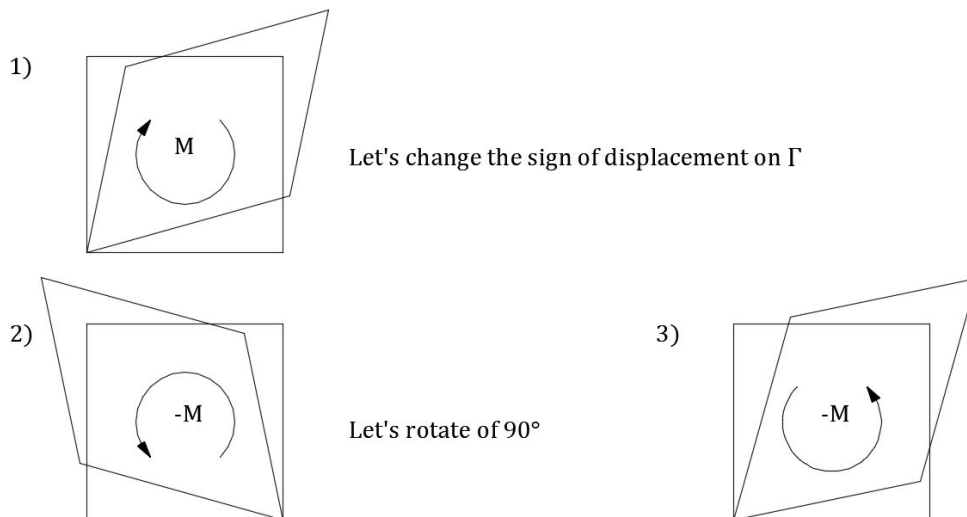
Figure 4.2: Proof that the resultant moment is null.

Therefore, $M = 0$ must be valid.

The same analyses are valid for the first integral on the right side of (4.1.19).

It is now possible to prove that the choice of the displacement $u'_{1i} = \epsilon^0_{ij} x_j$ extended to all the point of the RVE is strictly admissible in the special case of purely deviatoric type of kinematic loading on the RVE. To examine in a complete way a purely deviatoric kunematic loading it is sufficient to consider $\bar{\epsilon}_{12} = \bar{\epsilon}_{21}$ as the only non-zero strain components in the RVE. All the other possible cases could be approached in the same way.
Equation (4.1.19) thus becomes:

$$\langle \sigma^B_{2ij} * \epsilon'_{1ij} \rangle = \frac{1}{V} \left[\int_\Gamma p^B_j x_i \, d\Gamma + \int_\Omega b^B_j x_i \, d\Omega \right] \cdot \bar{\epsilon}_{ij} \tag{4.1.22}$$

In the two-dimensional case (4.1.22) becomes:

$$\begin{aligned}
\langle \sigma^B_{2ij} * \epsilon'_{1ij} \rangle = &\frac{1}{V} \left[\int_\Gamma p^B_1 x_2 \, d\Gamma + \int_\Omega b^B_1 x_2 \, d\Omega \right] \cdot \bar{\epsilon}_{21} \\
&+ \frac{1}{V} \left[\int_\Gamma p^B_2 x_1 \, d\Gamma + \int_\Omega b^B_2 x_1 \, d\Omega \right] \cdot \bar{\epsilon}_{12}
\end{aligned} \tag{4.1.23}$$

The quantities in square brackets represent couples, thus one can consider:

$$\int_\Omega \sigma^B_{2ij}(2T) * \epsilon'_{1ij}(2T) \, d\Omega = M_{12} \cdot \bar{\epsilon}_{21} + M_{21} \cdot \bar{\epsilon}_{12} \tag{4.1.24}$$

Let's rotate the reference system of 90. In the new reference system the left side of (4.1.24) is unchanged and M_{12} and M_{21} are the same as before (they remain unchanged with respect to rotation of the reference system), whereas the shear strains $\bar{\epsilon}_{21}$ and $\bar{\epsilon}_{12}$ change their signs into $-\bar{\epsilon}_{21}$ and $-\bar{\epsilon}_{12}$.
Thus the following result is also valid:

$$\int_\Omega \sigma^B_{2ij}(2T) * \epsilon'_{1ij}(2T) \, d\Omega = -\left[M_{12} \cdot \bar{\epsilon}_{21} + M_{21} \cdot \bar{\epsilon}_{12} \right] \tag{4.1.25}$$

which is real only if

$$\langle \sigma^B_{2ij} * \epsilon'_{1ij} \rangle = 0 \tag{4.1.26}$$

$\square$

As a consequence of this reasoning, under this type of loading for a macroscopically isotropic viscoelastic RVE, the Carini and Mattei functional (2015) becomes:

$$\overline{\text{TPE}}[u'_{1i}] = \frac{1}{2} \int_\Omega A\epsilon'_{1ij}(2T) * \epsilon'_{1ij}(2T) \, d\Omega \tag{4.1.27}$$

Surprisingly, if the boundary displacement are purely volumetric, it is impossible to prove that $\langle \sigma^B_{2ij} * \epsilon'_{1ij} \rangle = 0$.
An analogous procedure can be applied to the Total Complementary Energy like functional, considering as loading conditions only surface tractions producing a constant stress field over the RVE.

Upper bounds derived from functional (4.1.27)

We choose, for the arbitrary compatible strain field $\epsilon'_{1ij}(x_r, t)$, the same definition of eq. (4.1.2), constant in space and governed in time by the Heaviside function $\mathcal{H}(t)$.

According to the definitions of operator A of eq. (4.1.13), of the stress $\sigma_{2ij} = A\epsilon_{1hk} + B\epsilon_{2hk}$, and of the adopted convolutive bilinear form, the $\overline{\text{TPE}}$ functional of eq. (4.1.27), evaluated in the solution of the RVE problem, is explicitly written as follows:

$$\overline{\text{TPE}}_{\text{sol}} = \frac{1}{2} \int_\Omega \int_{0^-}^{2T} \int_{0^-}^{T} R_{ijhk}(2T - t - \tau) \, d\epsilon_{1ij}(\tau) \, d\epsilon_{1hk}(t) \, d\Omega \qquad (4.1.28)$$

For this functional, the following minimum theorem holds:

$$\overline{\text{TPE}}[u_{1i}] = \min_{u'_{1i}} \overline{\text{TPE}}[u'_{1i}] \qquad (4.1.29)$$

Recall now that eq. (4.1.28) denotes the free energy density for this problem; thus, the following result holds:

$$\frac{1}{V} \overline{\text{TPE}}_{\text{sol}} = \frac{1}{2} \bar{\epsilon}_{ij} R^h_{ijhk}(2T) \bar{\epsilon}_{hk} \qquad (4.1.30)$$

where $R^h_{ijhk}(2T)$ denotes the homogenized value of the relaxation kernel.

The minimum theorem of eq. (4.1.29) allows therefore one to write

$$\bar{\epsilon}_{ij} R^h_{ijhk}(2T) \bar{\epsilon}_{hk} \le \left\langle A\epsilon'_{1ij}(2T) * \epsilon'_{1ij}(2T) \right\rangle \quad \forall \epsilon'_{1ij} \quad \text{strictly admissible} \qquad (4.1.31)$$

From this, recalling the definition (4.1.13) of operator A and exploiting the choice (4.1.2) for $\epsilon'_{1ij}(t)$, one obtains finally the desired upper bound to the homogenized relaxation kernel:

$$\bar{\epsilon}_{ij} R^h_{ijhk}(2T) \bar{\epsilon}_{hk} \le \bar{\epsilon}_{ij} \left\langle R_{ijhk}(2T) \right\rangle \bar{\epsilon}_{hk} \qquad (4.1.32)$$

which, taking T as an arbitrary time, becomes valid for a generic time t.

One can produce an upper bound to the homogenized creep function $C^h_{ijhk}(t)$ in a similar way, starting now from the Total Complementary Energy like functional. Now the loading condition on the RVE must be defined in terms of prescribed tractions; in a fully analogous way to what is usually done in creep laboratory test, we consider the following loading:

$$p_j(x_r, t) = \langle \sigma_{ij}(x_r, t) \rangle n_i = \sigma^0_{ij}(t) n_i \quad \text{in } \Gamma_p = \Gamma \qquad (4.1.33)$$

with

$$\sigma^0_{ij}(t) = \bar{\sigma}_{ij} \mathcal{H}(t) \qquad (4.1.34)$$

Next, one proceeds in a way analogous to the one illustrated here above. One chooses also for σ'_{1ij} the distribution given by eq. (4.1.34). After passages completely similar to those leading to eq. (4.1.32), which we omit for brevity, one obtains the following upper bound to the homogenized creep function:

$$\bar{\sigma}_{ij} C^h_{ijhk}(2T) \bar{\sigma}_{hk} \le \bar{\sigma}_{ij} \left\langle C_{ijhk}(2T) \right\rangle \bar{\sigma}_{hk} \qquad (4.1.35)$$

once more holding for any generic time t.

This Chapter directly follows the theory described in Chapter 2 about the viscoelastic behaviour of structural materials.

We consider the case of a macroscopically isotropic material.

Consider a composite material with N phases, denote by c_i the volume fraction of each phase (i) and denote by $R^{(i)}(t)$ and $C^{(i)}(t)$ a scalar relaxation and creep kernel component of phase (i), respectively.

As shown in the introduction, strict lower bounds were already defined by Huet (1995) (who proved them, using the Principle of Virtual Work), whereas we obtained upper bounds valid exclusively under the hypothesis of deviatoric strains.

The proposed upper bounds for the scalar homogenized relaxation $R^h(t)$ and creep $C^h(t)$ kernel components read as follows:

- *upper bound* to the relaxation kernel, shear component:

$$R^h(t) \leq \sum_{i=1}^{N} c_i \cdot R^{(i)}(t) \quad \forall t \tag{4.1.36}$$

- *upper bound* to the creep kernel, shear component:

$$C^h(t) \leq \sum_{i=1}^{N} c_i \cdot C^{(i)}(t) \quad \forall t \tag{4.1.37}$$

Whereas, the lower bounds for the scalar homogenized relaxation $R^h(t)$ and creep $C^h(t)$ kernel components read as follows:

- *lower bound* to the relaxation kernel, shear and volumetric components:

$$R^h(t) > \frac{1}{\sum_{i=1}^{N} \frac{c_i}{R^{(i)}(t)}} \quad \forall t \tag{4.1.38}$$

- *lower bound* to the creep kernel, shear and volumetric components:

$$C^h(t) > \frac{1}{\sum_{i=1}^{N} \frac{c_i}{C^{(i)}(t)}} \quad \forall t \tag{4.1.39}$$

It is interesting to notice that bounds (4.1.36) and (4.1.37) become, in the limit case when all phases are linear elastic, identical to the Voigt upper bounds in linear elasticity; and, obviously, both lower bounds (4.1.38) and (4.1.39) become, in the same limit case, identical to the Reuss lower bounds in linear elasticity.

Therefore, all these results can be considered extensions to linear viscoelasticity of these two basic, first-order bounds in elasticity.

For the linear viscoelastic case, both at the initial time $t = 0$ and for $t \to \infty$ they should therefore coincide with the Voigt and Reuss bounds, and, for intermediate times, they can be expected to be affected by errors of the same order of magnitude as the Voigt and Reuss ones. The lower bounds, as we have already stated, prove to be always verified.

In this Chapter, our aim is to verifying the upper bounds for examples with deviatoric strains. Numerical tests are performed even on systems subjected to volumetric strains, proving that upper bounds are not valid.

Also an example of an uniaxial system with elastic and viscoelastic materials arranged in series is presented, in order to prove that an upper bound can be extrapolated from the TPE functional (4.1.11).

4.2 Analysis of an uniaxial system with elastic and viscoelastic materials arranged in series

Consider the problem in Fig. 4.3.
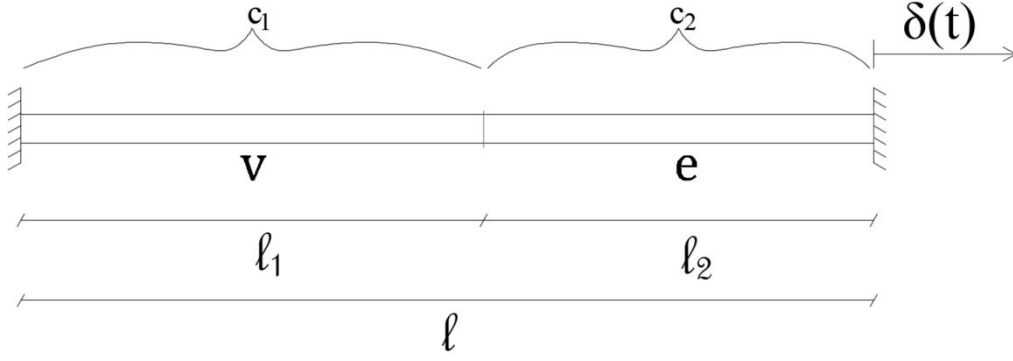
Figure 4.3: System with elastic and viscoelastic materials arranged in series.

Namely, a rod with constant unitary cross-sectional area, of length l, with elastic and viscoelastic materials arranged in series subjected to a displacement $\delta(t)$, defined as:

$$\delta(t) = \Delta \cdot \mathcal{H}(t) \tag{4.2.1}$$

where Δ is constant and $\mathcal{H}(t)$ is the Heaviside function.

Phase 1 of the composite is viscoelastic (V), with length l_1 and volume fraction c_1, governed by a standard two-parameter solid rheologic model of the Maxwell type, for which, the volumetric relaxation kernel is written as follows (Migliacci, 1979):

$$R_1(t) = E_1 \cdot e^{-\frac{E_1 t}{\eta_1}} \tag{4.2.2}$$

Phase 2 of the composite is elastic (E), with volume fraction c_2 and Young modulus E_2. The data used in this example are:

$c_1 = 0.7$; $E_1 = 12000$ MPa; $\eta_1 = 20000$ MPa sec
$c_2 = 0.3$; $E_2 = 6000$ MPa

The homogenized value of the relaxation kernel can be obtained using the Laplace transforms:

$$R^h(t) = \mathcal{L}^{-1}\left[\frac{1}{\frac{c_1}{\mathcal{L}(R_1)} + \frac{c_2}{\mathcal{L}(E_2)}}\right] = \frac{E_1 E_2 \cdot e^{-\frac{E_1 E_2 c_1 t}{E_1 \eta_1 c_2 + E_2 \eta_1 c_1}}}{E_1 c_2 + E_2 c_1} \tag{4.2.3}$$

Whereas the mean value, defined in (4.1.36), is:

$$\langle R(t)\rangle = E_1 \cdot e^{-\frac{E_1 t}{\eta_1}} \cdot c_1 + E_2 \cdot c_2 \tag{4.2.4}$$

The curves of Figure 4.4 plot the relaxation function normalized by the elastic Young modulus E_2.

As it is possible to deduce, the mean value does non constitute an upper bound for this structure.
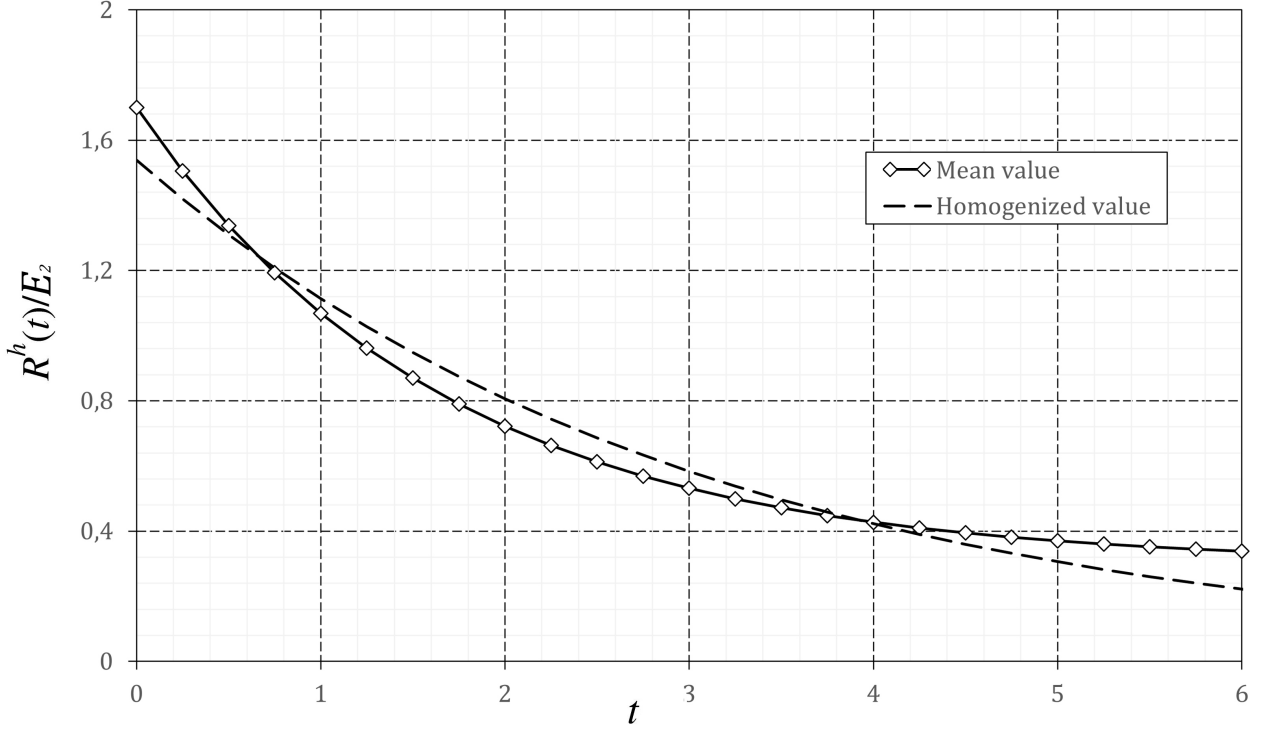
Figure 4.4: Normalized homogenized relaxation kernel $R^h(t)/E_2$ as a function of time t. Comparison between the mean value and the homogenized relaxation kernel of a system with elastic and viscoelastic materials arranged in series.

Recalling Carini-Mattei functional (4.1.11) and applying it to this particular example (assuming to know ϵ_{2ij}) it is possible to deduce an upper bound.
Before the splitting, the functional is written as

$$
\begin{aligned}
\text{TPE} &= +\frac{1}{2}\int_0^l \int_{0^-}^{2T} \int_{0^-}^{2T-t} R(2T-t-\tau)d\left(\frac{du}{dx}(x,t)\right)d\left(\frac{du}{dx}(x,\tau)\right)dx \\
&= +\frac{1}{2}\int_0^{l_1} \int_{0^-}^{2T} \int_{0^-}^{2T-t} R_1(2T-t-\tau)d\left(\frac{du}{dx}(x,t)\right)d\left(\frac{du}{dx}(x,\tau)\right)dx \\
&\quad +\frac{1}{2}\int_0^{l_2} \int_{0^-}^{2T} \int_{0^-}^{2T-t} R_2(2T-t-\tau)d\left(\frac{du}{dx}(x,t)\right)d\left(\frac{du}{dx}(x,\tau)\right)dx
\end{aligned}
\tag{4.2.5}
$$

where l_1 and l_2 are the lengths associated with the first and second phase of the composite. Using an elastic analysis, one can obtain the elongation of the first phase, meaning the displacement of the intermediate point between the two phases (called u_M):

$$
u_M = \Delta l_1 = \frac{\delta \cdot c_1}{E_1 \cdot \sum_{i=1}^2 \frac{c_i}{E_i}} = \frac{\delta \cdot c_1}{E_1 \cdot \left(\frac{c_1}{E_1} + \frac{c_2}{E_2}\right)} = \Delta \cdot \frac{c_1 E_2}{c_2 E_1 + c_1 E_2}
\tag{4.2.6}
$$

This result can be extended to the viscoelastic case through the correspondence principle with Laplace transforms.
The functional (written for a single phase) is splitted into two subintervals of the same ampli-

tude.

$$
\begin{aligned}
\text{TPE} =& \frac{1}{2}\langle A\epsilon_1 * \epsilon_1\rangle + \langle \tilde{B}\epsilon_1 * \epsilon_2\rangle\\
=& \frac{1}{2}\int_0^l \int_{0^-}^T \int_{0^-}^T R(2T - t - \tau)d\epsilon_1(\tau)d\epsilon_1(t)\,dx + \int_0^l \int_T^{2T} \int_{0^-}^{2T-t} R(2T - t - \tau)d\epsilon_1(\tau)d\epsilon_2(t)\,dx
\end{aligned}
$$

$$
\begin{aligned}
=& \frac{1}{2}\int_0^l \left[\int_{0^-}^T R(2T - t)\epsilon_1(0)d\epsilon_1(t) + \int_{0^-}^T \int_0^T R(2T - t - \tau)\frac{\partial \epsilon_1}{\partial \tau}d\tau\,d\epsilon_1(t)\right]dx\\
& + \int_0^l \left[\int_T^{2T} R(2T - t)\epsilon_1(0)d\epsilon_2(t) + \int_T^{2T}\int_0^{2T-t} R(2T - t - \tau)\frac{\partial \epsilon_1}{\partial \tau}d\tau\,d\epsilon_2(t)\right]dx
\end{aligned}
$$

$$
\begin{aligned}
=& \frac{1}{2}\int_0^l \left[R(2T)\epsilon_1(0)\epsilon_1(0) + \int_0^T R(2T - t)\epsilon_1(0)\frac{\partial \epsilon_1}{\partial t}dt\right]dx\\
& + \frac{1}{2}\int_0^l \left[\int_0^T R(2T - t)\epsilon_1(0)\frac{\partial \epsilon_1}{\partial \tau}d\tau + \int_0^T\int_0^T R(2T - t - \tau)\frac{\partial \epsilon_1}{\partial \tau}d\tau\,\frac{\partial \epsilon_1}{\partial t}dt\right]dx\\
& + \int_0^l \left[\int_T^{2T} R(2T - t)\epsilon_1(0)\frac{\partial \epsilon_2}{\partial t}dt + \int_T^{2T}\int_0^{2T-t} R(2T - t - \tau)\frac{\partial \epsilon_1}{\partial \tau}d\tau\,\frac{\partial \epsilon_2}{\partial t}dt\right]dx
\end{aligned}
$$

$$
\begin{aligned}
=& \frac{1}{2}\int_0^l \left[R(2T)\epsilon_1^2(0) + 2\epsilon_1(0)\int_0^T R(2T - t)\frac{\partial \epsilon_1}{\partial t}dt + \int_0^T\int_0^T R(2T - t - \tau)\frac{\partial \epsilon_1}{\partial \tau}\frac{\partial \epsilon_1}{\partial t}\,d\tau dt\right]dx\\
& + \int_0^l \left[\epsilon_1(0)\int_T^{2T} R(2T - t)\frac{\partial \epsilon_2}{\partial t}dt + \int_T^{2T}\int_0^{2T-t} R(2T - t - \tau)\frac{\partial \epsilon_1}{\partial \tau}\frac{\partial \epsilon_2}{\partial t}\,d\tau dt\right]dx
\end{aligned}
$$

$$
(4.2.7)
$$

Now we write the functional related to our analysis, assigning the subscript E for the elastic element and the subscript V for the viscoelastic element:

$$
\begin{aligned}
\text{TPE} =& \frac{l_E}{2}\left[E_2\epsilon_{1E}^2(0) + 2E_2\epsilon_{1E}(0)\int_0^T \frac{\partial \epsilon_{1E}}{\partial t}dt + E_2\int_0^T \frac{\partial \epsilon_{1E}}{\partial \tau}d\tau\int_0^T \frac{\partial \epsilon_{1E}}{\partial t}dt\right]\\
& + \frac{l_V}{2}\left[R_V(2T)\epsilon_{1V}^2(0) + 2\epsilon_{1V}(0)\int_0^T R_V(2T - t)\frac{\partial \epsilon_{1V}}{\partial t}dt + \int_0^T\int_0^T R_V(2T - t - \tau)\frac{\partial \epsilon_{1V}}{\partial \tau}\frac{\partial \epsilon_{1V}}{\partial t}\,d\tau dt\right]\\
& + l_E\left[E_2\epsilon_{1E}(0)\int_T^{2T} \frac{\partial \epsilon_{2E}}{\partial t}dt + E_2\int_T^{2T}\int_0^{2T-t} \frac{\partial \epsilon_{1E}}{\partial \tau}\frac{\partial \epsilon_{2E}}{\partial t}\,d\tau dt\right]\\
& + l_V\left[\epsilon_{1V}(0)\int_T^{2T} R_V(2T - t)\frac{\partial \epsilon_{2V}}{\partial t}dt + \int_T^{2T}\int_0^{2T-t} R_V(2T - t - \tau)\frac{\partial \epsilon_{1V}}{\partial \tau}\frac{\partial \epsilon_{2V}}{\partial t}\,d\tau dt\right]
\end{aligned}
$$

$$
(4.2.8)
$$

The following substitutions are performed:

$$
\epsilon_{1i} = \epsilon_1' = \bar{\epsilon}\cdot \mathcal{H}(t)\qquad i = E, V \tag{4.2.9}
$$

namely, we assign to the admissible solution over the first subinterval a mean value of strain

$$
\bar{\epsilon} = \frac{\delta(t)}{l} = \frac{\Delta}{l}\cdot (t) \tag{4.2.10}
$$

As for the second subinterval, we superimpose the exact solution of the problem, already calculated:

$$
\begin{aligned}
\epsilon_{2V} &= \frac{\Delta l_V}{l_V} = \frac{u_M}{l_V} \\
\epsilon_{2E} &= \frac{\Delta l_E}{l_E} = \frac{\delta(t) - u_M}{l_E}
\end{aligned}
\tag{4.2.11}
$$

considering that u_M is a function of $l \cdot \bar{\epsilon}$.

Making such substitutions within the functional (4.2.8) and performing some calculation, one gets:

$$
\text{TPE} = \frac{1}{2} \cdot l \cdot \bar{\epsilon}^2 \cdot R^{\text{TPE}}(2T)
\tag{4.2.12}
$$

In Figure 4.5 it is proved that:

$$
\frac{1}{2} R^h(2T) \cdot \bar{\epsilon}^2 \leq \frac{1}{2} \cdot R^{\text{TPE}}(2T) \cdot \bar{\epsilon}^2 \quad \Rightarrow \quad R^h(2T) \leq R^{\text{TPE}}(2T)
\tag{4.2.13}
$$
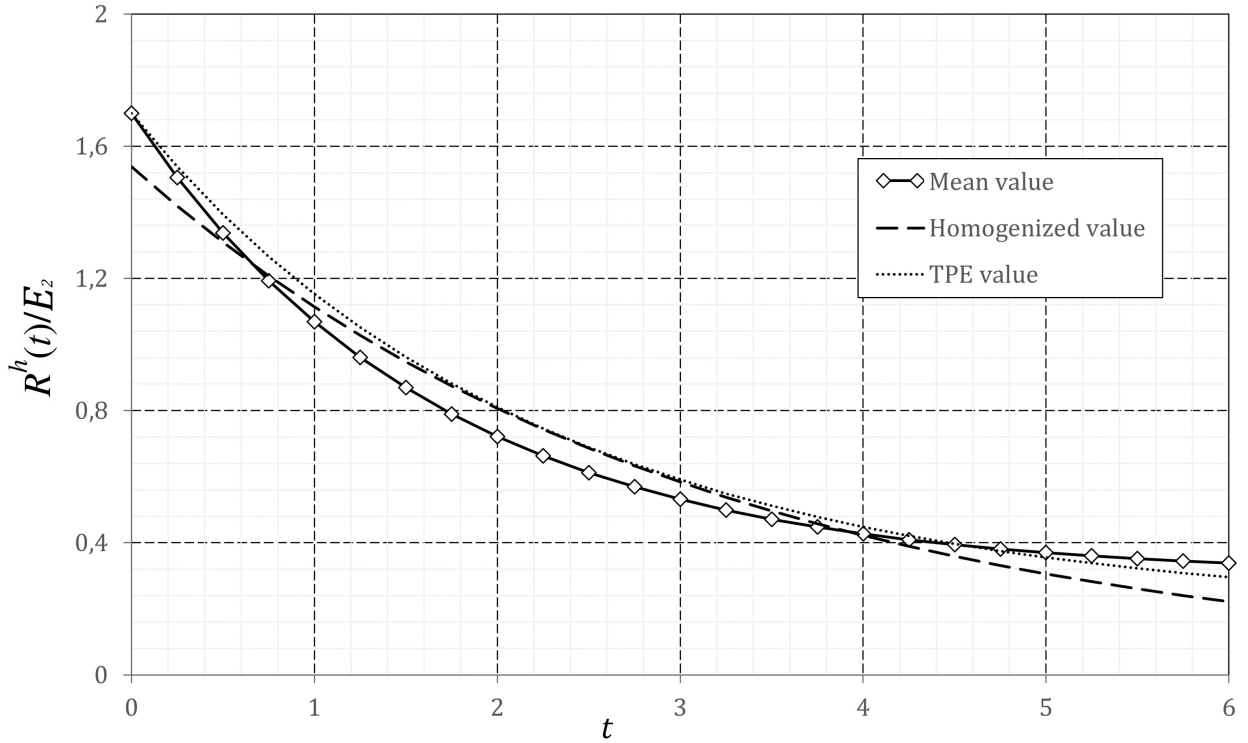
Figure 4.5: Normalized homogenized relaxation kernel $R^h(t)/E_2$ as a function of time t. Comparison between the mean value, the homogenized value and the relaxation kernel calculated with the TPE functional of a system with elastic and viscoelastic materials arranged in series.

4.3 Numerical tests on shear kernels

In this Section we will consider only shear viscous kernels.

In order to obtain numerical results, we now consider viscoelastic phases governed by a standard three-parameter solid rheologic model of the Kelvin–Voigt (or Zener) type, for which, for a generic phase (i), the shear relaxation kernel is written as follows (Bland, 1960):

$$R_S^{(i)}(t) = (G_E^{(i)} + G_V^{(i)}) - G_V^{(i)}\left[1 - \exp\left(-\frac{G_V^{(i)}t}{\eta_V^{(i)}}\right)\right] \tag{4.3.1}$$

where $G_E^{(i)}$ and $G_V^{(i)}$ are the shear moduli of the viscoelastic material, and $\eta_V^{(i)}$ is the viscosity coefficient. The corresponding shear creep kernel reads as follows (Bland, 1960):

$$C_S^{(i)}(t) = \frac{1}{(G_E^{(i)} + G_V^{(i)})} + \frac{G_V^{(i)}}{G_E^{(i)}(G_E^{(i)} + G_V^{(i)})}\left[1 - \exp\left(-\frac{G_E^{(i)}G_V^{(i)}t}{\eta_V^{(i)}(G_E^{(i)} + G_V^{(i)})}\right)\right] \tag{4.3.2}$$

The performance of bounds (4.1.36) – (4.1.39) was checked against Finite Element results obtained by means of the commercial code ABAQUS (Hibbitt et al., 2018). ABAQUS allows the modelling of linear viscoelastic materials through the definition of material parameters associated to the Prony series for relaxation only; this, for a Kelvin–Voigt material and for each phase (i), is written in ABAQUS in the following form:

$$\tau^{(i)}(t) = G_0^{(i)}\int_0^t\left\{1 - \frac{G_1^{(i)}}{G_0^{(i)}}\left[1 - \exp\left(-\frac{G_1^{(i)}\tau}{\eta_1^{(i)}}\right)\right]\right\}\dot{\gamma}^{(i)}\,d\tau, \quad i = 1,\ldots,N \tag{4.3.3}$$

and requires in input the values of $G_0^{(i)}$, $G_1^{(i)}/G_0^{(i)}$, and $\eta_1^{(i)}/G_1^{(i)}$, $i = 1,\ldots,N$. A match between eqs. (4.3.3) and (4.3.1) shows immediately that, in order to establish equivalence between ABAQUS and analytical results, one needs to set $G_0^{(i)} = G_E^{(i)} + G_V^{(i)}$, $G_1^{(i)} = G_V^{(i)}$, and $\eta_1^{(i)} = \eta_V^{(i)}$.

Several square RVEs with unit sides have been constructed, with different microstructures, each possessing at least a 10×10 array of inclusions of different shapes. A plane strain simple shear problem was considered, applying, in the case of relaxation, boundary displacements corresponding to a constant unit value for the average in-plane shear strain, and, for creep, boundary tractions corresponding to a unit value for the average in-plane shear stress. This setup represents of course a transversely isotropic problem, not a fully isotropic one; nevertheless, the considered loading conditions allow one to obtain information about the homogenized shear modulus of a macroscopically isotropic material.

Both loading conditions were applied as unit steps at $t = 0$. Quadrilateral 8-noded plane strain elements with reduced integration (`CPE8R` in ABAQUS notation) have always been adopted. At least 100 elements per each side of the RVE were adopted, arriving at 1000 per side in the case of the most complex microstructures.

The first set of analyses was run considering a two-phase material, the first $(i = 1)$ linear elastic and the second $(i = 2)$ linear viscoelastic. The material data have been taken equal to those adopted in Lahellec and Suquet (2007), i.e.,
$c_1 = 0.4$; $G^{(1)} = G_{el} = 166650$ MPa
$c_2 = 0.6$; $G_E^{(2)} = 26920$ MPa; $G_V^{(2)} = G_V = 13460$ MPa; $\eta_V^{(2)} = \eta_V = 10000$ MPa sec
The bulk modulus of the elastic phase plays no role (anyway, we set $\nu^{(1)} = 0$), and that of the viscous phase has been set equal to zero.

We first checked the validity of the bounds with this set of data for all the considered RVEs. Figures 4.6 and 4.7 report the relevant results, the first for relaxation and the second for

creep. In both Figures the time has been normalized by the relaxation time $t_V = \eta_V/G_V$; the curves of Figure 4.6 plot the relaxation function normalized by the elastic shear modulus G_{el}, and those of Figure 4.7 plot the creep function normalized once more by G_{el}. All the considered RVEs yield both families of curves lying within the respective bounds, and all tend to furnish similar relaxation and creep curves. In the rest of the examples we have considered just one of these RVEs, with the most (quasi) random microstructure.
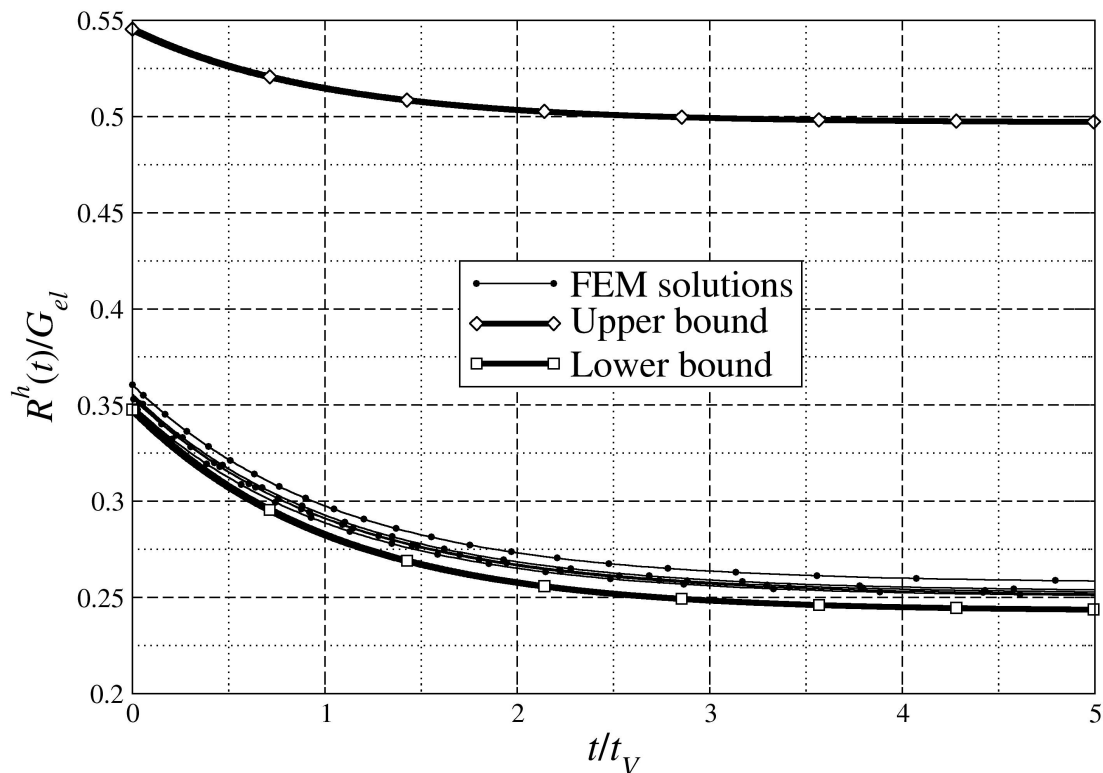
Figure 4.6: Normalized homogenized shear relaxation kernel $R^h(t)/G_{el}$ as a function of normalized time t/t_V for a 2-phase composite. Solid thick curves with white symbols plot lower (squares, eq. (4.1.38)) and upper (diamonds, eq. (4.1.36)) bounds; thin lines plot FEM solutions.
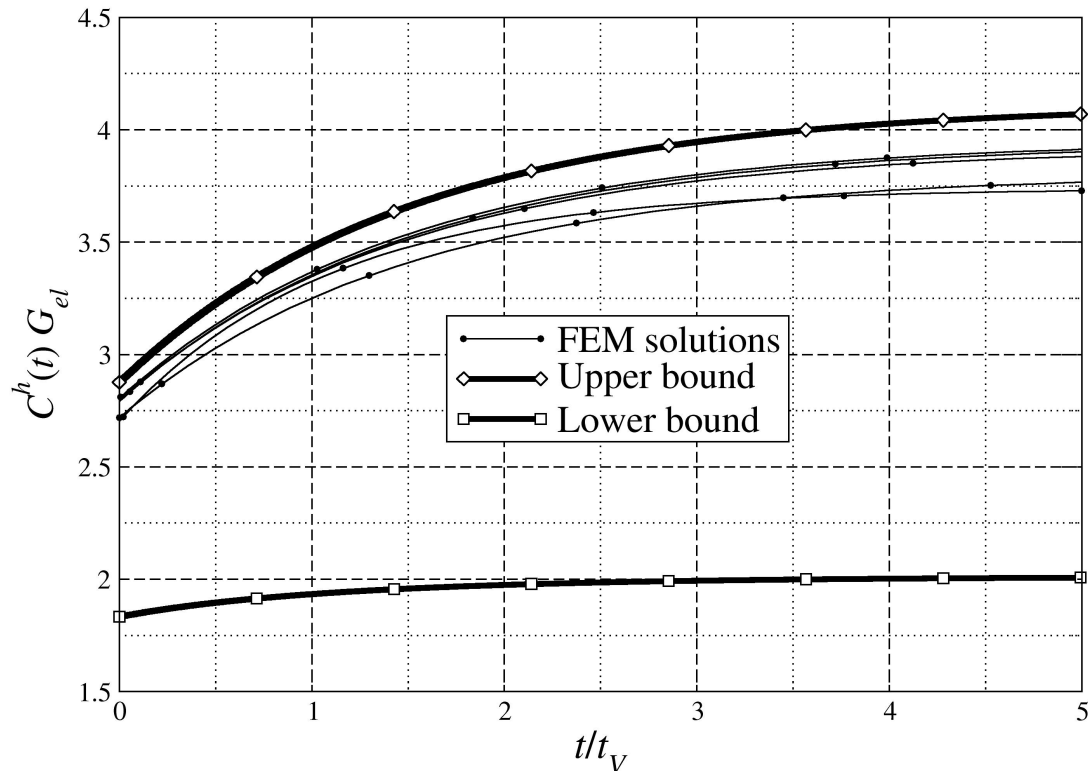
Figure 4.7: Normalized homogenized shear creep kernel $C^h(t)G_{el}$ as a function of normalized time t/t_V for a 2-phase composite. Solid thick curves with white symbols plot lower (squares, eq. (4.1.39)) and upper (diamonds, eq. (4.1.37)) bounds; thin lines plot FEM solutions.

A second group of analyses keeps fixed the volume fractions of the two phases, $c_1 = 0.4$ and $c_2 = 0.6$, and explores the sensitivity to the contrast between the elastic shear moduli of the two phases. Denoting by $k = G_{el}/(G_E^{(2)} + G_V^{(2)})$ this contrast, the starting data of the previous Figures have all $k = 4.1271$; three more cases have been run, with $k = 0.1, k = 1$, and $k = 10$, respectively.

Figures 4.8 and 4.9 plot now, again as a function of the normalized time, the relative errors between the bounds on the viscous kernels and the FEM results. Figure 4.8 refers to relaxation, and Figure 4.9 to creep. Here all the white symbols are lower bound errors, and all the black symbols refer to upper bound errors. Both figures show that all the bounds lie in their proper portion of the plane, and that the best results, as obvious, occur for $k = 1$. The errors remain for all times of the same order of magnitude ($\pm 80\%$ in the worst cases) as the errors on the instantaneous, (elastic, time $t = 0$) moduli, and in some cases increase by a small amount for increasing time, in others decrease.
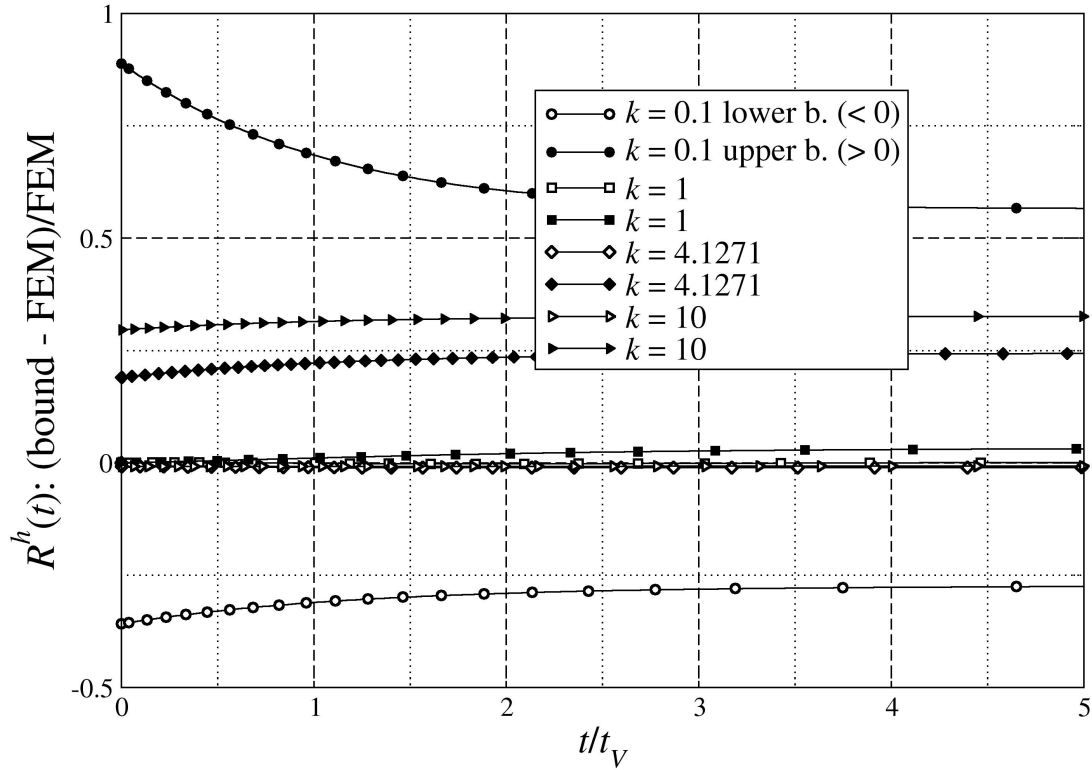
Figure 4.8: Relative error curves for the homogenized shear relaxation kernel $R^h(t)$ as a function of normalized time t/t_V for a 2-phase composite, for various values of the contrast parameter $k = G_{el}/(G_E^{(2)}+G_V^{(2)})$. White symbols denote lower bound errors (results of bound (4.1.38) minus FEM results divided by FEM results); black symbols denote upper bound relative errors. Other parameters as indicated in the text.
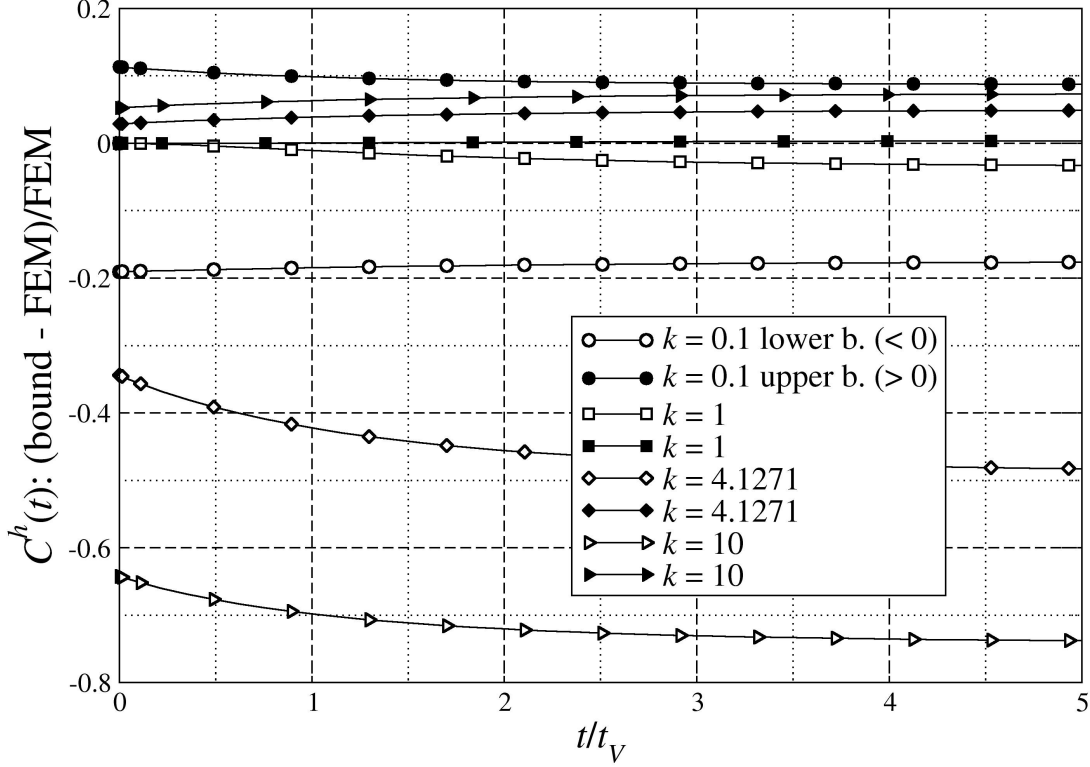
Figure 4.9: Relative error curves for the homogenized shear creep kernel $C^h(t)$ as a function of normalized time t/t_V, for a 2-phase composite, for various values of the contrast parameter $k = G_{el}/(G_E^{(2)}+G_V^{(2)})$. White symbols denote lower bound errors (results of bound (4.1.39) minus FEM results divided by FEM results); black symbols denote upper bound relative errors. Other parameters as indicated in the text.

Figures 4.10 and 4.11 show results concerning the sensitivity to the volume fractions, keeping the contrast equal to that of the first case, i.e., $k = 4.1271$. Four cases of volume fractions have been considered, namely $c_1 = 0.4$ as before, $c_1 = 0.1, c_1 = 0.6$, and $c_1 = 0.9$. This forced the adoption of different meshes for each case, with very dense ones for the case $c_1 = 0.9$.

Figures 4.10 and 4.11 plot again, still as a function of normalized time, the relative errors between the bounds on the viscous kernels and the FEM results, Figure 4.10 for relaxation and Figure 4.11 for creep. Both Figures show once more that all the bounds lie in their proper portion of the plane. The errors are now generally smaller than in the previous two figures, even for extreme values of the volume fractions; this is probably due to the value of the contrast k. The errors are always of the same order of magnitude as the initial, purely elastic ones.
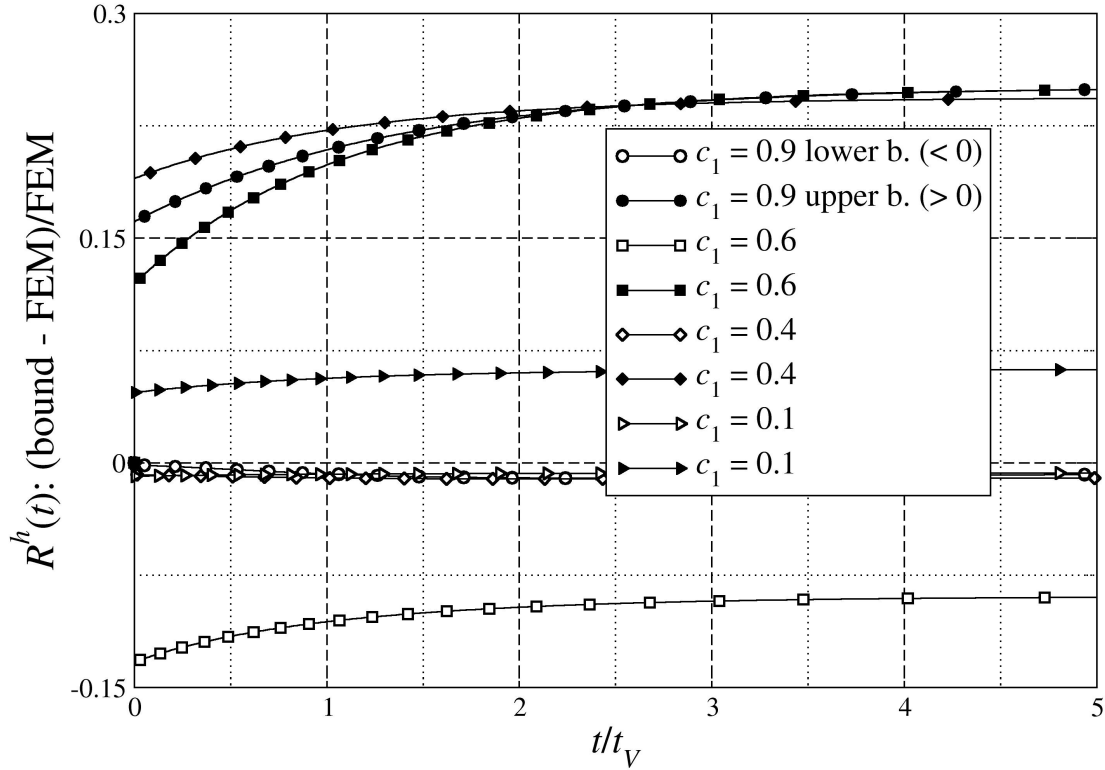
Figure 4.10: Relative error curves for the homogenized shear relaxation kernel $R^h(t)$ as a function of normalized time t/t_V, for a 2-phase composite, for various values of the volume fraction of the elastic phase c_1. White symbols denote lower bound errors (results of bound (4.1.38) minus FEM results divided by FEM results); black symbols denote upper bound relative errors. Other parameters as indicated in the text.
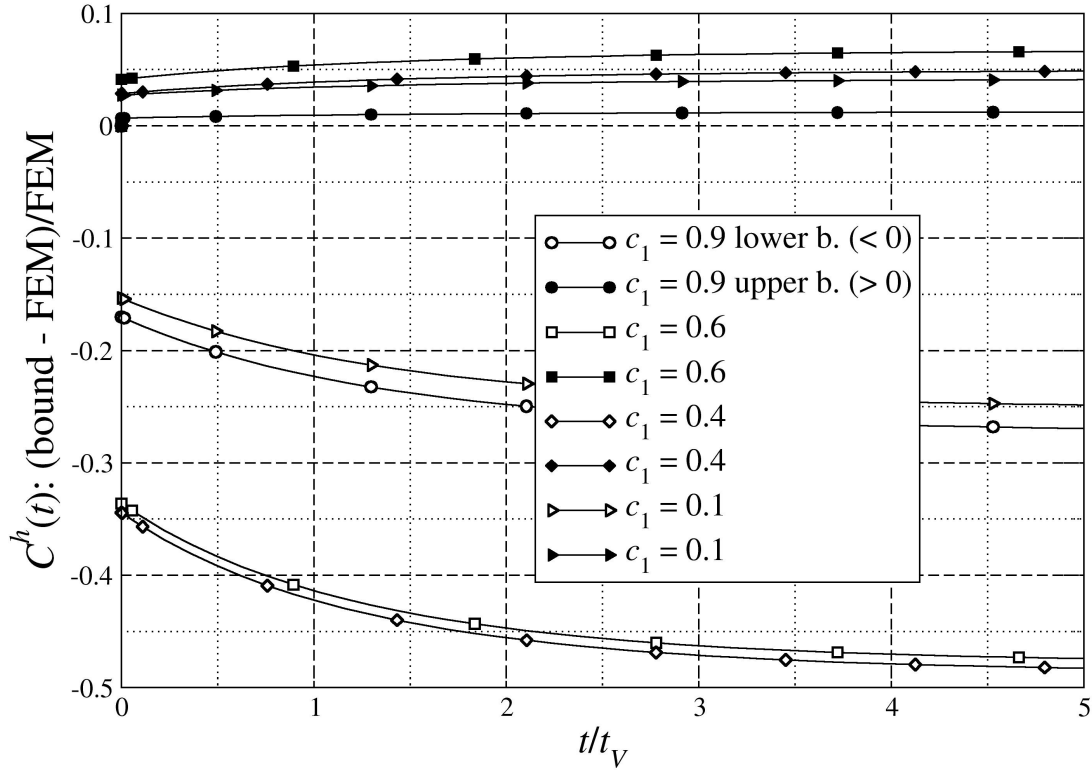
Figure 4.11: Relative error curves for the homogenized shear creep kernel $C^h(t)$ as a function of normalized time t/t_V, for a 2-phase composite, for various values of the volume fraction of the elastic phase c_1. White symbols denote lower bound errors (results of bound (4.1.39) minus FEM results divided by FEM results); black symbols denote upper bound relative errors. Other parameters as indicated in the text.

The next figures, 4.12 and 4.13, plot once more relative errors between analytical bounds and FEM results considering variations of the ratio $g_1 = G_V^{(2)}/(G_E^{(2)} + G_V^{(2)})$ in which the value of $G_V^{(2)}$ has been always kept fixed to its starting value $G_V^{(2)} = 13460$ MPa, so as to consider also limit cases of both absence of elasticity and very high elasticity in the viscous phase.
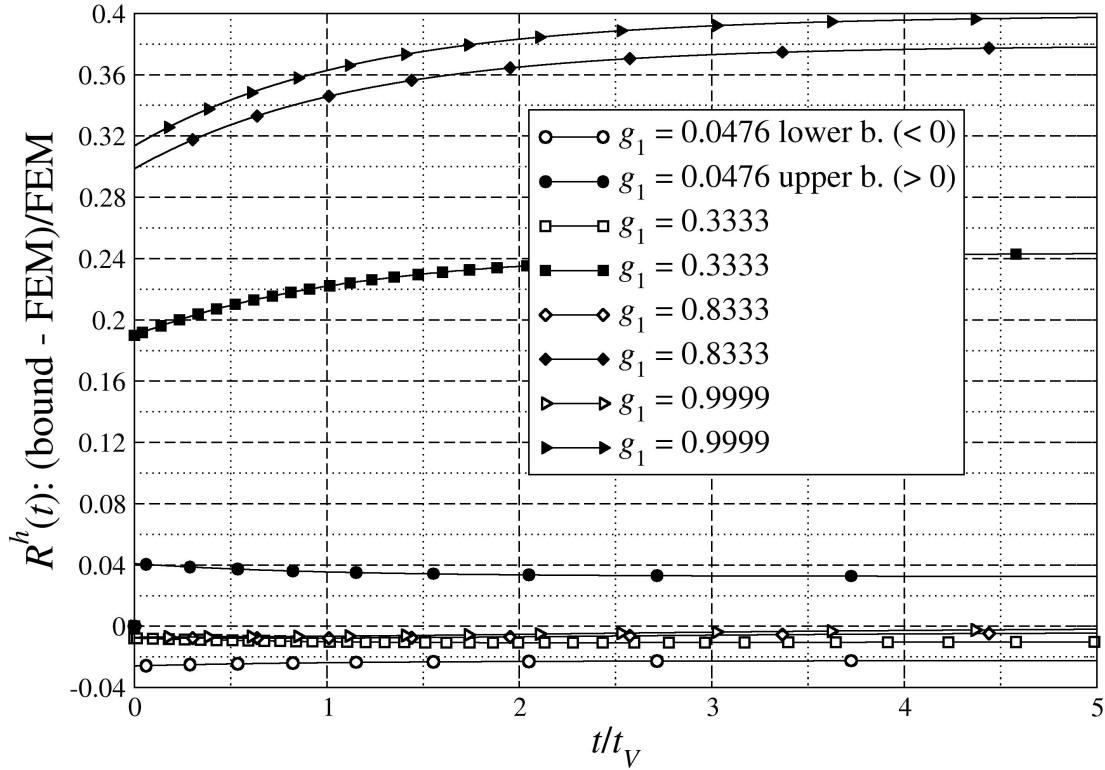
Figure 4.12: Relative error curves for the homogenized shear relaxation kernel $R^h(t)$ as a function of normalized time t/t_V, for a 2-phase composite, for various values of the ratio $g_1 = G_V^{(2)}/(G_E^{(2)} + G_V^{(2)})$ between the shear modulus of the viscous phase and the global one. White symbols denote lower bound errors (results of bound (4.1.38) minus FEM results divided by FEM results); black symbols denote upper bound relative errors. Other parameters as indicated in the text.
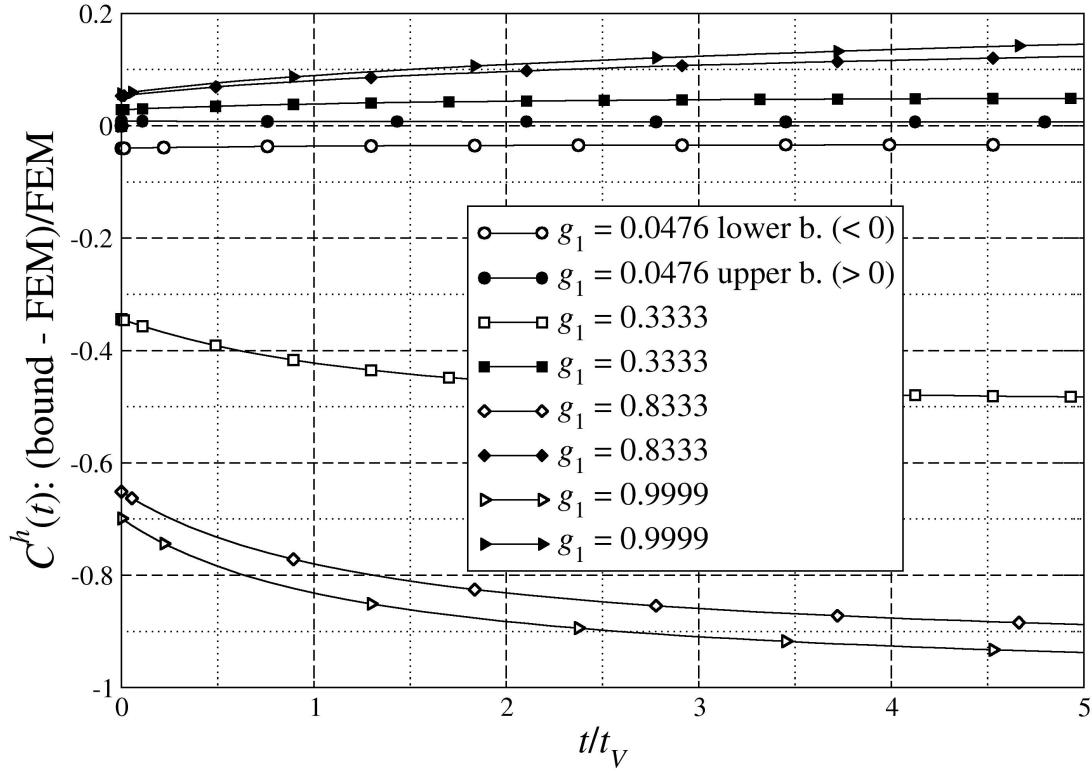
Figure 4.13: Relative error curves for the homogenized shear creep kernel $C^h(t)$ as a function of normalized time t/t_V, for a 2-phase composite, for various values of the ratio $g_1 = G_V^{(2)}/(G_E^{(2)} + G_V^{(2)})$ between the shear modulus of the viscous phase and the global one. White symbols denote lower bound errors (results of bound (4.1.39) minus FEM results divided by FEM results); black symbols denote upper bound relative errors. Other parameters as indicated in the text.

Figure 4.14 and 4.15, which still plot relative errors, refer to varying the relaxation time $t_V = \eta_V/G_V$ in the viscous phase, considering 4 different values $\eta_V = 10, 1000, 10000$, and 1000000 sec, and keeping all the other parameters fixed at their basic values reported above. Note that now the nondimensional time axes are in log scale, since the adoption of relaxation times covering a wide range of values — from $t_V = 7.429 \times 10^{-4}$ sec to $t_V = 74.2942$ sec — produces viscous kernels so different from each other that they can be plotted superimposed only by using such a scale.
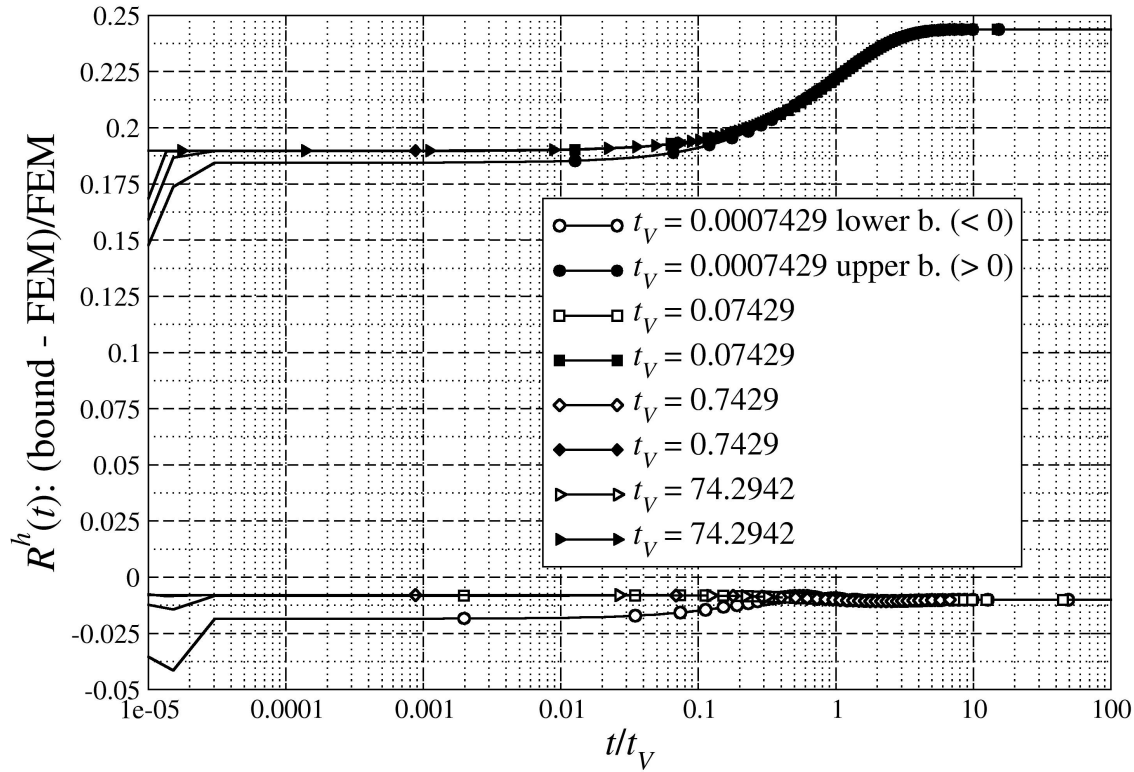
Figure 4.14: Relative error curves for the homogenized shear relaxation kernel $R^h(t)$ as a function of normalized time t/t_V, for a 2-phase composite, for various values of the relaxation time $t_V = \eta_V^{(2)}/G_V^{(2)}$. White symbols denote lower bound errors (results of bound (4.1.38) minus FEM results divided by FEM results); black symbols denote upper bound relative errors. Other parameters as indicated in the text.
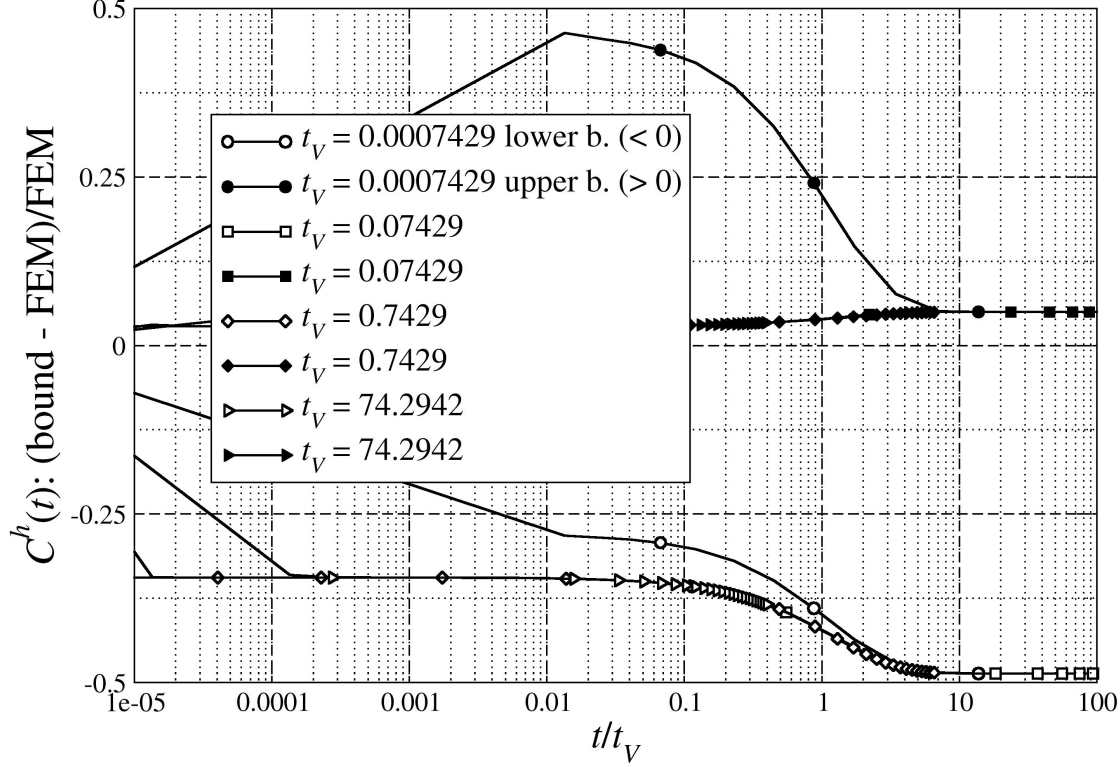
Figure 4.15: Relative error curves for the homogenized shear creep kernel $C^h(t)$ as a function of normalized time t/t_V, for a 2-phase composite, for various values of the relaxation time $t_V = \eta_V^{(2)}/G_V^{(2)}$. White symbols denote lower bound errors (results of bound (4.1.39) minus FEM results divided by FEM results); black symbols denote upper bound relative errors. Other parameters as indicated in the text.

All these results confirm the validity of the bounds derived in this work.

Finally, four more analyses — two relaxation and two creep — have been run for the case of a material having one elastic and three viscoelastic phases, in order to check the correctness of the bounds also in the presence of a more complicated microstructure. A first group concerns a high volume fraction of the elastic phase, with $c_1 = 0.9$; a second group the opposite case, with $c_1 = 0.1$.

The adopted data are as follows:

- case with $c_1 = 0.9$:
  $G^{(1)} = G_{el} = 166650$ MPa
  $c_2 = 0.05$; $G_E^{(2)} = 26920$ MPa; $G_V^{(2)} = 13460$ MPa; $\eta_V^{(2)} = 20000$ MPa
  $c_3 = 0.03333$; $G_E^{(3)} = 5384$ MPa; $G_V^{(3)} = 48456$ MPa; $\eta_V^{(3)} = 35998$ MPa
  $c_4 = 0.01667$; $G_E^{(4)} = 13056.2$ MPa; $G_V^{(4)} = 403.8$ MPa; $\eta_V^{(4)} = 150.01$ MPa

- case with $c_1 = 0.1$:
  $G^{(1)} = G_{el} = 166650$ MPa

$$c_2 = 0.5; \quad G_E^{(2)} = 13056.2 \text{ MPa}; \quad G_V^{(2)} = 403.8 \text{ MPa}; \quad \eta_V^{(2)} = 150.01 \text{ MPa}$$
$$c_3 = 0.3; \quad G_E^{(3)} = 5384 \text{ MPa}; \quad G_V^{(3)} = 48456 \text{ MPa}; \quad \eta_V^{(3)} = 35998 \text{ MPa}$$
$$c_4 = 0.1; \quad G_E^{(4)} = 26920 \text{ MPa}; \quad G_V^{(4)} = 13460 \text{ MPa}; \quad \eta_V^{(4)} = 20000 \text{ MPa}$$

These data cover a rather wide range of both relaxation times and of contrasts between elasticity of the elastic and the viscous phases, and are expected to provide a significantly severe test for the bounding equations.

Figures 4.16 and 4.17 now plot directly the normalized relaxation and creep kernels, in the same plot, as functions of a time t normalized with respect to the relaxation time $t_{V,m}$ of the viscous phase with the highest volume fraction. Figure 4.16 refers to the case $c_1 = 0.1$ (small elastic fraction), and Figure 4.17 to the case $c_1 = 0.9$ (high elastic fraction). In Figure 4.17 all the relaxation curves have been amplified by a factor of 10 in order to better show them, otherwise they would all appear as superimposed at $y \approx 0$.
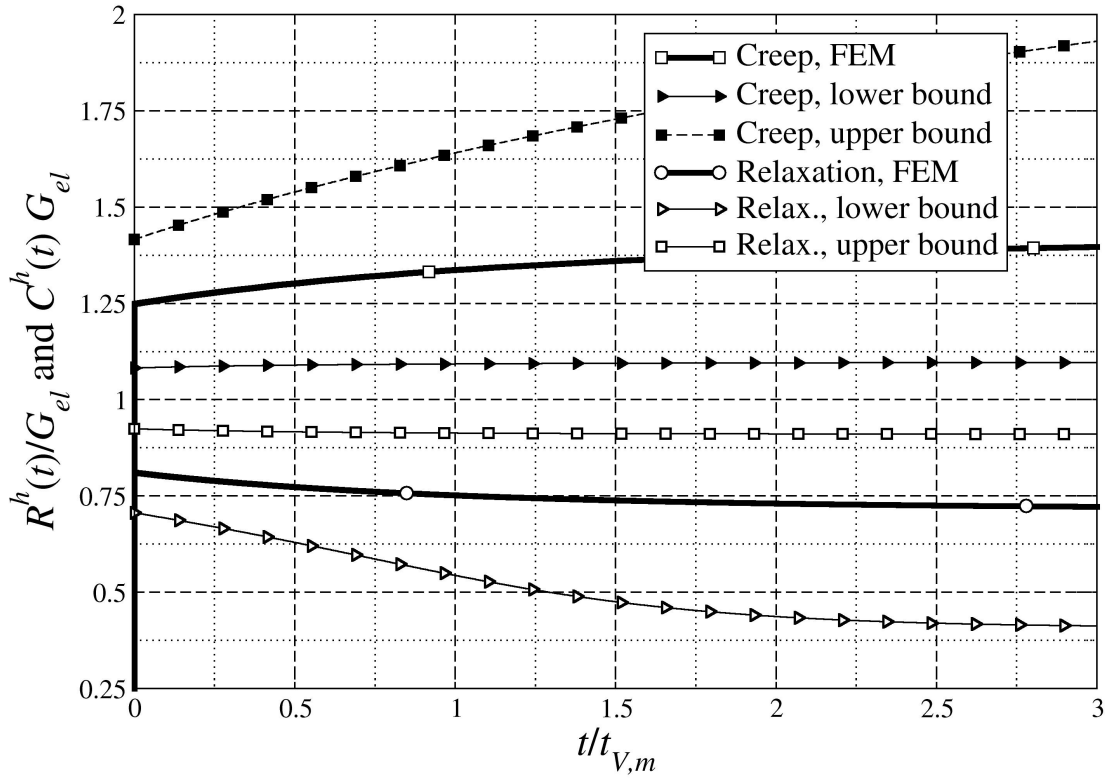
Figure 4.16: Normalized homogenized shear kernels as a function of normalized time t/t_V for a 4-phase composite, with $c_1 = 0.9$ (elastic), and $c_2 = 0.05, c_3 = 0.03333, c_4 = 0.01667$ (all viscoelastic). Thin curves with black symbols plot lower (right triangles, eq. (4.1.39)) and upper (squares, eq. (4.1.37)) bounds on the normalized homogenized creep kernel $C^h(t)G_{el}$; thin curves with white symbols plot lower (right triangles, eq. (4.1.38)) and upper (squares, eq. (4.1.36)) bounds on the normalized homogenized relaxation kernel $R^h(t)/G_{el}$; thick lines plot FEM solutions. Other parameters as indicated in the text.
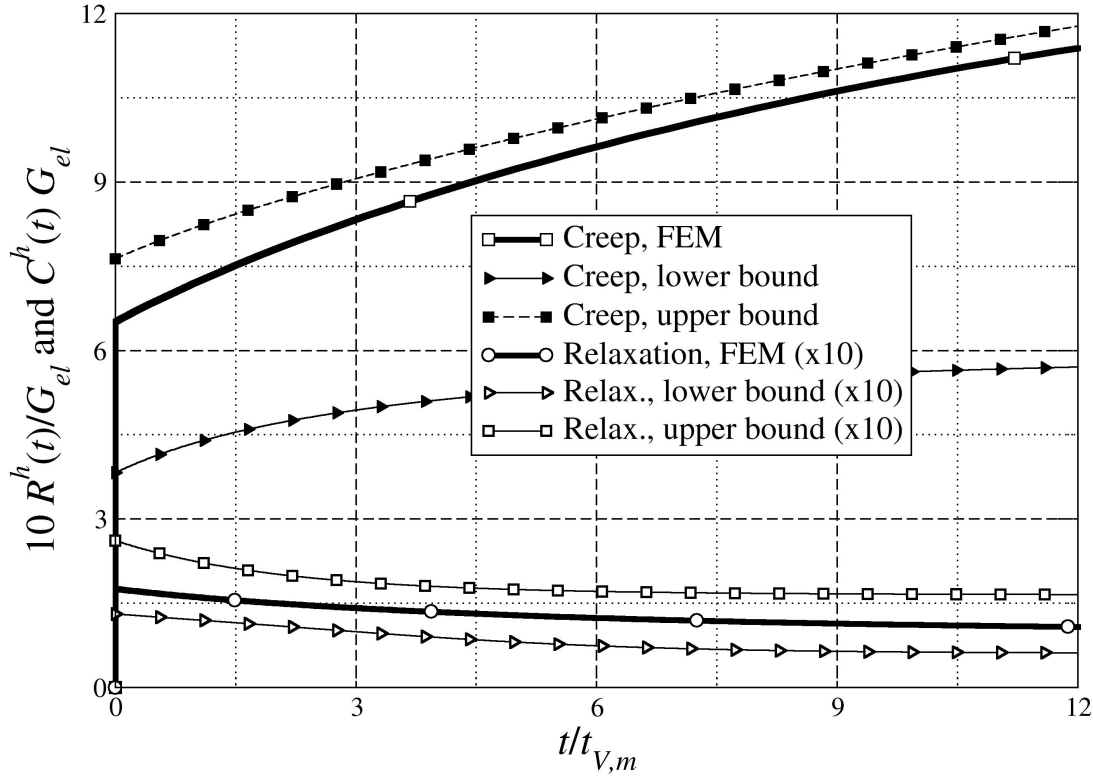
Figure 4.17: Normalized homogenized shear kernels as a function of normalized time t/t_V for a 4-phase composite, with $c_1 = 0.1$ (elastic), and $c_2 = 0.5, c_3 = 0.3, c_4 = 0.1$ (all viscoelastic). Thin curves with black symbols plot lower (right triangles, eq. (4.1.39)) and upper (squares, eq. (4.1.37)) bounds on the normalized homogenized creep kernel $C^h(t)G_{el}$; thin curves with white symbols plot lower (right triangles, eq. (4.1.38)) and upper (squares, eq. (4.1.36)) bounds on the normalized homogenized relaxation kernel $R^h(t)/G_{el}$; thick lines plot FEM solutions. Other parameters as indicated in the text.

All these results confirm once more the validity of the newly formulated bounds.

4.4 Numerical tests on volumetric kernels

In this Section we will consider only volumetric strains, unlike in the previous Section.

In order to obtain numerical results, we now consider viscoelastic phases governed by a standard two-parameter solid rheologic model of the Maxwell type, for which, for a generic phase (i), the volumetric relaxation kernel is written as follows (Migliacci, 1979):

$$R_V^{(i)}(t) = K_V^{(i)} \exp\left(-\frac{K_V^{(i)} t}{\eta_V^{(i)}} \right) \tag{4.4.1}$$

where $K_V^{(i)}$ is the bulk modulus of the viscoelastic material, and $\eta_V^{(i)}$ is the viscosity coefficient. The corresponding volumetric creep kernel reads as follows (Migliacci, 1979):

$$C_V^{(i)}(t) = \frac{1}{K_V^{(i)}} + \frac{t}{\eta_V^{(i)}} \tag{4.4.2}$$

Bounds (4.1.36) – (4.1.39) are compared with Finite Element results obtained by means of the commercial code ABAQUS (Hibbitt et al., 2018). ABAQUS allows the modelling of linear viscoelastic materials through the definition of material parameters associated to the Prony series for relaxation only; this, for a Maxwell material and for each phase (i), is written in ABAQUS in the following form:

$$p^{(i)}(t) = -K_0^{(i)} \int_0^t \left\{ 1 - \frac{K_1^{(i)}}{K_0^{(i)}} \left[1 - \exp\left(-\frac{K_1^{(i)} \tau}{\eta_1^{(i)}} \right) \right] \right\} \dot{\epsilon}^{vol\,(i)} \, d\tau, \quad i = 1, \dots, N \tag{4.4.3}$$

and requires in input the values of $K_0^{(i)}$, $K_1^{(i)}/K_0^{(i)}$, and $\eta_1^{(i)}/K_1^{(i)}$, $i = 1, \dots, N$. A match between eqs. (4.4.3) and (4.4.1) shows immediately that, in order to establish equivalence between ABAQUS and analytical results, one needs to set $K_0^{(i)} = K_V^{(i)}$, $K_1^{(i)} = K_0^{(i)} = K_V^{(i)}$, and $\eta_1^{(i)} = \eta_V^{(i)}$.

Two example are presented: the first one is a sphere, the second one is a RVE with unit sides with different microstructures, each possessing inclusions of different size. We start analysing the relaxation kernel, by applying boundary displacements corresponding to a constant unit value for the volumetric strain. This Section shows numerically that upper bounds are not valid for systems subject to volumetric strains and the analysis was limited only to relaxation kernels.

The considered loading conditions allow one to obtain information about the homogenized bulk modulus of a macroscopically isotropic material.

Loading conditions were applied as unit steps at $t = 0$. 4-node linear standard tetrahedral elements (3D stress family) (C3D4 in ABAQUS notation) have always been adopted.

The set of analyses was run considering a two-phase material, the first $(i = 1)$ linear elastic and the second $(i = 2)$ linear viscoelastic. The considered material data are:

$c_1 = 0.7$; $K^{(1)} = K_{el} = 1666.6667$ MPa

$c_2 = 0.3$; $K_V^{(2)} = 25000$ MPa; $\eta_V^{(2)} = \eta_V = 20000$ MPa sec

The Poisson's coefficient of both the elastic and the viscoelastic phase has been set equal to $\nu^{(1)} = \nu^{(2)} = 0.3$.

4.4.1 Analysis of a 3D system with volumetric strains

Elastic body with viscoelastic inclusions

Consider the problem of Figure 4.18, represented in 3D in ABAQUS.
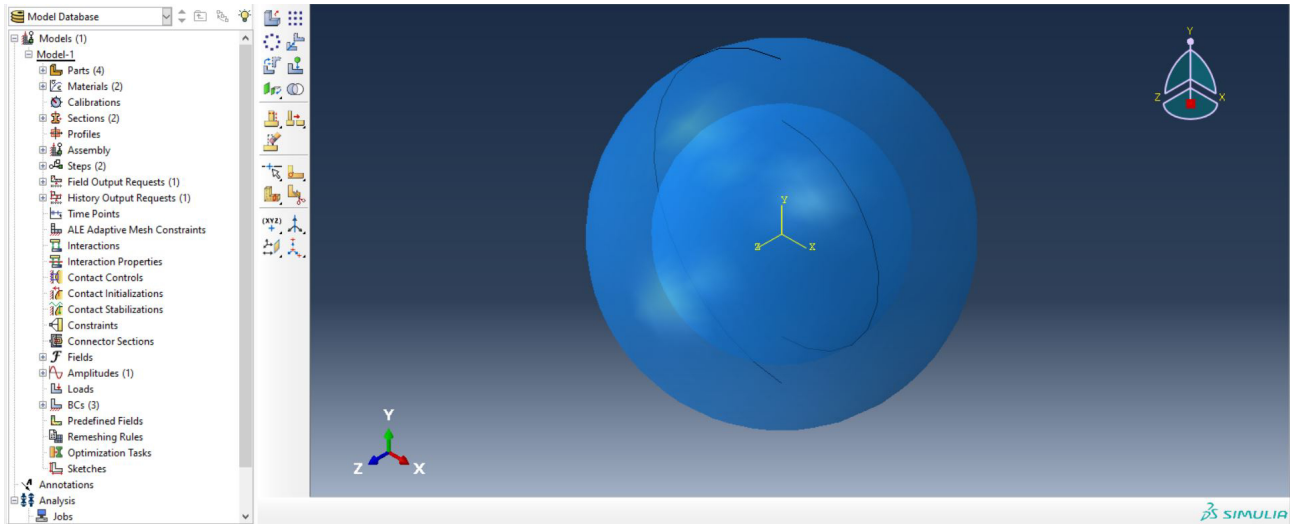
Figure 4.18: Sphere consisting of two phases with one inclusion, 3D representation from the program ABAQUS.

Meaning a sphere consisting of two phases, the first one with volume V_1 and the second one with volume V_2, subjected to radial displacement δ uniformly distributed, which creates a volumetric strain.

The analysis performed with one inclusion is replicated using four and eight inclusions (represented in Figures 4.19-4.20).
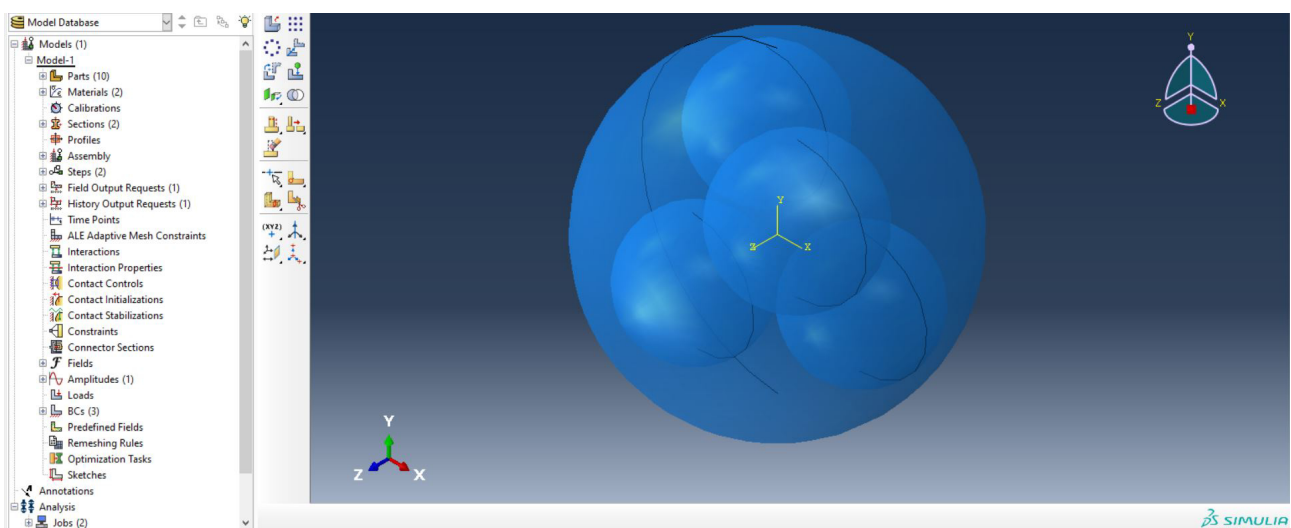
Figure 4.19: Sphere consisting of two phases with four inclusions, 3D representation in ABAQUS.
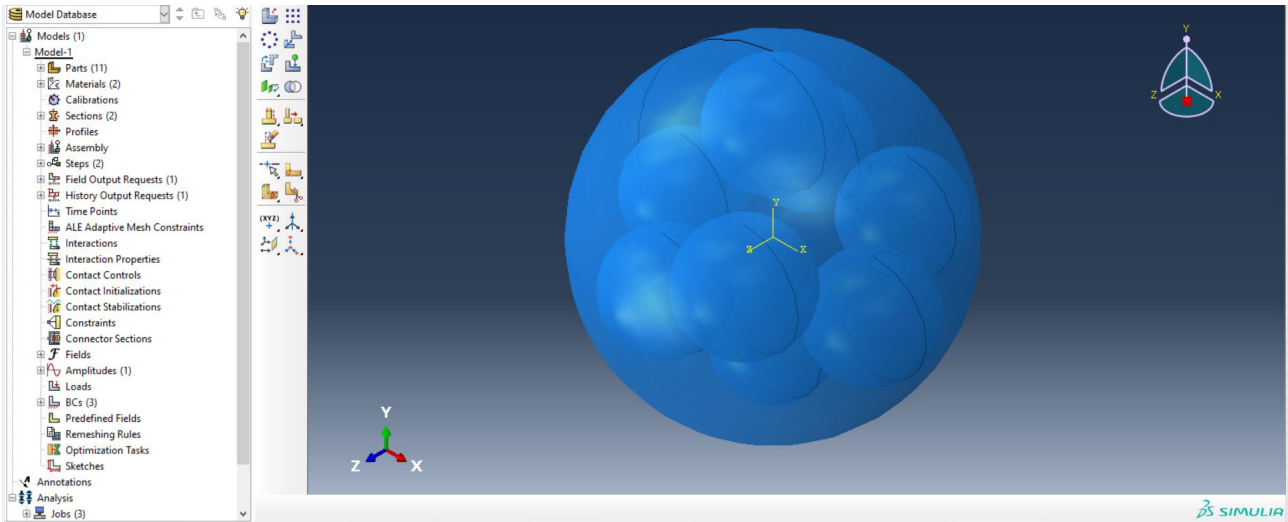
Figure 4.20: Sphere consisting of two phases with eight inclusions, 3D representation in ABAQUS.

Figure 4.21 plots the relaxation function normalized by the elastic bulk modulus K_{el} and shows a comparison between the mean value, defined in (4.1.36), and the homogenized value of the relaxation function using one, four and eight inclusions. The time has been normalized by the relaxation time $t_V = \eta_v/K_V$.

It is proved once again that the mean value does not constitute an upper bound for a system subject to volumetric strains.

The enlargement of Figure 4.22 shows the variation of the homogenized value of the relaxation kernel using one, four and eight inclusions. The case with eight inclusions overlaps the one with four inclusions. These results are larger than the case with just one inclusion at the beginning of the time range, afterwards they get lower and, finally, all results overlap at the end of the time range.
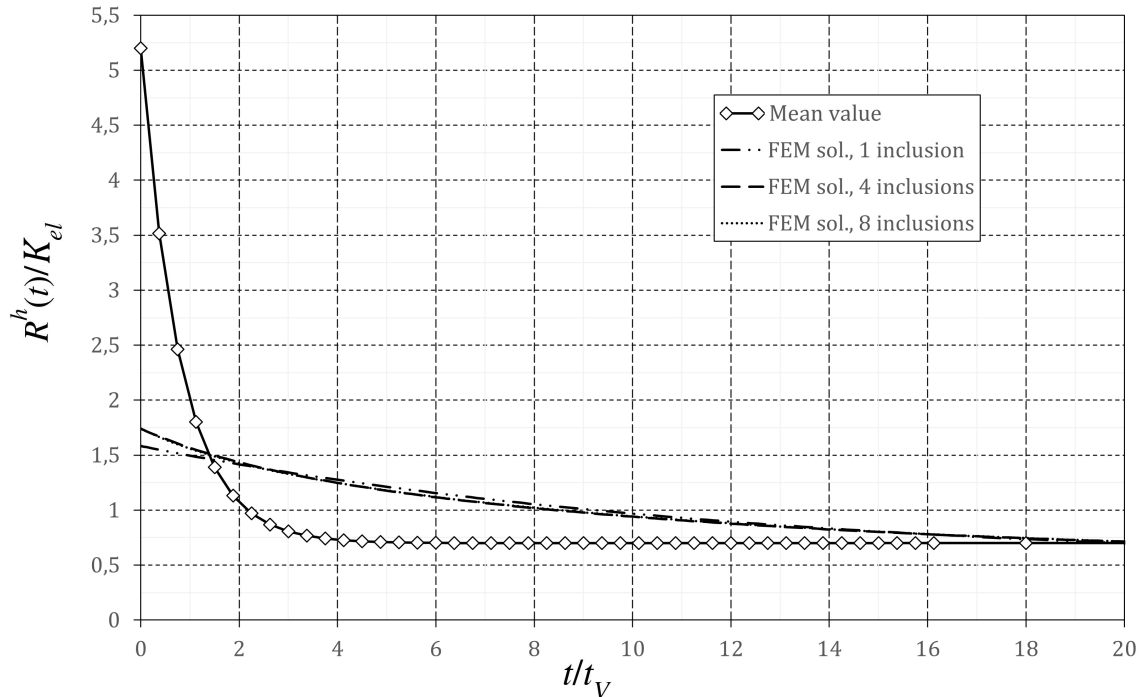
Figure 4.21: Normalized homogenized volumetric relaxation kernel $R^h(t)/K_{el}$ as a function of normalized time t/t_V. Comparison between the mean value (4.1.36) and the homogenized relaxation kernel of a 3D system with volumetric strains and viscoelastic inclusions using, respectively, one, four and eight inclusions.
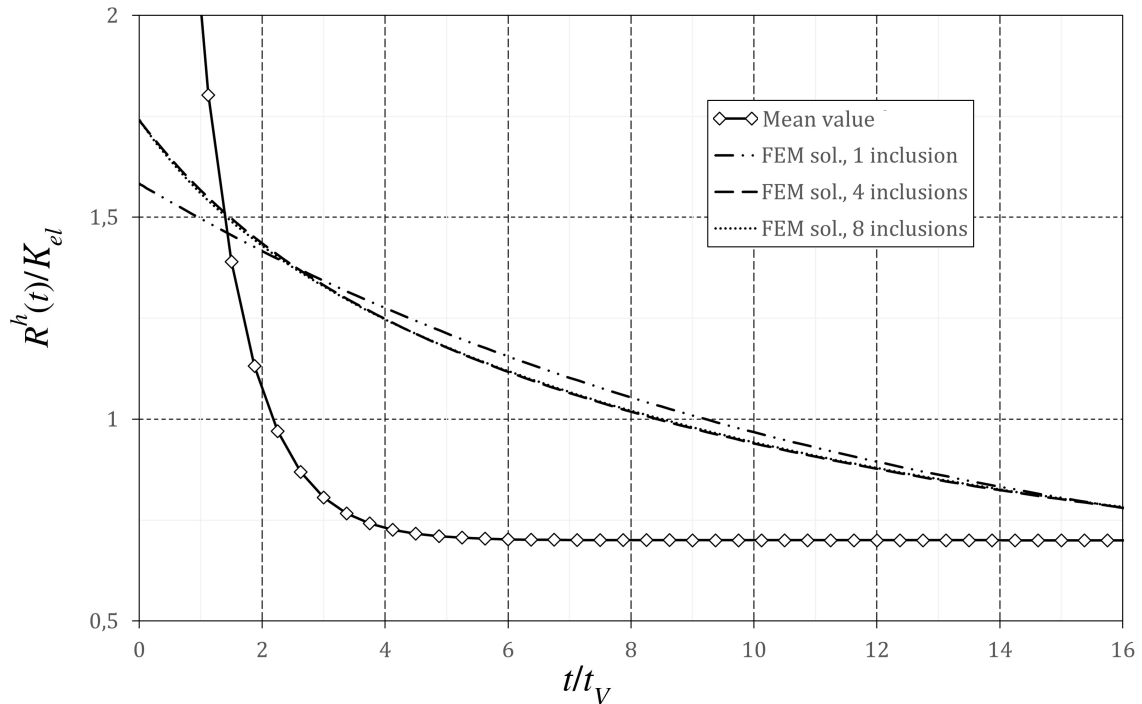
Figure 4.22: Normalized homogenized volumetric relaxation kernel $R^h(t)/K_{el}$ as a function of normalized time t/t_V. Comparison between the mean value (4.1.36) and the homogenized relaxation kernel of a 3D system with volumetric strains and viscoelastic inclusions using, respectively, one, four and eight inclusions - enlargement.

Viscoelastic body with elastic inclusions

Consider the same problem as in the previous Section, this time assigning an elastic material to the inclusions and a viscoelastic material to the matrix.

The whole process is not presented again for the sake of brevity, only the final results with one, four and eight inclusions (calculated with ABAQUS) are summarized in Figures 4.23-4.24.

Figure 4.23 shows a comparison between the mean value (4.1.36) and the homogenized value of the relaxation function using one, four and eight inclusions.

It is proved once again that the mean value does not constitute an upper bound for a system subject to volumetric strains.

The enlargement of Figure 4.24 shows the variation of the homogenized value with one, four and eight inclusions. The case with eight inclusions overlaps the one with four inclusions. These results are larger than the case with just one inclusion at the beginning of the time range, afterwards they get lower and, finally, all results overlap at the end of the time range.
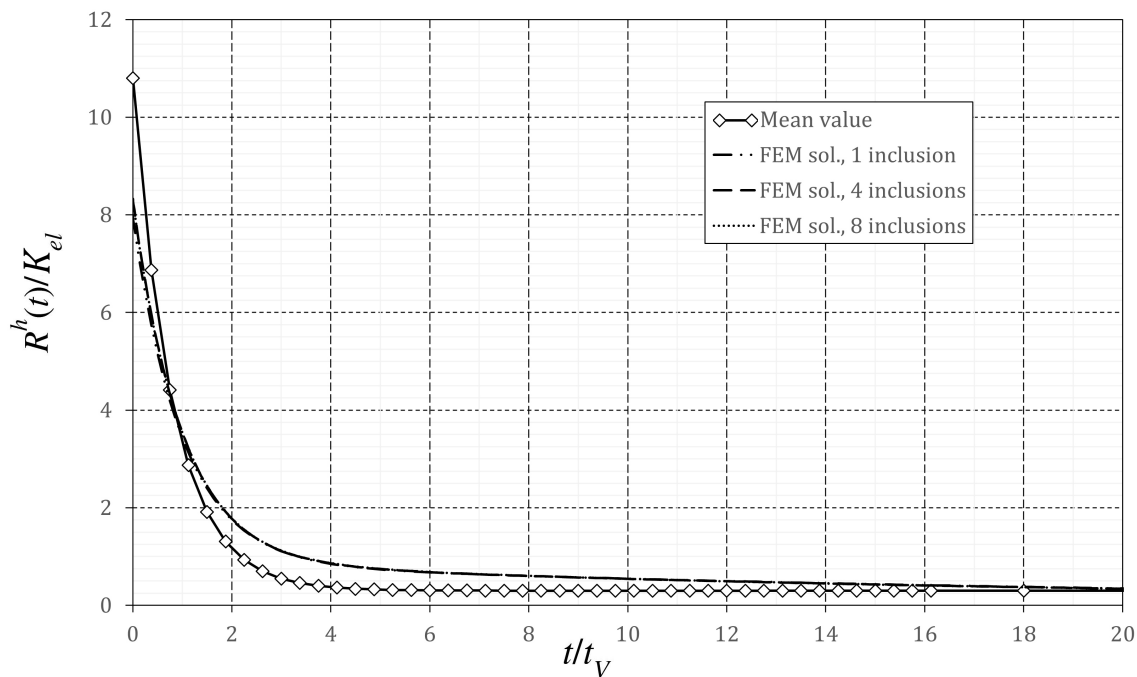
Figure 4.23: Normalized homogenized volumetric relaxation kernel $R^h(t)/K_{el}$ as a function of normalized time t/t_V. Comparison between the mean value (4.1.36) and the homogenized relaxation kernel of a 3D system with volumetric strains and elastic inclusions using, respectively, one, four and eight inclusions.
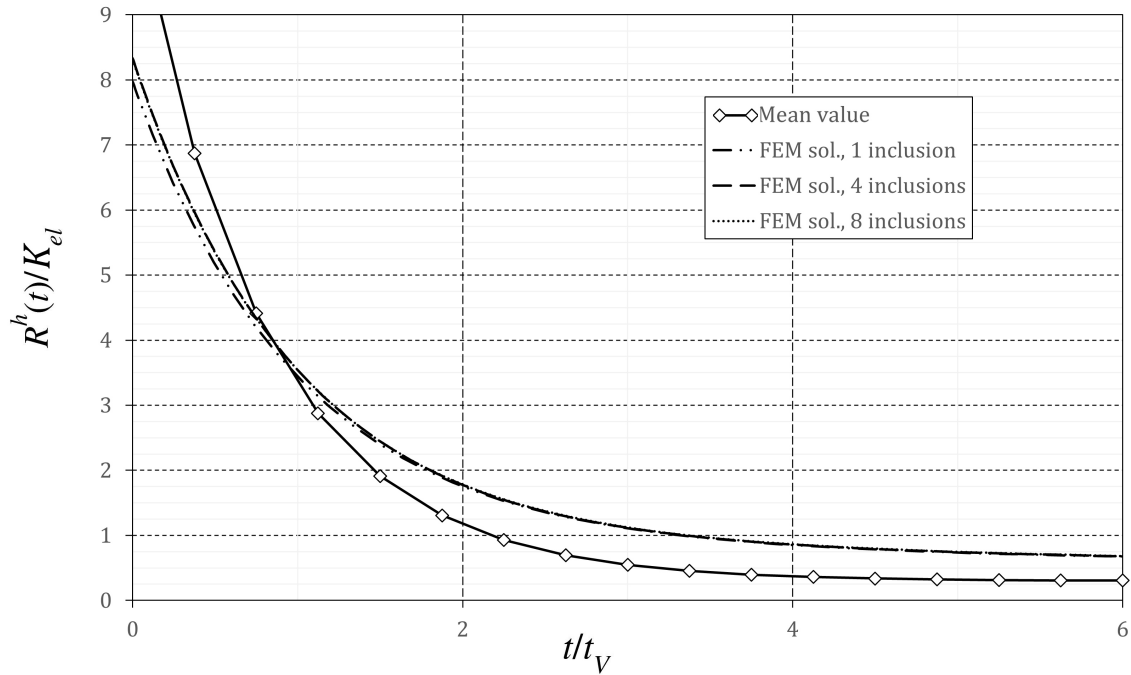
Figure 4.24: Normalized homogenized volumetric relaxation kernel $R^h(t)/K_{el}$ as a function of normalized time t/t_V. Comparison between the mean value (4.1.36) and the homogenized relaxation kernel of a 3D system with volumetric strains and elastic inclusions using, respectively, one, four and eight inclusions - enlargement.

4.4.2 Analysis of a RVE with volumetric strains

Elastic body with viscoelastic inclusions

Consider the problem of Figure 4.25, represented in 3D in ABAQUS.
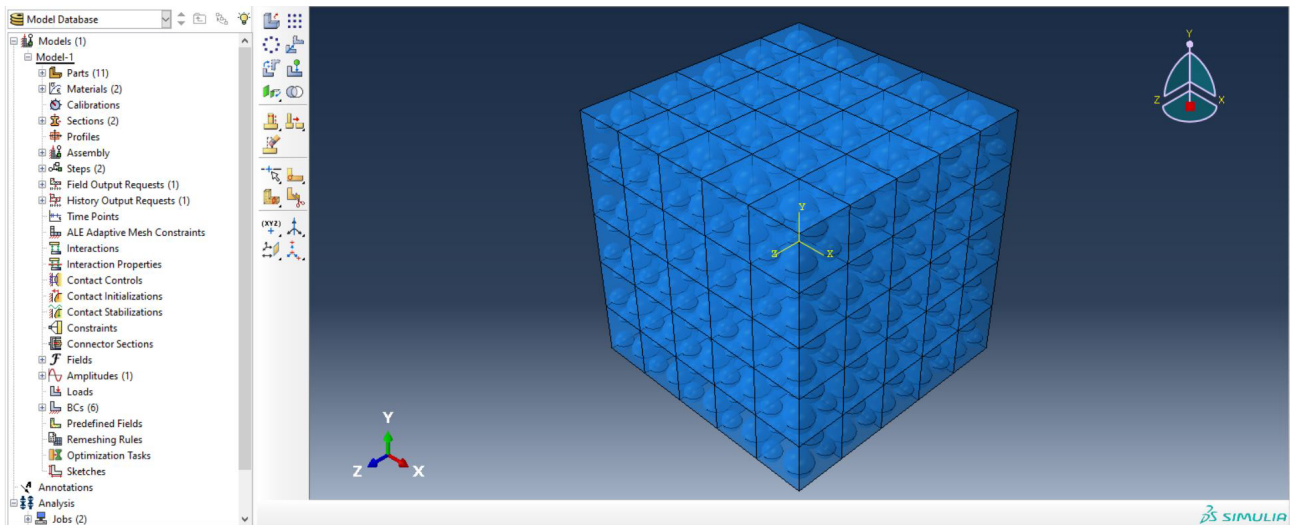
Figure 4.25: RVE consisting of two phases with different inclusions, 3D representation in ABAQUS.

Meaning a RVE consisting of two phases, the first one with volume V_1 and the second one with volume V_2, subjected to displacement δ perpendicular to the external faces of the cube. It is a combination of cubes (5×5×5), each containing seven spherical inclusions of different sizes.

Figure 4.26 plots the relaxation function normalized by the elastic elastic bulk modulus K_{el} and shows a comparison between the mean value, defined in (4.1.36), and the homogenized value of the relaxation function. The time has been normalized by the relaxation time $t_V = \eta_v / K_V$. It is proved once again that the mean value does not constitute an upper bound for a system subject to volumetric strains.
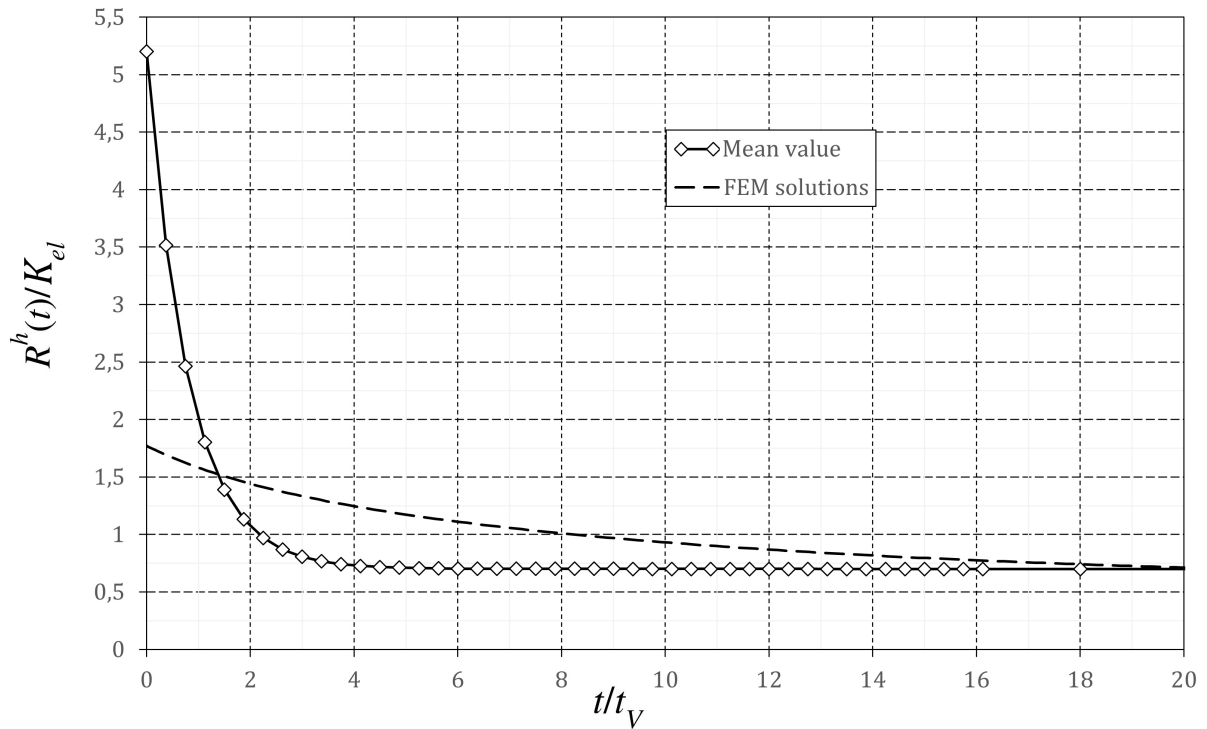
Figure 4.26: Normalized homogenized volumetric relaxation kernel $R^h(t)/K_{el}$ as a function of normalized time t/t_V. Comparison between the mean value (4.1.36) and the homogenized relaxation kernel of a 3D RVE system with volumetric strains and viscoelastic inclusions.

Viscoelastic body with elastic inclusions

Consider the same problem as in the previous Section, this time assigning an elastic material to the inclusions and a viscoelastic material to the matrix.

The whole process is not presented again for the sake of brevity, only the final result multiple inclusions (calculated with ABAQUS) is summarized in Figure 4.27, which shows a comparison between the mean value, defined in (4.1.36), and the homogenized value of the relaxation function.

It is proved once again that the mean value does not constitute an upper bound for a system subject to volumetric strains.
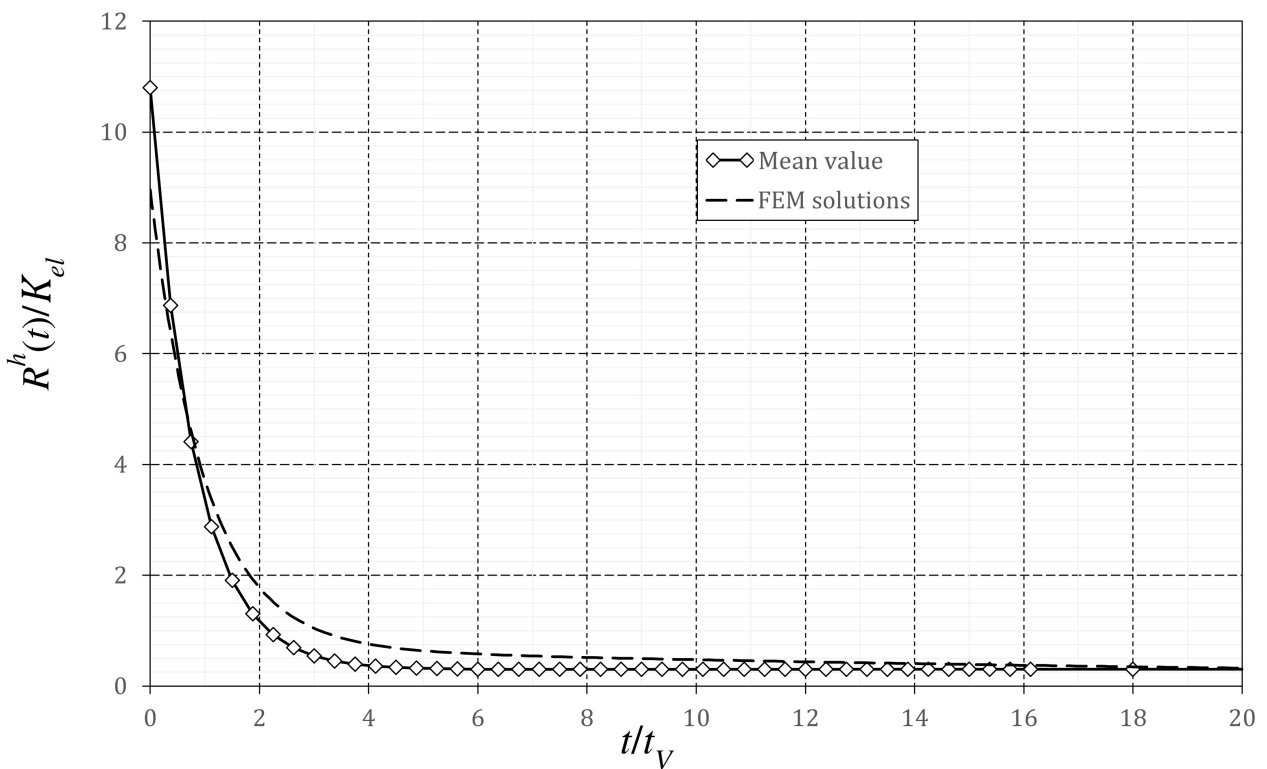
Figure 4.27: Normalized homogenized volumetric relaxation kernel $R^h(t)/K_{el}$ as a function of normalized time t/t_V. Comparison between the mean value (4.1.36) and the homogenized relaxation kernel of a 3D RVE system with volumetric strains and elastic inclusions.

4.5 Conclusions

We consider the case of macroscopically isotropic materials.

Upper and lower bounds have been described, as extensions of the bounds derived by Voigt and Reuss from extremal formulation valid for elasticity.

From Carini and Mattei (2015) upper bounds are obtained and proved only for deviatoric strains and several numerical simulations have been performed in order to verify these bounds, even with volumetric strains.

The lower bounds have already been proposed by Huet (1995) for the scalar homogenized relaxation $R^h(t)$ and creep $C^h(t)$ kernel components, who derived them from the Principle of Virtual Work. Therefore, there was no need in testing them again (in fact they only appear in the analysis of shear kernels).

On the other hand, the upper bounds are tested for bodies subjected to either volumetric or deviatoric strains.

From the first set of analyses, as expected, the upper bounds prove to be verified for deviatoric strains.

Nevertheless, when a body is subjected to volumetric strains, the proposed upper bound is no longer satisfied.

This particular issue could be an interesting starting point for subsequent research works.

References

ABAQUS Manuals, rel. 2018. Dassault Systèmes/SIMULIA, Jonston, Rhode Island, US.
Hibbit, H.D., Karlsson, B., Sorensen, P.

Bland, D.R., 1960. The theory of linear viscoelasticity. Pergamon Press, Oxford, UK.

Carini, A., Gelfi, P., Marchina, E., 1995. An energetic formulation for the linear viscoelastic problem. Part I: Theoretical results and first calculations. International Journal for Numerical Methods in Engineering, 38, 37-62.

Carini, A., Mattei, O., 2015. Variational formulations for the linear viscoelastic problem in the time domain. European Journal of Mechanics A/Solids, 54, 146-159.

Cherkaev, A.V., Gibiansky, L. V., 1994. Variational principles for complex conductivity, viscoelasticity, and similar problems in media with complex moduli. Journal of Mathematical Physics , 35, 127-145.

Franciosi, V., 1962. Scienza delle costruzioni: Teoria dell'elasticità e resistenza dei materiali. Liguori Editore, Napoli.

Gurtin, M.E., 1963. Variational principles in the linear theory of viscoelasticity. rchive for Rational Mechanics and Analysis, 16 (1), 34-50.

Huet, C., 1995. Bounds for the overall properties of viscoelastic heterogeneous and composite materials. Archives of Mechanics, 47(6), 1125-1155.

Lahellec, N., Suquet, P., 2007. Effective behaviour of linear viscoelastic composites: A time integration approach. International Journal of Solids and Structures, 44, 507-529.

Mandel, J., 1966. Cours de mécanique des milieux continus, Tome II. Gauthier-Villars, Paris.

Mattei, O., Milton, G. W. 2016. Bounds for the response of viscoelastic composites under antiplane loadings in the time domain. In: G. W. Milton, Extending the Theory of Composites to Other Areas of Science, Milton-Patton Publishing, Salt Lake City, USA.

Migliacci, A., 1979. Applicazioni dei principi di viscosità: strutture formate da aste di calcestruzzo in fase di viscosit'a lineare. Tamburini, Milano.

Milton, G. W., 1990. On characterizing the set of possible effective tensors of composites: the variational method and the translation method. Communications on Pure and Applied Mathematics, XL, 63-125.

Rafalski. P., 1969. The orthogonal projection method III. Linear viscoelastic problem. Bulletin of the Polish Academy of Sciences: Technical Sciences, 17, 167.

Reiss, R., Haug, E.J., 1978. Extremal principles for linear initial value problems of mathematical physics. International Journal of Engineering Science, 16, 231-251.

Staverman, A.J., Schwarzl, F., 1952. Thermodynamics of Viscoelastic Behavior. Proceedings of the National Academy of Sciences, The Netherlands 55, 474-485.

Tonti, E., 1973. On the variational formulation for linear initial value problems. Annali di Matematica Pura ed Applicata, Serie Quarta XCV, 331-359.

Tonti, E., 1984. Variational formulations for every nonlinear problem. International Journal of Engineering Science, 22 (11-12), 1343-1371.

Yosida, K., 1980. Functional Analysis. Springer-Verlag, Berlin, Heidelberg, New York.

Chapter 5

A variational approach to fracture mechanics

Notation

Greek and latin letters

- ϵ_{ij}: Small strain tensor components;

- F_j: Body force vector components;

- f_j: Surface traction vector components;

- V: Volume of the solid body;

- S_f/Γ_p: Loaded region of the boundary;

- u_j: Displacement vector components;

- h: Hardening component for the Capurso-Maier functional;

- λ: Plastic multiplier;

- φ: Yield function;

- $\bar{u}_j$: Prescribed displacement vector components;

- S_u/Γ_u: Constrained region of the boundary;

- V_E: Volume of the solid body in the elastic phase;

- V_P: Volume of the solid body in the plastic phase;

- Ω_∞: Infinite domain of the fracture mechanics problem;

- $w(x)$: Fracture opening;

- $p(w)$: Internal pressure of the fracture;

- l: Crack length;

- G: Energy-release rate;

- E: Young's modulus;

- H: Hardening term;

- G_0: Critical value of the Energy-release rate;

- η: Lagrange multiplier;

- D_j^l: Concentrated displacement discontinuity components;

- ν: Poisson's ratio;

- $\boldsymbol{K}$: Stress intensity factors vector;

- $s(t)$: Fracture extension in Salvadori and Carini (2011);

- $\vartheta(\boldsymbol{K})$: Actual crack state;

- K_1^C: Fracture toughness;

- $\kappa(t)$: Load factor;

- $\boldsymbol{E}$: Safe equilibrium domain;

- Ω: Region occupied by a solid body;

- $\bar{p}$: Prescribed pressure inside the fracture;

- Γ_w: Reference surface for the crack;

- $\boldsymbol{x}$: Field point;

- $\boldsymbol{\xi}$: Source point;

- r: Distance between the field point and the source point;

- $\boldsymbol{f}^i$: Vector of known terms;

- n_i: Unit outward normal vector components.

Symbols

- $=::$ Is defined as;

- $\dot{}$: Incremental variable;

- $\hat{}$: Admissible term;

- $_{\mathcal{L}}$: Lagrangian functional;

- ^{E}: Elastic component of a term;

- ^{P}: Plastic component of a term;

- $\in$: Belongs to.

Operators and functions

- $\mathcal{F}_{CM}$: Capurso-Maier functional;

- D_{ijhk}: Constitutive operator;

- $_{/i}$: Partial derivative operation;

- Δ: Subtraction operator;

- TPE: Total Potential Energy functional;

- G_{ij}: Green's operator;

- χ: Salvadori and Carini functional;

- TPE_{ext}: Total Potential Energy functional extended to the 2D/3D case;

- $\mathcal{F}_V$: Viscoelastic fracture mechanics functional;

- R_{pp}: Viscoelastic operator.

5.1   Introduction

The major aim of fracture mechanics is to find out which cracks constitute a potential risk for the global or partial failure of the structure and which do not.

From a practical point of view many cracks can be considered as harmless since they do not lead to failure of the structure but, it is well-known that micro-cracks and micro processes of de-cohesion deeply influence the macroscopic crack growth in materials.

The crack growth in materials can be regarded as an increasing of the opening displacement between the free surfaces that constitute the macroscopic crack. The evaluation of this parameter is important in structural design in order to investigate cracks propagation. The study of how cracks could develop inside the hosting medium is of fundamental importance in order to assess the safety of the component. In the present work, brittle materials are considered, i.e. the cohesion between surfaces is here neglected; furthermore non-penetrative condition between free surfaces is assumed and the loading conditions are assumed to be quasi-static, i.e. frictional or dynamic effects are assumed to be negligible.

Due to the importance of the topic, expecially from an engineering perspective, in this Chapter the aim is to derive new variational formulations and, in particular, new functionals for the study of the fracture mechanics problem.

In the first part of the Chapter, a functional is derived from the Total Potential Energy functional introduced by Capurso and Maier for the elastoplastic problem, expressed in an incremental form. In order to fully write the functional for a straight crack in an infinite domain Ω_∞, the variation of the energy-release rate is defined and a hardening component is obtained. Moreover, a formal analogy between the variation of the energy release-rate and the yield function for elastoplasticity is presented, as well as complementarity conditions, reminiscence of Kuhn-Tucker conditions. A minimum principle is proved for the derived functional and subsequently it is rewritten in a one-field form, depending either on the variation of the fracture opening caused by a crack elongation at constant pressure, or on the plastic distortion itself.

Furthermore, an analogy between the obtained one-field functional dependent only on the crack elongation and the functional derived in Salvadori-Carini (2011) is presented. Finally, the formulation is generalized to the case of a finite body in a two/three dimensional space and Bramble and Pasciak method is used to prove the minimum principle.

In the second part of the Chapter, a hint is given about a Free Energy type functional, deriving from Francfort-Marigo formulation (2008) of the fracture mechanics problem, which could be used to extend the fracture mechanics formulation to viscoelastic composites, thus to time-dependent problems.

In fact, since 1960 proposed models and methods for the study of crack propagation are referred only to elastic media. A more accurate theory should take into account the viscous materials properties and the exit from the elastic field of the material near the crack tip. The aim of future research is trying to extend the energetic formulation of Francfort and Marigo in order to simulate complex dynamic phenomena in viscoelastic media.

5.2 Capurso-Maier functional

5.2.1 Introduction

The aim of this work is to derive a Total Potential Energy (TPE) functional for fracture mechanics, analogous to the two-field functional $\mathcal{F}_{CM}$ used in elastoplastic formulation, as the one introduced by Capurso-Maier (Corradi dell'Acqua, 1992). The functional is expressed in incremental form as:

$$\mathcal{F}_{CM}(\dot{u}_i, \dot{\lambda}) = \frac{1}{2} \int_V D_{ijhk} \dot{\epsilon}_{ij} \dot{\epsilon}_{hk} \, dV - \int_V \dot{F}_j \dot{u}_j \, dV - \int_{S_f} \dot{f}_j \dot{u}_j \, dS + \frac{1}{2} \int_V h \dot{\lambda}^2 \, dV \qquad (5.2.1)$$

The functional must respect the following constraints

$$\dot{\epsilon}_{ij} = \frac{1}{2} \left(\dot{u}_{i/j} + \dot{u}_{j/i} \right) - \frac{\partial \varphi}{\partial \sigma_{ij}} \dot{\lambda} \qquad (5.2.2)$$

$$\dot{u}_j = \dot{\bar{u}}_j \quad on \ S_u \qquad (5.2.3)$$

$$\dot{\lambda} = 0 \quad in \ V_E \qquad (5.2.4)$$

$$\dot{\lambda} \geq 0 \quad in \ V_P \qquad (5.2.5)$$

where S_u/Γ_u is the constrained region of the boundary, V_E is the volume of the solid body in the elastic phase and V_P is the volume of the solid body in the plastic phase; To begin with, functional (5.2.1) can be written in a non-incremental form, exploiting Green's operator G_{pp}, that represents the pressure p on a normal surface $n(x)$, due to a unitary relative displacement concentrated in a point $\xi \in \Omega$ and acting on the unlimited space Ω_∞.

In the case of a symmetric problem, as the one sketched in Fig. 5.1, the functional takes the form:

$$\text{TPE} = -\frac{1}{2} \int_0^l \int_0^l G_{pp}(x - \xi) w(\xi) w(x) \, d\xi dx - \int_0^l p(x) w(x) \, dx \qquad (5.2.6)$$
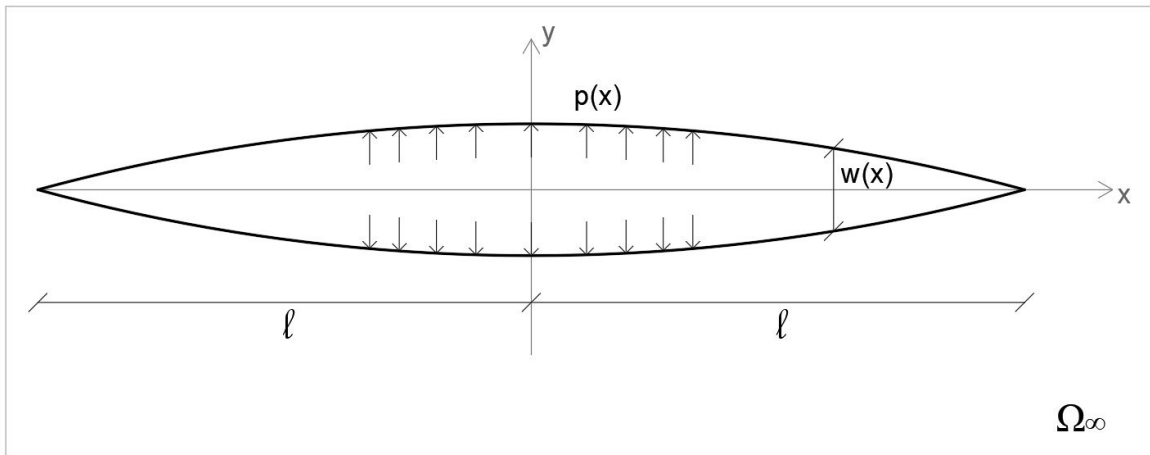
Figure 5.1: Fracture mechanics problem, defined in an infinite domain Ω_∞.

The first double integral in (5.2.6) is a strain energy, whereas the second one is the internal loads potential.

$p(x)$ is the pressure inside the fracture, $w(x)$ is the opening of the fracture, and $2l$ is the length

of the fracture.

Interpreting the first integral in (5.2.6) according to the Hadamard's sense, the equilibrium equation can be resembled:

$$-\int_0^l G_{pp}(x - \xi)w(\xi)\,d\xi = p(x) \tag{5.2.7}$$

Substituing the latter into (5.2.6), we get:

$$\text{TPE} = -\frac{1}{2}\int_0^l p(w)w(x)\,dx \tag{5.2.8}$$

5.2.2   Energy-release rate G

The energy-release rate G, if p is prescribed $(p(w) = \bar{p})$, is expressed as:

$$G = -\frac{\partial \text{TPE}}{\partial l}\bigg|_{\bar{p}} \tag{5.2.9}$$

Bringing the derivation formula inside the integral and substituting (5.2.8) in (5.2.9) one has:

$$G = \frac{1}{2}\int_0^l \left(p(w)\frac{\partial w}{\partial l}(x)\right)\bigg|_{\bar{p}}\,dx + \frac{1}{2}p(l)w(l) = \frac{1}{2}\int_0^l \left(p(w)\frac{\partial w}{\partial l}(x)\right)\bigg|_{\bar{p}}\,dx \tag{5.2.10}$$

in view of condition $w(l) = 0$.

In order to verify the validity of formula (5.2.10), one considers a crack immersed in an infinite domain Ω_∞ with constant internal pressure p.

Fracture opening reads (Carpinteri, 1992):

$$w(x) = 4p \cdot \frac{l}{E}\left[1 - \left(\frac{x}{l}\right)^2\right]^{1/2} \tag{5.2.11}$$

Its derivative with respect to l is:

$$\frac{\partial w}{\partial l} = \frac{4p}{E}\frac{1}{\sqrt{1 - \left(\frac{x}{l}\right)^2}} \tag{5.2.12}$$

Substituting (5.2.12) in (5.2.10), the latter becomes:

$$G = \frac{2p^2}{E}\int_0^l \frac{1}{\sqrt{1 - \left(\frac{x}{l}\right)^2}}\,dx \tag{5.2.13}$$

Performing the following change of variable

$$\frac{x}{l} = X \qquad dX = \frac{dx}{l} \qquad dx = l \cdot dX \tag{5.2.14}$$

$$x = 0 \quad \Rightarrow \quad X = 0 \tag{5.2.15}$$

$$x = l \quad \Rightarrow \quad X = 1 \tag{5.2.16}$$

equation (5.2.13) can be expressed as:

$$G = \frac{2p^2l}{E} \int_0^1 \frac{1}{\sqrt{1-X^2}} \, dX, \tag{5.2.17}$$

thus confirming the attainment of the well-known solution

$$G = \frac{\pi l p^2}{E} \tag{5.2.18}$$

5.2.3 Definition of $\dot{G}$

In order to write functional (5.2.1) in an incremental form, the form of $\dot{G}$ is needed. To this aim, one recalls the expression of the energy-release rate G, namely:

$$G = \frac{1}{2} \int_0^l p(w) \frac{\partial w(x)}{\partial l} \, dx \tag{5.2.19}$$

Bearing in mind that $\dfrac{\partial w}{\partial l} \cdot \dot{l}$ represents the variation of the fracture opening w caused by a crack elongation of constant pressure, one has

$$\left. \frac{\partial w}{\partial l} \right|_{p=0} \cdot \dot{l} = 0, \tag{5.2.20}$$

if there is no crack elongation.

Therefore, it is possible to state that the crack opens linearly with the superimposed load, at the same $\dot{l}$ and $\dfrac{\partial w}{\partial l}$ could be treated as a linear function of p, namely

$$\frac{\partial w}{\partial l} = p \cdot f(x, l) \tag{5.2.21}$$

with $f(x, l)$ independent from p.

Thus, the energy release rate (5.2.19) becomes:

$$G = \frac{1}{2} \int_0^l p^2 \cdot f(x, l) \, dx \tag{5.2.22}$$

The variation of G can thus be additively decomposed in a contribution due to the pressure variation $\dot{p}$ and a contribution due to the crack elongation $\dot{l}$. It reads:

$$
\begin{aligned}
\dot{G} =& \frac{\partial G}{\partial p} \cdot \dot{p} + \frac{\partial G}{\partial l} \cdot \dot{l} \\
=& \frac{1}{2} \left(\int_0^l 2p \cdot f(x, l) \, dx \right) \cdot \dot{p} + \frac{1}{2} \left(\int_0^l p^2 \cdot \frac{\partial f(x, l)}{\partial l} \, dx \right) \cdot \dot{l}
\end{aligned}
\tag{5.2.23}
$$

Equation (5.2.23) does not contain boundary terms coming from the derivation inside an integral, because, there, the load is zero ($p = 0$).

Considering that in this case $\dot{p}$ is constant with respect to the variable x and recalling (5.2.21),

$\dot{G}$ can be expressed as

$$\dot{G} = \int_0^l \dot{p} \cdot \frac{\partial w}{\partial l} \, dx + \left(\frac{1}{2} \int_0^l p \cdot \frac{\partial^2 w}{\partial l^2} \, dx \right) \cdot \dot{l} \tag{5.2.24}$$

The second term of equation (5.2.24) resembles the hardening component introduced in plasticity theory. Considering in fact the formal analogy that exists between the energy-release rate G and the yield function φ (see Salvadori and Carini, 2011 for details), one has:

$$\dot{\varphi} = \frac{\partial \varphi}{\partial \sigma} \cdot \dot{\sigma} - H \cdot \dot{\lambda} \tag{5.2.25}$$

It is worth noting that, contrarily to what happens in plasticity, in fracture mechanics the second term in (5.2.25) has a positive sign, thus decreasing the resistance. It can be considered as a negative hardening.

From a comparison between equations (5.2.24) and (5.2.25) the hardening term can be expressed as

$$\left(\frac{1}{2} \int_0^l p \cdot \frac{\partial^2 w}{\partial l^2} \, dx \right) = H \tag{5.2.26}$$

It is worth mentioning that H is not known a priori and this constitutes a huge issue for numerical analyses.

In order to evaluate the correctness of the form (5.2.24), one considers the benchmark of a straight crack in an infinite domain Ω_∞.

In this case, as already proved in (5.2.18), the energy-release rate holds:

$$G = \frac{\pi}{E} l p^2 \tag{5.2.27}$$

Its variation reads:

$$\begin{aligned}
\dot{G} &= \frac{\partial G}{\partial p} \cdot \dot{p} + \frac{\partial G}{\partial l} \cdot \dot{l} \\
&= \frac{\pi}{E} \left[2p \cdot l \cdot \dot{p} + p^2 \cdot \dot{l} \right]
\end{aligned} \tag{5.2.28}$$

Comparing equation (5.2.24) to (5.2.28) one obtains:

$$\int_0^l \dot{p} \cdot \frac{\partial w}{\partial l} \, dx = 2 \frac{\pi}{E} p l \cdot \dot{p} \quad \Rightarrow \quad \int_0^l \frac{\partial w}{\partial l} \, dx = 2 p l \frac{\pi}{E} \tag{5.2.29}$$

$$\frac{1}{2} \int_0^l p \cdot \frac{\partial^2 w}{\partial l^2} \cdot \dot{l} \, dx = \frac{\pi}{E} p^2 \cdot \dot{l} \quad \Rightarrow \quad \frac{1}{2} \int_0^l \frac{\partial^2 w}{\partial l^2} \, dx = p \frac{\pi}{E} \tag{5.2.30}$$

Considering that the fracture opening increment can be additively decomposed in a contribution due to load increment $\dot{p}$ and a contribution due to plastic distortion $\dot{l}$, one has

$$\dot{w} = \frac{\partial w}{\partial p} \cdot \dot{p} + \frac{\partial w}{\partial l} \cdot \dot{l} = \dot{w}^E + \dot{w}^P \tag{5.2.31}$$

In the light of equation (5.2.31), the parameter $\dot{G}l$ gains the form

$$
\begin{aligned}
\dot{G}l &= \int_0^l \dot{p} \cdot \frac{\partial w}{\partial l} \dot{l} \, dx + \left(\frac{1}{2} \int_0^l p \cdot \frac{\partial^2 w}{\partial l^2} \, dx \right) \cdot \dot{l}^2 \\
&= \int_0^l \dot{p} \cdot \dot{w}^P \, dx + H \cdot \dot{l}^2
\end{aligned}
\tag{5.2.32}
$$

5.2.4 Complementarity conditions

Crack propagation is governed at time t by the following conditions, reminiscence of Kuhn-Tucker conditions of plasticity

$$
(G - G_0)\dot{l} = 0 \qquad G - G_0 \le 0 \qquad \dot{l} \ge 0
\tag{5.2.33}
$$

In the hypothesis of irreversible crack growth, if the second condition is valid, the crack is stationary ($\dot{l} = 0$) and if the third one is valid, it means that G has reached the critical value G_0 and the crack propagates.

Time derivation of the first of conditions (5.2.33) leads to:

$$
\dot{G}\dot{l} + (G - G_0)\frac{d\dot{l}}{dt} = 0
\tag{5.2.34}
$$

Analogously to what happens in plasticity, in a plastic zone, namely when $G = G_0$, the second term of (5.2.34) vanishes and one retrieves the so-called consistency condition, namely:

$$
\dot{G}\dot{l} = 0
\tag{5.2.35}
$$

Therefore, in a plastic zone, complementarity conditions can be written as:

$$
\dot{G}\dot{l} = 0 \qquad \dot{G} \le 0 \qquad \dot{l} \ge 0
\tag{5.2.36}
$$

which complete the analogy with the complementarity conditions written in terms of the yield function $\dot{\varphi}$:

$$
\dot{\varphi}\dot{\lambda} = 0 \qquad \dot{\varphi} \le 0 \qquad \dot{\lambda} \ge 0
\tag{5.2.37}
$$

From equation (5.2.37), the formal equality $\dot{l} = \dot{\lambda}$ descends, which is proved in Salvadori and Carini, 2011.

5.2.5 Total Potential Energy functional

The Total Potential Energy functional, written in incremental form, for an admissible solution $(\hat{w}, \hat{l})$ is expressed as:

$$
\text{TPE}(\hat{w}, \hat{l}) = -\frac{1}{2} \int_0^l \int_0^l G_{pp}(x - \xi)\hat{w}^E(x)\hat{w}^E(\xi) \, d\xi dx - \int_0^l \dot{p}(x)\hat{w}(x) \, dx - \frac{1}{2}H \cdot \hat{l}^2.
\tag{5.2.38}
$$

Functional (5.2.38) is minimized in the correspondence of the solution $(\dot{w}, \dot{l})$, provided that the following constraints are satisfied:

$$
\dot{l} \ge 0 \quad \text{if } G = G_0
\tag{5.2.39}
$$

$$\dot{l} = 0 \quad \text{if } G < G_0. \tag{5.2.40}$$

Denoting with

$$\Delta \text{TPE} = \text{TPE}(\hat{\dot{w}}) - \text{TPE}(\dot{w}), \quad \Delta \dot{w} = \hat{\dot{w}} - \dot{w}, \quad \Delta \dot{l} = \hat{\dot{l}} - \dot{l}, \tag{5.2.41}$$

it must be proved that $\Delta \text{TPE} \geq 0$.

Considering the last term of functional (5.2.38), which involves the hardening operator H, one has

$$-\frac{1}{2} H \hat{\dot{l}}^2 + \frac{1}{2} H \dot{l}^2 = -\frac{1}{2} H (\hat{\dot{l}}^2 - \dot{l}^2). \tag{5.2.42}$$

Since the square of the variation $\Delta \dot{l}$ can be expressed as

$$\begin{aligned}
\Delta \dot{l}^2 &= (\hat{\dot{l}} - \dot{l})^2 = \hat{\dot{l}}^2 - 2\hat{\dot{l}} \cdot \dot{l} + \dot{l}^2 \\
&= (\hat{\dot{l}}^2 - \dot{l}^2) + 2\dot{l}^2 - 2\hat{\dot{l}} \cdot \dot{l}
\end{aligned} \tag{5.2.43}$$

one finally has

$$(\hat{\dot{l}}^2 - \dot{l}^2) = \Delta \dot{l}^2 + 2\dot{l}(\hat{\dot{l}} - \dot{l}) = \Delta \dot{l}^2 + 2\Delta \dot{l} \cdot \dot{l} \tag{5.2.44}$$

The result obtained in (5.2.44) is also valid for $\Delta \dot{w}^E$.

Equation (5.2.41) thus becomes

$$\begin{aligned}
\Delta \text{TPE} = &-\frac{1}{2} \int_0^l \int_0^l G_{pp}(x - \xi) \Delta \dot{w}^E(x) \Delta \dot{w}^E(\xi)\, d\xi dx - \int_0^l \dot{p}(x) \Delta \dot{w}(x)\, dx \\
&- \int_0^l \int_0^l G_{pp}(x - \xi) \dot{w}^E(x) \Delta \dot{w}^E(\xi)\, d\xi\, dx - \frac{1}{2} H \Delta \dot{l}^2 - H \Delta \dot{l} \cdot \dot{l}
\end{aligned} \tag{5.2.45}$$

The first and fourth members of (5.2.45) must satisfy the conditions already presented by Maier and Frangi in 1998 (H must be negative and the first integral is positive due to the properties of G_{pp}). Grouping these two terms and denoting them with symbol Δ^* and recalling the property $G_{pp}(x - \xi) = G_{pp}(\xi - x)$ one has

$$\begin{aligned}
\Delta \text{TPE} = &\Delta^* - \int_0^l \dot{p}(x) \Delta \dot{w}(x)\, dx - \int_0^l \int_0^l G_{pp}(x - \xi) \dot{w}^E(x) \Delta \dot{w}^E(\xi)\, d\xi\, dx - H \Delta \dot{l} \cdot \dot{l} \\
= &\Delta^* - \int_0^l \dot{p}(x) \Delta \dot{w}^E(x)\, dx - \int_0^l \dot{p}(x) \Delta \dot{w}^P(x)\, dx \\
&- \int_0^l \int_0^l G_{pp}(x - \xi) \dot{w}^E(x) \Delta \dot{w}^E(\xi)\, d\xi\, dx - H \Delta \dot{l} \cdot \dot{l}
\end{aligned} \tag{5.2.46}$$

Recalling that

$$-\int_0^l G_{pp}(x - \xi) \dot{w}^E(\xi) d\xi = \dot{p}(x), \tag{5.2.47}$$

equation (5.2.46) reduces to

$$
\begin{aligned}
\Delta\text{TPE} =& \Delta^* - \int_0^l \dot{p}(x)\Delta\dot{w}^P(x)\,dx - H\Delta\dot{l}\cdot\dot{l} \\
=& \Delta^* - \left[\int_0^l \dot{p}(x)\frac{\partial w}{\partial l}(x)\,dx + H\cdot\dot{l}\right]\Delta\dot{l}
\end{aligned}
\tag{5.2.48}
$$

in view of the validity of complementarity conditions (5.2.36)). Since the variation of the energy release rate $\dot{G}$ can be expressed according to (5.2.24), one finally has

$$
\begin{aligned}
\Delta\text{TPE} =& \Delta^* - \dot{G}\Delta\dot{l} \\
=& \Delta^* - \dot{G}\dot{\hat{l}} + \dot{G}\dot{l}
\end{aligned}
\tag{5.2.49}
$$

The product $\dot{G}\dot{l}$ vanishes because of the validity of consistency condition for the solution, while $-\dot{G}\dot{\hat{l}} \geq 0$. This concludes the proof, namely

$$
\Delta\text{TPE} \geq 0
\tag{5.2.50}
$$

Stationarity of the functional

In order to prove the stationarity of functional (5.2.38), one needs to compute its first variation. To this aim, one denotes with $\text{TPE}_{\mathcal{L}}$ the Lagrangian Functional

$$
\text{TPE}_{\mathcal{L}} = -\frac{1}{2}\int_0^l\int_0^l G_{pp}(x-\xi)\dot{w}^E(x)\dot{w}^E(\xi)\,d\xi dx - \int_0^l \dot{p}(x)\dot{w}(x)\,dx - \frac{1}{2}H\cdot\dot{l}^2 + \eta(\dot{l}-\alpha^2)
\tag{5.2.51}
$$

where η is a Lagrange multiplier and α^2 is a necessary definite-positive parameter in order to include the constraint of the problem.

The stationarity of $\text{TPE}_{\mathcal{L}}$ with respect to η reproduces exactly the constraint $\dot{l} \geq 0$ expressing the irreversibility of the process. In fact, the first variation leads to the equality $\delta\eta(\dot{l}-\alpha^2) = 0$ from which one has $\dot{l} = \alpha^2 \geq 0$.

Imposing the stationarity of (5.2.51) with respect to the other variables, namely $\dot{w}^E, \dot{l}$, and α, one has

$$
\begin{aligned}
\delta\text{TPE}_{\mathcal{L}} =& -\frac{1}{2}\int_0^l\int_0^l G_{pp}(x-\xi)\delta\dot{w}^E(x)\dot{w}^E(\xi)\,d\xi dx \\
& -\frac{1}{2}\int_0^l\int_0^l G_{pp}(x-\xi)\dot{w}^E(x)\delta\dot{w}^E(\xi)\,d\xi dx \\
& -\int_0^l \dot{p}(x)\delta\dot{w}(x)\,dx - \frac{1}{2}H\cdot\delta\dot{l}\dot{l} - \frac{1}{2}H\cdot\dot{l}\delta\dot{l} + \eta(\delta\dot{l} - 2\delta\alpha\alpha) \\
\\
=& -\int_0^l\int_0^l G_{pp}(x-\xi)\dot{w}^E(\xi)\delta\dot{w}^E(x)\,d\xi dx \\
& -\int_0^l \dot{p}(x)\delta\dot{w}(x)\,dx - H\cdot\dot{l}\delta\dot{l} + \eta(\delta\dot{l} - 2\delta\alpha\alpha)
\end{aligned}
$$

$$= -\int_0^l \int_0^l G_{pp}(x-\xi)\dot{w}^E(\xi)\delta\dot{w}^E(x)\,d\xi dx - \int_0^l \dot{p}(x)\delta\dot{w}^E(x)\,dx$$

$$- \int_0^l \dot{p}(x)\delta\dot{w}^P(x)\,dx - H \cdot \dot{l}\delta\dot{l} + \eta(\delta\dot{l} - 2\delta\alpha\alpha)$$

$$= -\int_0^l \int_0^l G_{pp}(x-\xi)\dot{w}^E(\xi)\delta\dot{w}^E(x)\,d\xi dx - \int_0^l \dot{p}(x)\delta\dot{w}^E(x)\,dx$$

$$- \int_0^l \dot{p}(x)\delta\left(\frac{\partial w}{\partial l}\dot{l}\right)\,dx - H \cdot \dot{l}\delta\dot{l} + \eta(\delta\dot{l} - 2\delta\alpha\alpha)$$

$$\tag{5.2.52}$$

$$= -\int_0^l \int_0^l G_{pp}(x-\xi)\dot{w}^E(\xi)\delta\dot{w}^E(x)\,d\xi dx - \int_0^l \dot{p}(x)\delta\dot{w}^E(x)\,dx$$

$$- \int_0^l \dot{p}(x)\frac{\partial w}{\partial l}\delta\dot{l}\,dx - H \cdot \dot{l}\delta\dot{l} + \eta(\delta\dot{l} - 2\delta\alpha\alpha)$$

$$= -\int_0^l \delta\dot{w}^E(x)\left[\int_0^l G_{pp}(x-\xi)\dot{w}^E(\xi)\,d\xi + \dot{p}(x)\right]dx$$

$$- \delta\dot{l}\left[\int_0^l \dot{p}(x)\frac{\partial w}{\partial l}\,dx + H \cdot \dot{l} - \eta\right] - 2\eta\delta\alpha\alpha = 0$$

It is therefore necessary to verify the validity of the equality

$$\delta\text{TPE}_{\mathcal{L}} = 0 \quad \forall\delta\dot{w}^E, \ \forall\delta\dot{l}, \ \forall\delta\alpha. \tag{5.2.53}$$

The variation $\delta\text{TPE}_{\mathcal{L}}$, as expressed in (5.2.52), can be expressed as the sum of three different contributions, called Ψ_1, Ψ_2, and Ψ_3, respectively, where:

$$\Psi_1 = -\int_0^l \delta\dot{w}^E(x)\left[\int_0^l G_{pp}(x-\xi)\dot{w}^E(\xi)\,d\xi + \dot{p}(x)\right]dx$$

$$\Psi_2 = -\delta\dot{l}\left[\int_0^l \dot{p}(x)\frac{\partial w}{\partial l}\,dx + H \cdot \dot{l} - \eta\right] \tag{5.2.54}$$

$$\Psi_3 = -2\eta\delta\alpha\alpha = 0$$

Equilibrium equation can be recovered imposing that $\Psi_1 = 0 \quad \forall\delta\dot{w}^E$, namely

$$\int_0^l G_{pp}(x-\xi)\dot{w}^E(\xi)\,d\xi + \dot{p}(x) = 0 \tag{5.2.55}$$

To prove these results, Gebbia fundamental solutions in linear elasticity are recalled (Carini and De Donato, 1992). These solution refer to the case of a concentrated displacement discontinuity (whose components are D_j^l $j = 1, 2, 3$) in a given material point $\boldsymbol{\xi}$ (crossing a surface Γ with normal $\boldsymbol{l}$) of a 3D elastic homogeneous and isotropic unbounded continuum.
Let $G_{i\alpha}^{pp}$ be the effect (in a given material point $\boldsymbol{x}$) in terms of tractions $p(x)$ on the surface of normal $\boldsymbol{n}$.

The following relation is valid:

$$G_{i\alpha}^{pp}(\boldsymbol{x}, \boldsymbol{\xi}, \boldsymbol{n}, \boldsymbol{l})D_\alpha^l = p_i(\boldsymbol{x}) \tag{5.2.56}$$

where index i is representative of components of effects in $\boldsymbol{x}$ and index α is representative of components of causes in $\boldsymbol{\xi}$.
The full expression of $G_{i\alpha}^{pp}$ is

$$G_{i\alpha}^{pp}(\boldsymbol{x}, \boldsymbol{\xi}, \boldsymbol{n}, \boldsymbol{l}) = \frac{\nu \cdot E}{2(1-\nu)(1+\nu)} \cdot f_{i\alpha}^{pp}(\boldsymbol{x}, \boldsymbol{\xi}, \boldsymbol{n}, \boldsymbol{l}) + \frac{E}{2(1-\nu)(1+\nu)} \cdot g_{i\alpha}^{pp}(\boldsymbol{x}, \boldsymbol{\xi}, \boldsymbol{n}, \boldsymbol{l}) \tag{5.2.57}$$

For the 2D case the following relations hold

$$f_{i\alpha}^{pp}(x, \xi, \boldsymbol{n}, \boldsymbol{l}) = 0 \tag{5.2.58}$$

$$g_{i\alpha}^{pp}(x, \xi, \boldsymbol{n}, \boldsymbol{l}) = \frac{1}{2\pi r^2} \left(\delta_{i\alpha}\delta_{kj} + \delta_{ki}\delta_{\alpha j} - \delta_{\alpha k}\delta_{ij} + 2\delta_{\alpha k}r_{/i}r_{/j} + 2\delta_{ij}r_{/\alpha}r_{/k} - 8r_{/i}r_{/j}r_{/\alpha}r_{/k} \right) l_k n_j \tag{5.2.59}$$

where $r_{/i} = \dfrac{x_i - \xi_i}{r}$, where r is the distance between $\boldsymbol{x}$ and $\boldsymbol{\xi}$.
In the simplest case, meaning superimposing $\alpha, i = 1$ and $j, k = 2$, one has:

$$g_{11}^{pp}(x, \xi, \boldsymbol{n}, \boldsymbol{l}) = \frac{1}{2\pi r^2} \tag{5.2.60}$$

Therefore, equation (5.2.57) reduces to

$$G_{11}^{pp}(x, \xi, \boldsymbol{n}, \boldsymbol{l}) = \frac{E}{2(1-\nu)(1+\nu)} \cdot \frac{1}{2\pi(x-\xi)^2} \tag{5.2.61}$$

Exploiting expression (5.2.11) for fracture opening, from (5.2.55), one can express the increment $\dot{w}^E$ in terms of pressure increment $\dot{p}$, namely

$$\dot{w}^E(\xi) = \frac{\partial w}{\partial p} \cdot \dot{p} = 4 \cdot \frac{l}{E} \left[1 - \left(\frac{x}{l}\right)^2 \right]^{1/2} \cdot \dot{p} \tag{5.2.62}$$

In the range $[-l, l]$, equation (5.2.55) leads to

$$\int_{-l}^l G_{pp}(x-\xi)\dot{w}^E(\xi)\, d\xi + \dot{p}$$

$$\frac{E}{4\pi(1-\nu^2)} \cdot \frac{4}{E} \cdot \dot{p} \cdot \int_{-l}^l \frac{1}{(x-\xi)^2} \sqrt{l^2 - \xi^2}\, d\xi + \dot{p}$$

$$\frac{1}{\pi(1-\nu^2)} \cdot \dot{p} \cdot \int_{-l}^l \frac{1}{(x-\xi)^2} \sqrt{l^2 - \xi^2}\, d\xi + \dot{p} \tag{5.2.63}$$

$$\frac{1}{\pi(1-\nu^2)} \cdot \dot{p} \cdot [-\pi] + \dot{p}$$

$$-\frac{\dot{p}}{(1-\nu^2)} + \dot{p} = 0$$

If the Poisson coefficient vanishes, the equality $\Psi_1 = 0$, $\forall \delta \dot{w}^E$ is proved.

Imposing that $\Psi_2 = 0$, $\forall \delta \dot{l}$ and $\Psi_3 = 0$, $\forall \delta \dot{\alpha}$, one has

$$\int_0^l \dot{p}(x) \frac{\partial w}{\partial l} \, dx + H \cdot \dot{l} - \eta = 0 \tag{5.2.64}$$

$$2\eta\alpha = 0 \tag{5.2.65}$$

From equation (5.2.64), and recalling the definition of the variation of energy-release rate (5.2.24), the equality between $\dot{G}$ and the Lagrange multiplier derives, namely

$$\dot{G} = \int_0^l \dot{p}(x) \frac{\partial w}{\partial l} \, dx + H \cdot \dot{l} = \eta \tag{5.2.66}$$

Substituing equation (5.2.66) in (5.2.65), one gets

$$\dot{G} \cdot \alpha = 0 \tag{5.2.67}$$

In view of the equality $\alpha^2 = \dot{l}$, verified at the beginning of the present Section, one finally derives the stationarity of the functional (5.2.51), since $\dot{G} \cdot \dot{l} = 0$ because of consistency condition.

5.2.6   One-field functional

The two-fields functional (5.2.38) can be transformed into a one-field one. To this aim, one recalls that the fracture opening can be decomposed into two independent contributions. One is the elastic fracture opening $\dot{w}^E$, and the other one is the plastic crack aperture $\dot{w}^P$. Accordingly, the fracture opening variation can be expressed as the sum of an increment due to the variation of the external loads $\dot{p}$, and an irreversible increment due to the variation of crack length $\dot{l}$, namely

$$\dot{w} = \frac{\partial w}{\partial p} \cdot \dot{p} + \frac{\partial w}{\partial l} \cdot \dot{l} = \dot{w}^E + \dot{w}^P \tag{5.2.68}$$

Assuming for simplicity that $\dot{w}^E$ is constant, taking into account equilibrium equation (5.2.55), functional (5.2.38) reads

$$
\begin{aligned}
\text{TPE}(\dot{w}^P, \dot{l}) = &-\frac{1}{2} \int_0^l \int_0^l G_{pp}(x - \xi) \dot{w}^E(x) \dot{w}^E(\xi) \, d\xi dx - \int_0^l \dot{p}(x) \dot{w}(x) \, dx - \frac{1}{2} H \cdot \dot{l}^2 \\
= &-\frac{1}{2} \int_0^l \int_0^l G_{pp}(x - \xi) \dot{w}^E(x) \dot{w}^E(\xi) \, d\xi dx - \int_0^l \dot{p}(x) \dot{w}^E(x) \, dx \\
&- \int_0^l \dot{p}(x) \dot{w}^P(x) \, dx - \frac{1}{2} H \cdot \dot{l}^2 \\
\\
= &-\frac{1}{2} \int_0^l \int_0^l G_{pp}(x - \xi) \dot{w}^E(x) \dot{w}^E(\xi) \, d\xi dx + \int_0^l \int_0^l G_{pp}(x - \xi) \dot{w}^E(x) \dot{w}^E(\xi) \, d\xi dx \\
&- \int_0^l \dot{p}(x) \dot{w}^P(x) \, dx - \frac{1}{2} H \cdot \dot{l}^2 \\
\\
= &+\frac{1}{2} \int_0^l \int_0^l G_{pp}(x - \xi) \dot{w}^E(x) \dot{w}^E(\xi) \, d\xi dx - \int_0^l \dot{p}(x) \dot{w}^P(x) \, dx - \frac{1}{2} H \cdot \dot{l}^2 \\
\\
= &-\frac{1}{2} \int_0^l \dot{p}(x) \dot{w}^E(x) \, dx - \int_0^l \dot{p}(x) \dot{w}^P(x) \, dx - \frac{1}{2} H \cdot \dot{l}^2
\end{aligned}
$$

$$(5.2.69)$$

It is worth mentioning the validity of the following constraint

$$\dot{l} \geq 0 \quad \Rightarrow \quad \dot{w}^P(l) \geq 0 \quad \text{if } G = G_0 \tag{5.2.70}$$

where $\dot{w}^P(l)$ means that $\dot{w}^P$ depends on the crack length.

Furthermore, since the term $-\frac{1}{2} \int_0^l \dot{p}(x) \dot{w}^E(x) \, dx$, as stated, is a known term, it can be omitted from the functional (5.2.69). In order to write the functional as a function of $\dot{w}^P$, the following hypothesis is introduced

$$\dot{l} = \beta \dot{w}^P(l), \tag{5.2.71}$$

where β is a proportionality coefficient between $\dot{l}$ and $\dot{w}^P(l)$, namely to express $\dot{l}$ as a function of the increase of the crack opening due to plastic distortion.

Recalling expression (5.2.26) for the hardening parameter H, the last term of the functional (5.2.69) gains the form

$$
\begin{aligned}
H\dot{l}^2 &= \left(\frac{1}{2} \int_0^l p \cdot \frac{\partial^2 w}{\partial l^2} \, dx \right) \cdot \dot{l}^2 \\
&= \left(\frac{1}{2} \int_0^l p \cdot \frac{\partial^2 w}{\partial l^2} \, dx \right) \cdot \beta^2 (\dot{w}^P(l))^2 \\
&= \left(\frac{\beta^2}{2} \int_0^l p \cdot \frac{\partial^2 w}{\partial l^2} \, dx \right) \cdot (\dot{w}^P(l))^2 = \tilde{H} \cdot (\dot{w}^P(l))^2
\end{aligned}
\tag{5.2.72}
$$

The functional (5.2.69) is then written as a function of $\dot{w}^P$:

$$\text{TPE}(\dot{w}^P) = -\frac{1}{2}\tilde{H} \cdot (\dot{w}^P(l))^2 - \int_0^l \dot{p}(x)\dot{w}^P(x)\,dx, \tag{5.2.73}$$

which turns out to be a functional constituted by a quadratic part and a linear one.

In order to express functional (5.2.69) as dependent solely on $\dot{l}$, bearing in mind that $\dot{w}^P = \frac{\partial w}{\partial l} \cdot \dot{l}$ and that $\dot{w}^E$ is constant, equation (5.2.69) can be written in the following form

$$\text{TPE} = -\frac{1}{2}\int_0^l\int_0^l G_{pp}(x-\xi)\dot{w}^E(x)\dot{w}^E(\xi)\,d\xi dx - \int_0^l \dot{p}(x)\dot{w}(x)\,dx - \frac{1}{2}H \cdot \dot{l}^2$$

$$= -\frac{1}{2}\int_0^l \dot{p}(x)\dot{w}^E(x)\,dx - \int_0^l \dot{p}(x)\dot{w}^P(x)\,dx - \frac{1}{2}H \cdot \dot{l}^2$$

$$\tag{5.2.74}$$

$$= -\frac{1}{2}\int_0^l \dot{p}(x)\dot{w}^E(x)\,dx - \int_0^l \dot{p}(x)\frac{\partial w}{\partial l} \cdot \dot{l}\,dx - \frac{1}{2}H \cdot \dot{l}^2$$

$$= -\frac{1}{2}\int_0^l \dot{p}(x)\dot{w}^E(x)\,dx - \int_0^l \dot{p}(x)\frac{\partial w}{\partial l}\,dx \cdot \dot{l} - \frac{1}{2}H \cdot \dot{l}^2$$

Since $\dot{l} \geq 0$ *if* $G = G_0$, one finally has

$$\text{TPE}(\dot{l}) = -\frac{1}{2}H \cdot \dot{l}^2 - \int_0^l \dot{p}(x)\frac{\partial w}{\partial l}\,dx \cdot \dot{l} \tag{5.2.75}$$

Analogy with the functional obtained by Salvadori and Carini (2011)

In this Subsection, the goal is to define an analogy between the one-field functional (5.2.75) and the functional obtained by Salvadori and Carini (2011). In the above-mentioned reference, in fact, it has been proved that the crack front velocity as solution of the global quasi-static fracture propagation problem, minimizes a constrained quadratic functional. In particular, the following theorem has been stated:

Provided that $\frac{\partial \varphi}{\partial \boldsymbol{K}^*} \cdot \boldsymbol{K}^{(1)} < 0$ the crack tip velocity $\dot{s}(t)$ that solves the global quasi-static fracture propagation problem at time t minimizes the function:

$$\chi(\dot{s}) = -\frac{1}{2}\frac{\partial \varphi}{\partial \boldsymbol{K}^*}(t) \cdot \boldsymbol{K}^{(1)}(t)\dot{s}^2 - \frac{\partial \varphi}{\partial \boldsymbol{K}^*}(t) \cdot \dot{\boldsymbol{K}}^*(t)\dot{s} \tag{5.2.76}$$

under the constraint:

$$\dot{s} \geq 0 \tag{5.2.77}$$

A stability requirement has been derived in Salvadori and Carini (2011), expressing the condition under which the crack propagation is governed by the increment of the external loads. It holds

$$\frac{\partial \varphi}{\partial \boldsymbol{K}^*} \cdot \boldsymbol{K}^{(1)} < 0. \tag{5.2.78}$$

Condition (5.2.78) corresponds to $H < 0$. Exactly as in (5.2.75), also functional (5.2.76) is a one-field functional and it comprises a quadratic component and a linear one. It is a reminiscence of Ceradini's theorem for standard dissipative systems theory. Crack propagation is considered as an irreversible phenomenon, hence the constraint (5.2.77). Functional (5.2.76) departs from the Stress Intensity Factors (SIFs) vector expansion in powers of crack elongation s, performed in Amestoy M. et al. (1986) and Amestoy M. and Leblond J.B. (1992). In particular, denoting with $\mathbf{K}(t)$ the SIFs vector at any crack tip at time t, at time instant $\tau \geq t$ the expansion takes the general form

$$\boldsymbol{K}(\kappa(\tau), s(\tau)) = \boldsymbol{K}^*(\kappa(\tau)) + \boldsymbol{K}^{(1/2)}(\kappa(\tau))\sqrt{s(\tau)} + \boldsymbol{K}^{(1)}(\kappa(\tau))s(\tau) + O(s^{3/2}). \qquad (5.2.79)$$

It details the behavior of SIFs at a generic crack tip due to an irreversible change in the geometry at the same crack tip. Factors $\mathbf{K}^*$ and $\mathbf{K}^{(1/2)}$ in (5.2.79) are termed universal, because they obey to the autonomy concept. They are in fact independent on body geometry and here they are expressed as functions of the load factor $\kappa(\tau)$, which determines the proportional increase of the external loading and has no requirements apart from being non negative. Term $\mathbf{K}^{(1)}$, instead, depends on the geometry of the body and on the curvature of the elongated branch. The mathematical representation of the onset of crack propagation is given by the equation

$$\varphi(\mathbf{K}) = \vartheta(\mathbf{K}) - \vartheta(K_1^C) = 0, \qquad (5.2.80)$$

where function φ is expressed as the difference between the actual crack state $\vartheta(\mathbf{K})$ and a critical one, depending on the value of the fracture toughness K_1^C. Function ϑ is peculiar of any crack propagation criterion (see Salvadori 2008). Cracks cannot advance if $\varphi < 0$ and this inequality allows to define the so-called *safe equilibrium domain*

$$\boldsymbol{E} = \{\{K_1^*, K_2^*\} \in \boldsymbol{R}_0^+ \times \boldsymbol{R} | \varphi(K_1^*, K_2^*) < 0\}, \qquad (5.2.81)$$

which is a reminiscence of the elastic domain in plasticity.
Its boundary defines the onset of crack propagation, namely

$$\partial\boldsymbol{E} = \{\{K_1^*, K_2^*\} \in \boldsymbol{R}_0^+ \times \boldsymbol{R} | \varphi(K_1^*, K_2^*) = 0\}, \qquad (5.2.82)$$

which is a reminiscence of the yield surface in plasticity.
Propagation is governed by the following conditions, reminiscence of Kuhn-Tucker conditions of plasticity

$$\varphi\dot{s} = 0 \qquad \varphi \leq 0 \qquad \dot{s} \geq 0, \qquad (5.2.83)$$

analogous to (5.2.33). If the *Maximum Energy Release Rate* (MERR) is chosen as the propagation criterion, function φ assumes the following form

$$\varphi = \frac{1}{2}\frac{1-\nu^2}{E}\left(||\boldsymbol{K}^*||^2 - (K_1^C)^2\right). \qquad (5.2.84)$$

If $\varphi < 0$ at time t, there is a load increment $\delta\kappa$ small enough not to lengthen the crack:

$$at\ t\ s.t.\ \varphi(\boldsymbol{K}) < 0 \quad \exists \delta\kappa > 0\ s.t.$$
$$\delta\boldsymbol{K} = \frac{\boldsymbol{K}(t)}{\kappa(t)}\delta\kappa, \quad \varphi(\boldsymbol{K} + \delta\boldsymbol{K}) < 0 \qquad (5.2.85)$$

This describes the first stage of the cracking process, namely *loading without crack growth*.

When the onset of the propagation is reached because of the increment of the external loads, the second phase starts: *stable crack growth.*

$$at\ t\ s.t.\ \varphi(\boldsymbol{K}) = 0 \quad \exists \delta\kappa > 0\ s.t.$$
$$\delta\boldsymbol{K}^* = \frac{\boldsymbol{K}^*(t)}{\kappa(t)}\delta\kappa, \quad \delta\boldsymbol{K} = \delta\boldsymbol{K}^* + \boldsymbol{K}^{(1/2)}(t)\sqrt{s} + O(\delta\kappa, s) \tag{5.2.86}$$

The latter condition is a reminiscence of Colonnetti's decomposition of stresses in plasticity. The variation of the SIFs $\delta\mathbf{K}$, in fact, is decomposed as due to an elastic contribution $\delta\mathbf{K}^*$ and to a distortion, represented by the crack elongation s, which reverses itself into the stiffness factor $\mathbf{K}^{(1/2)}$.

The consistency condition is derived from (5.2.83) by performing a time derivative at $\varphi = 0$, namely

$$\dot{\varphi}\dot{s} = 0, \quad \dot{\varphi} \leq 0, \quad \dot{s} \geq 0, \tag{5.2.87}$$

which recall the conditions (5.2.36).

Owing to equation (5.2.86) and to consistency condition (5.2.87), for $\dot{s}(t) > 0$, the time derivative of function φ can be properly defined. One has

$$\dot{\varphi}(t) = \frac{\partial\varphi}{\partial\boldsymbol{K}^*}(t) \cdot \left(\dot{\boldsymbol{K}}^*(t) + \boldsymbol{K}^{(1)}(t)\dot{s}(t)\right) + h.o.t = 0 \tag{5.2.88}$$

Recalling Colonnetti's work, $\dot{\boldsymbol{K}}^*(t)$ is a contribution which is associated with an inelastic distortion $\dot{s}(t)$, but, in the hypotheses made by Salvadori and Carini (2011), it is a purely elastic contribution due to $\dot{\kappa}(t)$. Equation (5.2.88) sets the condition for a stable crack growth, required for the validity of theorem (5.2.76), and inherently, for the transition to the unstable phase. It reads

$$\dot{\kappa}(t) > 0 \rightarrow \frac{\partial\varphi}{\partial\mathbf{K}^*}(t) \cdot \mathbf{K}^{(1)}(t) < 0. \tag{5.2.89}$$

The analogies existing between the two one-field functionals (5.2.76) and (5.2.38) are summarized in Table 5.1.

	TPE($\dot{l}$)	$\chi(\dot{s})$
Inelastic variable	$\dot{l}$	$\dot{s}$
Constraint	$\dot{l} \geq 0$	$\dot{s} \geq 0$
Quadratic component	$-\frac{1}{2}H \cdot \dot{l}^2$	$-\frac{1}{2}\frac{\partial \varphi}{\partial \mathbf{K}^*}(t) \cdot \mathbf{K}^{(1)}(t)\dot{s}^2$
Stability condition	$H < 0$	$\frac{\partial \varphi}{\partial \mathbf{K}^*}(t) \cdot \mathbf{K}^{(1)}(t) < 0$
Geometry dependent term	H	$\mathbf{K}^{(1)}$
Linear component	$-\int_0^l \dot{p}(x)\frac{\partial w}{\partial l}\,dx \cdot \dot{l}$	$-\frac{\partial \varphi}{\partial \mathbf{K}^*}(t) \cdot \dot{\mathbf{K}}^*(t)\dot{s}$
Elastic contributions	$\dot{p}$	$\dot{\mathbf{K}}^*(t)$
Kuhn-Tucker conditions	$(G - G_0)\dot{l} = 0\,;\, G - G_0 \leq 0\,;\, \dot{l} \geq 0$	$\varphi\dot{s} = 0\,;\, \varphi \leq 0\,;\, \dot{s} \geq 0$
Consistency conditions	$\dot{G}\dot{l} = 0\,;\, \dot{G} \leq 0\,;\, \dot{l} \geq 0$ with $G = G_0$	$\dot{\varphi}\dot{s} = 0\,;\, \dot{\varphi} \leq 0\,;\, \dot{s} \geq 0$ with $\varphi = 0$

Table 5.1: Summary of the analogies between the one-field functional (5.2.38) dependent on $\dot{l}$, obtained in the present work, and the one-field functional (5.2.76) dependent on $\dot{s}$ obtained by Salvadori and Carini (2011).

5.2.7 Generalization of the problem

The goal of this Section is to extend the obtained functional (5.2.38) to the case of a body Ω defined in a two or three-dimensional space. One considers the problem of Fig. 5.2:
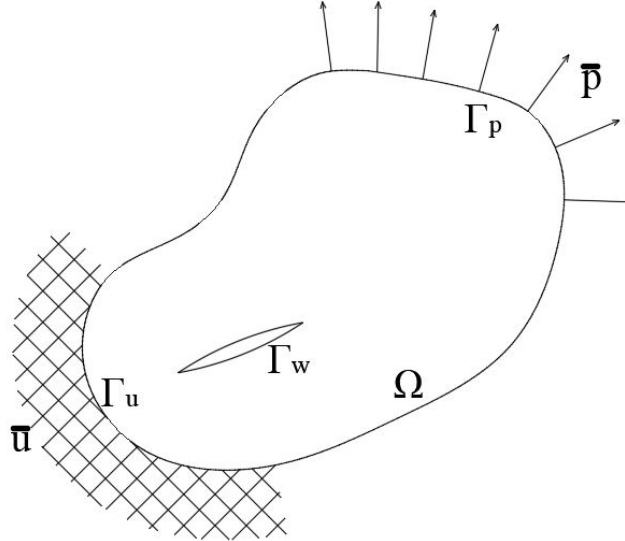
Figure 5.2: Body Ω with a crack of boundary Γ_w, subjected to Dirichlet and Neumann boundary conditions.

The mathematical formulation of the fracture mechanics problem is based on the following set of hypotheses:

- a domain $\Omega \subset \mathbb{R}^d$, where $d = 2, 3$ is the spatial dimension of the problem;

- small displacements and strains are assumed, in the sense that the equilibrium relations are not affected by configuration changes and the kinematic compatibility equations are linear;

- displacements $\bar{\boldsymbol{u}}$ are imposed over Γ_u (Dirichlet boundary conditions) and tractions $\bar{\boldsymbol{p}}$ are imposed over Γ_p (Neumann boundary conditions).

The geometric description of the crack implies two boundaries: Γ_w^+ and Γ_w^-, which shape its edges, with respect to a reference surface Γ_w.
The *relative opening displacement* function is defined here with $\boldsymbol{w}$.

The direct boundary integral formulation is based on the use of Green's functions (reunited in the matrices $\boldsymbol{G_{uu}}$ and $\boldsymbol{G_{pu}}$) which represent, respectively, the components of the displacement vector u_i (i=1,2,3) at the point $\boldsymbol{x}$ and the components of the traction vector p_i (i=1,2,3) on a surface of normal $\boldsymbol{n}(\boldsymbol{x})$, due to a unit force concentrated in a point $\boldsymbol{\xi} \in \Omega$ and acting on the unlimited space Ω_∞.
To define the dual form, the Green functions this time are $\boldsymbol{G_{up}}$ and $\boldsymbol{G_{pp}}$, which represent respectively, the components of the displacement vector u_i (i=1,2,3) at the point $\boldsymbol{x}$ and the components of the traction vector p_i (i=1,2,3) on surface of normal $\boldsymbol{n}(\boldsymbol{x})$, due to a unitary relative displacement concentrated in a point $\boldsymbol{\xi} \in \Omega$ and acting on the unlimited space Ω_∞.
The first subscript of $\boldsymbol{G}$, therefore, specifies the nature of the effect, while the second is associated with the dual of the source which causes this effect.
$\boldsymbol{x}$ and $\boldsymbol{\xi}$ denote the so-called *field-point* and *source-point*.

The classical bilinear form:

$$\mathcal{A}(\mathbf{u}, \mathbf{p}) = \int_{\Gamma} \mathbf{u} \cdot \mathbf{p} \, d\mathbf{x} \tag{5.2.90}$$

puts the two spaces U and P in duality, with $\boldsymbol{u} \in U$ and $\boldsymbol{p} \in P$.

It is possible to prove the following symmetry properties of Green's functions:

$$\mathcal{A}(\mathbf{q}, \mathbf{G_{uu}p}) = \mathcal{A}(\mathbf{p}, \mathbf{G_{uu}q}) \tag{5.2.91}$$

$$\mathcal{A}(\mathbf{u}, \mathbf{G_{pp}v}) = \mathcal{A}(\mathbf{v}, \mathbf{G_{pp}u}) \tag{5.2.92}$$

$$\mathcal{A}(\mathbf{u}, \mathbf{G_{pu}p}) = \mathcal{A}(\mathbf{p}, \mathbf{G_{up}u}) \tag{5.2.93}$$

In the integration process, if the point $\boldsymbol{x}$ tends to the boundary (considering that $\boldsymbol{r} = \boldsymbol{x} - \boldsymbol{\xi}$), Green functions bring out singularities.

These behaviours have already been extensively discussed in the past and summarized in Table 5.2:

Kernel	Asymptotic behaviour when $r \to 0$		Name
	2D	3D	
$\mathbf{G_{uu}}$	$O(log(\boldsymbol{r}))$	$O(\boldsymbol{r}^{-1})$	Weak singularity (integrable)
$\mathbf{G_{up}}, \mathbf{G_{pu}}$	$O(\boldsymbol{r}^{-1})$	$O(\boldsymbol{r}^{-2})$	Strong singularity
$\mathbf{G_{pp}}$	$O(\boldsymbol{r}^{-2})$	$O(\boldsymbol{r}^{-3})$	Hypersingularity

Table 5.2: Summary of the singularities of Green's functions when $\boldsymbol{r} = \boldsymbol{x} - \boldsymbol{\xi} \longrightarrow 0$.

Integrals with strong singularities must be interpreted according to their distributional nature of the Cauchy Principal Value.

Similarly, the hypersingular kernel must be interpreted according to its distributional nature of the finite part of Hadamard.

Schematization of the problem

The Galerkin scheme of the BIE (Boundary Integral Equations) formulation, applied to the fracture mechanics problem in incremental form, leads to the following operator form:

$$\left| \begin{array}{ccc} \int_{\Gamma_u} \mathbf{G_{uu}}[\cdot] \, d\boldsymbol{\xi} & -\int_{\Gamma_p} \mathbf{G_{up}}[\cdot] \, d\boldsymbol{\xi} & -\int_{\Gamma_w} \mathbf{G_{up}}[\cdot] \, d\boldsymbol{\xi} \\ -\int_{\Gamma_u} \mathbf{G_{pu}}[\cdot] \, d\boldsymbol{\xi} & \int_{\Gamma_p} \mathbf{G_{pp}}[\cdot] \, d\boldsymbol{\xi} & \int_{\Gamma_w} \mathbf{G_{pp}}[\cdot] \, d\boldsymbol{\xi} \\ -\int_{\Gamma_u} \mathbf{G_{pu}}[\cdot] \, d\boldsymbol{\xi} & \int_{\Gamma_p} \mathbf{G_{pp}}[\cdot] \, d\boldsymbol{\xi} & \int_{\Gamma_w} \mathbf{G_{pp}}[\cdot] \, d\boldsymbol{\xi} \end{array} \right| \cdot \left| \begin{array}{c} \dot{\mathbf{p}}^{\mathbf{E}} \\ \dot{\mathbf{u}}^{\mathbf{E}} \\ \dot{\mathbf{w}}^{\mathbf{E}} \end{array} \right| = \left| \begin{array}{c} \dot{\mathbf{f}}^{\mathbf{u}} \\ \dot{\mathbf{f}}^{\mathbf{P}} \\ \dot{\mathbf{f}}^{\mathbf{w}} \end{array} \right| \begin{array}{c} \text{on } \Gamma_u \\ \text{on } \Gamma_p \\ \text{on } \Gamma_w \end{array} \tag{5.2.94}$$

Under the hypothesis of smooth boundaries, the vectors of the known terms hold:

$$\dot{\boldsymbol{f}}^{\boldsymbol{u}}(\boldsymbol{x}) = \frac{1}{2}\dot{\boldsymbol{u}} - \int_{\Gamma_p} \boldsymbol{G_{uu}}\dot{\boldsymbol{p}} \, d\boldsymbol{\xi} + \int_{\Gamma_u} \boldsymbol{G_{up}}\dot{\boldsymbol{u}} \, d\boldsymbol{\xi} \tag{5.2.95}$$

$$\dot{\boldsymbol{f}}^{\boldsymbol{p}}(\boldsymbol{x}) = -\frac{1}{2}\dot{\boldsymbol{p}} + \int_{\Gamma_p} \boldsymbol{G_{pu}}\dot{\boldsymbol{p}} \, d\boldsymbol{\xi} - \int_{\Gamma_u} \boldsymbol{G_{pp}}\dot{\boldsymbol{u}} \, d\boldsymbol{\xi} \tag{5.2.96}$$

$$\dot{\boldsymbol{f}}^{\boldsymbol{w}}(\boldsymbol{x}) = \frac{1}{2}\dot{\boldsymbol{p}} + \int_{\Gamma_p} \boldsymbol{G_{pu}}\dot{\boldsymbol{p}}\, d\boldsymbol{\xi} - \int_{\Gamma_u} \boldsymbol{G_{pp}}\dot{\boldsymbol{u}}\, d\boldsymbol{\xi} \tag{5.2.97}$$

Equation (5.2.94) can be written in the compact form:

$$\boldsymbol{L}\dot{\boldsymbol{y}}^{\boldsymbol{E}} = \dot{\boldsymbol{f}} \tag{5.2.98}$$

The operator $\boldsymbol{L}$ is symmetric with respect to the bilinear form (5.2.90):

$$\mathcal{A}(\boldsymbol{Lu}, \boldsymbol{v}) = \mathcal{A}(\boldsymbol{u}, \boldsymbol{Lv}) \tag{5.2.99}$$

It is therefore possible to write in full the functional Total Potential Energy, thus extending the functional (5.2.38):

$$\text{TPE}_{ext}(\dot{\boldsymbol{u}}, \dot{\boldsymbol{p}}, \dot{\boldsymbol{w}}, \dot{l}) = \frac{1}{2}\int_{\Gamma} \dot{\boldsymbol{y}}^{\boldsymbol{E}}\boldsymbol{L}\dot{\boldsymbol{y}}^{\boldsymbol{E}} - \int_{\Gamma} \dot{\boldsymbol{f}}\dot{\boldsymbol{y}} - \frac{1}{2}\boldsymbol{H}\dot{l}^2$$

$$\begin{aligned}
= \quad & \frac{1}{2}\int_{\Gamma_u} \dot{\boldsymbol{p}}^{\boldsymbol{E}}(\boldsymbol{x}) \int_{\Gamma_u} \boldsymbol{G_{uu}}\dot{\boldsymbol{p}}^{\boldsymbol{E}}(\boldsymbol{\xi})\, d\boldsymbol{\xi}\, d\boldsymbol{x} - \frac{1}{2}\int_{\Gamma_u} \dot{\boldsymbol{p}}^{\boldsymbol{E}}(\boldsymbol{x}) \int_{\Gamma_p} \boldsymbol{G_{up}}\dot{\boldsymbol{u}}^{\boldsymbol{E}}(\boldsymbol{\xi})\, d\boldsymbol{\xi}\, d\boldsymbol{x} \\
& - \frac{1}{2}\int_{\Gamma_u} \dot{\boldsymbol{p}}^{\boldsymbol{E}}(\boldsymbol{x}) \int_{\Gamma_w} \boldsymbol{G_{up}}\dot{\boldsymbol{w}}^{\boldsymbol{E}}(\boldsymbol{\xi})\, d\boldsymbol{\xi}\, d\boldsymbol{x} - \frac{1}{2}\int_{\Gamma_p} \dot{\boldsymbol{u}}^{\boldsymbol{E}}(\boldsymbol{x}) \int_{\Gamma_u} \boldsymbol{G_{pu}}\dot{\boldsymbol{p}}^{\boldsymbol{E}}(\boldsymbol{\xi})\, d\boldsymbol{\xi}\, d\boldsymbol{x} \\
& + \frac{1}{2}\int_{\Gamma_p} \dot{\boldsymbol{u}}^{\boldsymbol{E}}(\boldsymbol{x}) \int_{\Gamma_p} \boldsymbol{G_{pp}}\dot{\boldsymbol{u}}^{\boldsymbol{E}}(\boldsymbol{\xi})\, d\boldsymbol{\xi}\, d\boldsymbol{x} + \frac{1}{2}\int_{\Gamma_p} \dot{\boldsymbol{u}}^{\boldsymbol{E}}(\boldsymbol{x}) \int_{\Gamma_w} \boldsymbol{G_{pp}}\dot{\boldsymbol{w}}^{\boldsymbol{E}}(\boldsymbol{\xi})\, d\boldsymbol{\xi}\, d\boldsymbol{x} \\
& - \frac{1}{2}\int_{\Gamma_w} \dot{\boldsymbol{w}}^{\boldsymbol{E}}(\boldsymbol{x}) \int_{\Gamma_u} \boldsymbol{G_{pu}}\dot{\boldsymbol{p}}^{\boldsymbol{E}}(\boldsymbol{\xi})\, d\boldsymbol{\xi}\, d\boldsymbol{x} + \frac{1}{2}\int_{\Gamma_w} \dot{\boldsymbol{w}}^{\boldsymbol{E}}(\boldsymbol{x}) \int_{\Gamma_p} \boldsymbol{G_{pp}}\dot{\boldsymbol{u}}^{\boldsymbol{E}}(\boldsymbol{\xi})\, d\boldsymbol{\xi}\, d\boldsymbol{x} \\
& + \frac{1}{2}\int_{\Gamma_w} \dot{\boldsymbol{w}}^{\boldsymbol{E}}(\boldsymbol{x}) \int_{\Gamma_w} \boldsymbol{G_{pp}}\dot{\boldsymbol{w}}^{\boldsymbol{E}}(\boldsymbol{\xi})\, d\boldsymbol{\xi}\, d\boldsymbol{x} \\
& - \int_{\Gamma_u} \dot{\boldsymbol{p}}(\boldsymbol{x}) \cdot \dot{\boldsymbol{f}}^{\boldsymbol{u}}(\boldsymbol{x})\, d\boldsymbol{x} - \int_{\Gamma_p} \dot{\boldsymbol{u}}(\boldsymbol{x}) \cdot \dot{\boldsymbol{f}}^{\boldsymbol{p}}(\boldsymbol{x})\, d\boldsymbol{x} - \int_{\Gamma_w} \dot{\boldsymbol{w}}(\boldsymbol{x}) \cdot \dot{\boldsymbol{f}}^{\boldsymbol{w}}(\boldsymbol{x})\, d\boldsymbol{x} \\
& - \frac{1}{2}\boldsymbol{H}\dot{l}^2
\end{aligned}$$

$$\tag{5.2.100}$$

Vector $\dot{\boldsymbol{y}}$ can be additively decomposed in a contribution due to load increment and a contribution due to plastic distortion $\dot{l}$

$$\boldsymbol{y}^{\dot{\boldsymbol{E}}} = \dot{\boldsymbol{y}} - \boldsymbol{y}^{\dot{\boldsymbol{P}}}, \quad \boldsymbol{y}^{\dot{\boldsymbol{P}}} = \boldsymbol{N} \cdot \dot{l}, \tag{5.2.101}$$

with

$$\boldsymbol{N} = \left[\frac{\partial \boldsymbol{y}}{\partial l}\right] \tag{5.2.102}$$

Furthermore, the following definition of the hardening operator $\boldsymbol{H}$ holds:

$$\boldsymbol{H} = \frac{1}{2}\int_{\Gamma} \boldsymbol{f}(\boldsymbol{x}) \cdot \left[\frac{\partial^2 \boldsymbol{y}}{\partial l^2}\right] d\boldsymbol{x} \tag{5.2.103}$$

The goal, once again, is to prove that a field $\dot{\hat{y}}$ is the solution of the fracture mechanics problem if and only if it minimizes the functional (5.2.100) under the constraint

$$\dot{l} \geq 0 \tag{5.2.104}$$

Sufficient condition

In order to prove it, it is necessary to consider the Lagrangian functional:

$$\text{TPE}_{ext_{\mathcal{L}}}(\dot{\boldsymbol{u}}, \dot{\boldsymbol{p}}, \dot{\boldsymbol{w}}, \eta, \dot{l}, \alpha) = \text{TPE}_{ext}(\dot{\boldsymbol{u}}, \dot{\boldsymbol{p}}, \dot{\boldsymbol{w}}) + \eta(\dot{l} - \alpha^2) = \frac{1}{2}\int_{\Gamma} \dot{\boldsymbol{y}}^{\boldsymbol{E}} \boldsymbol{L} \dot{\boldsymbol{y}}^{\boldsymbol{E}} - \int_{\Gamma} \dot{\boldsymbol{f}}\dot{\boldsymbol{y}} - \frac{1}{2}\boldsymbol{H}\dot{l}^2 + \eta(\dot{l} - \alpha^2) \tag{5.2.105}$$

where η is a Lagrange multiplier.

The stationarity of $\text{TPE}_{ext_{\mathcal{L}}}$ with respect to η reproduces exactly the constraint (5.2.104), since $\delta\eta(\dot{l} - \alpha^2) = 0 \Rightarrow \dot{l} = \alpha^2 \geq 0$.

The stationarity is therefore calculated with respect to the other variables $\dot{\boldsymbol{u}}, \dot{\boldsymbol{p}}, \dot{\boldsymbol{w}}, \dot{l}, \alpha$.

It gives

$$\begin{aligned}
\delta\text{TPE}_{ext_{\mathcal{L}}}(\dot{\boldsymbol{u}}, \dot{\boldsymbol{p}}, \dot{\boldsymbol{w}}, \dot{l}, \alpha) &= \frac{1}{2}\int_{\Gamma} \delta\dot{\boldsymbol{y}}^{\boldsymbol{E}} \boldsymbol{L}\dot{\boldsymbol{y}}^{\boldsymbol{E}} + \frac{1}{2}\int_{\Gamma} \dot{\boldsymbol{y}}^{\boldsymbol{E}} \boldsymbol{L}\delta\dot{\boldsymbol{y}}^{\boldsymbol{E}} - \int_{\Gamma} \dot{\boldsymbol{f}}\delta\dot{\boldsymbol{y}} - \frac{1}{2}\boldsymbol{H}\delta\dot{l}\dot{l} - \frac{1}{2}\boldsymbol{H}\dot{l}\delta\dot{l} + \eta(\delta\dot{l} - 2\delta\alpha\alpha) \\
&= \int_{\Gamma} \delta\dot{\boldsymbol{y}}^{\boldsymbol{E}} \boldsymbol{L}\dot{\boldsymbol{y}}^{\boldsymbol{E}} - \int_{\Gamma} \dot{\boldsymbol{f}}\delta\dot{\boldsymbol{y}} - \delta\dot{l}\boldsymbol{H}\dot{l} + \eta(\delta\dot{l} - 2\delta\alpha\alpha) = 0
\end{aligned} \tag{5.2.106}$$

After algebraic manipulations, one has:

$$\begin{aligned}
\delta\text{TPE}_{ext_{\mathcal{L}}}(\dot{\boldsymbol{u}}, \dot{\boldsymbol{p}}, \dot{\boldsymbol{w}}, \dot{l}, \alpha) &= \int_{\Gamma} \delta\dot{\boldsymbol{y}}^{\boldsymbol{E}} \boldsymbol{L}\dot{\boldsymbol{y}}^{\boldsymbol{E}} - \int_{\Gamma} \dot{\boldsymbol{f}}(\delta\dot{\boldsymbol{y}}^{\boldsymbol{E}} + \delta\dot{\boldsymbol{y}}^{\boldsymbol{P}}) - \delta\dot{l}\boldsymbol{H}\dot{l} + \eta(\delta\dot{l} - 2\delta\alpha\alpha) \\
&= \int_{\Gamma} \delta\dot{\boldsymbol{y}}^{\boldsymbol{E}}\left[\boldsymbol{L}\dot{\boldsymbol{y}}^{\boldsymbol{E}} - \dot{\boldsymbol{f}}\right] - \int_{\Gamma} \dot{\boldsymbol{f}}\delta\dot{\boldsymbol{y}}^{\boldsymbol{P}} - \delta\dot{l}\boldsymbol{H}\dot{l} + \eta(\delta\dot{l} - 2\delta\alpha\alpha) \\
&= \int_{\Gamma} \delta\dot{\boldsymbol{y}}^{\boldsymbol{E}}\left[\boldsymbol{L}\dot{\boldsymbol{y}}^{\boldsymbol{E}} - \dot{\boldsymbol{f}}\right] - \int_{\Gamma} \dot{\boldsymbol{f}}\delta\left[\frac{\partial\boldsymbol{y}}{\partial l}\dot{l}\right] - \delta\dot{l}\boldsymbol{H}\dot{l} + \eta(\delta\dot{l} - 2\delta\alpha\alpha) \\
&= \int_{\Gamma} \delta\dot{\boldsymbol{y}}^{\boldsymbol{E}}\left[\boldsymbol{L}\dot{\boldsymbol{y}}^{\boldsymbol{E}} - \dot{\boldsymbol{f}}\right] - \int_{\Gamma} \dot{\boldsymbol{f}}\frac{\partial\boldsymbol{y}}{\partial l}\delta\dot{l} - \delta\dot{l}\boldsymbol{H}\dot{l} + \eta(\delta\dot{l} - 2\delta\alpha\alpha) \\
&= \int_{\Gamma} \delta\dot{\boldsymbol{y}}^{\boldsymbol{E}}\left[\boldsymbol{L}\dot{\boldsymbol{y}}^{\boldsymbol{E}} - \dot{\boldsymbol{f}}\right] - \delta\dot{l}\left[\int_{\Gamma} \dot{\boldsymbol{f}}\frac{\partial\boldsymbol{y}}{\partial l} + \boldsymbol{H}\dot{l} - \eta\right] - 2\eta\delta\alpha\alpha = 0
\end{aligned} \tag{5.2.107}$$

Thus, the problem reduces to the following system of equations:

$$\int_{\Gamma} \boldsymbol{L}\dot{\boldsymbol{y}}^{\boldsymbol{E}} - \dot{\boldsymbol{f}} = 0 \tag{5.2.108}$$

$$\int_{\Gamma} \dot{\boldsymbol{f}}\frac{\partial\boldsymbol{y}}{\partial l} + \boldsymbol{H}\dot{l} - \eta = 0 \tag{5.2.109}$$

$$2\eta\alpha = 0 \tag{5.2.110}$$

The first equation is the equilibrium equation.

From the second equation and recalling the definition of the variation of energy-release rate

(5.2.24), the equality between $\dot{\boldsymbol{G}}$ and the Lagrange multiplier derives, namely

$$\dot{\boldsymbol{G}} = \int_{\Gamma} \dot{\boldsymbol{f}} \frac{\partial \boldsymbol{y}}{\partial l} + \boldsymbol{H} \dot{l} = \eta \qquad (5.2.111)$$

Substituing equation (5.2.111) in (5.2.110), one gets

$$\dot{\boldsymbol{G}} \cdot \alpha = 0 \qquad (5.2.112)$$

In view of the equality $\alpha^2 = \dot{l}$, verified at the beginning of the present Section, one finally derives the stationarity of the functional (5.2.100), since $\dot{\boldsymbol{G}} \cdot \dot{l} = 0$ because of consistency condition.

Necessary condition

For what regards the the necessary condition, one needs to compute the difference between the functional (5.2.100) in an admissible solution and in the exact solution, proving that the result is always greater than zero.

Denoting with $\mathrm{TPE}_{ext}(\dot{\hat{\boldsymbol{u}}}, \dot{\hat{\boldsymbol{p}}}, \dot{\hat{\boldsymbol{w}}}, \dot{\hat{l}})$ the functional (5.2.100) computed in the admissible solution and with $\mathrm{TPE}_{ext}(\dot{\boldsymbol{u}}, \dot{\boldsymbol{p}}, \dot{\boldsymbol{w}}, \dot{l})$ the same functional at the exact solution, one needs to prove that

$$\Delta \mathrm{TPE}_{ext} = \mathrm{TPE}_{ext}(\dot{\hat{\boldsymbol{u}}}, \dot{\hat{\boldsymbol{p}}}, \dot{\hat{\boldsymbol{w}}}, \dot{\hat{l}}) - \mathrm{TPE}_{ext}(\dot{\boldsymbol{u}}, \dot{\boldsymbol{p}}, \dot{\boldsymbol{w}}, \dot{l}) \geq 0 \qquad (5.2.113)$$

After defining the following quantities

$$\Delta \dot{\boldsymbol{u}} = \dot{\hat{\boldsymbol{u}}} - \dot{\boldsymbol{u}}, \ \ \Delta \dot{\boldsymbol{p}} = \dot{\hat{\boldsymbol{p}}} - \dot{\boldsymbol{p}}, \ \ \Delta \dot{\boldsymbol{w}} = \dot{\hat{\boldsymbol{w}}} - \dot{\boldsymbol{w}}, \ \ \Delta \dot{l} = \dot{\hat{l}} - \dot{l}, \qquad (5.2.114)$$

the variation of TPE_{ext} reads

$$
\begin{aligned}
\Delta \mathrm{TPE}_{ext} =& \frac{1}{2} \int_{\Gamma} \Delta \dot{\boldsymbol{y}}^{\boldsymbol{E}} \boldsymbol{L} \Delta \dot{\boldsymbol{y}}^{\boldsymbol{E}} - \int_{\Gamma} \dot{\boldsymbol{f}} \Delta \dot{\boldsymbol{y}} + \int_{\Gamma} \dot{\boldsymbol{y}}^{\boldsymbol{E}} \boldsymbol{L} \Delta \dot{\boldsymbol{y}}^{\boldsymbol{E}} - \frac{1}{2} \boldsymbol{H} \Delta \dot{l}^2 - \boldsymbol{H} \Delta \dot{l} \cdot \dot{l} \\
=& \ \frac{1}{2} \int_{\Gamma} \Delta \dot{\boldsymbol{y}}^{\boldsymbol{E}} \boldsymbol{L} \Delta \dot{\boldsymbol{y}}^{\boldsymbol{E}} - \frac{1}{2} \boldsymbol{H} \Delta \dot{l}^2 \\
& - \int_{\Gamma} \dot{\boldsymbol{f}} (\Delta \dot{\boldsymbol{y}}^{\boldsymbol{E}} + \Delta \dot{\boldsymbol{y}}^{\boldsymbol{P}}) + \int_{\Gamma} \dot{\boldsymbol{y}}^{\boldsymbol{E}} \boldsymbol{L} \Delta \dot{\boldsymbol{y}}^{\boldsymbol{E}} - \boldsymbol{H} \Delta \dot{l} \cdot \dot{l} \\
\\
=& \ \frac{1}{2} \int_{\Gamma} \Delta \dot{\boldsymbol{y}}^{\boldsymbol{E}} \boldsymbol{L} \Delta \dot{\boldsymbol{y}}^{\boldsymbol{E}} - \frac{1}{2} \boldsymbol{H} \Delta \dot{l}^2 \\
& + \int_{\Gamma} \Delta \dot{\boldsymbol{y}}^{\boldsymbol{E}} \left[\boldsymbol{L} \dot{\boldsymbol{y}}^{\boldsymbol{E}} - \dot{\boldsymbol{f}} \right] - \int_{\Gamma} \dot{\boldsymbol{f}} \Delta \dot{\boldsymbol{y}}^{\boldsymbol{P}} - \boldsymbol{H} \Delta \dot{l} \cdot \dot{l} \\
\\
=& \ \frac{1}{2} \int_{\Gamma} \Delta \dot{\boldsymbol{y}}^{\boldsymbol{E}} \boldsymbol{L} \Delta \dot{\boldsymbol{y}}^{\boldsymbol{E}} - \frac{1}{2} \boldsymbol{H} \Delta \dot{l}^2 \\
& + \int_{\Gamma} \Delta \dot{\boldsymbol{y}}^{\boldsymbol{E}} \left[\boldsymbol{L} \dot{\boldsymbol{y}}^{\boldsymbol{E}} - \dot{\boldsymbol{f}} \right] - \Delta \dot{l} \left[\int_{\Gamma} \dot{\boldsymbol{f}} \frac{\partial \boldsymbol{y}}{\partial l} + \boldsymbol{H} \dot{l} \right]
\end{aligned}
\qquad (5.2.115)
$$

The third member of (5.2.115) vanishes as it is the equilibrium equation of the problem. Recalling the definition of the variation of energy-release rate (5.2.24), one finally has:

$$\Delta \text{TPE}_{ext} = \frac{1}{2} \int_{\Gamma} \Delta \dot{\boldsymbol{y}}^{\boldsymbol{E}} \boldsymbol{L} \Delta \dot{\boldsymbol{y}}^{\boldsymbol{E}} - \frac{1}{2} \boldsymbol{H} \Delta \dot{l}^2 - \dot{\hat{l}} \dot{\boldsymbol{G}} + \dot{l} \dot{\boldsymbol{G}} \tag{5.2.116}$$

The term $-\dot{\hat{l}} \dot{\boldsymbol{G}}$ in (5.2.116) is positive semidefinite, while the term $\dot{l} \dot{\boldsymbol{G}}$ is null, due to the consistency condition (5.2.87).

Hardening operator $\boldsymbol{H}$ is defined as negative, therefore a hypothesis on the sign of the operator $\boldsymbol{L}$ is needed.

Defined as in (5.2.94), the operator $\boldsymbol{L}$ has no sign, but there are two possibilities to fix this issue:

- evaluate a self-balanced solid, therefore without having to superimpose displacements. In this case all components defined on Γ_u vanish;

- carry out an inversion of the type proposed by Bramble and Pasciak, in order to guarantee the positive definition of $\boldsymbol{L}$.

Bramble and Pasciak method for the positive definition of the operator $\boldsymbol{L}$

Bramble and Pasciak method (Carini, Diligenti, Salvadori 1997) is exploited here to derive the positive definition of the operator $\boldsymbol{L}$. First, one considers the following transformations:

$$\boldsymbol{A} = \int_{\Gamma_u} \mathbf{G_{uu}}[\cdot] \, d\boldsymbol{\xi} \tag{5.2.117}$$

$$\tilde{\boldsymbol{B}} = \begin{vmatrix} -\int_{\Gamma_u} \mathbf{G_{pu}}[\cdot] \, d\boldsymbol{\xi} \\ -\int_{\Gamma_u} \mathbf{G_{pu}}[\cdot] \, d\boldsymbol{\xi} \end{vmatrix} \tag{5.2.118}$$

$$\tilde{\boldsymbol{B}}^* = \begin{vmatrix} -\int_{\Gamma_p} \mathbf{G_{up}}[\cdot] \, d\boldsymbol{\xi} & -\int_{\Gamma_w} \mathbf{G_{up}}[\cdot] \, d\boldsymbol{\xi} \end{vmatrix} \tag{5.2.119}$$

$$\tilde{\boldsymbol{C}} = \begin{vmatrix} -\int_{\Gamma_p} \mathbf{G_{pp}}[\cdot] \, d\boldsymbol{\xi} & -\int_{\Gamma_w} \mathbf{G_{pp}}[\cdot] \, d\boldsymbol{\xi} \\ -\int_{\Gamma_p} \mathbf{G_{pp}}[\cdot] \, d\boldsymbol{\xi} & -\int_{\Gamma_w} \mathbf{G_{pp}}[\cdot] \, d\boldsymbol{\xi} \end{vmatrix} \tag{5.2.120}$$

$$\dot{\boldsymbol{U}}^{\boldsymbol{E}} = \begin{vmatrix} \dot{\mathbf{u}}^{\mathbf{E}} \\ \dot{\mathbf{w}}^{\mathbf{E}} \end{vmatrix} \tag{5.2.121}$$

$$\dot{\boldsymbol{f}}^{\boldsymbol{\Sigma}} = \begin{vmatrix} \dot{\mathbf{f}}^{\mathbf{P}} \\ \dot{\mathbf{f}}^{\mathbf{w}} \end{vmatrix} \tag{5.2.122}$$

In the light of (5.2.117)-(5.2.122),the problem (5.2.94) can be rewritten in operatorial form as:

$$\begin{vmatrix} \boldsymbol{A} & \tilde{\boldsymbol{B}}^* \\ \tilde{\boldsymbol{B}} & -\tilde{\boldsymbol{C}} \end{vmatrix} \cdot \begin{vmatrix} \dot{\mathbf{p}}^{\mathbf{E}} \\ \dot{\boldsymbol{U}}^{\boldsymbol{E}} \end{vmatrix} = \begin{vmatrix} \dot{\mathbf{f}}^{\mathbf{u}} \\ \dot{\boldsymbol{f}}^{\boldsymbol{\Sigma}} \end{vmatrix} \tag{5.2.123}$$

In order to derive the positive definition of the operator $\boldsymbol{L}$, one multiplies both members of (5.2.123) by the operator $\tilde{\boldsymbol{P}}$, defined as

$$\tilde{\boldsymbol{P}} = \begin{vmatrix} \boldsymbol{A} \boldsymbol{A}_0^{-1} - \boldsymbol{I} & \mathbf{0} \\ \tilde{\boldsymbol{B}} \boldsymbol{A}_0^{-1} & -\boldsymbol{I} \end{vmatrix}, \tag{5.2.124}$$

where $\boldsymbol{A}_0^{-1}$ is an operator that makes $\boldsymbol{A}$ symmetric and positive definite. The system (5.2.123) thus becomes

$$
\left|
\begin{array}{cc}
(\boldsymbol{A} - \boldsymbol{A}_0)\boldsymbol{A}_0^{-1}\boldsymbol{A} & (\boldsymbol{A} - \boldsymbol{A}_0)\boldsymbol{A}_0^{-1}\tilde{\boldsymbol{B}}^* \\
\tilde{\boldsymbol{B}}\boldsymbol{A}_0^{-1}(\boldsymbol{A} - \boldsymbol{A}_0) & \tilde{\boldsymbol{C}} + \tilde{\boldsymbol{B}}\boldsymbol{A}_0^{-1}\tilde{\boldsymbol{B}}^*
\end{array}
\right|
\cdot
\left|
\begin{array}{c}
\dot{\mathbf{p}}^{\mathbf{E}} \\
\dot{\boldsymbol{U}}^{E}
\end{array}
\right|
=
\left|
\begin{array}{c}
(\boldsymbol{A} - \boldsymbol{A}_0)\boldsymbol{A}_0^{-1}\dot{\mathbf{f}}^{\mathbf{u}} \\
\tilde{\boldsymbol{B}}\boldsymbol{A}_0^{-1}\dot{\mathbf{f}}^{\mathbf{u}} - \dot{\boldsymbol{f}}^{\boldsymbol{\Sigma}}
\end{array}
\right|
\tag{5.2.125}
$$

The system (5.2.125) can be extended as

$$
\left|
\begin{array}{ccc}
\boldsymbol{D} & \boldsymbol{E}^* & \boldsymbol{F}^* \\
\boldsymbol{E} & \boldsymbol{Q} & \boldsymbol{R}^* \\
\boldsymbol{F} & \boldsymbol{R} & \boldsymbol{S}
\end{array}
\right|
\cdot
\left|
\begin{array}{c}
\dot{\mathbf{p}}^{\mathbf{E}} \\
\dot{\mathbf{u}}^{\mathbf{E}} \\
\dot{\mathbf{w}}^{\mathbf{E}}
\end{array}
\right|
=
\left|
\begin{array}{c}
\dot{\mathbf{g}}^{\mathbf{u}} \\
\dot{\mathbf{g}}^{\mathbf{P}} \\
\dot{\mathbf{g}}^{\mathbf{w}}
\end{array}
\right|
\begin{array}{l}
su\ \Gamma_u \\
su\ \Gamma_p \\
su\ \Gamma_w
\end{array}
,
\tag{5.2.126}
$$

for which the following relations hold:

$$
\boldsymbol{D} = (\boldsymbol{A} - \boldsymbol{A}_0)\boldsymbol{A}_0^{-1}\boldsymbol{A}
\tag{5.2.127}
$$

$$
\boldsymbol{E} = -\int_{\Gamma_u} \mathbf{G}_{\mathbf{pu}}\boldsymbol{A}_0^{-1}(\boldsymbol{A} - \boldsymbol{A}_0)[\cdot]\, d\boldsymbol{\xi}
\tag{5.2.128}
$$

$$
\boldsymbol{E}^* = -\int_{\Gamma_p} (\boldsymbol{A} - \boldsymbol{A}_0)\boldsymbol{A}_0^{-1}\mathbf{G}_{\mathbf{up}}[\cdot]\, d\boldsymbol{\xi}
\tag{5.2.129}
$$

$$
\boldsymbol{F} = -\int_{\Gamma_u} \mathbf{G}_{\mathbf{pu}}\boldsymbol{A}_0^{-1}(\boldsymbol{A} - \boldsymbol{A}_0)[\cdot]\, d\boldsymbol{\xi}
\tag{5.2.130}
$$

$$
\boldsymbol{F}^* = -\int_{\Gamma_w} (\boldsymbol{A} - \boldsymbol{A}_0)\boldsymbol{A}_0^{-1}\mathbf{G}_{\mathbf{up}}[\cdot]\, d\boldsymbol{\xi}
\tag{5.2.131}
$$

$$
\boldsymbol{Q} = -\int_{\Gamma_p} \mathbf{G}_{\mathbf{pp}}[\cdot]\, d\boldsymbol{\xi} + \int_{\Gamma_u} \mathbf{G}_{\mathbf{pu}}\left[\boldsymbol{A}_0^{-1}\int_{\Gamma_p} \mathbf{G}_{\mathbf{up}}[\cdot]\, d\boldsymbol{\xi}\right]\, d\boldsymbol{\xi}
\tag{5.2.132}
$$

$$
\boldsymbol{R} = -\int_{\Gamma_p} \mathbf{G}_{\mathbf{pp}}[\cdot]\, d\boldsymbol{\xi} + \int_{\Gamma_u} \mathbf{G}_{\mathbf{pu}}\left[\boldsymbol{A}_0^{-1}\int_{\Gamma_p} \mathbf{G}_{\mathbf{up}}[\cdot]\, d\boldsymbol{\xi}\right]\, d\boldsymbol{\xi}
\tag{5.2.133}
$$

$$
\boldsymbol{R}^* = -\int_{\Gamma_w} \mathbf{G}_{\mathbf{pp}}[\cdot]\, d\boldsymbol{\xi} + \int_{\Gamma_u} \mathbf{G}_{\mathbf{pu}}\left[\boldsymbol{A}_0^{-1}\int_{\Gamma_w} \mathbf{G}_{\mathbf{up}}[\cdot]\, d\boldsymbol{\xi}\right]\, d\boldsymbol{\xi}
\tag{5.2.134}
$$

$$
\boldsymbol{S} = -\int_{\Gamma_w} \mathbf{G}_{\mathbf{pp}}[\cdot]\, d\boldsymbol{\xi} + \int_{\Gamma_u} \mathbf{G}_{\mathbf{pu}}\left[\boldsymbol{A}_0^{-1}\int_{\Gamma_w} \mathbf{G}_{\mathbf{up}}[\cdot]\, d\boldsymbol{\xi}\right]\, d\boldsymbol{\xi}
\tag{5.2.135}
$$

$$
\dot{\boldsymbol{g}}^{\boldsymbol{u}} = (\boldsymbol{A} - \boldsymbol{A}_0)\boldsymbol{A}_0^{-1}\dot{\mathbf{f}}^{\mathbf{u}}
\tag{5.2.136}
$$

$$
\dot{\boldsymbol{g}}^{\boldsymbol{p}} = -\int_{\Gamma_u} \mathbf{G}_{\mathbf{pu}}\boldsymbol{A}_0^{-1}\dot{\mathbf{f}}^{\mathbf{u}}\, d\boldsymbol{\xi} - \dot{\mathbf{f}}^{\mathbf{P}}
\tag{5.2.137}
$$

$$
\dot{\boldsymbol{g}}^{\boldsymbol{w}} = -\int_{\Gamma_u} \mathbf{G}_{\mathbf{pu}}\boldsymbol{A}_0^{-1}\dot{\mathbf{f}}^{\mathbf{u}}\, d\boldsymbol{\xi} - \dot{\mathbf{f}}^{\mathbf{w}}
\tag{5.2.138}
$$

It is therefore possible to rewrite the Total Potential Energy functional (5.2.100) in the following way:

$$
\begin{aligned}
\mathrm{TPE}_{ext}(\dot{\boldsymbol{u}}, \dot{\boldsymbol{p}}, \dot{\boldsymbol{w}}, \dot{l}) = & \frac{1}{2} \int_{\Gamma} \dot{\boldsymbol{y}}^{\boldsymbol{E}} \boldsymbol{L} \dot{\boldsymbol{y}}^{\boldsymbol{E}} - \int_{\Gamma} \dot{\boldsymbol{f}} \dot{\boldsymbol{y}} - \frac{1}{2} \boldsymbol{H} \dot{l}^2 \\
= & \ \frac{1}{2} \int_{\Gamma_u} \dot{\boldsymbol{p}}^{\boldsymbol{E}} \boldsymbol{D} \dot{\boldsymbol{p}}^{\boldsymbol{E}} \, d\boldsymbol{x} + \frac{1}{2} \int_{\Gamma_p} \dot{\boldsymbol{u}}^{\boldsymbol{E}} \boldsymbol{Q} \dot{\boldsymbol{u}}^{\boldsymbol{E}} \, d\boldsymbol{x} + \frac{1}{2} \int_{\Gamma_w} \dot{\boldsymbol{w}}^{\boldsymbol{E}} \boldsymbol{S} \dot{\boldsymbol{w}}^{\boldsymbol{E}} \, d\boldsymbol{x} \\
& + \int_{\Gamma_p} \dot{\boldsymbol{u}}^{\boldsymbol{E}} \boldsymbol{E} \dot{\boldsymbol{p}}^{\boldsymbol{E}} \, d\boldsymbol{\xi} + \int_{\Gamma_w} \dot{\boldsymbol{w}}^{\boldsymbol{E}} \boldsymbol{F} \dot{\boldsymbol{p}}^{\boldsymbol{E}} \, d\boldsymbol{\xi} + \int_{\Gamma_w} \dot{\boldsymbol{w}}^{\boldsymbol{E}} \boldsymbol{R} \dot{\boldsymbol{u}}^{\boldsymbol{E}} \, d\boldsymbol{\xi} \qquad (5.2.139) \\
& - \frac{1}{2} \boldsymbol{H} \dot{l}^2 \\
& - \int_{\Gamma_u} \dot{\boldsymbol{p}} \cdot \dot{\boldsymbol{g}}^{\boldsymbol{u}} \, d\boldsymbol{x} - \int_{\Gamma_p} \dot{\boldsymbol{u}} \cdot \dot{\boldsymbol{g}}^{\boldsymbol{p}} \, d\boldsymbol{x} - \int_{\Gamma_w} \dot{\boldsymbol{w}} \cdot \dot{\boldsymbol{g}}^{\boldsymbol{w}} \, d\boldsymbol{x}
\end{aligned}
$$

As in Carini, Diligenti and Salvadori (1997) (where the proof is omitted for the sake of brevity), it is now possible to conclude that the solution of the problem is the one which solves the minimization problem:

$$
\begin{cases}
\min \left[\mathrm{TPE}_{ext}(\dot{\boldsymbol{u}}, \dot{\boldsymbol{p}}, \dot{\boldsymbol{w}}, \dot{l}) \right] \\
\dot{l} \geq 0
\end{cases}
\qquad (5.2.140)
$$

5.3 Viscoelastic fracture mechanics

An interesting line of future research, which unfortunately has not been developed in the work of this thesis due to time restrictions, is the topic of viscoelastic fracture mechanics.

Starting from Francfort-Marigot formulation (2008), namely a variational model for quasistatic crack evolution in a brittle material given by a contribution of a surface energy and a contribution of bulk energy, which is a revisitation of Griffith's energetic criterion, a functional of the Free Energy type is written in a non-incremental form.

For an admissible solution, it could be written as

$$
\mathcal{F}_V = -\frac{1}{2} \int_0^{\hat{l}} \int_0^{\hat{l}} \int_{0^-}^T \int_{0^-}^T R_{pp}(x-\xi; 2T-t-\tau) d\hat{w}(\xi;\tau) d\hat{w}(x;t) \, d\xi dx
$$
$$
- \int_0^{\hat{l}} \int_{0^-}^T p(x; 2T-t) d\hat{w}(x;t) \, dx + G_0 \cdot \hat{l}(T)
$$

(5.3.1)

with the constraint $\hat{l} \geq l(t)$.

Green's functions are replaced by functions (here denoted with R_{pp}), recalling relaxation kernels of viscoelastic composites, whose properties of positive definiteness should be defined in advance.

In order to prove that the solution of the problem is the minimum of functional (5.3.1), one needs to prove that the difference between the functional computed in the correspondence of an admissible solution, here denoted with $\hat{\mathcal{F}}_V$, and the functional computed in the correspondence of the exact solution, is non negative, namely

$$
\Delta \mathcal{F}_V = \hat{\mathcal{F}}_V - \mathcal{F}_V \geq 0
$$

(5.3.2)

The stationarity of functional (5.3.1) needs to be proved starting from the Lagrangian functional

$$
\mathcal{F}_{V_\mathcal{L}} = -\frac{1}{2} \int_0^{\hat{l}} \int_0^{\hat{l}} \int_{0^-}^T \int_{0^-}^T R_{pp}(x-\xi; 2T-t-\tau) d\hat{w}(\xi;\tau) d\hat{w}(x;t) \, d\xi dx
$$
$$
- \int_0^{\hat{l}} \int_{0^-}^T p(x; 2T-t) d\hat{w}(x;t) \, dx + G_0 \cdot \hat{l}(T) + \eta[\hat{l} - (l(T) + \alpha^2)]
$$

(5.3.3)

where η is a Lagrange multiplier and α^2 is a necessary definite-positive parameter in order to include the constraint of the problem. To this aim, the Gateaux derivative of functional (5.3.1) needs to be zero, namely

$$
\frac{d}{d\epsilon} \mathcal{F}_{V_\mathcal{L}}(l + \epsilon \tilde{l}, w + \epsilon \tilde{w})|_{\epsilon=0} = 0
$$

(5.3.4)

Once again, the stationarity of $\mathcal{F}_{V_\mathcal{L}}$ with respect to η returns the constraint $l \geq l(T)$ ($\delta \eta[\hat{l} - (l(t) + \alpha^2)] = 0 \Rightarrow \hat{l} = l(T) + \alpha^2 \geq l(T)$).

5.4 Conclusions

Starting from Capurso-Maier incremental functional for the elastic-plastic case as expressed in equation (5.2.1), an analogous formulation has been obtained for the fracture mechanics case in Section 5.2.5. It materializes in equation (5.2.38).

The negative hardening component is obtained from the incremental form of the energy-release rate in Section 5.2.3 and it results to be dependent on the geometry of the crack, thus is not known a priori. The complementary conditions are re-obtained for fracture mechanics. They govern the fracture propagation problem at each time instant, as expressed by equations (5.2.33) and(5.2.36). The stationarity of the functional (5.2.38) is demonstrated in Section 5.2.5 and a minimum principle is derived. The functional (5.2.38) is re-formulated as a one-field functional in Section 5.2.6 and an analogy with the functional introduced by Salvadori and Carini (2011) (see equation (5.2.76)) is presented.

Furthermore, the problem is generalized to a solid body in a two/three-dimensional space in Section 5.2.7.

Starting from Francfort-Marigo work (2008) a non incremental formulation, in a Free Energy form, could be used to extend the fracture mechanics formulation to viscoelastic composites.

References

Amestoy, M., Leblond, J.B., 1992. Crack paths in plane situations - ii. detailed form of the expansion of the stress intensity factors. International Journal of Solids and Structures, 29, pp. 465-501.

Amestoy, M., Bui, H.D., Leblond, J.B., 1986. Facteurs dintensit des contraintes dune fissure branche. Comptes Rendus de l'Acadmie des Sciences , Paris, 303, pp. 985-988.

Brinker, R., 1990. Crack tip parameters for growing cracks in linear viscoelastic materials. Dept. of Building Technology and Structural Engineering, Aalborg University. Fracture and Dynamics vol. R9007, No. 19.

Carini, A., De Donato, O., 1992. Fundamental solutions for linear viscoelastic continua. International Journal of Solids and Structures, 29, No. 23, 2989-3009.

Carini, A., Diligenti, M., Salvadori, A., 1997. Extremal formulations for elastic and elastic-plastic analysis by boundary integral equations. XIII Congresso Nazionale AIMETA, Siena 29 september - 3 october.

Carpinteri, A., 1992. Meccanica dei materiali e della frattura. Editore Pitagora, Bologna.

Chambolle, A., Francfort, G., Marigo, J., 2009. When and how do cracks propagate? Journal of Mechanics and Physics of Solids, 57, No. 9, 1614-1622.

Chaoufi, J., Gamby, D., 1993. A possible way of applying Shapery's viscoelastic fracture model to creep crack growth in carbon-epoxy composites. Advanced Composites Letters, 2, No.3, 93-95.

Christensen, R.M., 1979. A rate-dependent criterion for crack growth. International Journal of Fracture, 15, 3-21.

Corradi dell'Acqua, L., 1992. Meccanica delle strutture, il comportamento dei mezzi continui. Ed. McGraw-Hill, Milano.

Francfort, G., Marigo, J., 1998. Revisiting brittle fracture as an energy minimization problem. Journal of Mechanics and Physics of Solids, 46, No. 8, 1319-1342.

Francfort, G., Marigo, J., 2008. The Variational Approach to Fracture. Journal of Elasticity, 91.

Golden, J.M., Graham, G.A.C., 1990. Energy balance criteria for viscoelastic fracture. Quarterly of Applied Mathematics, 48, No. 3, 401-413.

Liang, R.Y., Zhou, J., 1997. Energy based approach for crack initiation and propagation in viscoelastic solid. Engineering Fracture Mechanics, 58, 71-85.

Maier, G., Frangi, A., 1998. Symmetric boundary element method for "discrete" crack model

of fracture processes. Computer Assisted Mechanics and Engineering Sciences, 5, 201-226.

Maugin, G.A., 1992. The thermomechanics of plasticity and fracture. Cambridge University Press, Cambridge.

McCartney, L.N., 1980. Discussion: "A rate-dependent criterion for crack growth", by R.M. Christensen. International Journal of Fracture, 16, 229-232.

Salvadori, A., 2008. A plasticity framework for (linear elastic) fracture mechanics. Journal of the Mechanics and Physics of Solids, 56, pp. 2092-2116

Salvadori, A., Carini, A., 2011. Minimum theorems in incremental linear elastic fracture mechanics. International Journal of Solids and Structures, 48, 1362-1369.

Stolz, C., 2011. Analysis of Stability and Bifurcation in Non linear Mechanics with Dissipation. Entropy, 13, 332-366.

Syngellakis, S., Wu, J., 2003. Boundary element applications to polymer fracture. Transaction on Modelling and Simulations, 35, 83-92.

Chapter 6

On the dynamic stability of elastic structures subjected to follower forces and some curiosities about systems showing instability in tension

Notation

Greek and latin letters

- M: Concentrated mass;
- m: Distributed mass;
- μ: Mass per unit length;
- ω: Frequency of the small vibrations of the rod;
- u: Lagrangian coordinate;
- K: Stiffness coefficient;
- $\mathcal{E}$: Total energy of a conservative system;
- P: Concentrated follower load;
- p: Distributed follower load;
- Q: Concentrated conservative load;
- l: Length of the rod;
- J: Moment of inertia;
- F: Transverse static force;
- E: Young's modulus;
- a: Coordinate of the intermediate support;

- a^*: Transition value;

- $v(z)$: Deflected curve;

- Φ: Rotation.

Symbols

- $\hat{}$: Admissible solution.

Operators and functions

- ^{n}: n^{th} spatial derivative operation;

- $\dot{}$: Derivation with respect to the time variable;

- f: Leipholz's functional;

- $\dot{}$: Derivation with respect to the time variable;

- U: Deformation energy.

6.1 A variational approach for the dynamic stability problem

Leipholz (1978) spent many years trying to reconcile the fact that structural problems with follower forces are nonconservative, thus the classical variational principles following Hamilton's principle cannot be applied, with the fact that, in some way, a variational approach should yet be possible.
He defined a bilinear functional, applicable to nonconservative systems, like Beck's rod, and proved that there exist a stationary principle.

Starting from Beck's rod (Fig. 6.1) of length l, with bending stiffness EJ, mass per unit length μ, clamped at a lower end and subjected to a compressive follower load P at the free end, one can write the following differential equation with relevant boundary conditions:

$$EJv^{IV} + Pv^{II} - \mu\omega^2 v = 0$$
$$v(0) = v^I(0) = v^{II}(l) = v^{III}(l) = 0 \tag{6.1.1}$$

In (6.1.1) ω is the frequency of the small vibrations of the rod, $v(z)$ is the lateral displacement and z is the coordinate of the axis of the rod.
Consider the following functional:

$$f(\hat{v}) = \int_0^l \left[EJ\hat{v}^{IV}(z) + P\hat{v}^{II}(z) - \mu\omega^2\hat{v}(z) \right] \cdot \hat{v}^{II}(l-z)\,dz \tag{6.1.2}$$

The latter functional proves to be particularly interesting for our research because it contains a convolution product with respect to the space variable instead of the time variable.
The stationary principle holds:

$$f(v) = \underset{\hat{v}}{\text{stat}}\, f(\hat{v}) \tag{6.1.3}$$

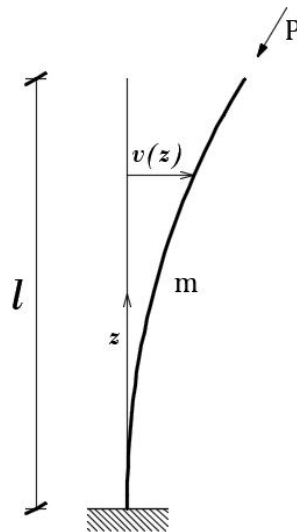and the critical loads are obtained.

Figure 6.1: Beck's rod: clamped at one end with a concentrated follower force on the free end and with a distributed mass m.

The advantage of using a convolutive functional is clear after what has been described in Chapter 2 and in Chapter 3.

A splitting of the lenght of the beam would formally double the unknowns: the variables defined in the first sub-interval and those defined in the second one. This approach could lead to the definition f a min-max principle, as already pointed out in Chapter 2 and Chapter 3.

In conclusion, Leipholz (1978) defined a functional valid for analysis with distributed mass m. Our goal is to obtain results for different systems, in particular, structures with one concentrated mass.

It is important to emphasize that there are still many intermediate problems, which have not been addressed in the context of this thesis, such as structures with two or more concentrated masses or systems with both distributed and concentrated masses. This could be an interesting topic for future researches.

6.2 Part I: Conjecture on the dynamic instability of structures subjected to compressive follower forces

6.2.1 Introduction

Within the framework of the second-order theory, some classical stability problems, whose critical load corresponded to dynamic instability, were considered in the paper by Feriani and Carini (2017). The main focus was on plain systems with just one lumped mass. This idealization, together with the assumption of negligible axial strain and the adoption of the second-order theory, reduced the considered systems to a single Lagrangian coordinate. In this way, static methods could be applied to derive the analytical expression of the stiffness coefficient and to study the dynamic stability, starting with a well-known example, namely, a cantilever beam with a lumped mass at the free end subjected to a follower load (Panovko, Gubanova, 1967). In this Chapter, a new lumped mass system is studied: a straight-axis beam with constant cross-sectional area and stiffness, mass-free, hinged at one end, simply supported at an intermediate point (with a sliding plane parallel to the beam axis) and with the other end free, where a lumped mass is present and a follower force is applied. As in the examples shown in Feriani and Carini (2017), in this example the first asymptote of the stiffness coefficient corresponds to the critical load, due to divergence at infinity. It is shown that this critical load is equal to the buckling load due to divergence of an auxiliary structure, which differs from the original one in that the concentrated mass is replaced by a constraint that blocks the corresponding Lagrangian coordinate.

6.2.2 The stability problem with follower forces

A classical stability problem involving a straight-axis Euler Bernoulli beam without damping, with a concentrated mass M, inflecting in a plane, subjected to follower loads is discussed. No allowance is made for axial strain, and displacements are assumed to be small. This idealization reduces the system to a single Lagrangian coordinate u. Therefore, the equation of motion due to an initial perturbation can be written in the form:

$$M\ddot{u} + Ku = 0 \qquad (6.2.1)$$

where the stiffness coefficient K takes second-order effects into account. It follows that stability depends on the sign of the stiffness coefficient. If it is positive, the motion is oscillatory and bounded. If it is negative, the motion is unbounded and non-oscillatory (divergence). Since the system possesses just one Lagrangian coordinate, unbounded oscillatory motion (flutter) cannot occur. In fact, a dynamical system that can be schematized with a lumped mass constrained by a linear spring and for which motion is governed by (6.2.1) is a conservative system with total energy $\mathcal{E}$ (kinetic plus potential) equal to

$$\mathcal{E} = \frac{1}{2}M\ddot{u}^2 + \frac{1}{2}Ku^2 \qquad (6.2.2)$$

which is conserved during the motion. The stability of such a system can therefore be studied statically by using Dirichlet's theorem and then going on to determine the sign of K. If $K > 0$ the potential energy in the initial undeformed configuration is minimum and the system is stable whereas if $K < 0$ the potential energy in the initial undeformed configuration is maximum and the system is unstable.

In Feriani and Carini (2017) systems depicted in Fig. 6.2a, 6.2b and 6.2c have already been studied. Referring, for simplicity, to the system in Fig. 6.2a, the dependence of the stiffness coefficient on the applied load is nonlinear, due to the adopted mass modelling, so the change of sign of the stiffness coefficient may occur due to the presence of an asymptote. As the compressive load slowly increases from zero, the stiffness coefficient increases and consequently the vibration frequency increases. When the load tends to the critical value, the stiffness coefficient tends to infinity and the corresponding mass displacement tends to zero (Panovko, Gubanova, 1967). If the load is slightly higher than the critical load, the other branch of the function is involved and the stiffness coefficient is negative, corresponding to non-oscillatory unbounded motion. This phenomenon of stable-to-unstable transition is named divergence at infinity (Felippa, 2014) and it is caused by ignoring the distributed mass of the column. It is a dynamic instability, since it depends on the mass properties of the structure, and it can occur in systems that possess just one Lagrangian coordinate and are subjected to follower loads. In these cases, divergence at infinity can be studied by analysing the sign of the stiffness coefficient, i.e., although divergence at infinity is a dynamic instability, a static method can be applied. The phenomenon of divergence at infinity also occurs for the structures in Fig. 6.2b and 6.2c. In this Chapter, a new lumped mass system is studied: a straight-axis beam with constant cross-sectional area and stiffness, massless, hinged at one end, simply supported at an intermediate point at a distance a from the hinge and with the other end free in which there is a lumped mass and a follower force is applied (Fig. 6.3a). In the case of uniformly distributed mass, the system was studied by Zorii and Chernukha (1971) and later by Elishakoff and Hollkamp (1987). Intuitively, for $a \longrightarrow 0$ one should find the results already obtained in Feriani and Carini (2016), while for $a \longrightarrow l$ one should find again the Eulerian critical load. This implies (as indeed already pointed out in Zorii and Chernukha (1971) and later by Elishakoff and Hollkamp (1987)) that there should exist a transition value $a = a^*$ such that when $a < a^*$ there is instability by divergence at infinity, while for $a > a^*$ there is Eulerian instability by divergence.

6.2.3   Applying a static method to detect divergence at infinity

Consider the example in Fig. 6.3a, i.e., a straight-axis beam of length l, with a constant cross-section and moment of inertia J, with no distributed mass, hinged at one end, simply supported at an intermediate point at distance a from the hinge and with the other end free in which
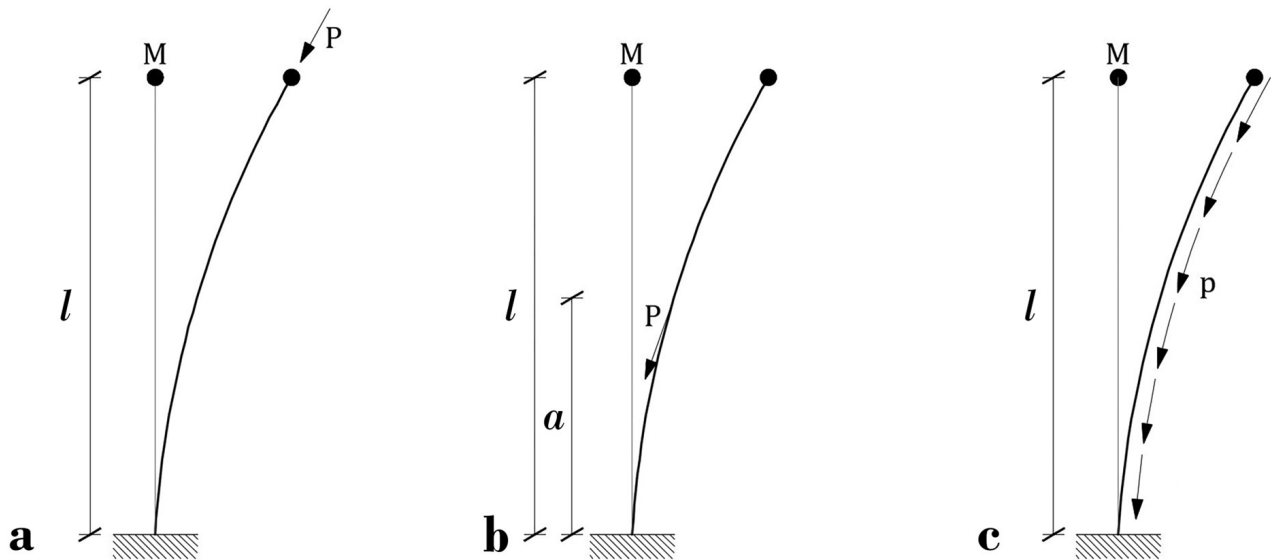
Figure 6.2: Cantilever beam with lumped mass subject to (a) a follower force P at the free end, (b) to a follower force P applied at an intermediate point, and (c) to a uniformly distributed follower force p.
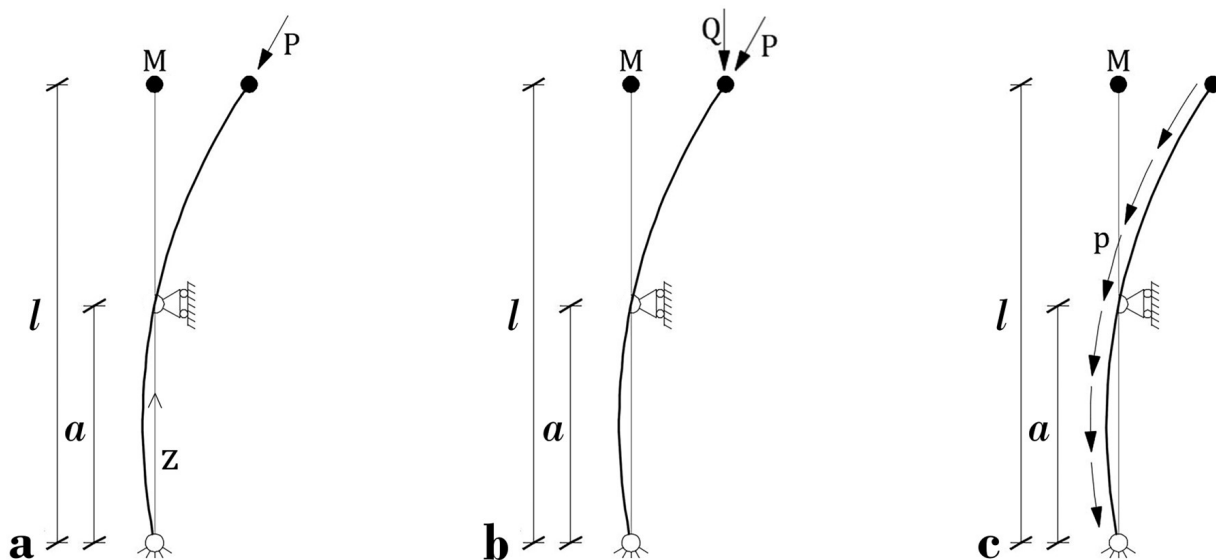

Figure 6.3: Beam hinged at one end, free at the other end, simply supported at an intermediate point, with a mass concentrated at the free end and subject to (a) a follower force P at the free end, (b) a conservative force Q and a follower force P at the free end, and (c) a uniformly distributed follower force p.

there is a concentrated mass M and a follower force P is applied. The stiffness coefficient K is determined by using the direct method, that is, neglecting the mass and applying a transverse static force F acting transversely to the beam at the free end such as to produce a unit displacement in the direction of F.

Having chosen, as shown in Fig. 6.3a, the hinged end as the origin of the z-coordinate along the axis of the beam and denoting by E the Young's modulus, the deflected curve $v(z)$, can be obtained by prescribing

$$EJv_i^{IV} + Pv_i^{II} = 0 \ \ with \ \ i = 1 \ \ for \ \ 0 \le z \le a, \ \ i = 2 \ \ for \ \ a \le z \le l \tag{6.2.3}$$

with boundary conditions:

$$v_1(0) = 0, \ \ v_1^{II}(0) = 0, \ \ v_2(l) = 1, \ \ v_2^{II}(l) = 0 \tag{6.2.4}$$

and with the continuity conditions:

$$v_1(a) = v_2(a) = 0, \ \ v_1^I(a) = v_2^I(a), \ \ v_1^{II}(a) = v_2^{II}(a). \tag{6.2.5}$$

By solving the equation of the deflected curve, it is possible to determine K:

$$K = -EJv_2^{III}(l) = P\alpha \cdot \frac{a\sin(\alpha a)}{\alpha a^2 \sin(\alpha l) - \alpha al \sin(\alpha l) + l\sin(\alpha a) \cdot [\cos(\alpha a)\sin(\alpha l) - \cos(\alpha l)\sin(\alpha a)]} \tag{6.2.6}$$

with $\alpha^2 = P/EJ$.

Assuming $c = a/l$, Fig. 6.4 shows the dimensionless stiffness coefficient Kl^3/EJ as a function of αl for different c. For $c = 0$ a well-known case is found (Panovko, Gubanova, 1967). In this case, asymptotes occur as

$$\tan(\alpha l) = \alpha l \tag{6.2.7}$$

and the first asymptote (divergence at infinity) corresponds to $(P_{cr}l^2)EJ = 20.1934$. If $c = 1$ another well-known case is obtained: the pinned-pinned Euler rod to which corresponds the Eulerian critical load $(P_{cr}l^2)EJ = 9.8696$. Analysing the same graph as c increases from zero to one, we move from instability by divergence at infinity to Eulerian instability by divergence. Such a transition occurs when $c = 0.5$.
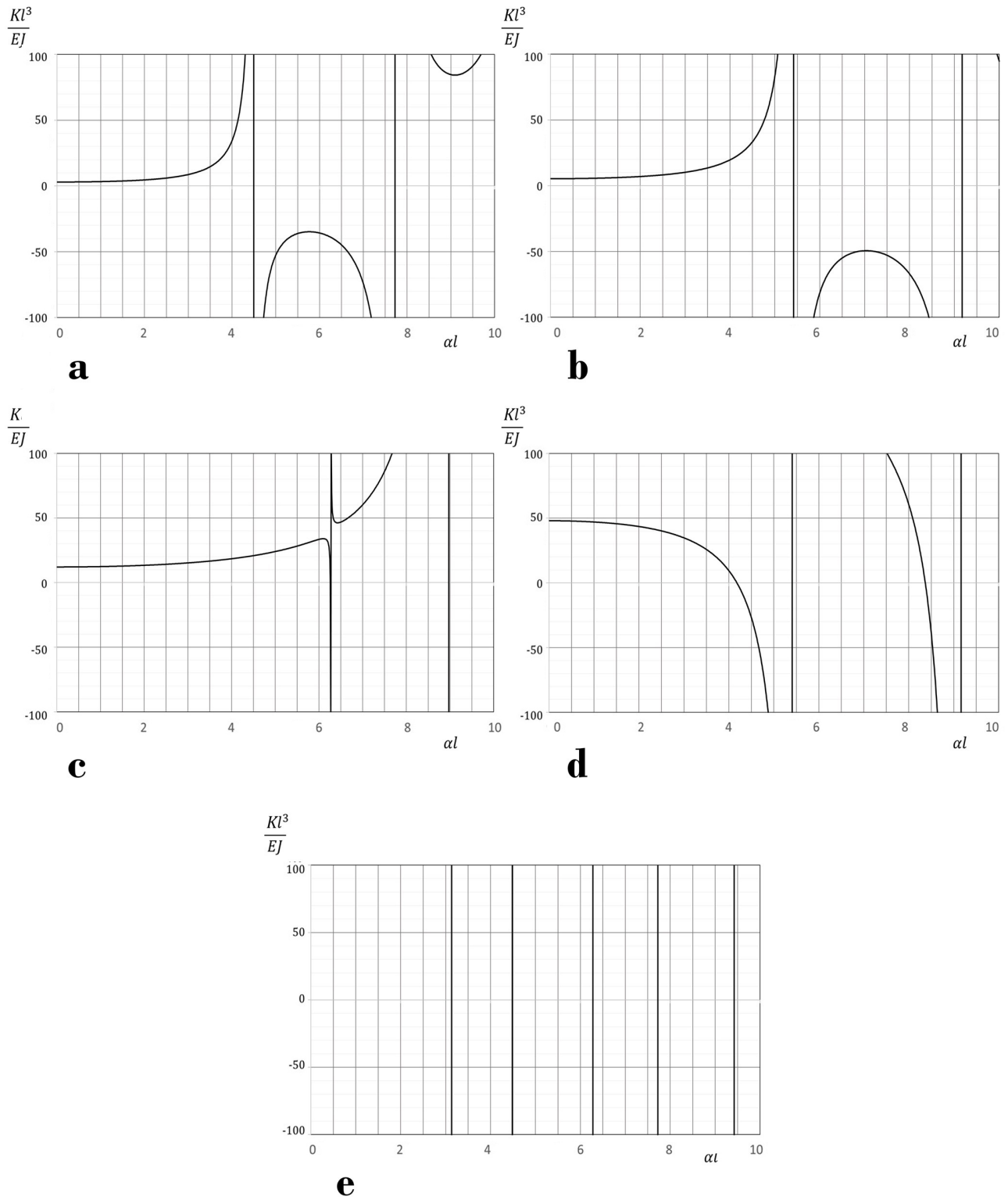
Figure 6.4: Dimensionless stiffness coefficient Kl^3/EJ versus αl when (a) $c = 0$, (b) $c = 0.25$, (c) $c = 0.5$, (d) $c = 0.75$, (e) $c = 1$.

Comparing the critical load by divergence at infinity with the Eulerian critical load by divergence of an auxiliary structure.

Consider $c = 0$. As it is well known, (6.2.7) coincides with the equation that determines the Euler buckling load of a clamped-pinned beam. This coincidence is due to the fact that when the critical load is approached by slowly increasing the applied follower load, the stiffness coefficient tends to infinity (Fig. 6.4a) and the displacement of the free end tends to zero. This fact happens for all values of c between 0 and 0.5, that is, when there is instability by divergence at infinity. A general hypothesis already highlighted in Feriani and Carini (2016) is confirmed: when instability is due to divergence at infinity, if one considers an auxiliary structure, different from the original one in that the lumped mass is replaced by a constraint that blocks the corresponding Lagrangian coordinate, and if the critical load of this new structure is due to divergence, that is, it does not depend on the mass distribution, then it coincides with the critical load by divergence at infinity of the original structure. It is then noticed that for $c \geq 0.5$ the critical load coincides with the Eulerian critical load of the massless beam. Therefore, it can be assumed that, in general, if one wants to determine the dynamic critical load of a linear elastic structure subjected to follower forces in the small displacements regime, it suffices to determine the minimum critical load between the one determined with the auxiliary structure first introduced in Fig. 6.5a and the one determined statically (looking for equilibrium configurations other than the trivial) starting from the assigned structure in Fig. 6.5b. Table 6.1 shows the values of the critical loads thus deduced. It can be seen that for $0 \leq c \leq 0.5$ the correct critical loads are those of the auxiliary structure while for $0.5 \leq c \leq 1$ the correct critical loads are those derived statically from the actual structure.
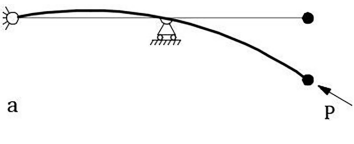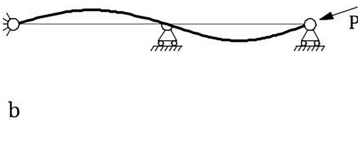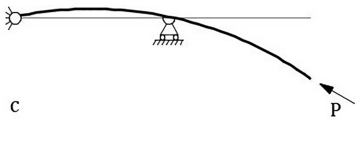
$c = \dfrac{a}{l}$	a	b	c
0	$(P_{cr}l^2)EJ =$20.1934	20.1934	∞
0.1	23.2248	23.2248	986.9604
0.2	27.0533	27.0533	246.7401
0.3	31.7550	31.7550	109.6623
0.4	36.7999	36.7999	61.6850
0.5	39.4784	39.4784	39.4784
0.6	27.4156	36.7999	27.4156
0.7	20.1420	31.7550	20.1420
0.8	15.4213	27.0533	15.4213
0.9	12.1847	23.2248	12.1847
1	9.8696	20.1934	9.8696

Table 6.1: Critical loads for different values of c for (a) the real beam, (b) the auxiliary beam, and (c) the real beam without lumped mass with a concentrated follower load P.
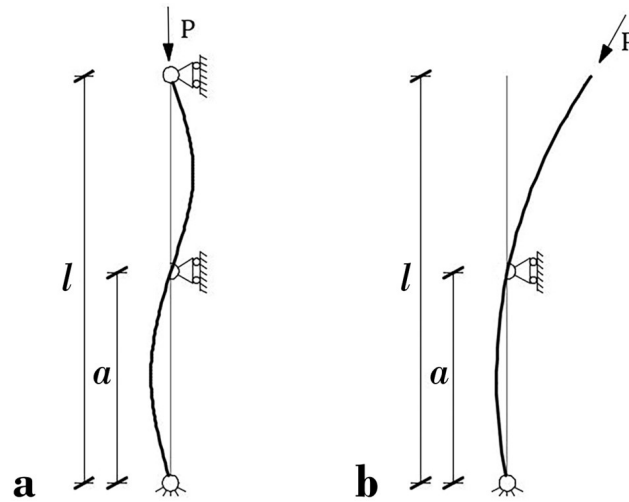
Figure 6.5: (a) Auxiliary structure, (b) real beam without lumped mass.

The same analysis can be performed on the problem of Fig. 6.3b, where the beam is subjected to both a follower and a conservative concentrated load. In Tables 6.2-6.6, the results of the dynamic analysis are compared to the results obtained by the static analysis on the auxiliary beam and on the real beam without the lumped mass, for different values of P an Q.

If P has a lower value compared to Q the real values coincide with those of the real beam without lumped mass, whereas, when P increases, the real values coincide with those of the auxiliary structure.

$c = \dfrac{a}{l}$ $P = 0$			
0	$((P+Q)_{cr}l^2)EJ = 2.467401$	20.193421	2.467401
0.1	2.832306	23.224779	2.832306
0.2	3.283024	27.053319	3.283024
0.3	3.845285	31.755046	3.845285
0.4	4.551082	36.799947	4.551082
0.5	5.434132	39.478418	5.434132
0.6	6.510622	36.799947	6.510622
0.7	7.726004	31.755046	7.726004
0.8	8.873959	27.053319	8.873959
0.9	9.636865	23.224779	9.636865
1	9.869604	20.193421	9.869604

Table 6.2: Critical loads for different values of c for (a) the real beam, (b) the auxiliary beam, and (c) the real beam without lumped mass with a concentrated follower load P and a concentrated conservative load Q. Here $P = 0$.
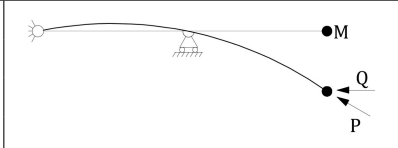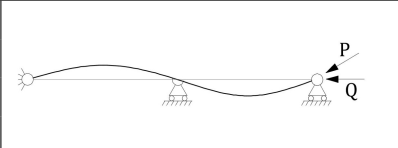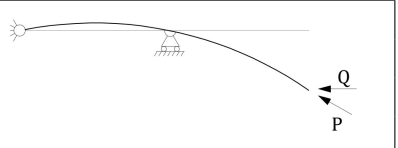
$c = \dfrac{a}{l}$ $P = 0.5Q$			
0	$((P+Q)_{cr}l^2)EJ =4.386491$	20.193421	4.386491
0.1	5.027210	23.224779	5.027210
0.2	5.792053	27.053319	5.792053
0.3	6.694040	31.755046	6.694040
0.4	7.724921	36.799947	7.724921
0.5	8.824308	39.478418	8.824308
0.6	9.839700	36.799947	9.839700
0.7	10.534591	31.755046	10.534591
0.8	10.727142	27.053319	10.727142
0.9	10.445219	23.224779	10.445219
1	9.869604	20.193421	9.869604

Table 6.3: Critical loads for different values of c for (a) the real beam, (b) the auxiliary beam, and (c) the real beam without lumped mass with a concentrated follower load P and a concentrated conservative load Q. Here $P = 0.5Q$.
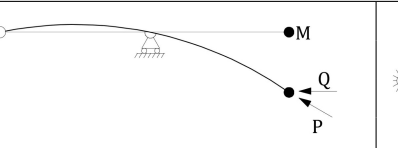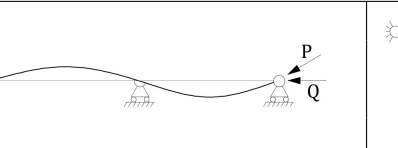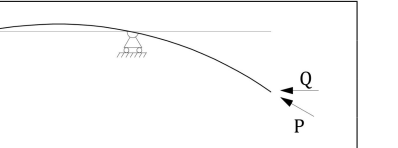
$c = \dfrac{a}{l}$ $P = Q$			
0	$((P+Q)_{cr}l^2)EJ =9.866812$	20.193421	9.866812
0.1	10.557424	23.224779	10.557424
0.2	11.285784	27.053319	11.285784
0.3	12.004017	31.755046	12.004017
0.4	12.621084	36.799947	12.621084
0.5	13.003321	39.478418	13.003321
0.6	13.012767	36.799947	13.012767
0.7	12.593363	31.755046	12.593363
0.8	11.825351	27.053319	11.825351
0.9	10.869127	23.224779	10.869127
1	9.869604	20.193421	9.869604

Table 6.4: Critical loads for different values of c for (a) the real beam, (b) the auxiliary beam, and (c) the real beam without lumped mass with a concentrated follower load P and a concentrated conservative load Q. Here $P = Q$.
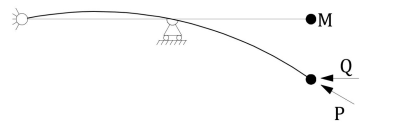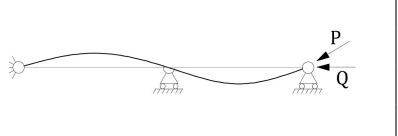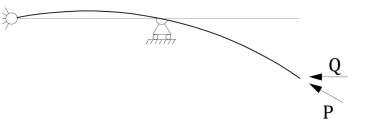
$c = \dfrac{a}{l}$ $P = 1.5Q$			
0	$((P+Q)_{cr}l^2)EJ =$ 20.190719	20.193421	∞
0.1	23.224779	23.224779	986.960440
0.2	27.053319	27.053319	115.479420
0.3	31.755046	31.755046	94.568172
0.4	36.799947	36.799947	76.718834
0.5	18.714629	39.478418	18.714629
0.6	15.813116	36.799947	15.813116
0.7	14.060247	31.755046	14.060247
0.8	12.528197	27.053319	12.528197
0.9	11.128291	23.224779	11.128291
1	9.869604	20.193421	9.869604

Table 6.5: Critical loads for different values of c for (a) the real beam, (b) the auxiliary beam, and (c) the real beam without lumped mass with a concentrated follower load P and a concentrated conservative load Q. Here $P = 1.5Q$.

$c = \dfrac{a}{l}$ $P = 10Q$			
0	$((P+Q)_{cr}l^2)EJ =$ 20.193420	20.193421	1.013006×10^{15}
0.1	23.224779	23.224779	986.960440
0.2	27.053319	27.053319	246.740110
0.3	31.755046	31.755046	104.574488
0.4	36.799947	36.799947	65.450961
0.5	39.478418	39.478418	39.478418
0.6	25.757606	36.799947	25.757606
0.7	18.921044	31.755046	18.921044
0.8	14.778474	27.053319	14.778474
0.9	11.943393	23.224779	11.943393
1	9.869604	20.193421	9.869604

Table 6.6: Critical loads for different values of c for (a) the real beam, (b) the auxiliary beam, and (c) the real beam without lumped mass with a concentrated follower load P and a concentraded conservative load Q. Here $P = 10Q$.
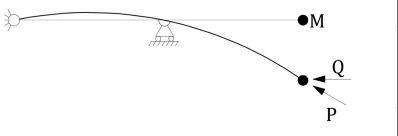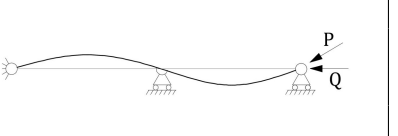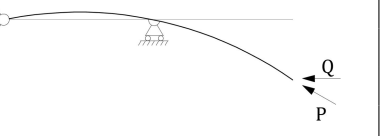
The same analysis can be performed on the problem of Fig. 6.3c. This particular problem requires a numerical analysis, using the finite element method.

The beam is thus subdivided into standard linear finite elements with two nodes. Each node has two degrees of freedom: the translation v and the rotation ϕ.

The tangent stiffness matrix and the mass matrix are computed and, in Table 6.7, the results of the dynamic analysis are compared to the results obtained by the static analysis on the auxiliary beam and on the real beam without the lumped mass. In this problem, it can be seen that for $0 \leq c \leq 0.3$ the correct critical loads are those of the auxiliary structure while for $0.4 \leq c \leq 1$ the correct critical loads are those derived statically from the actual structure.
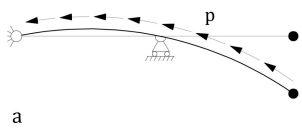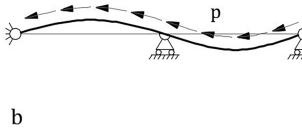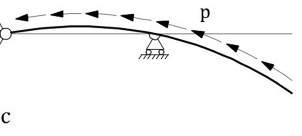
$c = \dfrac{a}{l}$	a	b	c
0	$(p_{cr}l^3)EJ =$57.0162	57.0162	∞
0.1	69.4495	69.4495	1262.9830
0.2	82.4450	82.4450	276.1083
0.3	88.7741	88.7741	129.0508
0.4	76.9404	80.0298	76.9404
0.5	52.3994	65.6796	52.3994
0.6	38.8634	53.8126	38.8634
0.7	30.6110	45.1049	30.6110
0.8	25.2281	38.7692	25.2281
0.9	21.5499	34.0918	21.5499
1	18.9567	30.5741	18.9567

Table 6.7: Critical loads for different values of c for (a) the real beam, (b) the auxiliary beam, and (c) the real beam without lumped mass with a distributed follower load p.

6.2.4 Conclusions

In conclusion, a conjecture can be formulated: consider a system with just one Lagrangian coordinate and, if instability is due to divergence at infinity, consider an auxiliary structure, differing from the original one in that the lumped mass is replaced by a constraint blocking the corresponding Lagrangian coordinate. The critical load of such new structure is due to divergence and it coincides with the critical load by divergence at infinity of the original structure. Therefore, within the second order theory, considering structures with intermediate supports, a static method was detected to determine the critical load due to divergence at infinity in systems subjected to follower loads where the mass is modelled just as a lumped mass. The critical load is determined statically by taking the minimum value between the Eulerian critical load of an auxiliary structure and the Eulerian critical load of the given structure.

6.3 Part II: Conservative systems showing instability in tension

6.3.1 Introduction

According to Ziegler (1977), conservative systems, like the one of Fig. 6.6a, exhibiting instability in tension were first detected by Grammel (Biezeno and Grammel 1954, cited in Ziegler 1977). Zaccaria et al. (2011) observe that structures like the one of Fig. 6.6a have compressed parts. Nevertheless, actually, the structure of Fig. 6.6a is fully equivalent to the structure of Fig. 6.6b where there are no compressed parts, but a linear rotational spring of negative stiffness equal to $-Pa$. Zaccaria et al. (2011) found another class of structures showing instability in tension and proved experimentally such phenomenon. In particular, Zaccaria et al. consider two inextensible elastic rods clamped at one end and joint through a slider (see Fig. 6.7). In Feriani and Carini (Feriani and Carini, 2017) two conservative systems showing instability due to a tensile load are presented. However, their load cannot be defined as "dead load" according to Zaccaria et al. (2011). In particular, in Feriani and Carini (2017) the example depicted in Fig. 6.8a is considered. It is obtained by symmetrizing the load of Fig. 6.8b. It corresponds to summing Beck's and Reut's non conservative loading conditions, where in each case the vertical load is equal to $P/2$. The resulting applied load is conservative. In Feriani and Carini (2017) the transverse displacement of the free end is considered. The stiffness coefficient K, that is, the transverse force on the free end needed to produce a unit displacement, was calculated. In order to determine the stiffness coefficient, consider the equation $EJv^{IV} + Pv^{II} = 0$ together with the boundary conditions written hereafter: $v(0) = 0$, $v'(0) = 0$ $v(l) = 1$, $EJv''(l) = -P/2$. Once the deflected curve $v(z)$ is known, the stiffness coefficient, which is equal to the transverse force applied at the free end, can be determined by prescribing equilibrium. If $P < 0$ the stiffness coefficient K, as a function of P, presents only one root. Thus, a critical load by divergence is obtained when the conservative system of Fig. 6.8a is subjected to traction and the dimensionless critical load $-Pl^2/EJ = 5.7569$ is found. Similarly, the symmetrization of the system of Fig. 6.9b leads to the conservative system of Fig. 6.9a, that is subject to instability when a traction load is applied. Using the same procedure exploited for the first case Feriani and Carini obtained $-pl^3/EJ = 21.3897$. In this section a new system is studied: a straight-axis beam of length l with constant cross-sectional area and stiffness, hinged at one end, simply supported at an intermediate point distant a from the hinge is presented and two different follower forces causing traction are applied. The first one leads to a "generalized" Beck column in the sense that when $c = a/l = 0$ the Beck column is realized. The second one leads to a "generalized" Reut column in the sense that when $c = 0$ the Reut column is realized. A new analogy between the generalized Beck plus generalized Reut column and the elastic circular arch is shown. A discussion on the results obtained is presented. In particular, it will be shown that there is a close relationship between the Zaccaria et al. structure and the Feriani and Carini structure.
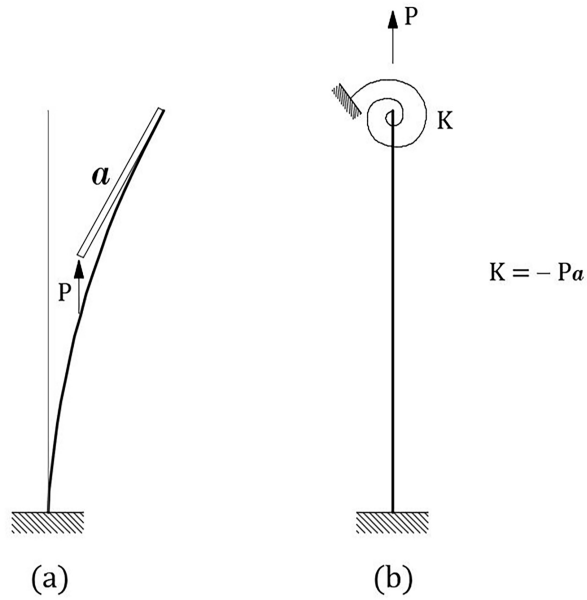
Figure 6.6: (a) Buckling by tension: the axial load P is applied at the end of a rigid handle of length a with is pointing downwards and is in alignment with the tangent of the deflection curve at the upper end; (b) An equivalent structure.
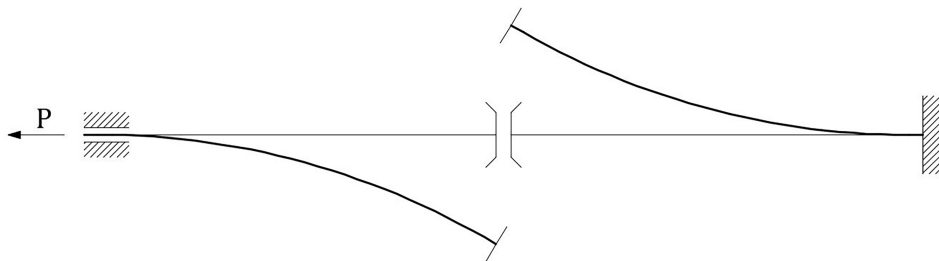
Figure 6.7: Elastic system under tensile dead loading composed by two inextensible elastic rods clamped at one end and jointed through a slider, a device allowing only relative sliding between the two connected pieces (Zaccaria et al. (2011)).

Figure 6.8: (a) A beam clamped at one end under conservative load at the other end. The conservative load is obtained symmetrizing the non conservative follower force (b), (Feriani and Carini, 2017).

Figure 6.9: (a) A beam clamped at one end, under distributed conservative load obtained symmetrizing the non conservative distributed follower load (b). (Feriani and Carini, 2017).

6.3.2 Some remarks about the generalized Reut column, the generalized Beck column and the elastic circular arch

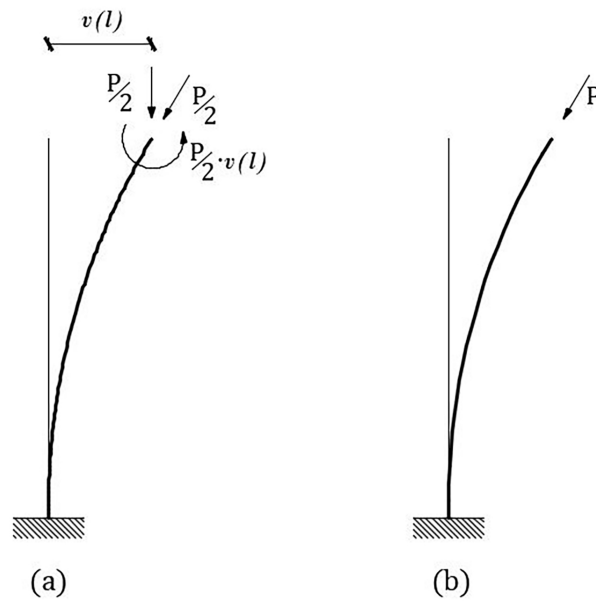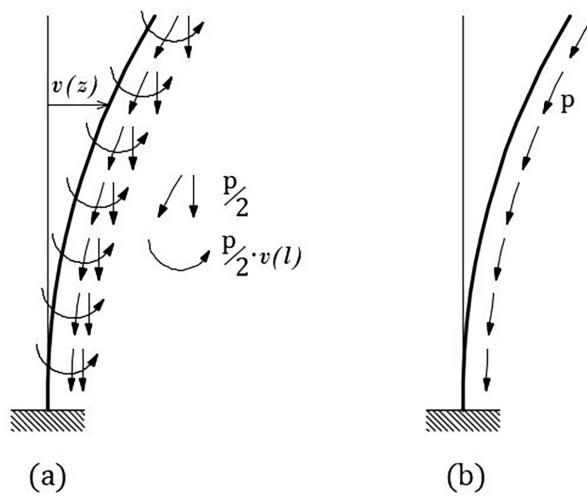As it is well known, the generalized Beck (Fig. 6.10a) and Reut (Fig. 6.10b) columns are classical examples of non-conservative problems. When $c = 0$ the beams specialize into Beck and Reut columns. When $c = 1$ they both become beams hinged at one end, simply supported at the other end, and the loads from non-conservative become conservative. The generalized Beck (Fig. 6.10a) and Reut (Fig. 6.10b) columns are governed, in the absence of inertial forces, by the following equations, with the relevant boundary conditions, all in terms of transversal displacements $v(z)$ only:

generalized Beck column:
$$\begin{cases} EJ\dfrac{\mathrm{d}^4 v}{\mathrm{d}z^4} + P\dfrac{\mathrm{d}^2 v}{\mathrm{d}z^2} = 0 \\[2mm] v(0) = 0, \quad \dfrac{\mathrm{d}^2 v}{\mathrm{d}z^2}\Big|_0 = 0, \quad v(a) = 0, \quad \dfrac{\mathrm{d}^2 v}{\mathrm{d}z^2}\Big|_l = 0, \quad \dfrac{\mathrm{d}^3 v}{\mathrm{d}z^3}\Big|_l = 0 \end{cases}$$
$$(6.3.1)$$

generalized
Reut column:
$$\begin{cases} EJ\dfrac{\mathrm{d}^4 v}{\mathrm{d}z^4} + P\dfrac{\mathrm{d}^2 v}{\mathrm{d}z^2} = 0 \\[2mm] v(0) = 0, \quad \dfrac{\mathrm{d}^2 v}{\mathrm{d}z^2}\Big|_0 = 0, \quad v(a) = 0, \quad \left[\dfrac{\mathrm{d}^2 v}{\mathrm{d}z^2} + \dfrac{P}{EJ}v\right]_l = 0, \quad \left[\dfrac{\mathrm{d}^3 v}{\mathrm{d}z^3} + \dfrac{P}{EJ}\dfrac{\mathrm{d}v}{\mathrm{d}z}\right]_l = 0. \end{cases}$$
$$(6.3.2)$$

Let us now consider the new problem of Fig. 6.11a, where the same column is subjected to the non-conservative loads of the generalized Beck and Reut columns simultaneously. It is easy to derive the relevant governing equation and boundary conditions as follows:

generalized Beck
+ Reut column:
$$\begin{cases} EJ\dfrac{\mathrm{d}^4 v}{\mathrm{d}z^4} + 2P\dfrac{\mathrm{d}^2 v}{\mathrm{d}z^2} = 0 \\[2mm] v(0) = 0, \quad \dfrac{\mathrm{d}^2 v}{\mathrm{d}z^2}\Big|_0 = 0, \quad v(a) = 0, \quad \left[\dfrac{\mathrm{d}^2 v}{\mathrm{d}z^2} + \dfrac{P}{EJ}v\right]_l = 0, \quad \left[\dfrac{\mathrm{d}^3 v}{\mathrm{d}z^3} + \dfrac{P}{EJ}\dfrac{\mathrm{d}v}{\mathrm{d}z}\right]_l = 0. \end{cases}$$
$$(6.3.3)$$

It is possible now to recognize that this new problem is conservative.
In fact, as is easy to see, the differential operator, including boundary conditions, related to Reut's rod is the adjoint operator of the operator related to Beck's rod. Therefore, the sum operator of the two problems turns out to be self-adjoint. This means that the Beck's rod plus Reut's rod system is conservative.
This is corroborated by the following nice analogy. Consider the arch beam in Figure 6.11b. The governing equation of the arch problem of Fig. 6.11b in terms of radial displacements $v(s)$ only, with the relevant boundary conditions, is written as follows:

Circular
arch problem:
$$\begin{cases} \dfrac{\mathrm{d}^4 v}{\mathrm{d}s^4} + \dfrac{2}{R^2}\dfrac{\mathrm{d}^2 v}{\mathrm{d}s^2} + \dfrac{v}{R^4} = 0 \\[2mm] v(0) = 0, \quad \dfrac{\mathrm{d}^2 v}{\mathrm{d}s^2}\Big|_0 = 0, \quad v(a) = 0, \quad \left[\dfrac{\mathrm{d}^2 v}{\mathrm{d}s^2} + \dfrac{1}{R^2}v\right]_l = 0, \quad \left[\dfrac{\mathrm{d}^3 v}{\mathrm{d}s^3} + \dfrac{1}{R^2}\dfrac{\mathrm{d}v}{\mathrm{d}s}\right]_l = 0. \end{cases}$$
$$(6.3.4)$$

We immediately recognize that this equation and relevant boundary conditions are highly similar to those of the generalized Beck + Reut columns (Fig. 6.11a) when $1/R^2$ in Eq. (6.3.4) is substituted by P/EJ, except for the presence of the term v/R^4 in Eq. (6.3.4). If the new arch beam of Fig. 6.11b is now considered, with a bed of springs having negative stiffness $K = -EJ/R^4$, the above term v/R^4 of Eq. (6.3.4) disappears and then the set of equations (6.3.4) becomes the same as Eq. (6.3.3) governing the generalized Beck + Reut column problem (Fig. 6.11a). Then, this allows to state that the generalized Beck + Reut column problem is conservative and the total potential energy will be analogous to the following deformation energy of the arch of Fig. 6.11b:

$$U(v) = \frac{1}{2} \int_0^l EJ \left(\frac{\mathrm{d}^2 v}{\mathrm{d}s^2} + \frac{v}{R^2} \right)^2 \mathrm{d}s - \frac{EJ}{2R^4} \int_0^l v^2 \, \mathrm{d}s. \tag{6.3.5}$$

After replacing $1/R^2$ by P/EJ, we arrive, by virtue of the analogy, at the following form of the total potential energy:

$$U(v) = \frac{1}{2} \int_0^l EJ \left(\frac{\mathrm{d}^2 v}{\mathrm{d}s^2} \right)^2 \mathrm{d}s + P \int_0^l v \frac{\mathrm{d}^2 v}{\mathrm{d}s^2} \, \mathrm{d}s \tag{6.3.6}$$

which, with integration by parts, becomes

$$U(v) = \frac{1}{2} \int_0^l EJ \left(\frac{\mathrm{d}^2 v}{\mathrm{d}s^2} \right)^2 \mathrm{d}s + P \int_0^l \left(\frac{\mathrm{d}v}{\mathrm{d}s} \right)^2 \mathrm{d}s + Pv(l) \frac{\mathrm{d}v}{\mathrm{d}s}(l) \tag{6.3.7}$$

where we recognize the strain energy of the beam $\frac{1}{2} \int_0^l EJ \left(\frac{\mathrm{d}^2 v}{\mathrm{d}s^2} \right)^2 \mathrm{d}s$ and the potential energy of the external loads $P \int_0^l \left(\frac{\mathrm{d}v}{\mathrm{d}s} \right)^2 \mathrm{d}s + Pv(l) \frac{\mathrm{d}v}{\mathrm{d}s}(l)$.

6.3.3 Stability of the new conservative systems

Consider first the example in Fig. 6.11a (with tensile loads). As it can be seen, it is obtained by symmetrizing the load in Fig. 6.10a and it corresponds to the sum of the generalized Beck and Reut loading conditions. The resulting load is conservative and, therefore, the buckling conditions are independent of the mass distribution and the critical buckling load can be obtained with the standard energy criterion. In the specific case, the results shown in Table 6.8 are obtained. It can be seen that tensile buckling is possible for any c except for $c = 1$. As c increases, the critical load also increases. For $c = 0$, the results presented in Feriani and Carini (2017) are obtained again. Similarly, the symmetrization of the second example (Fig. 6.12a), for which the finite element method is used, leads to a conservative system that can buckle under tension. The results are shown in Table 6.9 changing the value of c, meaning, by changing the position of the intermediate support. For $c = 0$, as the number of degrees of freedom increases, the value of the dimensionless critical load tends to 21.389 as in Feriani and Carini (2017). In Table 6.10 the tensile dimensionless critical load obtained for $c = 0.5$ is listed as a function of the number n finite elements adopted.
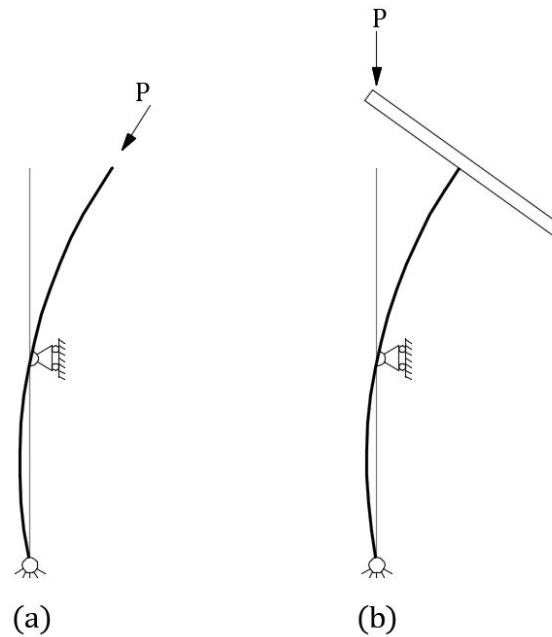
Figure 6.10: Beam hinged at one end, free at the other end, simply supported at an intermediate point, and subjected to (a) a follower force P at the free end (generalized Beck column), (b) a force P which is always directed along the initial undeformed axis, with a fixed direction line of acting (generalized Reut column).
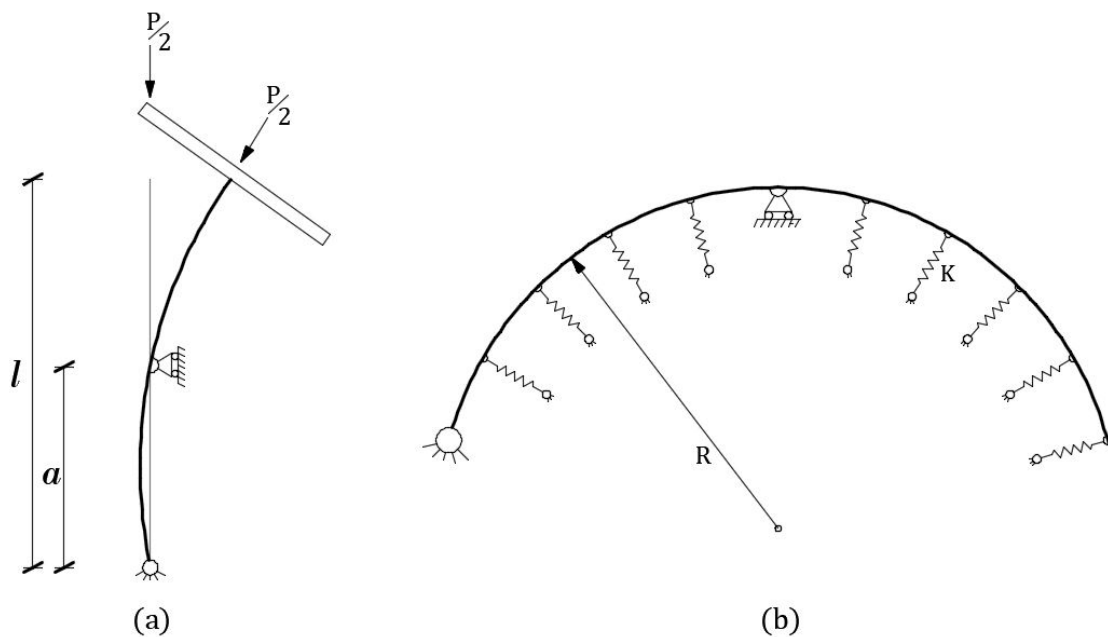

Figure 6.11: (a) An example of conservative load as sum of non-conservative loads, (b) An analogous system: the circular arch on a bed of springs with stiffness $K = -EJ/R^4$.

$c = a/l$	0	0.1	0.2	0.3	0.4	0.5	0.6	0.7	0.8	0.9	1
$P_{cr}l^2/EJ$	5.76	6.64	7.84	9.55	12.12	16.33	24.05	40.74	88.35	343.01	∞

Table 6.8: Values of dimensionless critical loads related to the structure of Fig. 6.11a.
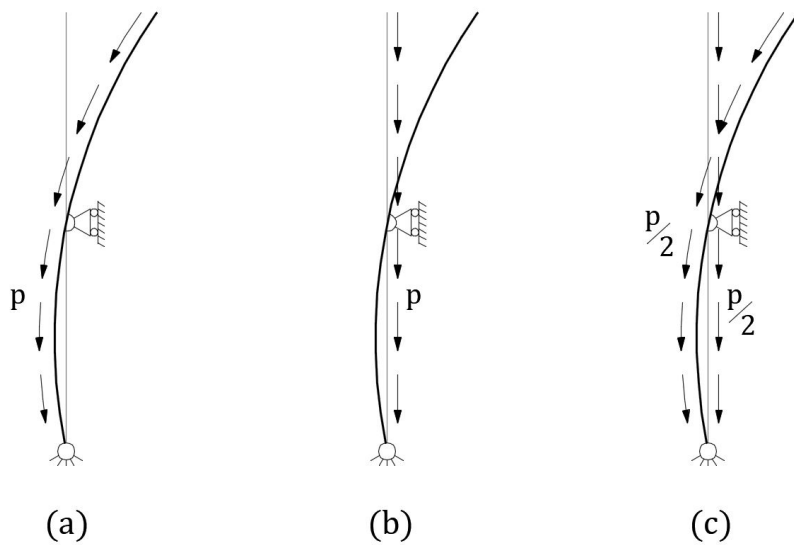

Figure 6.12: (a) Uniformly distributed follower force p; (b) Uniformly distributed force p with a fixed direction; (c) Conservative load as sum of the previous two non-conservative loads.

$c = a/l$	0	0.1	0.2	0.3	0.4	0.5	0.6	0.7	0.8	0.9	1
$\dfrac{p_{cr}l^3}{EJ}$	21.39	26.65	34.82	48.45	73.10	122.14	233.34	544.79	1827.31	15134.24	∞

Table 6.9: Values of dimensionless critical loads related to the structure of Fig. 6.12.

n	2	4	6	8	10
$p_{cr}l^3/EJ$	129.2980	123.2868	122.3634	122.1920	122.1435

Table 6.10: Values of dimensionless critical loads related to the structure of Fig. 6.12 for various discretizations and for $c = 0.5$.

6.3.4 Discussion and Conclusions

Two new structures are studied that exhibit instability when a traction load is applied. These structures specialize into two others, already presented in Feriani and Carini (2017). A nice analogy is shown between the generalized Beck + Reut column and the elastic circular arch problem. In Zaccaria et al. (2011) "dead loads" are defined as loads that are applied at a point in the structure and remain applied at that point even after displacement has occurred and always maintain the original direction. Other loads are termed "live loads". In Zaccaria et al. (2011) the structure in Fig. 6.7, subjected to a "dead" load, which shows tensile instability, was studied. In Feriani and Carini (2017), another structure exhibiting tensile instability, but subjected to "live" loads, was considered. Consider the equilibrium of the slider present in the structure of Fig. 6.7. The internal actions in the slider result as in Fig. 6.13a. It is evident that the conservative loads applied to the structure of Fig. 6.11a are identical to the internal actions in the slider to which a "dead" load is added (see Fig. 6.13). Therefore, barring a "dead" load, the load applied in one structure coincides with the constraining reaction in the other and vice versa. In conclusion, it seems that the definition of "dead" load must somehow consider the set of active and reactive loads.
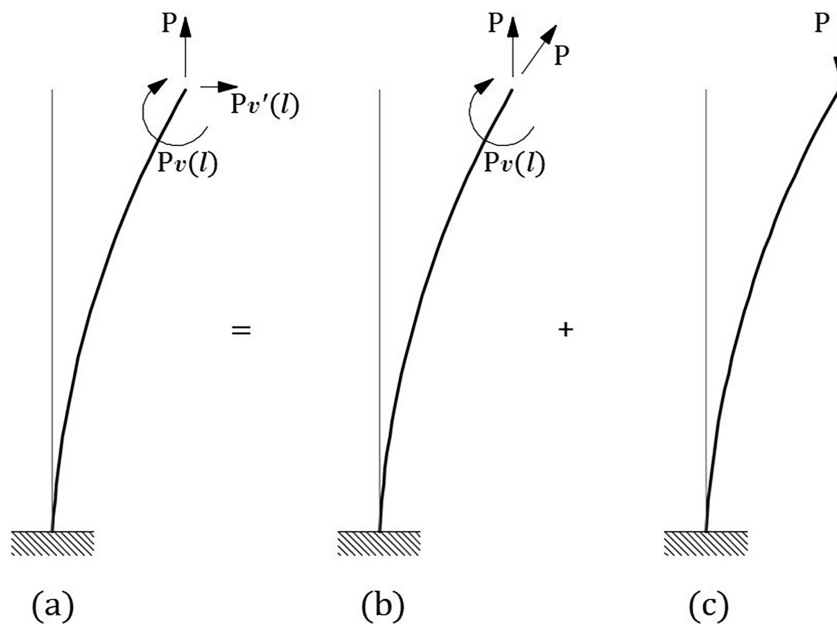

Figure 6.13: (a) Slider internal actions; (b) Beck plus Reut beams; (c) Beam subjected to a *dead* conservative load.

References

Bisenzio, C., Grammel, R., 1954. Engineering Dynamics. Princeton: D. Van Nostrand Co., Ltd.

Bolotin, V.V., 1963. Nonconservative Problems of the Theory of Elastic Stability. Pergamon Press, London.

Elishakoff, I., Hollkamp, J., 1987. Computerized symbolic solution for a nonconservative system in which instability occurs by flutter in one range of a parameter and by divergence in another. Computer Methods in Applied Mechanics and Engineering 62, 27-46.

Felippa, C., 2014. Nonlinear Finite Element Methods. Department of Aerospace Engineering Sciences. University of Colorado at Boulder, Spring, www.colorado.edu.

Feriani, A., Carini, A., 2017. Some considerations on dynamic stability. in A. Zingoni (Ed.), Insights and Innovations in Structural Engineering, Mechanics and Computation, Proceedings of Sixth International Conference on Structural Engineering, Mechanics and Computation, Cape Town (South Africa), 2016-09-05 / 2016-09-07.

Leipholz, H., 1970. Stability Theory. Academic Press, London.

Leipholz, H., 1974. On conservative elastic systems of the first and second kind. Ingenieur-Archiv 43, 255-271.

Leipholz, H., 1978. On a variational principle for Beck's rod. Mechanics Research Communications, 5(1), 45-49.

Leipholz, H., 1984. An alternative to Liapunov's stability method. Computer methods in applied mechanics and engineering 43, 293-313.

Leipholz, H., 1984. An alternative to Liapunov's stability method and its application to higher-order systems. Computer methods in applied mechanics and engineering 47, 299-314.

Leipholz, H., 1986. On principles of stationarity for non-selfadjoint rod problems. Computer Methods in Applied Mechanics and Engineering, 59, 215-226.

Leipholz, H., 1987. On Galerkin's method interpreted as a generalized integral transformation. Computer methods in applied mechanics and engineering 65, 177-189.

Panovko, Y., Gubanova, I., 1967. Stability and oscillations of elastic systems: Models, paradoxes and errors. second ed., Nunka Press, Moscow.

Zaccaria, D., Bigoni, D., Misseroni, D., Noselli, G., 2011. Structures buckling under tensile dead load. Proceedings of the Royal Society of London, A 467, 1686-1700.

Ziegler, H., 1977. Principles of structural stability. 2nd Ed., Basel: Birkhuser Verlag.

Zorii, L.M., Chernukha, Yu A., 1971. Influence of supports on the dynamic stability of elastic column. Prikl. Makh. 7(2) 134-136 (in Russian).

Chapter 7

Conclusions

The mathematical formulation of phenomena that evolve over time generally requires the resolution of systems of differential equations with initial conditions. These particular problems cannot be often solved analytically and, therefore, numerical integration techniques are used in order to obtain an accurate approximation of the solution.

An interesting alternative that could be exploited is the variational approach. As it has already been pointed out in the context of this thesis, variational methods are valid both for a qualitative study of the problem (study of existence and uniqueness of the solution, its regularity, etc.), and for a quantitative study, namely from a numerical point of view (evaluation of convergence, estimation of the error of the approximate solution). This thesis addresses the application of variational principles to several evolution problems of engineering interest such as the linear viscoelastic problem, the heat conduction problem, the derivation of upper bounds to the homogenized viscous kernels of liner viscoelastic composites, the extension of the Capurso-Maier functional to fracture mechanics and the analysis of dynamical instability of systems with one Lagrangian coordinate.

The common thread of all these different and complex problems is the exploitation of functionals based on convolutive bilinear forms. In fact, Tonti (1973) highlighted the crucial role played by the choice of a suitable bilinear form, in order to provide a variational formulation for the given problem. In particular, he showed how the use of a bilinear form of the convolutive type allows one to provide a variational formulation for initial value problems, making unnecessary their transformation into problems with only boundary conditions.

Furthermore, if one decomposes the time integration interval (or the space integration interval as in the dynamic instability analysis) of the problem into two sub-intervals of equal length, as shown in Carini and Mattei (2015), new variational formulations can be derived: in fact, by the adopted time splitting, one is able to isolate a part of the functional that represents the free energy of the system and is, therefore, in general, semidefinite positive. In conclusion, the use of the convolutive (and biconvolutive) bilinear forms provides good numerical results as well.

During the thesis (and overall during the PhD), several scripts have been developed in Matlab to solve all the problems and, as for the chapter concerning the definition of bounds, the RVEs and models have been analysed using the ABAQUS software.

A great deal of work remains to be done.

As for the linear viscoelastic problem and the heat conduction problem, the choice of the most suitable time shape functions remains an open issue, here solved with a trial and error method. Moreover, the behaviour of the solution calculated using the splitted functionals with a reduction of degrees of freedom on the second subinterval still needs a theoretical explanation.

Upper bounds for the relaxation and creep kernels for bodies subjected to volumetric strains haven't been defined yet.

Regarding the fracture mechanics problem, the issue of the determination of the hardening component, which strictly depends on the geometry of the crack, thus is not known a priori, constitutes a significant obstacle.

Furthermore, only a hint on a possible variational formulation applicable to viscoelastic composites is given.

As for the dynamic stability Chapter, there are still many intermediate problems to take into account, which have not been addressed in the context of this thesis, such as structures with two or more concentrated masses or systems with both distributed and concentrated masses.

References

Carini, A., Mattei, O., 2015. Variational formulations for the linear viscoelastic problem in the time domain. European Journal of Mechanics A/Solids, 54, 146-159.

Tonti, E., 1973. On the variational formulation for linear initial value problems. Annali di Matematica Pura ed Applicata, Serie Quarta XCV, 331-359.